THERMODYNAMIC STUDY ON ABSORPTION REFRIGERATION SYSTEMS USING AMMONIA/IONIC LIQUID WORKING PAIRS

Hifni Mukhtar Ariyadi

Hifni Mukhtar Ariyadi

THERMODYNAMIC STUDY ON ABSORPTION REFRIGERATION SYSTEMS USING AMMONIA/IONIC LIQUID WORKING PAIRS

UNIVERSITAT ROVIRA I VIRGILI

DOCTORAL THESIS

Supervised by:
Prof. Alberto Coronas

Department of Mechanical Engineering

TARRAGONA
2016

UNIVERSITAT ROVIRA I VIRGILI
DEPARTAMENT D'ENGINYERIA MECÀNICA

Escola Tècnica Superior d'Enginyeria Química (ETSEQ).
Av. Països Catalans 26. 43007 Tarragona (Spain)

I state that the present study entitled "Thermodynamic Study on Absorption Refrigeration Systems Using Ammonia/Ionic Liquid as Working Fluid" presented by Mr. Hifni Mukhtar Ariyadi for the award of the Degree of Doctor has been carried out under our supervision at the Department of Mechanical Engineering, Rovira i Virgili University and it fulfils all the requirements to be eligible for the International Doctorate Award.

Tarragona, July 11th, 2016

Doctoral Thesis Supervisor

Prof. Alberto Coronas

Li Llah, Fi Llah, Bi Llah...

Dedicated to my beloved family

"The best of people are those that bring most benefit to the rest of mankind."
Muhammad (570 CE –632 CE)

Acknowledgements

Special thanks and love to my family, Mas Afnin, Mbak Anggun, Dik Anies, Dik Yazid, and my cute nephew Elvio, for their unconditional support and motivation over these years.

Of course, this thesis could not be completed without the participation and assistance of so many colleagues, friends and well-wishers whose names may not all the enumerated. Their contributions are sincerely appreciated and gratefully acknowledged.

Abstract

Absorption refrigeration system is a good known technology as it can utilize renewable energy such as solar and geothermal energy or waste heat sources, thus carries a primary energy saving and emission reduction. In addition, the absorption system has no vibration and noise and contains natural substances and therefore, environmentally friendly and becomes a competitive alternative to the conventional mechanical-driven vapour compression refrigeration systems. One most common working fluid in absorption refrigeration cycle is ammonia/water. In this working pair, the characteristics of water is volatile, thus as absorbent, it is necessary to add an additional component, rectifier, to minimize the amount of water coming to the condenser. Hence, to overcome these drawbacks, finding a suitable working pair is inevitable.

As a new type of fluids with a great solvent character and other interesting properties such as a good thermal stability and very low vapour pressure, ionic liquids can be good candidates as absorbents for absorption systems to overcome drawbacks associated with the conventional working pairs. Nevertheless, research on both thermodynamic properties and application of ammonia/ionic liquid mixtures for absorption cycle applications still remains scarce. This thesis was aimed to analyse the feasibility and the performance of ionic liquids as absorbents for ammonia refrigerant in absorption refrigeration systems. Ionic liquids, novel and tailor-made absorbents, can be used with ammonia as working pairs for absorption refrigeration cycles and give some advantages such as elimination of the rectification process in ammonia/water systems.

The selection of an appropriate model to describe the vapour-liquid equilibrium properties ammonia/ionic liquid mixtures was firstly carried out in this research as the solubility of the working fluids is one of the most important properties the simulation results were undoubtedly dependent to the thermodynamic model of the vapor-liquid equilibrium. Among four different models studied in this research, both NRTL and RK-Soave model show their ability to calculate the vapor-liquid equilibrium of ammonia/ionic liquid mixtures with high accuracy. Although the calculation results using NRTL model were slightly less accurate than those of RK-Soave model, the NRTL model is considered as the simplest model in comparison with other thermodynamic models. Subsequently, NRTL model is chosen to evaluate the performances of absorption refrigeration systems using ammonia/ionic liquid mixtures available in the literature. Among five ammonia/ionic liquid working fluids studied, at certain operation conditions the ammonia/[emim][NTf$_2$] working fluid presented the highest COP than other ammonia/ionic liquid mixtures. However, although the COP of the system working with ammonia ammonia/[emim][NTf$_2$] was higher than the systems with other working fluids, its circulation ratio was the highest among other working fluids and thus the solution mass flowrate per unit of cooling load (R) was also the highest among other working fluids. It means that at the same ionic liquid mass flow rate and at the same operation conditions, the system working with ammonia/[emim][NTf$_2$] mixture produces lower cooling capacity. On contrary, the COP of the system

working with ammonia ammonia/[bmim][BF$_4$] was lower than the systems with other working fluids and its f and R values were the lowest among other working fluids.

Apart of ammonia/ionic liquid mixtures available in the literature, new selected ammonia/ionic liquid mixtures working pair for absorption refrigeration applications are theoretically studied and analysed, and compared with the performance of ammoni/LiNO$_3$ working pair. Among all of new ammonia/ionic liquid working fluids studied only [N$_{1113}$][NTf$_2$] presented higher *COP* than that of ammonia/LiNO$_3$ at certain operation conditions and the highest circulation ratio among other working fluids. The circulation ratios (*f*) and R values of the absorption systems working with ammonia/ionic liquid working fluids at same operation conditions were somehow higher as compared with that of ammonia/LiNO$_3$. Finally the viscosities of ammonia/ionic liquids mixtures were generally higher than that of ammonia/LiNO$_3$ however, surprisingly the viscosity of ammonia/[N$_{111}$(2OH)] [NTf$_2$] was lower than that of ammonia/LiNO$_3$, which may be a competitive absorbent for water absorbent substitution for ammonia-based absorption refrigeration systems in comparison with LiNO$_3$.

In addition to the simulation and theoretical investigation, a measurement setup to study the absorption capacity of the ammonia vapor in ionic liquids in a pool type absorber was also developed and studied to find the most suitable ionic liquid as an absorbent for ammonia refrigerant. Furthermore, it is also important to find the most suitable absorber configuration for the proposed ammonia/ionic liquids absorption systems. Among all measured ionic liquids, [EtOHmim]$^+$ based ionic liquids shows higher absorption capacity than [emim]$^+$ based ionic liquids, which means that the OH structure in the cation may improve the absorption capacity of ammonia. In addition [BF$_4$]$^-$ anion shows slightly higher absorption capacity than other anions with same cation. However, in the beginning of the process [emim]$^+$ based ionic liquids show higher absorption capacity than [EtOHmim]$^+$ based ionic liquids.

The ammonia/ionic liquid working fluid can provide competitive performance in comparison with conventional absorbent for ammonia refrigerant. However, some drawbacks still remain to be solved such as the relatively low solubility of ammonia into ionic liquids which affects the solution circulation mass flow ratio and relatively high viscosity of ionic liquid in comparison with other conventional absorbent which may affect the performance of the absorber and solution pump.

List of Publications

Articles in Scientific Journals

1. **Ariyadi, H. M.**, and Coronas, A., *Absorption Capacity of Ammonia into Ionic Liquids for Absorption Refrigeration Applications*, Journal of Physics: Conference Series (Accepted).

2. **Ariyadi, H. M.**, and Coronas, A., *Performance Absorption Refrigeration Systems Based on Ammonia Refrigerant and Selected Ionic Liquid Absorbents,* Applied Thermal Engineering (In preparation).

3. **Ariyadi, H. M.**, and Coronas, A., *Simple Method for Screening Ionic Liquid Absorbents for Ammonia Refrigerant Based on Solubility Data for Absorption Heat Pumps*. International Journal of Refrigeration (In preparation).

4. **Ariyadi, H. M.**, Salavera, D., Bourouis, M., and Coronas, A., *Measurements of Absorption Capacity of Ammonia into Ionic Liquids*, International Communications in Heat and Mass Transfer (In preparation).

Workshop and Conference Proceedings and Presentations

1. **Ariyadi, H. M.**, Salavera, D., Cera-Manjarres, A., Coronas, A., *1-(2-Hydroxyethyl)-3-Methylimidazolium Tetrafluoroborate and Bis(Trifluoro-Methylsulfonyl)Imide as Absorbents of Ammonia in Absorption Refrigeration Applications*, 26th EUCHEM on Molten Salts and Ionic Liquids, 3– 8 July 2016, Vienna, Austria (Poster Presentation).

2. **Ariyadi, H. M.**, and Coronas, A., *Absorption Capacity of Ammonia into Ionic Liquids for Absorption Refrigeration Applications*, 7th European Thermal-Sciences Conference, 19–23 June, 2016, Krakow, Poland (Oral Presentation). ISBN: 978-83-7464-868-4

3. **Ariyadi, H. M.**, Maiya, M. P., Vallès, M., Salavera, D., and Coronas, A., *Measurement of Ammonia Absorption in New Absorbent - Preliminary Results*, Proceedings of the 28th International Conference on Efficiency, Cost, Optimization, Simulation and Environmental Impact of Energy Systems, 30 June–3 July 2015, Pau, France (Oral Presentation). ISBN: 978-2-9555539-0-9

4. **Ariyadi, H. M.**, and Coronas, A., *Analysis And Evaluation of 2,2,2-Trifluoroethanol/Ionic Liquids as New Working Pairs for Heat Transformers*, Proceeding of 9º Congreso Nacional de Ingeniería Termodinámica, 3– 5 June 2015, Cartagena, Spain (Oral Presentation). ISBN: 978-84-606-8931-7

5. **Ariyadi, H. M.**, and Coronas, A., *Simulation of Absorption Refrigeration Cycle with Ammonia Ionic Liquid Mixtures using Equation of State*, 4th International Workshop on Ionic Liquids: Advanced Energy Applications, 15–16 January 2015, Tarragona, Spain (Poster Presentation).

6. **Ariyadi, H. M.**, Maiya, M. P., Vallès, M., Salavera, D., and Coronas, A., *Preliminary Study of the Measurement of Ammonia Absorption Capacity in Ionic Liquids*, 4th International Workshop on Ionic Liquids: Advanced Energy Applications, 15–16 January 2015, Tarragona, Spain (Poster Presentation).

7. **Ariyadi, H. M.**, Albornoz, J., Quinteros-Lama, H., and Segura, H., *Barotropic Behavior in Binary and Ternary Mixtures Composed of Ionic Liquids*, International Workshop on Ionic Liquids 2014, 24–25 March 2014, Concepción, Chile (Oral Presentation).

8. Quinteros-Lama, H., **Ariyadi, H. M.**, Albornoz, J., Coronas, A., and Segura, H., *Progressive Modelling of Ionic Liquids from Minimal to Detailed Experimental Data*, International Workshop on Ionic Liquids 2014, 24–25 March 2014 Concepción, Chile (Oral Presentation).

9. **Ariyadi, H. M.,** and Coronas, A., *Analysis and Evaluation of Ammonia/Ionic Liquid Mixtures as New Working Pairs for Absorption Applications*, Workshop of Solar Absorption Refrigeration Systems Operating with Ionic Liquids, 21–22 February 2014, Chennai, India (Oral Presentation).

10. **Ariyadi, H. M.**, Coronas, A. and Bourouis, M., *Simulation Study of Heat and Mass Transfer Processes in Tubular Vertical Falling Film Absorbers Using Water-(LiBr+LiI+LiNO3+LiCl) as Working Fluid*, International Workshop on New Working Fluids for Absorption Heat Pumps and Refrigeration Systems (Eurotherm Seminar No. 100), 22–23 July 2013, Tarragona, Spain (Poster Presentation).

11. **Ariyadi, H. M.**, Salavera, D., and A Coronas, A., *Modelling of Phase Equilibria and Thermophysical Properties of Ionic Liquids and Molecular Solvents with PC-SAFT*, International Workshop on New Working Fluids for Absorption Heat Pumps and Refrigeration Systems (Eurotherm Seminar No. 100), 22–23 July 2013, Tarragona, Spain (Oral Presentation).

12. **Ariyadi, H. M.**, Salavera, D., and Coronas, A., *Performance Simulation of the Absorption Refrigeration Cycle with Some Ammonia/IL Mixtures with ASPEN Plus*, 2nd International Workshop on Ionic Liquids: Alternative Benign Materials for Renewable Energy and its Applications, 16–17 January 2013, Pune, India (Oral Presentation).

Scientific Reports

1. Albornoz, J., **Ariyadi, H.M.**, Segura, H., Coronas, A., *Report on the prediction model based upon group contribution method for thermophysical properties of ionic liquids*, FP7-People-2010-IRSES Program (NARILAR -New Working Fluids based on Natural Refrigerants and Ionic Liquids for Absorption Refrigeration, Grant Number 269321), 2015.

2. Albornoz, J., **Ariyadi, H.M.**, Segura, H., Coronas, A., *Report on the validation of the prediction model*, FP7-People-2010-IRSES Program (NARILAR -New Working Fluids based on Natural Refrigerants and Ionic Liquids for Absorption Refrigeration, Grant Number 269321), 2015

3. **Ariyadi, H.M.**, Maiya, M. P., Coronas, A., *Report on the experimental study of absorption and desorption process with the selected working pairs*, FP7-People-2010-IRSES Program (NARILAR -New Working Fluids based on Natural Refrigerants and Ionic Liquids for Absorption Refrigeration, Grant Number 269321), 2015.

Contents

List of Tables

List of Figures

Nomenclature

A	Interface area (cm^2)
C	Constant
COP	Coefficient of performance
C_p	Isobaric mass heat capacity (kJ/kg·K)
$C_{p,m}$	Isobaric molar heat capacity (kJ/kmol·K)
f	Solution mass flow ratio
G^E	Excess Gibbs energy (kJ/kmol)
H^E	Excess molar enthalpy (kJ/kmol)
h^E	Excess mass enthalpy (kJ/kg)
h	Specific mass enthalpy (kJ/kg)
Δh_{mix}	Heat of mixing (kJ/kg)
Δh_v	Enthalpy of Evaporisation (kJ/kg)
IL	Ionic liquid
l	Slope
m	Mass flow rate (kg/s)
m_f	Mass flux (g/s cm^2)
MW	Molecular weight (g/mol)
NRTL	Non-random two-liquid
P	Pressure (bar)
P_c	Critical pressure (bar)
Q	Thermal load (kW)
q	Specific thermal load (kW/kg)
R	Solution mass flowrate per unit of cooling load (kg/MW·s)
RK-EOS	Reidlich-Kwong equation of state
RTIL	Room temperature ionic liquid
S^E	Excess entropy (kJ/kmol·K)
SHX	Solution heat exchanger
T	Temperature (ºC)
T_c	Critical temperature (K)
V	Specific volume (m^3/kg)

V_m	Specific molar volume (cm^3/mol)
VLE	Vapour-liquid equilibrium
W	Mechanical work (kW)
x	Mole fraction
X	Concentration (% mass)

Subscripts

1,2, …	Component/stream number 1, 2, …
ABS	Absorber
COND	Condenser
EVAP	Evaporator
g	vapour phase
GEN	Generator
IL	Ionic liquid
l	Liquid phase
p	Solution pump
r	refrigerant
s	solution
st	strong
SHX	Solution heat exchanger
w	weak

Greek letters

ε	Heat exchanger effectiveness
γ	Activity coefficient
ρ	Density (kg/m^3)
ρ_m	Molar density (kmol/m^3)
ω	Acentric factor

Ionic Liquids

[bmim][BF_4]	1-butyl-3-methylimidazolium tetrafluoroborate
[bmim][PF_6]	1-butyl-3-methylimidazolium hexafluorophosphate
[bmim][Zn_2Cl_5]	1-butyl-3-methylimidazolium Zn_2Cl_5

Chapter 1

Introduction

1.1. Background and Justification

Absorption refrigeration system is a good known technology. The absorption systems, which can utilize renewable energy such as solar and geothermal energy or waste heat sources such as exhausts of diesel engines and industrial plants to produce cold, carries a primary energy saving, and thus emission reduction. In addition, the absorption systems contain natural refrigerant and thus, environmentally friendly and becomes a competitive alternative to the conventional mechanical-driven vapour compression refrigeration systems. In addition, as the absorption systems are thermally-driven, the absorption machine has no vibration and noise, can increase the number of hours of operation in Combined Heat Power Plant or boilers especially in summer, when the heating needs are less. Similar to the vapour compression cycle, absorption cycle is based on the cooling and heating process associated with phase changes of evaporation and condensation of refrigerant fluid at different temperatures and pressures. The working fluid consists of refrigerant and absorbent, so that the boiling temperature can be modified by changing the pressure or composition of the mixture.

A wide variety of refrigerant-absorbent combinations (both organic and inorganic) have been suggested for vapour absorption cooling systems. Most of these are two component systems. The two most common working fluids in absorption refrigeration cycle are water–LiBr and ammonia–water. In water–LiBr working fluid, LiBr solution works as absorbent and water as refrigerant. The water–LiBr absoprtion cycle is basically used for cooling applications, with the cooling

temperature above 5°C. The working pressure is vacuum in some components and the working operation condition is also limited by the crystallization of the salt. Nevertheless, the water-LiBr working fluid is non toxic and non flammable, thus safe and easy to handle and maintain.

In ammonia-water working fluid, water works as absorbent and ammonia works as refrigerant. The ammonia-water absorption cycle is used mainly for refrigeration purpose, since it can produce cold below 0°C. Being natural fluids, both are emission free and ozone friendly resulting with zero global warming potential (GWP) and ozone depletion potential (ODP). However, the characteristics of ammonia is toxic, so it is necessary to be handled carefully. In addition, the characteristics of water is volatile, thus as absorbent, it is necessary to add an additional component, rectifier, to minimize the amount of water coming to the condenser.

Some other important combinations other than ammonia-water and water-lithium bromide are CFC, HCFC and HFC refrigerants namely R21, R22 and R134a with organic absorbents such as DMF, DMETEG and DMAC. Though HCFC and HFC based systems are found to be thermodynamically superior, high GWP and chemical instability problems are major hurdles in using them for large-scale applications. Hence, finding a suitable working pair is inevitable. As a new type of fluids with a great solvent character and other interesting properties such as a good thermal stability and very low vapour pressure, ionic liquids can be excellent candidates as absorbents for absorption systems to overcome drawbacks associated with the conventional working pairs and to extend the operating range of absorption systems for different boundary conditions.

Ionic liquids, or often referred as room temperature ionic liquids (RTIL), have the character of molten salts, which are stable at room temperature [8-12]. These liquids, which usually consist of organic cation and inorganic anion, have negligible vapour pressure and thermally stable to temperatures well above those in vapor compression refrigeration systems [8]. In addition, the thermophysical properties of ionic liquids can be adjusted and controlled by the selection and combination of the cation and anion pair. This has led to the concept of ionic liquids

being "designer solvents" [12-13]. Although for this to be achieved requires not just a post hoc rationalization of the ionic liquids' properties, but the ability to predict them [12], these unique characteristics make ionic liquids to be a potential candidate as a novel absorbent for absorption system eliminating the drawbacks of conventional working fluids.

The unique charachteristic of ionic liquids have made these liquids become interesting candidate as absorbent in combination with refrigerants to constitute new working pairs for absorption cycle. Compared with organic solvents, the advantages of IL are mainly embodied in the following aspects [14].

1. Most ionic liquids exist as liquid at a wide range around room temperature. The boiling points of ionic liquids are much higher than those of refrigerants because of the ignorable vapour pressure. In the generation process, the refrigerant can be easily separated from ionic liquid with high purity in the cycle.

2. The heat capacity of ionic liquid solution is small, which is beneficial in improving the cycle efficiency.

3. Solubility with inorganic or organic species and the affinity with refrigerants are good, which is in favour of enhancing the performance.

4. Ionic liquids have high chemical and thermal stability, high thermal decomposition temperature, and are non-flammable.

5. The chemical and physical properties of ionic liquids can be adjusted by the design of anion and cation.

To date, many researchers have investigated the thermophysical properties of working pairs consisting of ionic liquids and common refrigerants, such as water, ammonia, alcohol, and HFCs, for absorption cycle [1-8, 15-18]. In the case of ammonia refrigerant, the use of ionic liquids (ILs) as an alternative to water as absorbent in the absorption refrigeration cycle gives some advantages such as elimination of the rectification process in ammonia/water systems. The use of ionic liquids as absorbent with ammonia as refrigerant in the absorption refrigeration cycle has been discussed by researchers in recent years [1−7]. According to them, one of the main advantages in comparison with a conventional ammonia/water absorption

refrigeration cycle is that the ammonia-ionic liquid absorption refrigeration systems may not require the costly rectifier unit needed for traditional ammonia/water system due to there being practically no vapour pressure for the absorbent.

Although the use of ionic liquids as absorbent for ammonia refrigerant looks very promising, the research on both thermodynamic properties and application of ammonia/ionic liquid mixtures for absorption cycle applications is still remains scarce. For instance, one of the most important properties necessary to study absorption cycle's working fluids, solubility data of ammonia/ionic liquid mixtures are only limited by those measured by Yokozeki and Shifflet [1-2] and Li et al. [3]. In addition, most of ionic liquids measured in their research were imidazolium based ionic liquids. Furthermore, investigations related to the application of ammonia/ionic liquid working fluids in absorption refrigeration systems are so far limited to the theoretical studies and computational simulation. The experimental studies on the absorption refrigeration systems working with ammonia/ionic liquid fluids are so far not reported in the literature.

Therefore, it is necessary to extend the study of ammonia/ionic liquid mixtures as working fluid for absorption cycle applications, not only with ammonia/ionic liquid mixtures available in the literature, but it is also necessary to study, develop, and propose other ionic liquids that may be suitable as absorbent for ammonia refrigerant for absorption cycle applications.

1.2. Research Objectives

The main objective of this research was to study the performance and the feasibility of ionic liquids as absorbent for ammonia refrigerant in absorption refrigeration systems. Not only studying the ammonia/ionic liquid mixtures available in the literature, this research also covered the new selected ammonia/ionic liquid mixtures which consist of non-imidazolium based ionic liquids proposed by our research group. These new selected ammonia/ionic liquid mixtures present better properties particularly solubility with ammonia refrigerant [19]. Theoretical and experimental study on ammonia/ionic liquid working fluids have been conducted to

provide information in the operation and efficiency of absorption refrigeration systems working with ammonia/ionic liquid pairs.

To reach the above mentioned objective, the more specific objectives were raised as follows

1. To review on the absorption refrigeration technologies and working fluids with emphasize on ammonia/ionic liquid working pairs. The basic criteria for working fluids selection were also reviewed.

2. To estimate the performance of absorption systems using ammonia/ionic liquid working fluids using limited data, particularly solubility.

3. To select an appropriate model to describe the vapour-liquid equilibrium properties of the binary systems of ammonia/ionic liquid mixtures to correlate the thermophysical properties needed to investigate the thermal performance of the absorption systems based on ammonia/ionic liquid working fluids.

4. To analyse of the performance of absorption refrigeration systems using various ammonia/ionic liquid working pairs by means of thermodynamic simulations using the software program ASPEN Plus. The ammonia/ionic liquid mixture studied were taken from open literature.

5. To analyse of the performance of absorption refrigeration systems using new selected ammonia/ionic liquid working pairs using Engineering Equation Solver (EES). The use of EES enables to understand well the problems that might occurs in oftware program ASPEN Plus.

6. To design and construct a setup to measure the absorption capacity of the ammonia vapour in ionic liquids in a pool type absorber and analyse the measurement result.

1.3.   Thesis Structure

This thesis was composed in following chapters:

Chapter 1 is dedicated to explain the background and justifications of this research that raise to the motivation and objectives of this thesis. Moreover, the research projects that involved in this thesis are also described.

Chapter 2 presents an overview of the absorption refrigeration technologies. In this chapter, the basic description of the absorption refrigeration systems was described in comparison with mechanical vapour compression refrigeration systems. Furthermore, the operation principle of basic absorption refrigeration processes, the working fluid mixtures commonly used in the absorption refrigeration system, and the main requirements of the working mixtures were analyzed. The new working fluid mixtures based on ionic liquid absorbent for absorption refrigeration application were also discussed. Finally, methods used for *COP* evaluation using limited data, particularly solubility data for working mixture pre-selection were described and applied.

Chapter 3 of this thesis is aimed to study the ability of different model to calculate the vapor-liquid phase equilibrium of ammonia/ionic liquid mixtures and to select an appropriate model used to correlate the thermophysical properties needed to investigate the thermal performance of the absorption systems based on ammonia/ionic liquid working fluids. The models studied in this chapter include Non-Random Two-Liquids, Redlich-Kwong-Soave cubic equation of state, and Perturbed-Chain Statistical Associating Fluid Theory (PC-SAFT). In addition, a model based on groups contribution methods UNIFAC was also studied. Using selected thermodynamic method, the PTx diagram were built and the *COP* of the systems were estimated.

Chapter 4 provides the performance analysis of absorption refrigeration systems using various ionic liquids as absorbents and ammnonia as a refrigerant. The thermodynamic performance simulation of the single effect absorption refrigeration cycle with ammonia/ionic liquid pairs were studied and analysed in this chapter. The simulation were carried out using ASPEN Plus using the experimental VLE data available in the literature.

Chapter 5 presents the performance analysis of absorption refrigeration systems using new selected ionic liquids as absorbents and ammnonia as a

refrigerant. The thermodynamic performance simulation of single effect absorption refrigeration cycle with new selected ammonia/ionic liquid pairs were simulated using Engineering Equation Solver (EES), by using the experimental VLE data measured by our research group. Moreover, the effect of the viscosity of ionic liquids on the absorption systems was also studied.

Chapter 6 is aimed to the development of a setup and to measure the absorption capacity of ammonia vapour in ionic liquids in a pool type absorber. This investigation is essential in order to identify the most suitable ionic liquid as an absorbent for ammonia refrigerant. The detail of the methodology and experimental setup were explained in this chapter and measurement results of absorption capacity of ammonia into ionic liquid are discussed in this chapter.

Chapter 7 summarizes the major findings in this thesis and gave an overview of the further work required.

1.4. Description of the Projects Involved in the Thesis

This work was carried out within the following projects

1. FP7-People-2010-IRSES Programme (PIRSES-GA-2010-269321) entitled "New Working Fluids based on Natural Refrigerant and Ionic Liquids for Absorption Refrigeration – NARILAR", coordinated by Applied Thermal Engineering Research Group (CREVER) of Universitat Rovira I Virgili with the participation of Universidade de Lisboa (Portugal), Universidad de Concepción (Chile), Indian Institute of Technology Madras (India), Council of Scientific and Industrial Research (India) and Anna University (India) (2011-2015).

2. PRI-PIBIN-2011-1177 - Solar Absorption Refrigeration Systems Operating with Ionic Liquids as Absorbents and Ammonia as Refrigerant (SARSIL project) coordinated by Applied Thermal Engineering Research Group (CREVER) of Universitat Rovira I Virgili in collaboration with the Indian Institute of Technology Madras (India) (2012-2014).

3. "Development of New Working Fluids, Components and Configurations for High Performance Absorption Heat Pumps-AHP2", in cooperation between Universitat Rovira I Virgili and Universidad de Vigo.

The main goal of this project is to develop new working fluids and components for absorption heat pumps and refrigeration systems that enlarge the operation range, improve the performance and increase the energy efficiency in new configurations. These new working fluids to be developed are the mixtures of ionic liquid based absorbent and natural refrigerants, such as ammonia, carbon dioxide, and water.

The project involves different research groups with specific objectives which are developed in according to their expertise and facilities available in each research group, but that are bounded among them. To reach the global objective, the following tasks were carried out

1. Design of ionic liquids taking into consideration the desirable properties of absorbents to be used in absorption refrigeration systems.

2. Synthesize and characterisation of ionic liquids.

3. Measurement of thermophysical properties of pure ionic liquids necessary for absorption refrigeration applications.

4. Measurement of thermophysical properties of ionic liquid and ammonia mixtures necessary for absorption refrigeration applications.

5. Development of thermodynamic models to accurately estimate and predict the thermodynamic and transport properties.

6. Analysis of the performance of absorption refrigeration systems using various ionic liquids as absorbents and ammonia as a refrigerant by means of thermodynamic simulations.

7. Design of components and configurations of absorption refrigeration systems.

1.5.   References

[1]   Yokozeki, A., Shiflett, M.B., Vapor–liquid equilibria of ammonia + ionic liquid mixtures. *Applied Energy*. 2007; 84; 1258-1273

[2] Yokozeki, A., Shiflett, M.B., Ammonia solubilities in room-temperature ionic liquids, ammonia solubilities in room-temperature ionic liquids. *Ind. Eng. Chem. Res*. 2007; 46; 1605-1610

[3] Li, G., Zhou, Q., Zhang, X., Wang, L., Zhang, S., Lia, J., Solubilities of ammonia in basic imidazolium ionic liquids. *Fluid Phase Equilibria*. 2010 ;297(1); 34–39

[4] Ruiz, E, Ferro, V.R., de Riva, J., Moreno, D., Palomar, J., Evaluation of ionic liquids as absorbents for ammonia absorption refrigeration cycles using COSMO-based process simulations. *Applied Energy*. 2014; 123; 281–291

[5] Palomar, J., Gonzalez-Miquel, M., Bedia, J., Rodriguez, F., Rodriguez, J. J., Task-specific ionic liquids for efficient ammonia absorption. *Separation and Purification Technology*. 2011; 82; 43–52

[6] Bedia. J., Palomar, J., Gonzalez-Miquel, M., Rodriguez, F., Rodriguez, J. J., Screening ionic liquids as suitable ammonia absorbents on the basis of thermodynamic and kinetic analysis. *Separation and Purification Technology*. 2012; 95; 188–195

[7] Kotenko. O., Moser, H., and Rieberer, R., Thermodynamic Analysis Of Ammonia/Ionic Liquid Absorption Heat Pumping Processes. *Proc. Int. Sorption Heat Pump Conf*. 2011; 89-796

[8] Kim, Y. J., Kim, S., Joshi, Y. K., Fedorov, A. G., and Paul, A., Kohl, P. A., Thermodynamic analysis of an absorption refrigeration system with ionic-liquid/refrigerant mixture as a working fluid. *Energy*. 2012; 44; 1005-1016

[9] Hayes, R., Warr, G. G., and Atkin, R., Structure and Nanostructure in Ionic Liquids. *Chem. Rev*. 2015; 115; 6357−6426

[10] Ghandi, K., A Review of Ionic Liquids, Their Limits and Applications, *Green and Sustainable Chemistry*. 2014; 4; 44-53

[11] Welton, T., Room-temperature ionic liquids: solvents for synthesis and catalysis, *Chemical Reviews*, 1999; 99(8); 2071–2083

[12] Hallet, J. P., Welton, T., Room-temperature ionic liquids: solvents for synthesis and catalysis.2, *Chem. Rev*. 2011; 111; 3508–3576

[13] Freemantle, M., Designer Solvents: Ionic liquids may boost clean technology development. *Chem. Eng. News*. 1998; 76 (13); 32

[14] Zheng, D., Dong, L., Huang, W., Wu, X., Nie, N., A review of imidazolium ionic liquids research and development towards working pair of absorption cycle, *Renewable and Sustainable Energy Reviews*, 2014, 37, 47–68

[15] Shiflett M.B., Yokozeki, A., Solubilities and diffusivities of carbon dioxide in ionic liquids: [Bmim][PF6] and [Bmim][BF4], *Ind. Eng. Chem. Res*., 2004; 44; 4453–64.

[16] Kim, K.S., Bae-Kun Shin, B. K., Lee, H., and Ziegler, F., Refractive index and heat capacity of 1-butyl-3-methylimidazolium bromide and 1-butyl-3-methylimidazolium tetrafluoroborate, and vapor pressure of binary systems for 1-butyl-3-methylimidazolium bromide + trifluoroethanol and 1-butyl-3-

methylimidazolium tetrafluoroborate + trifluoroethanol. *Fluid Phase Equilibria*, 2004, 218, 215–220

[17] Wang, J., Zheng, D., Fan, L., and Dong, L., Vapor pressure measurement for the water + 1,3-dimethylimidazolium chloride system and 2,2,2-trifluoroethanol + 1-ethyl-3-methylimidazolium tetrafluoroborate system. *J. Chem. Eng. Data,* 2010, 55, 2128–2132

[18] Currás, M. R., Costa Gomes, M. F., Husson, P., Padua, A. A. H., and Garcia, J., Calorimetric and volumetric study on binary mixtures 2,2,2-trifluoroethanol + (1-butyl-3-methylimidazolium tetrafluoroborate or 1-ethyl-3-methylimidazolium tetrafluoroborate). *J. Chem. Eng. Data*, 2010, 55, 5504–5512

[19] Cerra-Manjarres, A., PhD Thesis, Universitat Rovira i Virgili, Spain, 2015

Chapter 2

Overview of the Absorption Refrigeration Technologies and Working Fluids

2.1. Introduction

In this chapter an overview of the absorption refrigeration technologies is presented. The basic description of the absorption refrigeration systems is described in comparison with mechanical vapour compression refrigeration systems. Following a discussion of the operation principle of basic absorption refrigeration processes, the working fluid mixtures commonly used in the absorption refrigeration system and the main requirements of the working mixtures will be analyzed. The new working fluid mixture based on ionic liquid as an absorbent for absorption refrigeration application will be discussed. Finally, methods used for *COP* evaluation using limited data for working mixture pre-selection are described.

2.2. Absorption Refrigeration System

Absorption refrigeration system is a system that uses a heat source (e.g., solar energy, a fossil-fuelled flame, waste heat from factories, or district heating systems) which provides the energy needed to drive the cooling process [1]. This system operates based on absorption process rather than compression process [2].

Similar to vapour compression system, the cooling effect is produced through evaporation process of the refrigerant in the evaporator and the heat absorbed in the evaporator is released to the atmosphere via the condenser. The vapour absorption

refrigeration system also comprises of all the processes taking place in vapour compression refrigeration system such as condensation, expansion, evaporation, and compression.

Although both absorption system and compression system have similarities in producing cooling effect in the evaporator, they have some differences. The differences of absorption system and compression system can be schematically compared in Figure 2.1.
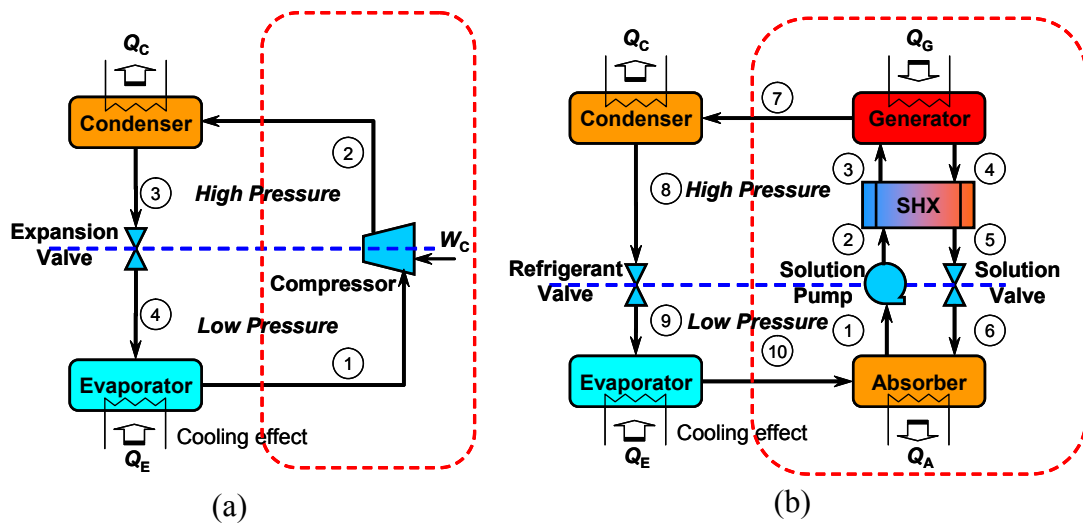
Figure 2.1. Schematic diagram of (a) mechanical vapour cooling compression system and (b) absorption cooling systems

As it can be seen in Figure 2.1, one of the major differences between mechanical vapour compression system and absorption system is the method of transferring the refrigerant from the lower pressure system to the higher pressure system. In the vapour compression system, the refrigerant is transferred from the lower pressure system to the higher pressure systems by mechanical compressor. The mechanical compressor sucks the refrigerant vapour and compresses it to the high pressure. In addition, the mechanical compressor also creates the refrigerant flow in the whole compression cycle. In the absorption system, the refrigerant is transferred from the lower pressure system to the higher pressure systems through a mechanism of absorption and desorption process carried out by two different devices called as absorber and generator (desorber), respectively, together with solution pump, solution valve, and solution heat exchanger. Therefore the compressor in the vapour compression system is replaced by the absorber and generator loop or it can be called

as "chemical compressor". In addition, the refrigerant flow in the whole absorption cycle is created by absorption process of the refrigerant in the absorber by the solution called absorbent and transported to the generator using solution pump. The absorption process at the absorber and desorption process at the generator make it possible to use a solution pump with low power input to increase the pressure between the condenser and the evaporator [3].

The presence of the absorption and desorption devices replacing the mechanical compressor has a consequence in the increase the overall system volume. However the displacement volume and power consumption for compression of the liquid in absorption refrigeration system are much smaller as compared with vapour compression systems.

Another major difference between the vapour compression and vapour absorption cycle is the method in which the energy input is given to the system. In vapour compression systems, the energy input needed to operate the cycle is provided in the form of mechanical work to drive the compressor. This mechanical work input usually comes from the electric motor run by the electricity. In the absorption systems, the energy input needed to operate the cycle is provided in the form of the heat to separate the refrigerant from the solution in the generator. This heat source can be supplied from renewable energy such as solar, geothermal energy, and biomass or waste heat sources such as exhausts on diesel engines and industrial plants [4]. The heat can also be created by other sources like natural gas, kerosene, heater, etc. though these sources are usually used only in the small systems [2]. As the absorption refrigeration systems are operated using heat source and the only component of this system with moving mechanical parts is the liquid pump, these systems has very lower vibration and thus lower noise with no lubrication needed than those of mechanical compression systems.

Another difference between the vapour compression and vapour absorption cycle is the working fluid used. In vapour compression systems, the working fluid used is only refrigerant fluid. Most vapour compression systems commonly use chlorofluorocarbon refrigerants (CFCs) because of their excellent thermophysical properties. It is through the restricted use of CFCs, due to depletion of the ozone layer that will make absorption systems more prominent [4]. In absorption

refrigeration system, the working fluid used is usually a pair of absorbent and refrigerant fluid. The two most common working fluids in absorption refrigeration cycle are water/LiBr and ammonia/water. In water/LiBr working fluid, water works as refrigerant and aqueous LiBr solution works as absorbent and in ammonia/water system ammonia works as refrigerant and water works as absorbent.

2.2.1. Principle of Absorption Refrigeration Process

Absorption refrigeration system basically consists of four main components, namely absorber, desorber (generator), condenser, and evaporator. In addition, it requires working fluid which consists of refrigerant and absorbent. Other supporting components necessary for the basic absorption refrigeration cycle are solution pump, solution valve, refrigerant valve, and solution heat exchanger (SHX). In this system, the refrigerant undergoes a phase change in the condenser and evaporator, and the absorbent solution undergoes a concentration change in the absorber and the generator.

The basic absorption refrigeration process can be schematically drawn in Dühring diagram as shown in Figure 2.2. The solution leaving from absorber (stream 1) is moved to the higher pressure system by solution pump, creating high pressure cold stream (stream 2). Ideally the solution leaving the absorber is in saturation condition taking into account the absorber pressure (lower pressure) and temperature. This solution is rich in refrigerant fluid therefore it can be named as rich solution.

The high pressure cold stream is then preheated in the solution heat exchanger using the heat transferred from the solution leaving the generator. The rich solution leaving the solution heat exchanger (stream 3) then enters the generator. In the generator, vaporization/desorption process takes place creating refrigerant vapour and poor solution. The desorption process between the absorbent and refrigerant is usually endothermic process, therefore to undergo this process the heat needs to be supplied from the external source such as solar, geothermal energy, and biomass or waste heat sources such as exhausts on diesel engines and industrial plants (Q_{GEN}).

The refrigerant vapour leaving the generator (stream 7) comes to the refrigerant loop and enters the condenser. In the condenser, condensation process takes place and all refrigerant is condensed into saturated liquid corresponds to the

condenser pressure (higher pressure) and temperature. The heat released from this condensation process is discharged to the atmosphere (Q_{COND}) through a cooling system at ambient temperature.
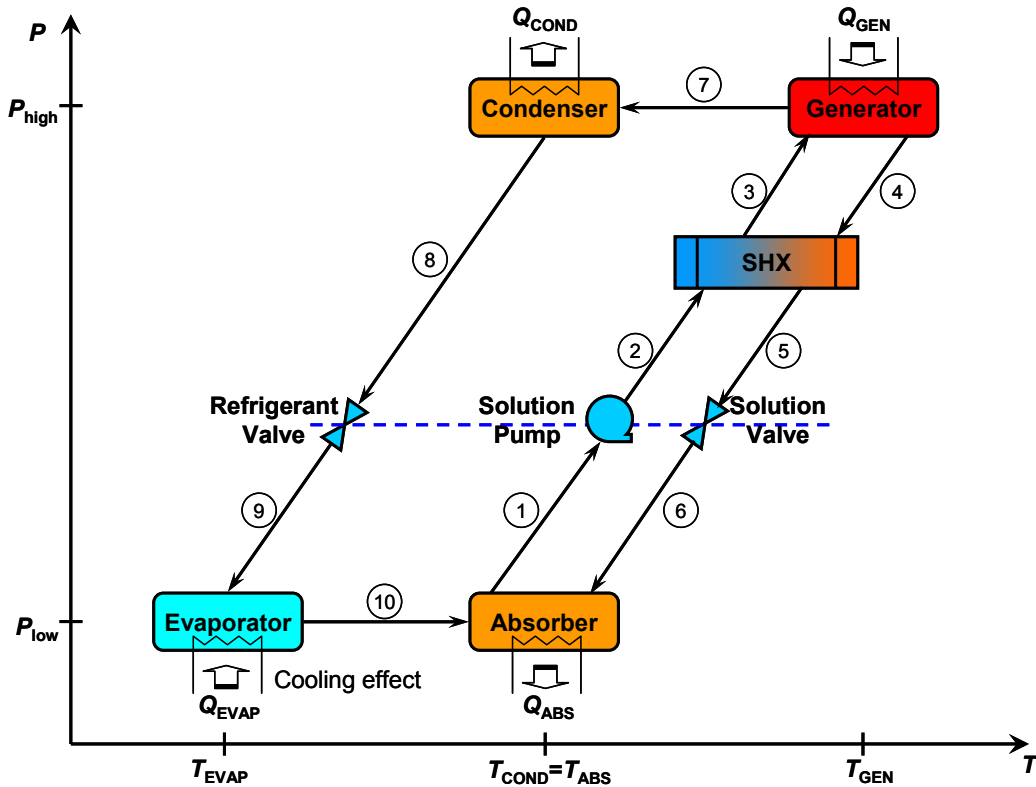
Figure 2.2. Schematic diagram of an absorption refrigeration system in Dühring diagram

The saturated liquid refrigerant leaving from the condenser (stream 8) moves to the evaporator through refrigerant valve to reduce its pressure to the evaporator pressure (low pressure). This expansion process in the refrigerant valve is an isenthalpic expansion. The refrigerant leaving the refrigerant valve (stream 9) enters the evaporator and the evaporation process takes place.

As the saturation temperature of the refrigerant at lower pressure is much lower than room temperature, the heat from desired cooling chamber (Q_{EVAP}) is absorbed to the evaporator creating the evaporation process to the refrigerant, and therefore gives cooling effect to the cooling/refrigeration chamber.

Back to the solution loop in the generator, the solution leaving the generator (stream 4) has low concentration in refrigerant and thus it is called as poor solution.

As the stream leaving from the generator has high temperature, it can be useful to utilize the heat of this stream to pre-heat the rich solution before entering the generator. The heat from the solution leaving the generator is transferred to the rich solution entering the generator by means of solution heat exchanger (SHX).

The poor solution leaving the solution heat exchanger moves to the absorber through solution valve to reduce its pressure to the lower pressure. Similar with the expansion process in the refrigerant valve, the expansion process in the solution valve is also an isenthalpic expansion. The poor solution leaving the solution valve (stream 6) enters the absorber to undergo the absorption process.

The poor solution enters the absorber is in sub-cooled condition corresponds to its temperature and absorber pressure. Therefore, when the vapour refrigerant (stream 10) enters the absorber, the refrigerant vapour is absorbed by the solution. As the absorption process takes place, the mixing process also takes place. The mixing process between absorbent and refrigerant is usually exothermic process, and therefore during the absorption process the heat is released from the solution and the solution temperature increases. To maintain the absorption process remains take place at desired temperature (absorber temperature), the heat of absorption needs to be dissipated to the ambient. This heat is dissipated to the ambient (Q_{ABS}) by means of cooling system at ambient temperature.

Once the solution reach its saturation condition corresponds to absorber pressure and temperature, the solution is unable to absorb more vapour refrigerant. This solution then leaves the absorber to the generator and the solution loop is completed.

One of the key parameters to evaluate the performance of absorption refrigeration cycle is what so called as coefficient of performance (*COP*) which is defined as the ratio of available useful cooling output of the system to the total power supplied to the system. The *COP* can be mathematically written as

$$COP = \frac{Q_{EVAP}}{Q_{GEN} + W_p} \qquad (2.1)$$

where Q_{EVAP} and Q_{GEN} are the cooling output of the evaporator and the heat input of the generator, respectively and W_p is the working input of the solution pump.

The work input of the solution pump W_p is negligible relative to the heat input in the generator therefore the pump work is usually neglected for the purposes of analysis.

The process taking place in each component in the absorption refrigeration system is summarized in Table 2.1.

Table 2.1. Main components and processes in absorption refrigeration system

Components	States	Process
Absorber	$6,10 \rightarrow 1$	Absorption of refrigerant into absorbent Heat of absorption release to ambient
Solution Pump	$1 \rightarrow 2$	Isentropic solution pressurization
Solution Heat Exchanger	$2 \rightarrow 3$ and $4 \rightarrow 5$	Regenerative pre-heating
Generator	$3 \rightarrow 4,7$	Vaporization of refrigerant from solution Heat of desorption induction from heat source
Condenser	$7 \rightarrow 8$	Refrigerant condensation Heat rejection to ambient
Evaporator	$9 \rightarrow 10$	Refrigerant vaporisation Heat absorption from the device/chamber
Solution Valve	$5 \rightarrow 6$	Isenthalpic solution expansion
Refrigerant Valve	$8 \rightarrow 9$	Isenthalpic refrigerant expansion

2.3.   Conventional Working Fluid Mixtures

Similar to the compression cycle, absorption cycle is based on the cooling and heating process associated with phase changes of evaporation and condensation of refrigerant fluid at different temperatures and pressures. The working fluid in absorption cycle consists of refrigerant and absorbent, so that the boiling temperature of the working fluid can be modified by changing the pressure or composition of the mixture.

The performance and efficiency of the absorption refrigeration systems are also determined a large degree by the properties of the working fluids [5]. Both the first cost and the operating cost of an absorption machine are strongly dependent on the working fluid properties [6]. Therefore it is important to select the best candidate

among some candidates of ionic liquids as an absorbent for ammonia refrigerant in the absorption systems in order to get the best performance and efficiency in absorption systems.

Generally, a good absorption refrigeration system fluid absorbent should meet a number of important requirements, which are [4-10]:

1. *Absence of solid phase*

A good refrigerant–absorbent pair should not form a solid phase over the range of composition and temperature to which it will be operated. The presence of solid phase can block the system components and shorten the life time of the equipment and thus reduce the overall performance.

2. *Large boiling temperature difference*

A good absorbent should be less volatile than the refrigerant so that it can be separated easily by heating. The elevation of boiling (the difference in boiling point between the pure refrigerant and the mixture at the same pressure) should be as large as possible.

3. *Good affinity and solubility*

The absorbent should have a strong affinity with the refrigerant under the conditions in which absorption takes place. This affinity allows less absorbent to be circulated for the same refrigerating effect, and therefore, sensible heat losses are less. Also, a smaller liquid heat exchanger is required to transfer heat from the absorbent to the pressurised refrigerant–absorbent solution. A disadvantage is that extra heat is required in the generator to separate the refrigerant from the absorbent. Thus ideally, the absorbent should have strong affinity with the refrigerant at low temperature (i.e. absorber temperature) yet have weak affinity with the refrigerant at high temperature (i.e. generator temperature)

4. *Favorable transport properties*

Transport properties that influence heat and mass transfer, e.g., viscosity, thermal conductivity, and diffusion coefficient should be favorable. In addition, viscosity plays an important role in the absorption refrigeration systems. Kim et al. [2] reported that higher viscosity of absorbent can cause an increased pressure drop in the compression loop, which would result in larger pumping power or larger pipes and system volume.

5. *Moderate operating pressure*

Moderate operating pressures should be used in order to avoid the use of heavy walled equipment and reduce the electrical power required to pump the fluids from the low pressure side to the high pressure side. Also, very low pressure (vacuum) will require the use of large volume equipment and special means of reducing pressure drop in the refrigerant vapour flow. Moderate operating pressure also allows the systems to be extended into multiple effects configuration without any problem of pressure, which gives rise to a considerable improvement of the heat ratio.

6. *High heat of vaporization*

The heat of vaporization of the refrigerant should be high in order to obtain a low circulation factor and consequently small irreversible losses. However, this gives rise to a high pressure ratio, which at high working pressure leads to a high pump energy requirement. Besides, in the case of a weak deviation from Raoult's Law, this leads to low working medium concentrations in the mixture, resulting in a high circulation factor.

7. *Ratio of enthalpies of dilution and evaporation*

The ratio of enthalpies of dilution and evaportaion should be low, preferably negative, for a single effect system. However, for a multiple effect system this value should not be too low in order to avoid too high a generator temperature.

8. *Good thermal and chemical Stability*

Good chemical stability is required to avoid the undesirable formation of gases, solids or corrosive substances. In addition, high thermal stability is required to prevent the decomposition of ions.

9. *Non-corrosive*

The fluids should be non-corrosive in order to reduce the maintenance cost of the system. If the fluids are corrosive, corrosion inhibitors should be used, which may influence the thermodynamic performance of the equipment and increase the maintenance cost.

10. *Safety*

Ideally, the fluids must be non-toxic and non-inflammable.

11. Economically feasible

Good working fluid should be low cost and economically feasible.
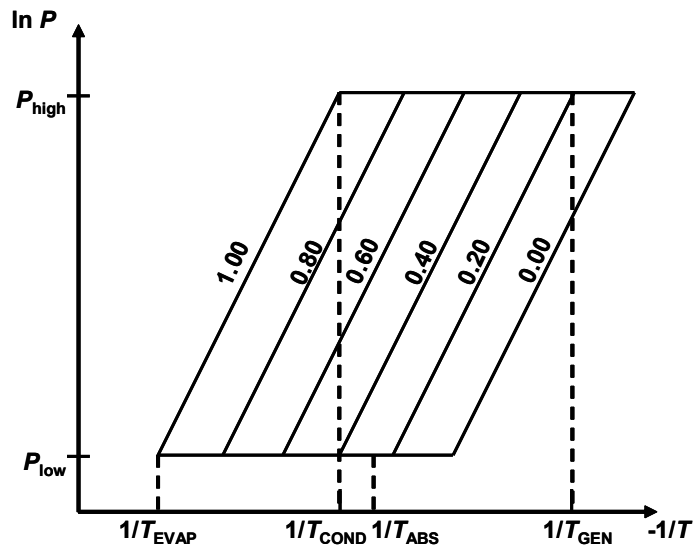
(a)
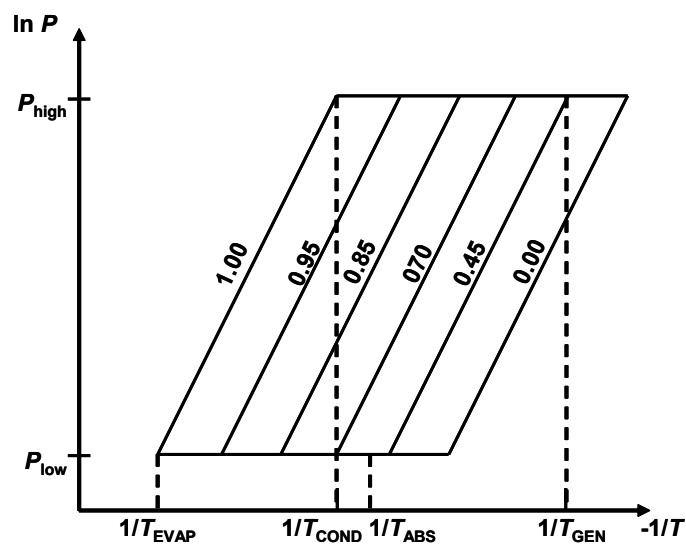
(b)

Figure 2.3. Schematic of Dühring diagram with working fluids: (a) having uniform vapour pressure distribution and (b) having non-uniform vapour pressure distribution

Moreover, in terms of refrigerant concentration in the absorbent-refrigerant mixture, it is interested to note in the Dühring diagram that the vapor pressure curves

at constant refrigerant mass concentrations distributed uniformly between the vapor curves of the pure refrigerant and pure absorbent are more desirable rather than those distributed non-uniformly in the whole range of mass concentration in order to have smaller solution mass flow ratio. The comparison of working fluid with uniform distribution and with non-uniform working fluid can be seen in Figure 2.3.

From Figure 2.3 it can be seen that at the same operation conditions working fluid mixtures with uniform vapour pressure distribution line have more refrigerant mass concentration in absorber-generator loop in comparison with working fluid mixtures with non-uniform vapour pressure distribution line. Therefore, the working fluid mixtures with uniform vapour pressure distribution line have lower solution flow rates than the fluid mixtures with non-uniform vapour pressure distribution line [11].

A wide variety of refrigerant/absorbent combinations (both organic and inorganic) have been suggested for vapour absorption cooling systems. Most of these are two component systems. The two most common working fluids in absorption refrigeration cycle are water/LiBr and ammonia/water. In water/LiBr working fluid, LiBr solution works as absorbent and water as refrigerant. The water/LiBr absoprtion cycle is basically used for cooling applications, with the cooling temperature above 5°C. The working pressure is vacuum in some components and the working operation condition is also limited by the crystallization of the salt. Nevertheless, the water/LiBr working fluid is non toxic and non flammable, thus safe and easy to handle and maintain.

In ammonia/water working fluid, water works as absorbent and ammonia works as refrigerant. The ammonia/water absorption cycle is used mainly for refrigeration purpose, since it can produce cold below 0°C. Being natural fluids, both are emission free and ozone friendly resulting with zero global warming potential (GWP) and ozone depletion potential (ODP). However, the characteristics of water is volatile, thus as absorbent, it is necessary to add an additional component, rectifier, to minimize the amount of water coming to the condenser.

Some other important combinations other than ammonia/water and water/lithium bromide are CFC, HCFC and HFC refrigerants namely R21, R22 and R134a with organic absorbents such as DMF, DMETEG and DMAC [4]. Though

HCFC and HFC based systems are found to be thermodynamically superior, high GWP and chemical instability problems are major hurdles in using them for large-scale applications. Hence, finding a suitable working pair is inevitable. As a new type of fluids with a great solvent character and other interesting properties such as a good thermal stability and very low vapour pressure, ionic liquids can be excellent candidates as absorbents for absorption systems to overcome drawbacks associated with the conventional working pairs and to extend the operating range of absorption systems for different boundary conditions.

2.3.1. Ammonia/Water

Ammonia/water mixture as a working fluid for refrigeration systems have been used since the mid of 19th century [12]. Since then, the use of ammonia/water working fluid has been extended for residential and commercial cooling and heating purposes.

Ammonia/water working fluid does not have any solid phase in wide range of temperature and pressure for absorption operation conditions thus free from crystallization problems. In addition, this working fluid is also thermally and chemically stable for a wide range of temperature and pressure condition for absorption refrigeration systems. High enthalpy of vaporization (1262 kJ/kg at 0ºC) which is necessary for efficient performance and compact size of the system and low freezing point of ammonia (-77ºC) which is enable to be applied for subzero temperature applications have made this compound becomes more desirable as refrigent. Being natural fluids, both are emission free and ozone friendly resulting with zero global warming potential (GWP) and ozone depletion potential (ODP). However absorption systems with ammonia/water working fluid require high activation temperatures (> 110ºC) to keep the refrigerant cooling capacity at the desired low evaporation temperatures and need high pressure as the vapour pressure of ammonia is relatively high. For instance, an evaporator temperature of 0°C corresponds to the saturation pressure of ammonia of 5.16 bar and a condenser temperature of 30ºC corresponds to the saturation pressure of water of 11.67 bar. The high refrigerant vapour pressure is the main reason why multiple effects of

absorption systems using ammonia/water are not available [13]. Thermal properties of ammonia/water mixture and their correlations could be found in literature [14-19]

Moreover, since the characteristics of water is volatile, thus, as absorbent, it is necessary to add an additional component, rectifier, to minimize the amount of water entering the condenser. Without a rectifier, the water would accumulate in the evaporator and offset the system performance. The use of a rectifier, which size increases reducing the evaporation temperature and thus increasing the generation temperature, and the fact that the refrigerant vapor coming to the condenser is not pure ammonia significantly affects the performance of the cycle with ammonia/water working fluid [13]. In addition, the characteristics of ammonia is toxic, so it is necessary to be handled carefully. There are other disadvantages such as its high corrosive action to copper and copper alloy [4].

The typical heat temperature input for single-effect ammonia/water absorption refrigeration cycle is between 120ºC and 132ºC with an approximate coefficient of performance of 0.9 [20]

2.3.2. Water/LiBr

Water/lithium bromide (water/LiBr) mixture as a working fluid for refrigeration systems have been used since around 1930 [4,21]. Since then, the use of water/lithium bromide working fluid has been extended for residential and commercial cooling and heating purposes [22].

Water/lithium bromide working fluid presents excellect characteristics such as the non-volatility of the absorbent (LiBr) and the high enthalpy of vaporization of refrigerant (water). The non-volatility of LiBr makes the absorption systems do not require rectification column as the refrigerant vapour coming from the generator has no absorbent content. The very high enthalpy of vaporization of water (2489 kJ/kg at 5ºC) is also one of the advantages of water/LiBr working fluid for efficient performance of the system. There are other advantages of water/LiBr such as non-toxic and high affinity between the absorbent and refrigerant.

However, crystallizations form when the mass fraction of the salt LiBr exceeds the solubility limit. This crystallization of LiBr can block the system components and thus shorten the life time of the equipment. The freezing point of

water is 0°C and thus restricts the use of the absorption systems limited to temperatures higher than 0°C. In addition, the vapour pressure of water is very low and thus it is necessary to operate the systems at sub-atmospheric conditions. For instance, an evaporator temperature of 5°C corresponds to the saturation pressure of water of 0.8726 kPa (0.009 atm) and a condenser temperature of 30°C corresponds to the saturation pressure of water of 4.246 kPa (0.042 atm). The low working pressure result that the equipments must be completely sealed. In addition, the low working pressure of water/LiBr absorption systems makes it possible to extend its application into multiple-effect systems. However, one should be careful in design of the systems due crystallisation limit of the solution. In addition, water/LiBr solution itself is highly aggressive to many metals including carbon steel and copper in the presence of dissolved oxygen [20]. Typical high operating temperatures are between 120 and 170°C with an approximate system efficiency ranging between 0.9 and 1.3 [20].

2.3.3. Other Working Fluids Based on Ammonia Refrigerant

Although not very common in comparison with ammonia/water working pair, some alternative absorbents for ammonia refrigerant have been investigated in order to improve the performance of ammonia-based absorption systems and to eliminate the drawbacks of ammonia/water absorption refrigeration systems such as the necessary of rectification column. Some of working fluids have been proposed for ammonia refrigerant for absorbent refrigeration systems, such as ammonia/(water+LiBr), ammonia/LiNO$_3$, ammonia/(LiNO$_3$+water), and ammonia/NaSCN, etc.

1. Ammonia/(water+LiBr)

The ternary systems ammonia/(water+LiBr) has been experimentally studied by Mclinden et al [22]. They used mass ratio of water and LiBr set at 48:52. Their results showed that the *COP* of the absorption heat pump operating with an ammonia/(water+LiBr) ternary mixture was about 0.05 lower than with conventional ammonia/water system. In addition, several factors indicated that the refrigerant

vapor entering the rectifier had significantly lower H_2O content with the ternary system.

2. Ammonia/LiNO$_3$

The use of ammonia/LiNO$_3$ as working fluid has been proposed in order to remove the necessary of rectification process. Based on simulation and theoretical study, this solution can produce cold at temperatures lower than 0 °C and offers a better *COP* than the ammonia/water solution [24-26]. However, the ammonia/LiNO$_3$ solution has higher viscosity than that of ammonia/water which may affect the overall heat transfer coefficient of the components.

Although theoretical study showed that the *COP* of absorption systems working with ammonia/LiNO$_3$ was higher than that of conventional ammonia/water working fluid, the experimental study on the performance of absorption refrigeration cycle working with ammonia/LiNO$_3$ show that the *COP* of the cycle was lower than that of ammonia/water[26]. Experimental investigation carried out by Rivera and Best [27] obtained that the heat transfer coefficients in boiling conditions for ammonia/LiNO$_3$ is two to three times lower than that of ammonia/H_2O. Heard [28] reported that the reduction in the achieved values of the *COP* and cooling capacity against the theoretical ones is mainly due to the low efficiency of the absorption process, penalized by the high viscosity of the solution.

3. Ammonia/(LiNO$_3$+water)

Some authors proposed ternary working fluid ammonia/(LiNO$_3$+water) [29-30]. The addition of water in the solution was aimed to reduced the viscosity of the solution and thus improved the heat and mass transfer coefficient in the absorber. Therefore, the performance of the cycle was expected to be improved.

The authors reported higher operation temperatures and significant *COP* improvements for the ternary mixture as compared to the binary mixture in heat pump applications. It was also observed that there is no need for rectification, which increases the cooling capacity. The ammonia/(LiNO$_3$+water) absorption refrigeration cycle can be operated without a distillation column, in this case the calculated water

---

content in the refrigerant entering the evaporator is less than 1.5% (in weight) for the selected operating conditions. In addition, it was concluded that the ammonia/LiNO$_3$ and NH$_3$/(LiNO$_3$+water) working fluid mixtures are suitable for use in absorption refrigeration cycles driven by low grade waste heat [26].

4. Ammonia/NaSCN

Similarly with ammonia/LiNO3 working fluid, the use of ammonia/NaSCN as working fluid for absorption refrigeration systems does not require rectification process as NaSCN is non-volatile. At certain operation condition, the *COP* of the systems operating with ammonia/NaSCN is higher than those the systems working with ammonia/LiNO3 and ammonia/water.

However, the solubility of ammonia in NaSCN is lower than those of ammonia/water and ammonia/LiNO3, thus the mass circulation ratio of the ammonia/NaSCN is higher than those of other absorbents. In addition, the heat source temperature of this cycle is limited because of the possibility of crystallization [24-25].

5. Ammonia/(water+NaOH)

Another attempt to overcome the drawbacks of conventional ammonia/water working fluid is by adding NaOH to the ammonia/water solution to improve the separation of NH$_3$ in the generator and reduce both chiller driving temperature and rectification losses. Cycle simulation based on their experimental data showed that the *COP* was about 20% higher than the conventional ammonia/water under same conditions and using a hydroxyl separation efficiency of 99% for NaOH [9,31].

2.4. *COP* Evaluation Using Limited Data for Working Mixture Pre-Selection

Ideally working fluid mixtures for absorption refrigeration applications should meet all criteria as mentioned in above section. However, to evaluate the feasibility of new working fluids based on above criteria it needs huge of properties information which are usually scarcely available in open literature. In addition, it

requires a long time and extended laboratory facilities to be able to measure all thermophysical properties for new proposed working fluid. On the other hand the final results and conclusions of the measurements are not necessarily in good agreement with all above-mentioned criteria.

Apart from above-mentioned ideal criteria of working mixtures for absorption refrigeration application, the feasibility and performance of working fluid in absorption refrigeration cycle can be theoretically studied using limited available data. The coefficient of performance (*COP*) of the absorption refrigeration systems can be calculated on different levels of sophistication, depending on the required precision and the availability of fluid data [32].

Normally the *COP* of the absorption refrigeration system is calculated using enthalpy-concentration-temperature diagram by applying energy balance in each components of the system and working pressure of the systems is calculated using vapor pressure diagram of the refrigerant based on condensation and evaporation (cooling) temperature of the cycle.

Nevertheless, the theoretical *COP* of the absorption refrigeration system can be calculated using Dühring diagram presenting pressure (ln *P*), temperature (1/*T*) and solution concentration. Assuming that absorber and condenser temperature are equal (fixed by cooling water temperature), the theoretical *COP* of the absorption refrigeration system is well-known and in a first order approximation proportional to the ratio of temperature thrust (T_{GEN} - T_{COND}) and temperature lift (T_{COND} - T_{EVAP}) [33]. This theoretical *COP* can be mathematically written as [34]

$$COP = \frac{Q_{EVAP}}{Q_{GEN}} = \frac{\dfrac{1}{T_{COND}} - \dfrac{1}{T_{GEN}}}{\dfrac{1}{T_{EVAP}} - \dfrac{1}{T_{COND}}} \tag{2.3}$$

where T_{EVAP}, T_{COND} and T_{GEN} are the temperature of evaporator, condenser, and generator, respectively. The simple schematic diagram of an absorption refrigeration system in Dühring diagram in inverse temperature scale is shown in Figure 2.4.
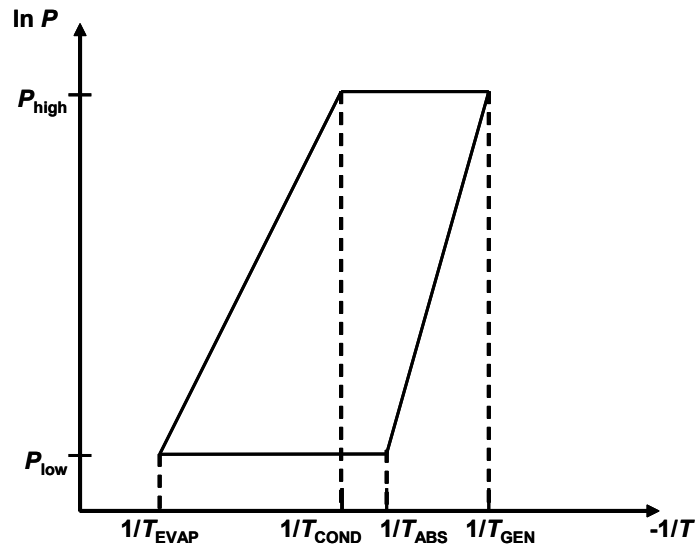
Figure 2.4. Schematic of Dühring diagram in inverse temperature scale

From Figure 2.4 it can be seen that the theoretical *COP* of a single effect absorption refrigeration system depends on the vapour pressure of the working fluids and can be obtained as a ratio of the axis line. Whereas the vapour pressure of a pure refrigerant is expressed by a function of temperature, the vapour pressure of working fluid mixture is given by a function of temperature and solution concentration. Hence, the vapour pressure of working fluid mixture can be written as

$$P = f(T, x_L) \tag{2.4}$$

where *P* is vapour pressure, *T* is temperature and x_L is concentration of one component in the mixture in liquid phase. In Clausius-Clapeyron equation, the vapour pressure of each pure component at low pressure (far from its critical pressure) can be described as a function of temperature and enthalpy of vaporization. The Clausius-Clapeyron equation for vapour pressure of pure components at low pressure is expressed as [35]

$$\ln P = -\frac{\Delta h_v}{R}\frac{1}{T} + C \tag{2.5}$$

where Δh_v is the enthalpy of vaporization, *R* is gas constant, and *C* is a constant. For binary working fluid mixtures, assuming that the vapour pressure of the absorbent is negligible, Equation (2.5) can be written as

$$\ln P = -\frac{\Delta h_v + \Delta h_{mix}}{R}\frac{1}{T} + C \tag{2.6}$$

Hifni M. Ariyadi, Doctoral Thesis, Universitat Rovira i Virgili, 2016

where Δh_{mix} is the heat of mixing of binary working fluid mixtures.

From Equation (2.6) it can be seen that the excess enthalpy of the working fluid mixtures affects the gradient/slope of the different vapour pressure line correspond to vapour pressure of pure refrigerant. Hence, from this description it can be distinguished that there are three variation of Dühring Diagram for working fluid mixture depending on the slope of the vapour pressure line at constant concentration (see Figure 2.5).

(a)

(b)

(c)
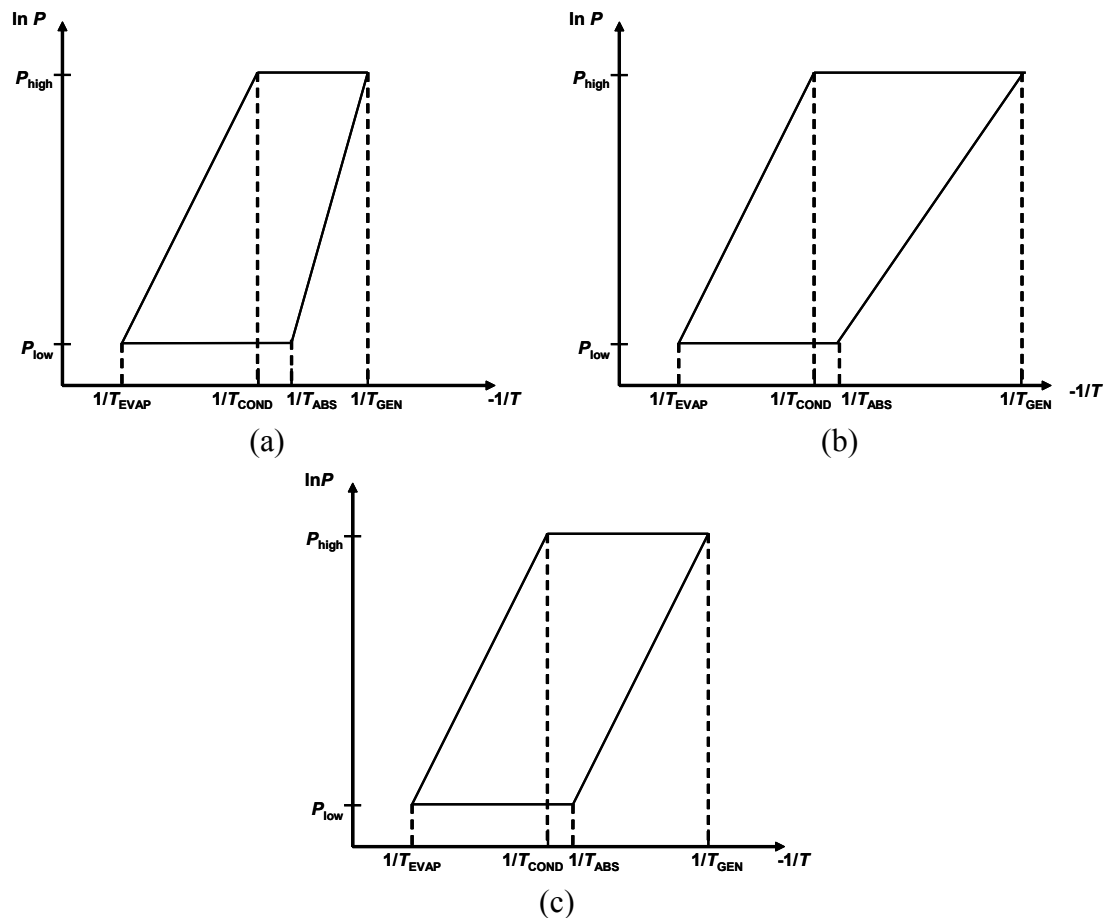
Figure 2.5. Schematic of Dühring diagram in inverse temperature scale with working fluid mixtures having (a) steeper slope (b) flatter slope and (c) parallel slope

For positive magnitude heat of mixing, as it is happened in conventional working fluid mixture, the line of vapour pressure at constant concentration in the Dühring diagram (ln P vs. $1/T$) becomes steeper (see Figure 2.5.(a)). In contrary, for negative magnitude heat of mixing the line of vapour pressure at constant concentration in the Dühring diagram (ln P vs. $1/T$) becomes flatter (see Figure 2.5.(b)). For zero magnitude heat of mixing the line of vapour pressure at constant

concentration in the Dühring diagram (ln P vs. $1/T$) remains parallel with the vapour pressure line of pure refrigerant (see Figure 2.54.(c)).

As mentioned above, the theoretical *COP* of a single effect absorption refrigeration system depends on the vapour pressure of the working fluids and can be obtained as a ratio of the axis line. As a consequence the range of *COP* in dependence of the sign of the excess enthalpy (or the slope of the vapour pressure line at constant concentration) can be estimated from the Dühring diagram. For positive magnitude heat of mixing, as it is happened in conventional working fluid mixture, the *COP* ranges between 0 and 1. In contrary, for negative magnitude heat of mixing the *COP* ranges between 1 and ∞. For zero magnitude heat of mixing the *COP* equals to 1. The ranges of *COP* in dependence of the excess enthalpy are summarized in Table 2.2.

Table 2.2. The ranges of COP in dependence of the sign of the excess enthalpy

Slope (*l*)	*COP*
$l > 0$	$0 - 1$
$l = 0$	1
$l < 0$	$1 - \infty$

For ammonia based working fluids, the values of maximum *COP* based on above approximation are presented in Table 2.3.

Table 2.3. Maximum *COP* of ammonia based working fluid

Working Fluids	T_{EVAP} (ºC)	$T_{ABS}=T_{COND}$ (ºC)	T_{GEN} (ºC)	max. *COP*
water/LiBr	5	30	58.36	0.95
ammonia/water	5	30	58.34	0.95
ammonia/LiNO$_3$	5	30	55.47	0.86
ammonia/NaSCN	5	30	57.89	0.94

The maximum *COP* presented in Table 2.3 was based on the evaporator temperature of 5ºC and condenser and absorber temperature of 30ºC. The *PTx* correlations for each working fluid were available in Engineering Equation Solver (EES) and were taken from literature [76-79].

From Table 2.3 it can be seen that the all conventional working fluids have maximum *COP* of less than 1 which mean that the slope of the concentration line of the working fluid mixtures in *PTx* diagram is steeper than the slope of refrigerant line. However, it also must be noted that steeper slope will reduce the minimum generator temperature limit. Hence, although the COP may be lower, the temperature needed to activate the cycle will be also lower.

Apart of above approximation method, according to Alefeld and Radermacher [32] and Ziegler [33], if the heat of evaporation (Δh_v) and heat of mixing (H^E) are known the coefficient of performance (*COP*) of a single effect absorption refrigeration cycle can be also calculated, as the slope of the vapor pressure line of the pure refrigerant in the Dühring diagram is proportional to the heat of evaporation while the slope of the vapor pressure line of the working mixture is proportional to the sum of the heats of evaporation and mixture (see Equation (2.5) and (2.6)).

Applying equation (2.5) and (2.6) into Eqaution (2.2), the evaporator cooling capacity and generator thermal load of a single effect absorption refrigeration cycle can be expressed the Equation (2.7) and (2.8), respectively.

$$Q_{EVAP} = \Delta h_v \qquad (2.7)$$
$$Q_{GEN} = \Delta h_v + \Delta h_{mix} \qquad (2.8)$$

Hence the *COP* of a single effect absorption refrigeration cycle can be calculated using the Equation (2.9).

$$COP = \frac{\Delta h_v}{\Delta h_v + \Delta h_{mix}} \qquad (2.9)$$

From Equation (2.7) it can be seen that the maximum *COP* does not vary strongly with changes in the working pair [33].

From these very simple considerations it can be concluded that the *COP* can not be raised above a limit in the order of one for a simple single-effect cycle. In addition, the temperature of the driving heat cannot be lowered beyond a certain temperature which can be derived from chilled water and cooling water temperature for a simple single-effect cycle.

Moreover, if other properties are available, such as enthalpy of vaporization, heat of mixing, and specific heat capacities of refrigerant and solution, the *COP* of an absorption system can be calculated with higher accuracy. The *COP* of an absorption refrigeration system has been described in Equation (2.3). For a cycle with 1 kg of refrigerant circulating in the system, the specific cooling thermal load, q_{EVAP}, can also be extended as in Equation (2.10) as summation of latent heat of the refrigerant and sensible heat of refrigerant, such as proposed by Alefeld and Radermacher [32].

$$q_{EVAP} = \Delta h_v - C_{p,r,l}(T_{COND} - T_{EVAP})$$ (2.10)

The specific generator thermal load, q_{GEN}, can also be described in Equation (2.11) as function of latent heat of phase change, sensible heat of the solution [32].

$$q_{GEN} = (\Delta h_v + \Delta h_{mix}) - C_{p,r,l}(T_{GEN} - T_{ABS}) + q_{SHX}$$ (2.11)

The sensible heat in the generator appears due to the difference of the solution mass flow and solution heat capacity between strong and weak solution in the circulation circuit. This sensible heat can be calculated by assuming a linear change in the specific heat capacity of the solution with regard to composition. Thus the correlation of heat capacity of the strong and weak solution can be written as Equation (2.12)

$$C_{p,s,st}f = C_{p,s,w}(f - 1) + C_{p,r}$$ (2.12)

The term q_{SHX} is the heat which is not recovered by the solution heat exchanger. In an ideal heat exchanger, all of the specific heat is transferred through the solution heat exchanger from the hot stream leaving the generator to the cold stream leaving the absorber. The specific heat transferred by an ideal heat exchanger can be written as Equation (2.13)

$$q_{SHX,id} = (f - 1)C_{p,s}(T_{GEN} - T_{ABS})$$ (2.13)

Therefore, heat which is not recovered by the solution heat exchanger can be calculated using Equation (2.14) [32].

$$q_{SHX} = (1 - \varepsilon_{SHX})(f - 1)C_{p,s}(T_{GEN} - T_{ABS})$$ (2.14)

Thus, the *COP* of an absorption refrigeration system can described in Equation (2.15)

$$COP = \frac{\Delta h_v - C_{p,r,l}\left(T_{COND} - T_{EVAP}\right)}{\left(\Delta h_v + \Delta h_{mix}\right) + C_{p,r,l}\left(T_{GEN} - T_{ABS}\right) + q_{SHX}} \qquad (2.15)$$

The *COP* estimation for ammonia based using Equation (2.15) is presented in Table 2.4. This evaluation was based on the operation condition similar to those published by Alefeld and Radermacher [32] with heat exchanger effectiveness of 1 and refrigerant mass flowrate of 1 kg/s.

Table 2.4. *COP* estimation of absorption refrigeration cycle with ammonia/ionic liquid working fluids

Parameters	Water/LiBr	NH₃/water	NH₃/LiNO₃	NH₃/NaSCN
T_{EVAP} (°C)	5	-10	-10	-10
T_{COND} (°C)	35	35	35	35
T_{ABS} (°C)	35	35	35	35
T_{GEN} (°C)	75	95	95	95
Δh_v (kJ/kg)	2405	1323	1323	1323
Δh_{mix} (kJ/kg)	246.4	213.6	387.5	208.6
$C_{p,r,l}$ (kJ/kg·K)	4.18	4.87	4.87	4.87
X_{ABS} (%wt. ref)	44.72	42.74	46.01	41.21
X_{GEN} (%wt. ref)	42.02	39.91	42.19	39.32
f	21.47	21.24	15.16	32.04
COP	0.81	0.57	0.52	0.57

Before observing Table 2.4, one must notes that those results are only approximation and thus are more intended for qualitative arguments than quantitatively exact results to help in understanding and discussing working fluid properties and their consequences for cycle design. Thus the error from this calculation should be tolerable [39]. From Table 2.4 it can be seen that using solubility data and properties of pure refrigerant, the estimated *COP* values of the cycle with new working fluids were under the maximum *COP* (as described in Table

2.3) and closer to the theoretical evaluation using detail parameters obtained from literature [37-38]. From Table 2.4 it also can be observed that new working fluids may not bring better *COP* in comparison with conventional working fluids. However, new working fluids may give other advantages such as elimination of rectification process and other advantages related with their transport properties such as more compact size in the main components etc [36].

Moreover, from these results it can be observed that vapour-liquid equilibrium data of the working fluid mixture plays an important role to analyse the performance of absorption refrigeration cycle. From these vapour-liquid equilibrium data, it is possible to create the Pressure-Temperature-Concentration (*PTx*) diagram which can be utilize to draw and to obtained the detail operation conditions of the absorption cycle from a given input. In addition the use *PTx* diagram of the working fluids enables us to estimate the heat of mixing of the working fluid mixture.

Therefore, the vapour-liquid equilibrium data is the minimum requirements needed to investigate the performance of absorption refrigeration cycle with new working pair. Obviously, the vapour-liquid equilibrium data of the working fluid must be solid and robust to improve the quality of the results. Furthermore, to be able to have solid *PTx* diagram of the working fluid, it is necessary to have a good correlation of vapor-liquid phase equilibrium of the working fluid using and to choose appropriate thermodynamic model to describe the vapour-liquid equilibrium properties of the working fluid mixtures.

2.5. Review of Ionic Liquids as Novel Absorbent for Ammonia Refrigerant

The ionic liquids have been used for wide applications, including in absorption process applications. Particularly in absorption refrigeration applications, the use of ionic liquids is relatively favorable due to negligible vapor pressure and relatively good solubility with other compounds. Especially in working fluid pair of ammonia and ionic liquid for absorption refrigeration application, some authors have been investigating the thermophysical properties of ammonia/ionic liquid mixtures

and studying the performance of ionic liquids as absorbent for ammonia refrigerant for absorption refrigeration applications.

The use of ionic liquids as absorbent for ammonia refrigerant was proposed in first time by Yokozeki and Shiflett [37-38] on 2007. Moreover, their invention on the use of ionic liquids as working fluid for absorption refrigeration cycle has been patented [40-42]. They measured the solubility of ammonia in some different ionic liquids (see Table 2.5 for details of ionic liquids) using static method. The solubility measurement was made at isothermal conditions of about 283, 298, 323, 348, and 373 K and ammonia mole fraction from 0.1 to 0.9. Their measurement data were correlated using cubic Reidlich-Kwong equation of state (RK-EOS). The use of cubic RK-EOS was chosen due to its availability to correlate the vapour-liquid equilibrium of mixture of ionic liquid with some various refrigerants [43-45].

Table 2.5. Ionic liquids studied by Yokozeki and Shiflett [37-38]

Ionic Liquids	MW	Abbreviations	No. data
1-ethyl-3-methylimidazolium acetate	170.11	[emim][Ac]	30
1-ethyl-3-methylimidazolium ethylsulfate	236.29	[emim][EtSO$_4$]	29
1-ethyl-3-methylimidazolium thiocyanate	169.25	[emim][SCN]	36
N,N-dimethylethanolammonium acetate	149.19	[DMEA][Ac]	32
1-butyl-3-methylimidazolium hexafluoro-phosphate	284.18	[bmim][PF$_6$]	29
1-hexyl-3-methylimidazolium chloride	202.73	[hmim][Cl]	30
1-ethyl-3-methylimidazoliumbis(trifluoro-methylsulfonyl)imide	391.31	[emim][NTf$_2$]	30
1-butyl-3-methylimidazolium tetrafluoroborate	226.02	[bmim][BF$_4$]	36

Their results show that the ammonia presented good solubility in the studied ionic liquids. The high solubility was nearly comparable to the case of ammonia/ water mixtures in molar compositions (i.e. negative deviations from Raoult's law), particularly for [hmim][Cl], [bmim][PF$_6$], and [DMEA][Ac] at 298 K. Another important result was that ammonia does not react with studied ionic liquids under the

experimental condition. In addition, excess properties (enthalpy, entropy, and Gibbs energy) calculated using Reidlich-Kwong EOS show all negative values.

Li et al. [46] determined the solubility of ammonia into four ionic liquids $[C_nMIM][BF_4]$ (n=2, 4, 6,and 8) and studied the effect of alkyl side chain length of ionic liquids on ammonia solubility. The measurements were carried out using static method at isothermally fixed temperatures of 293.15, 303.15, 313.15, 323.15 and 333.15 K and the pressure from 0 to 0.6 MPa. In addition to the high solubility of ammonia into studied ionic liquids, they found that, for ionic liquids having same anion, the solubility of ammonia into ionic liquid increase when the length of cations' alkyl increases, that is: $[C_8mim]^+ > [C_6mim]^+ > [C_4mim]^+ > [C_2mim]^+$. They analysed that increase of carbon chain length leads to the decrease of ionic liquids density, and thus generating more free volume and dissolving more ammonia molecules. Furthermore, the thermodynamic properties such as solution enthalpy, solution Gibbs free energy, solution entropy, and solution heat capacity of these systems were also obtained.

The solubility of ammonia into metal ion-containing ionic liquid $[bmim][Zn_2Cl_5]$ has been investigated by Chen et al [47] using static method. The measurements were performed at ammonia mole fraction of (0.83–0.94) and the temperature of (323.15–563.15) K. The total uncertainties of measurement were lower than 4.3%. The solubility data were then correlated using modified UNIFAC model, creating new group interaction parameters. Their results showed that the solubility of ammonia in $[bmim][Zn_2Cl_5]$ is higher than that in the other ionic liquids studied by Yokozeki and Shiflett [37-38].

Apart from experimental measurement of the solubility of ammonia in ionic liquids, some authors have been developing models to predict the thermophysical properties of ammonia/ionic liquid mixture, particularly on vapour-liquid equilibrium which is one of the most important properties for absorption refrigeration studies.

Shi and Maginn [48] performed a computational molecular simulation to predict the isotherms solubility of ammonia in the ionic liquid 1-ethyl-3-methylimidazolium bis(trifluoromethylsulfonyl)imide ([emim][NTf$_2$]). Their computational work was carried out using osmotic ensemble Monte Carlo simulation at temperatures of 298 K, 322K, and 348 K. Their results showed that, for vapour-

liquid equilibrium of pure ammonia, the simulations were in fair agreement with the experimental data with average deviation of 22.6%. For the solubility of ammonia/[emim][NTf$_2$] mixture, results from the simulations were also in fair agreement with experiment with the average absolute differences between simulations and experiments were 14.4%, 28.5%, and 25.6% at temperature of 298 K, 322 K, and 348 K, respectively. The activity coefficient of ammonia in [emim][NTf$_2$] varied between 0.5–0.8, indicating high solubility and negative deviations from Raoult's Law, and were in good agreement with the range of activity coefficients obtained experimentally. The enthalpy of mixing was negative in all cases, ranging from -2 to-11 kJ/mol. The magnitude of the enthalpy of mixing increases as the concentration of ammonia increases and as temperature decreases. Computed partial molar volumes are on the order of 25–30 cm^3/mol, and the expansion of the liquid is quite small where at ammonia mole fraction of 0.65, the total liquid volume expansion is only about 20%. The simulations show that ammonia interacts more strongly with the cation than the anion, due to hydrogen bonding interactions between the basic nitrogen atom on ammonia and the cation ring hydrogens. They finally suggested that solubilities can be tuned by adjusting the strength of the hydrogen bonding interactions between the cation and ammonia.

The use of UNIFAC model to predict vapour-liquid equilibrium of ammonia/ionic liquid mixture has been studied by Sun et al [49]. They used experimental solubility data of ammonia with four different ionic liquids to obtained new group interaction parameters. The four ionic liquids studied were 1-ethyl-3-methylimidazolium acetate ([emim][Ac]), 1-butyl-3-methylimidazolium tetrafluoro-borate ([bmim][BF$_4$]), 1,3-dimethylimidazolium dimethyl phosphate ([mmim]-[DMP]) and 1-ethyl-3-methylimidazolium ethylsulfate ([emim][EtSO$_4$]). The results showed that the model enable to predict the solubility of ammonia in four studied ionic liquids with the average relative deviation of pressure between the predicted and experimental data for the four systems was 9.35%. Furthermore, they implemented UNIFAC model to predict the values of infinite dilution activity coefficient and the absorption potential of 16 sets of ammonia/ionic liquid mixtures. They concluded that among different 16 studied ionic liquids, the working pair of ammonia/[bmim][Ac] has the best potential research value.

Research to propose new ionic liquids favorable with ammonia has been done by Palomar et al [51]. They developed a computational-experimental strategy research to propose new ionic liquids with favorable properties for NH_3 absorption. First, COSMO-RS method was used to analyze the solute–solvent intermolecular interactions and to perform a rational screening among 272 conventional and task-specific ionic liquids, for selecting a set of optimum cation–anion combinations for NH_3 absorption. The results obtained confirm the general suitability of COSMOS-RS method to predict gas–liquid equilibrium data in ionic liquid systems, such as, the solubility and Henry's law constants. Computational and experimental evidences probed that ammonia forms efficient intermolecular interactions with hydrogen bond donor groups present in the ionic liquid structure. As a conclusion, they proposed two new commercially available task-specific ionic liquids, 1-(2-hydroxyethyl)-3-methylimidazolium tetrafluoroborate [EtOHmim][BF$_4$] and (2-hydroxyethyl)-trimethyl ammonium bis(trifluorometanesulfonyl)imide ([choline]-[NTf$_2$]), whose characteristics would allow future implementation of novel ammonia absorption systems.

Recently, Cera-Manjarres [75] of CREVER Group of Rovira i Virgili through the same project with this thesis experimentally determined and modeled the most important thermophysical properties of selected ionic liquids and their binary mixtures with ammonia for absorption refrigeration applications. After carrying out a literature study, he selected six ionic liquids taking into account their low viscosity, high solubility to ammonia and high thermal stability: N-ethyl-N-(2-hydroxyethyl)-N,N-dimethyl with two different anions; 1) bis(trifluoromethylsulfonyl)imide and 2)trifluoromethane-sulfonate, 3) 1-(2-Hydroxyethyl)-3-methylimidazoliumtetra-luoroborate, 4) choline (trifluoromethylsulfonyl)imide, 5) 1-(2-Hydroxyethyl)-3-methylimidazolium bis(tr-fluoromethylsulfonyl)imide, and 6) N-Trimethyl-N-propylammonium bis(trifluoro-methylsulfonyl)imide.

The thermophysical properties of pure ionic liquids such as density, viscosity, thermal conductivity and heat capacity were measured using a vibrating tube densimeter, a piston type viscometer, a transient hot-wire method, and a Calvet Microcalorimeter, respectively. In case of ionic liquid-ammonia mixtures, vapor pressure, density and viscosity were measured at all composition range. The vapor

pressure was determined by means of static method. With the exception of thermal conductivity, all the thermophysical properties were measured in the temperature range of 293.15 K to 373.15 K. The vapor pressures of ionic liquid and ammonia binary mixtures present higher negative deviation from Raoult's law than ammonia-water at 303.15 K. The experimental data for each thermophysical properties of ionic liquids were correlated by means of algebraic polynomial equation, with an exception to the viscosity data which was correlated using Vogel type equation. All correlations had good agreement with the experimental data, with deviation lower than 1.2% for each thermophysical properties.

For the mixtures, Antoine type equation has been used to correlate the vapor pressure data. The results showed a good fit for the experimental data, especially at ammonia mole fraction higher than 0.4 and temperature higher than 313.15 K. All of these experimental data of pure ionic liquids and their mixtures with ammonia, in combination with the correlation of the each thermophysical properties, allow us to create a property database of ammonia/ionic liquid working pairs for absorption refrigeration applications.

From this review, it can be seen that properties of ammonia/ionic liquid working pairs have been gradually examined in recent years. However, among important properties necessary for absorption refrigeration studies, only solubility data of ammonia/ionic liquid mixtures were available in the literature. Other important properties, such as heat of dilution, density, and viscosity were not available. New set properties database necessary for absorption refrigeration studies was firstly proposed by our research group using new ammonia/ionic liquid working pairs. Given the tailor-made characteristic of the ionic liquid (i.e., various ionic liquids can be synthesized according to a given target or practical needs), the gap in this applied research field urgently needs to be filled. Moreover, it is necessary to study the interaction between ammonia and various ionic liquids, as well as to measure other thermophysical properties of their mixture, for the development of suitable working pairs for absorption cycle [52].

2.5.1. Issues on Ionic Liquids as Absorbent for Ammonia Refrigerant

As mentioned above, the use of ionic liquid as absorbent for ammonia refrigerant in absorption refrigeration systems may give some advantages such as unnecessary to add rectification column in the refrigerant outlet of the generator. However the applications of ionic liquids as absorbent for ammonia refrigerant in absorption refrigeration systems still remains some issues such as relatively high viscosity, different range of thermal stability, and relatively low solubility as compared to conventional absorbents.

1. Viscosity

Viscosity plays an important role in the absorption refrigeration systems. Kim et al. [2] reported that higher viscosity of absorbent can cause an increased pressure drop in the solution loop, which would result in larger pumping power or larger pipes and system volume. In addition, according to Römich et al. [65] a high viscosity can influence absorption negatively and increases the pressure drop within the process. Viscosity also plays an important role in the absorption process in the absorber as it influence the overall heat and mass transfer coefficient of the absorber.

Table 2.6. Viscosity of some pure ionic liquids at typical absorber
and desorber temperature of 30ºC and 100ºC, respectively

Ionic Liquid	Viscosity of Pure IL (cP) [66] at	
	Absorber	Generator
[bmim][BF$_4$]	78.83	9.11
[bmim][PF$_6$]	173.88	14.99
[emim][NTf$_2$]	27.34	5.51
[hmim][Cl]	6680.96	74.3
[emim][EtSO$_4$]	77.28	9.53
[emim][Ac]	97.98	9.35
[emim][SCN]	20.79	5.08

Although the experimental viscosity data of pure ionic liquids are available in open literature, the experimental viscosity data of ammonia/ionic liquid mixture still remains scarce. Table 2.6 show the viscosity of pure ionic liquids as proposed by Yokozeki and Shifflet at typical absorber and generator temperature based on study carried out by the author [37-38] and obtained from NIST database [66]. The

relatively high viscosity appears for almost all ionic liquids. The viscosities of the ionic liquids mentioned in Table 2.6 are between 20-6680 cP at a temperature of 30°C, which have significantly higher values than those of water (0.79 cP) at the same temperature [37-38].

Contrary to the analyses of Kim et al. [4] and Römich et al. [65], Ziegler [67] hypotheses that high viscosity in absorbent may give some advantages such as increasing the residence time of absorbent inside the absorber thus increase the absorption process.

2. Thermal Stability

Generally ionic liquids are stable up to 400 K [67–70]. However, in the case of a prolonged exposure to elevated temperatures, the effective decomposition temperature could be lower. Blake et al. [71] reported that the half-life of [bmim][PF$_6$] is only 138 days at 573 K, while at 423 K (the highest operating temperature of an absorption system), it could be more than 10 years. Since the degradation products of ionic liquids are often volatile compounds [72], the operating temperature needs to be kept within acceptable limits.

Moreover, some ionic liquids have relatively low thermal stability. For instance, [emim][EtSO$_4$] and [bmim][MeSO$_4$] decomposes at temperature of 50ºC [73]. Thus, it is important to understand the thermal stability of ionic liquid used as an absorbent for absorption systems, particularly in high temperature conditions such as in absorption heat transformers.

3. Solubility and circulation ratio

The solubility of ammonia as refrigerant into ionic liquid as an absorbent is one of the most important properties in absorption refrigeration applications. It describes the feasibility of an absorbent to be applied in absorption systems. A good absorbent must have good solubility and affinity with refrigerant, where it must easy to be absorbed in the absorber and must be easy to be separated in the generator. Thus for an amount of refrigerant, the absorbent required to operate the system can be minimized.

Another important parameter related to the solubility is circulation ratio. Solution circulation ratio (*f*) is defined as the ratio of the mass flow rate of the basic

solution per unit mass of refrigerant vapour generated in the generator is also used to evaluate the cycle performance. Mathematically, the solution circulation ratio can be described as

$$f = \frac{\dot{m}_s}{\dot{m}_r} \tag{2.2}$$

where $\dot{m}_s$ is strong solution mass flow rate and $\dot{m}_r$ is refrigerant mass flow rate.

Table 27 shows the circulation ratio (f) and concentration of ammonia/ ionic liquid mixture at typical absorber and generator operation conditions studied by the authors [37-38]. The concentration of ionic liquid at absorber temperature (30ºC) lies between 89.5 and 95.9 (% wt. of IL) and the concentration of ionic liquid at generator temperature (100ºC) lies between 878.5 and 91.8 (% wt. of IL). Thus, as a consequence the circulation ratio of the absorption systems with ammonia-ionic liquid working pairs is much higher as compared with conventional ammonia/water working pair.

Table 2.7. Circulation ratio (f) and concentration of ammonia/ ionic liquid mixture at typical absorber and desorber operation condition

Ionic Liquids	X_{GEN} (% wt. IL)	X_{ABS} (% wt. IL)	f	Ref.
[bmim][BF$_4$]	95.7	88.3	12.98	[36]
[bmim][PF$_6$]	94.5	89.0	17.27	[36]
[emim][NTf$_2$]	96.3	92.4	24.57	[36]
[hmim][Cl]	93.9	87.3	14.26	[36]
[emim][EtSO$_4$]	95.2	89.8	17.55	[37]
[emim][SCN]	92.7	85.2	12.42	[37]
[emim][Ac]	92.3	85.0	12.55	[37]
[DMEA][Ac]	84.1	73.1	7.60	[37]

4. Lack of reliable thermophysical properties data

The issues related with ionic liquids as absorbent for ammonia refrigerant in absorption refrigeration systems are not only related with the thermophysical properties of ionic liquids and their mixtures with ammonia. The advance research on the application of ammonia/ionic liquid working fluids in absorption refrigeration systems is strongly related to the availability of their thermophysical properties data. It is true that there has been a boom of thermophysical properties measurements for these fluids in the past decade. However, thermophysical properties data available in

open literature are still scarce and remains in limited range of temperatures and pressures when compared with the great number of existing ionic liquids. Thermophysical data available in the literature are limited to a reduced number of ionic liquids, with most of the data centered on imidazolium based ionic liquids and including anions such as hexafluorophosphate or tetrafluoroborate [75]. Moreover, among thermophysical properties available in the literature, discrepancies among thermophysical values for the same ionic liquids are being found among different laboratories as a result of purity, sample handling, and methods or procedures employed to measure such properties [75].

In addition, the information about their mixtures with natural refrigerants, particularly ammonia, are currently scarcer. For instance, there are only few available data of the solubility of ammonia into ionic liquids, which has been pioneered by Yokozeki and Shiflett [37-38]. Other experimental data, such as heat of mixing for ammonia/ionic liquid mixture which is important property for absorption simulation, so far is not available in the literature. The heat of mixing is only predicted using thermodynamic model from solubility data.

2.6. Conclusions

The overview of absorption technologies and working fluids has been presented in this chapter. The basic description of the absorption refrigeration systems is presented in comparison with mechanical vapour compression refrigeration system. A brief description of the operation principle of basic absorption refrigeration processes and conventional working fluid mixtures commonly used in the absorption refrigeration system and main requirements of the working mixtures were also analyzed.

Moreover, evaluation on the performance of the absorption refrigeration using limited data for working mixture pre-selection was also explained. This evaluation is important to estimate the performance of the systems when the experimental property data were limited or not available. To be able to evaluate the performance of the cycle, one must have at least the vapour-liquid equilibrium data of the working fluid mixture. Obviously, the vapour-liquid equilibrium data of the working fluid must be solid and robust to improve the quality of the results.

Furthermore, to be able to have solid *PTx* diagram of the working fluid, it is necessary to have a good correlation of vapor-liquid phase equilibrium of the working fluid using and to choose appropriate thermodynamic model to describe the vapour-liquid equilibrium properties of the working fluid mixtures. Hence, advance study on the thermodynamic model to describe the vapour-liquid equilibrium properties of the new working fluid mixtures is undoubtedly necessary before investigating the performance of the absorption cycle using new working fluids.

The review presents that properties of ammonia/ionic liquid working pairs have been gradually examined in recent years. However, the information related to the thermophysical properties of the mixtures of ammonia/ionic liquid systems still remains scarce. Among important properties necessary for absorption refrigeration studies, the information is limited to the solubility of ammonia in few ionic liquids mostly imidazolium based ionic liquids. Other information, such as excess enthalpy of ammonia/ionic liquid mixture which is important property for absorption simulation, so far is not available in the literature. New set properties database necessary for absorption refrigeration studies was firstly proposed by our research group using new ammonia/ionic liquid working pairs.

Furthermore, investigations related to the application of ammonia/ionic liquid working fluids in absorption refrigeration systems are so far limited to the theoretical studies and computational simulation. The experimental studies on the absorption refrigeration systems working with ammonia/ionic liquid fluids are so far not reported in the literature.

Although there are some issues related with ammonia/ionic liquid working fluids such as high viscosities and low solubility, given the unique characteristic and controllability of the ionic liquid structure (i.e., various ionic liquids can be synthesized according to a given target or practical needs), the gap in this applied research field urgently needs to be filled [51].

2.7.   References

[1]   Dossat, R. J., *Principles of Refrigeration*, fourth edition, Prentice Hall

[2]   Kim, Y. J., Kim, S., Joshi, Y. K., Fedorov, A. G., and Paul, A., Kohl, P. A., Thermodynamic analysis of an absorption refrigeration system with ionic-

liquid/refrigerant mixture as a working fluid, *Energy,* 2012, 44, 1005-1016

[3]   Chan, C.W.; Ling-Chin, J.; Roskilly, A.P., Reprint of "A review of chemical heat pumps, thermodynamic cycles and thermal energy storage technologies for low grade heat utilisation," *Appl. Therm. Eng.,* 2013, 53, 160–176

[4]   Srikhirin, P., Aphornratana, S., Chungpaibulpatana, S., A review of absorption refrigeration technologies, *Renewable and Sustainable Energy Reviews,* 2001, 5, 343–372

[5]   Perez-Blanco, H., Absorption heat pump performance for different types of solution, *Int. J. Refrig.,* 1984, 7(2),115–22

[6]   Killion, J. D., and Garimella, S., A critical review of models of coupled heat and mass transfer in falling-film absorption, *Int. J. Refrig.*, 2001, 24, 755-797

[7]   Florides, G., A., Kalogirou, S. A., Tassou, S. A., Wrobel, L. C., Design and construction of a LiBr–water absorption machine, *Energy Conversion and Management,* 2003, 44, 2483–2508

[8]   Holmberg P, Berntsson T., Alternative working fluids in heat transformers. *ASHRAE Trans.*, 1990, 96, 1582–9

[9]   Sun, J., Fu, L., Zhang, S., A review of working fluids of absorption cycles, *Renewable and Sustainable Energy Reviews*, 2012, 16, 1899–1906

[10]   Iedema, P. D., Mixtures for the absorption heat pump, *Int. J. Refrig.,* 1982, 5 (5), 262 – 273

[11]   Ziegler, F., Recent developments and future prospects of sorption heat pump systems, *Int. J. Therm. Sci.*, 1999, 38, 191-208

[12]   Kim, S. S., An Absorption Refrigeration System using Ionic Liquid and Hydrofluorocarbon Wokring Fluids, PhD Dissertation, 2014, Georgia Institute of Technology

[13]   Amaris, C., Intensification of NH3 Bubble Absorption Process using Advanced Surfaces and Carbon Nanotubes for NH_3/$LiNO_3$ Absorption Chillers, PhD Thesis, 2013, Universitat Rovira i Virgili, Tarragona, Spain

[14]   Park, Y. M., Sonntag, R. E., Thermodynamic properties of ammonia/water mixtures: a generalized equation-of-state approach. *ASHRAE Trans.,* 1990, 96, 150–9

[15]   El-Sayed YM, Tribus M., Thermodynamic properties of water-ammonia mixtures: theoretical implementation for use in power cycle analysis, *ASME Pub. AES*,1985,1, 89–95

[16]   Ziegler B, Trepp C. Equation of state for ammonia/water mixtures. *Int. J. Refrig.,* 1984, 7(2),101–6

[17]   Herold, K. E, Han, K., Moran, M. J., AMMWAT: a computer program for calculating the thermodynamic properties of ammonia and water mixtures using a Gibbs free energy formulation, *ASME Pub. AES*, 1988, 4, 65–75

[18]   Patek, J., Klomfar, J., Simple function for fast calculations of selected thermodynamic properties of ammonia/water system. *Int. J. Refrig.,*

1995,18(4), 228–34

[19] Tillner-Roth, R., Friend, D. G., Survey and assessment of available measurements on thermodynamic properties of the mixture {water+ammonia} *J. Phys. Chem. Ref. Data*, 1998, 27 (1), 45 – 61

[20] Herold, K. E.; Radermacher, R.; Klein, S. A. Absorption chillers and heat pumps; CRC Press: Boca Raton, FL, 1996

[21] Berestneff, A. A. Absorption refrigeration system. U.S. Patent No. 2,565,943, 1951

[22] Zogg, R. A., Feng, M. Y., Westphalen, D., Guide to Developing Air-Cooled LiBr Absorption for Combined Heat and Power Applications, *Distributed Energy Program Report*, US Department of Energy, 2005

[23] Mclinden, M. O,, Radermacher, R., An experimental comparison of NH3–H2O and NH_3–H_2O–LiBr mixtures in an absorption heat pump, *ASHRAE Transactions,* 1985,191,1837–46

[24] Sun, Da-We, Comparison of the Performances of NH_3-H_2O, NH_3-$LiNO_3$ and NH_3-NaSCN Absorption Refrigeration Systems, *Energy Convers. Mgmt.*, 1998, 39 (5/6), 357-368

[25] Garousi Farshi, L., Infante Ferreira, C. A., Mahmoudi, S. M. S., Rosen, M.A., First and second law analysis of ammonia/salt absorption refrigeration systems, *Int J Refrig.,* 2014, 40, 111-121

[26] Táboas, F., Bourouis, M., Vallès, M., Analysis of ammonia/water and ammonia/salt mixture absorption cycles for refrigeration purposes in fishing ships, *Applied Thermal Engineering*, 2014, 66, 603-611

[27] W. Rivera, R. Best, Boiling heat transfer coefficients inside a vertical smooth tube for water/ammonia and ammonia/lithium nitrate mixtures, *Int. J. Heat Mass Transfer,* 1999, 42 (5), 905-921.

[28] Heard, C.L., Ayala, R., Best, R., An experimental comparison of an absorption refrigerator using ammonia/water and ammonia/lithium nitrate, *Proc. of International Absorption Heat Pump Conference*, 1996, 245-252. Montreal, Canada

[29] Ehmke, H. J., Renz, M., Ternary working fluids for absorption systems with salt-liquid mixtures as absorber, *Proceedings of IIF-IIR Congress, Commission (B1-642)*, 1983, 289-296. Paris, France.

[30] Bokelmann, H., Steimle, F., Development of advanced heat transformers utilizing new working fluids, *Int. J. Refrig.*, 1986, 9 (1), 51-59

[31] Steiu, S., Salavera, D., Bruno, J. C., Coronas, A., A basis for the development of new NH_3–H_2O–sodium hydroxide absorption chillers. *Int. J. Refrig.*, 2009, 32, 577-87

[32] Georg Alefeld, Reinhard Radermacher, Heat Conversion Systems, CRC Press 1993

[33] Ziegler, F., Recent developments and future prospects of sorption heat pump systems, *Int. J. Therm. Sci.*, 1999, 38, 191-208

[34] Kotenko. O., Potential Analysis of Alternative Absorption Heat Pumping Processes with Special Emphasis on Sodium Hydroxide as Additive, Doctoral Thesis, Graz University of Technology, Austria, 2012

[35] Auracher, H., Glaser, H., Stephan, K., Thermodynamics of Mixtures and Elementary Processes in Absorption Heat Pumps, Heat Pump Fundamentals, Heat Pump Fundamentals, Volume 53 of the series NATO Advanced Study Institutes Series, 1980, 302-332

[36] Ziegler, F., Options for new working pairs – perceptions and misperceptions, *2014 International Sorption Heat Pump Conference (ISHPC2014)*, University of Maryland, College Park, MD, U.S.A. March 31 – April 3, 2014,

[37] Yokozeki, A., Shiflett, M.B., Ammonia solubilities in room-temperature ionic liquids, ammonia solubilities in room-temperature ionic liquids, *Ind. Eng. Chem. Res.*, 2007, 46, 1605-1610

[38] Yokozeki, A., Shiflett, M. B., Vapor–liquid equilibria of ammonia + ionic liquid mixtures, *Applied Energy*, 2007, 84, 1258-1273,

[39] Ziegler, F., The multiple meanings of the Stefan-number (and relatives) in refrigeration, *Int. J. Refrig.*, 2010, 33, 1343 -1349

[40] Shiflett, M. B., Yokozeki, A., Absorption Cycle Utilizing Ionic Liquid as Working Fluid, U.S. Patent No. 8,715,521 B2, Mat 6, 2014

[41] Shiflett, M. B., Yokozeki, A., Mixture of Ammonia and Ionic Liquids, United States Patent Application Publication, Pub. No. US 2008/0153697 A1, June 26, 2008

[42] Shiflett, M. B., Yokozeki, A., Absorption Cycle Utilizing Ionic Liquid as Working Fluid, International Application Publsihed under Patent Cooperation Treaty, No. WO 2006/084262 A1

[43] Yokozeki, A.; Shiflett, M. B., Global Phase Behaviors of Trifluoromethane in Room-Temperature Ionic Liquid [bmim][PF$_6$], *AIChE J.*, 2006, 52 (11), 3952

[44] Shiflett, M. B.; Yokozeki, A., Solubilities and Diffusivities of Carbon Dioxide in Ionic Liquids: [bmim][PF$_6$] and [bmim][BF$_4$], *Ind. Eng. Chem. Res.*, 2005, *44* (12), 4453

[45] Yokozeki, A., Solubility of refrigerants in various lubricants, *Int. J. Thermophys,.* 2001, 22, 1057

[46] Li, G., Zhou, Q., Zhang, X., Wang, L., Zhang, S., Lia, J., Solubilities of ammonia in basic imidazolium ionic liquids., *Fluid Phase Equilibria*, 2010, 297 (1), 34–39

[47] Chen, W., Liang, S., Guoa, Y., Guia, X., Tanga, D., Investigation on vapor–liquid equilibria for binary systems of metal ion-containing ionic liquid [bmim]Zn$_2$Cl$_5$/NH$_3$ by experiment and modified UNIFAC model, *Fluid Phase Equilibria,* 2013, 360, 1– 6

[48] Wei Shi and Edward J. Maginn, Molecular Simulation of Ammonia Absorption in the Ionic Liquid 1-ethyl-3-methylimidazolium bis(trifluoromethyl-sulfonyl)imide ([emim][Tf$_2$N]), *AIChE Journal*, 2009, 55 (9), 2414-2421

[49] Sun, G., Huang, W., Zheng, D., Dong, L., Wu, X., Vapor-Liquid Equilibrium Prediction of Ammonia-Ionic Liquid Working Pairs of Absorption Cycle using UNIFAC Model, *Chinese Journal of Chemical Engineering*, 2014, 22(1), 72-78

[50] Palomar, J., Gonzalez-Miquel, M., Bedia, J., Rodriguez, F., Rodriguez, J. J., Task-specific ionic liquids for efficient ammonia absorption, *Separation and Purification Technology*, 2011, 82, 43–52

[51] Zheng, D., Dong, L., Huang, W., Wu, X., Nie, N., A review of imidazolium ionic liquids research and development towards working pair of absorption cycle, *Renewable and Sustainable Energy Reviews*, 2014, 37, 47–68

[52] Wang, M., and Infante-Ferreira, C., Assessment of Vapor-Liquid Equilibrium Models for Ionic Liquids Based Absorption Systems, *Proceeding of ICR 2015*, August 16 – 22, Yokohama, Japan

[53] Vetere A., Again the Rackett equation, *Chem. Eng. J.*, 1992, 49, 27–33

[54] Harrison, B. K., Seaton, W. H., Solution to Missing Group Problem for Estimation of Ideal Gas Heat Capacities. *Ind. Eng. Chem. Res.*, 1988, 27, 1536

[55] Paulechka, Ya. U., Kabo, G. J., Blokhin, A. V., Vydrov, O. A., Magee, J. W., Frenkel, M. Thermodynamic Properties of 1-Butyl-3- methylimidazolium Hexafluorophosphate in the Ideal Gas State. *J. Chem. Eng. Data,* 2003, 48, 457

[56] Kotenko. O., Moser, H., and Rieberer, R., Thermodynamic Analysis Of Ammonia/Ionic Liquid Absorption Heat Pumping Processes. *Proc. Int. Sorption Heat Pump Conf.*, 2011, 89-796

[57] Aspen Plus (Version 7.3): Aspen technology Inc. (2012)

[58] Swarnkar, S. K., Srinivasa Murthy, S. S., Gardas, R. L., Venkatarathnam, G., Performance of a vapour absorption refrigeration system operating with ionic liquid-ammonia combination with water as cosolvent, *Applied Thermal Engineering*, 2014, 72 (2), 250-257

[59] Wang, J. F., Li, C.X., Wang, Z.H., Measurement and prediction of vapor pressure of binary and ternary systems containing 1-ethyl-3-methylimidazolium ethylsulfate, *J. Chem. Eng. Data,* 2007, 52, 1307-1312.

[60] Zhang, L., Ge, Y., Ji, D., Ji, J., Experimental measurement and modeling of vapour-liquid equilibrium for ternary systems containing ionic liquids: a case study for the system water + ethanol + 1-hexyl-3-methylimidazolium Chloride, *J. Chem. Eng. Data,* 2009, 54, 2322-2329.

[61] Calvar, N., Gonzalez, B., Gomez, E., Dominguez, A., Study of the behaviour of the azeotropic mixture ethanol water with imidazolium-based ionic liquids, *Fluid Phase Equilib.,* 2007, 259, 51-56.

[62] Guo, K., Bi, Y., Su, H., Hungpu, L., Experiment and correlation of vapor-liquid equilibrium of aqueous solution of hydrophilic ionic liquids: 1-ethyl-3-methylimidazolium acetate and 1-hexyl-3-methylimidazolium chloride, *J. Chem. Eng. Data,* 2012, 57, 2243-2251.

[63] Ruiz, E, Ferro, V.R., de Riva, J., Moreno, D., Palomar, J., Evaluation of ionic liquids as absorbents for ammonia absorption refrigeration cycles using

COSMO-based process simulations, *Applied Energy*, 2014, 123, 281–291

[64] Bedia. J., Palomar, J., Gonzalez-Miquel, M., Rodriguez, F., Rodriguez, J. J., Screening ionic liquids as suitable ammonia absorbents on the basis of thermodynamic and kinetic analysis. *Separation and Purification Technology,.* 2012, 95,188–195

[65] Roemich C., Schaber K., Berndt J.F., Schubert T.J.S., 2009, Arbeitsstoffgemische mit ionischen Fluessigkeiten fuer Absorptionswaermepumpen und Absorptionskaeltemaschinen, Endreport, Deutsche Bundesstiftung Umwelt (DBU), Germany, 44

[66] ILThermo V.2.0, NIST Standard Reference Database, US Secretary of Commerce. http://ilthermo.boulder.nist.gov/

[67] Heintz, A., Lehmann, J. K., Wertz, C., Thermodynamic properties of mixtures containing ionic liquids. 3. liquid-liquid equilibria of binary mixtures of 1-ethyl-3-methylimidazolium bis(trifluoromethylsulfonyl)imide with propanol, butanol, and pentanol, *J. Chem. Eng. Data,* 2003, 48, 472–4.

[68] Wilkes, J. S., Properties of ionic liquid solvents for catalysis, *J. Mol. Catal. A Chem.,* 2004, 214,11–7.

[69] Hagiwara, R., Ito, Y., Room temperature ionic liquids of alkylimidazoliumcations and fluoroanions, *J. Fluorine Chem.,* 2000, 105, 221–7.

[70] Blake, D. M., Moens, L., Rudnicki, D., Pilath, H., Lifetime of imidazolium salts at elevated temperatures, *J. Sol. Energy Eng.,* 2006,128, 54–7

[71] Scammells, P. J., Scott, J. L., Singer, R. D., Ionic liquids: the neglected issues, *Aust. J. Chem.,* 2005, 58, 155–69.

[72] Fernandez, A., Torrecilla, J. S., Garcia, J., and Rodriguez, F., Thermophysical Properties of 1-Ethyl-3-methylimidazolium Ethylsulfate and 1-Butyl-3-methylimidazolium Methylsulfate Ionic Liquids, *J. Chem. Eng. Data,* 2007, 52, 1979-1983

[73] Aparicio, S.; Atilhan, M.; Karadas, F., Thermophysical Properties of Pure Ionic Liquids: Review of Present Situation, *Ind. Eng. Chem.Res.*, 2010, 49, (20), 9580-9595

[74] Nieto de Castro, C. A., Thermophysical properties of ionic liquids: Do we know how to measure them accurately? *Journal of Molecular Liquids*, 156, (1), 10-17.

[75] Cerra-Manjarres, A., PhD Thesis, Universitat Rovira i Virgili, Spain, 2015

[76] Patek, J., and Klomfar, J., A computationally effective formulation of the thermodynamic properties of LiBr-H2O from 273 to 500 K over full composition range, *Int. J. of Refrigeration*, 2006, 29, 566-578,

[77] Chaudhari, S.K., Salavera, D., Coronas. A., Densities, Viscosities, Heat Capacities, and Vapor-Liquid Equilibria of Ammonia + Sodium Thiocyanate Solutions at Several Temperatures, *J. Chem. Eng. Data*, 2011, 56, 2861-2869

[78] Libotean, S., Salavera, D., Valles, M., Esteve, X., and Coronas, A., Vapor-

Liquid Equilibrium of Ammonia + Lithium Nitrate + Water and Ammonia + Lithium Nitrate Solutions from (293.15 to 353.15) K, *J. Chem. Eng. Data*, 2007, 52, 1050-1055

[79] Tillner-Roth, R., Friend, D.G., Survey and Assessment of Available Measurement on Thermodynamic Properties of the Mixture (Water+Ammonia), *J. Phys. Chem. Ref. Data*, 1998, 27 (1), 45-61

Chapter 3

Modelling of Vapor-Liquid Equilibrium and Derived Properties of Ammonia/Ionic Liquid Mixtures

3.1. Introduction

As mentioned in previous chapter, to be able to pre-select new working fluid for absorption refrigeration system, it is necessary to have a good understanding in the calculation or correlation of thermophysical properties of working fluids particularly vapor-liquid vapor-liquid equilibrium. However the correlation of thermodynamic characteristics and vapor-liquid vapor-liquid equilibrium of ammonia/ionic liquid mixtures remains an important objective. The use of equations of state has long been limited to systems of simple fluids; however, there is an increasing demand for models that are also suitable for even more complex fluids [1].

Therefore, it is important to select an appropriate model to describe the vapour-liquid equilibrium properties of the binary systems of ammonia/ionic liquid mixtures. This chapter is aimed to study the ability of different model to calculate the vapor-liquid equilibrium of ammonia/ionic liquid mixtures. Four different thermodynamic models to calculate the vapor-liquid vapor-liquid equilibrium of ammonia/ionic liquid mixtures will be studied and analyzed. These four thermodynamic models are Non-Random Two Liquid (NRTL) model, Reidlich-Kwong-Soave Equation of State (RK-Soave EOS), Perturbed-chain statistical

associating fluid theory (PC-SAFT) Equation of State, and UNIFAC model. The study has been carried out by firstly reviewing different thermodynamic models. Afterwards, some experimental vapour-liquid-equilibrium data from literature of ammonia/ionic liquid mixtures were calculated using different models. The experimental vapour-liquid-equilibrium data of Yokozeki and Shiflett [5-6] will be used as their data covers wide range of compositions and temperatures while other data from other authors were limited only in small composition range and temperatures and pressures. After both pure parameters and binary interaction were obtained, the vapor-liquid equilibrium calculation of ammonia and ionic liquid mixtures were studied and analyzed and the applicability of each model was investigated by taking into account both its precision and its simplicity.

Using selected model, it is possible to create *PTx* diagram of ammonia/ionic liquid mixtures and draw the solution cycle of ammonia/ionic liquid working pairs in the absorption system on the *PTx* diagram. In addition, the heat of mixing of the solution also can be estimated either using *PTx* diagram or using a thermodynamic model, and finally the *COP* of the absorption refrigeration system using ammonia/ionic liquid working fluids can be estimated

3.2. Non-Random Two Liquid Model (NRTL)

3.2.1. NRTL Equations and Parameters

The Non-Random Two Liquid model (NRTL) is an empirical equation proposed by Renon and Prausnitz [2] based on the local composition representation of the excess Gibbs energy, GE, of liquid mixtures.

The expression of excess Gibbs energy in NRTL model is given as [2]

$$G^E = x_1 x_2 \left(\frac{\tau_{21} G_{21}}{x_1 + x_2 G_{21}} + \frac{\tau_{12} G_{12}}{x_2 + x_1 G_{12}} \right) \tag{3.1}$$

where parameter G_{12} and G_{21} are given as

$$G_{12} = \exp(-\alpha_{12} \tau_{12}) \text{ and, } G_{21} = \exp(-\alpha_{21} \tau_{21}) \tag{3.2}$$

and parameter τ_{12} and τ_{21} are given as

$$\tau_{12} = a_{12} + \frac{b_{12}}{(T + 273.15)} + e_{12} \ln(T + 273.15) + f_{12}(T + 273.15) ;$$

and $\quad$ (3.3)

$$\tau_{21} = a_{21} + \frac{b_{21}}{(T + 273.15)} + e_{12} \ln(T + 273.15) + f_{12}(T + 273.15)$$

where $\alpha_{12} \neq \alpha_{12}$ and $b_{12} \neq b_{12}$. The parameter α_{12} and α_{21} are given as

$$\alpha_{12} = c_{12} + d_{12}\ T;\ \text{and}\ \alpha_{21} = c_{21} + d_{21}\ T \quad (3.4)$$

where $c_{12} = c_{12}$; and $d_{12} = d_{12}$.

$\qquad$ Parameters a_{12}, a_{21}, b_{12}, b_{21}, c_{12} and c_{21} are obtained from vapour-liquid equilibrium data [26] regression and are shown in table 2. The activity coefficient (γ) for component 1 and 2 in a binary mixture can be expressed in Equation (3.5) and (3.6).

$$\ln \gamma_1 = x_2^2 \left[\frac{\tau_{21} G_{21}^2}{(x_1 + x_2 G_{21})^2} + \frac{\tau_{12} G_{12}}{(x_2 + x_1 G_{12})^2} \right] \quad (3.5)$$

$$\ln \gamma_2 = x_1^2 \left[\frac{\tau_{12} G_{12}^2}{(x_2 + x_1 G_{12})^2} + \frac{\tau_{21} G_{21}}{(x_1 + x_2 G_{21})^2} \right] \quad (3.6)$$

Enthalpy and Excess Properties of the mixtures

$\qquad$ Excess enthalpy, which indicates the temperature dependence of the Gibbs energy, and hence also the activity coefficients, can be determined via Gibbs–Helmholtz relation as shown in Equation (3.7) [3].

$$\left(\frac{\partial (G^E / T)}{\partial T} \right)_{P,x} = -\frac{H^E}{T^2} \quad (3.7)$$

The excess enthalpy of ammonia/ionic liquids mixture can be estimated using Equation (3.8) [3].

$$H^E = -R\left(\frac{x_1 x_2 b_{21} G_{21} \left[x_1 (\alpha_{12}\tau_{21} - 1) - x_2 G_{21} \right]}{(x_1 + x_2 G_{21})^2} + \frac{x_1 x_2 b_{12} G_{12} \left[x_2 (\alpha_{12}\tau_{21} - 1) - x_1 G_{12} \right]}{(x_2 + x_1 G_{12})^2} \right) \quad (3.8)$$

Once the excess Gibbs energy G^E and excess enthalpy H^E, have been determined the isothermal excess entropy can be calculated by the fundamental thermodynamic relationship as shown in Equation (9)

$$TS^E = H^E - G^E \quad (3.9)$$

The enthalpy of ammonia/ionic liquid mixture solution can be written as

$$h = X_1 h_1 + X_2 h_2 + h^E \quad (3.10)$$

where h_1 is the specific mass enthalpy of pure ammonia and h_2 is the specific mass enthalpy of pure ionic liquid, which can be obtained from Equation (3.11).

$$h_2 = \int_{T_0}^{T} C_{p,IL} dT + h_0 \quad (3.11)$$

The enthalpy of reference, h_0, is set to be 200 kJ/kg at the reference point, following IIR (International Institute of Refrigeration) standard. The experimental VLE data of ammonia and ionic liquids mixtures are taken from Yokozeki and Shiflett [5-6]. In addition to the experimental VLE data from these author, the experimental VLE data of [bmim][BF$_4$] and ammonia mixture were also taken from Li et al. [7].

To be able to analyse the results and to compare with the experimental data, the absolute average deviation of the results is calculated. The absolute average deviation is calculated using equation (3.12).

$$AAD(\%) = \frac{100}{n_{pts}} \sum_{i=1}^{n_{pts}} \left| \frac{P_i^{exp} - P_i^{calc}}{P_i^{exp}} \right| \quad (3.12)$$

3.2.2. Results and Discussion

3.2.2.1. NRTL Parameters of Ammonia/Ionic Liquid Mixtures

To calculate the thermodynamic properties of ammonia/ionic liquid mixtures, the experimental VLE data of ammonia/ ionic liquid mixtures have been extracted and regressed from the literature. The detail results of NRTL parameters of pure ionic liquids and pure ammonia regressed from experimental data are given in the Table 3.1.

Table 3.1. NRTL parameters of ammonia (1)/ionic liquids (2) mixtures

Parameters	Ionic liquids (2)			
	[bmim][BF$_4$]	[bmim][PF$_6$]	[emim][Ac]	[emim][EtSO$_4$]
a_{ij}	24.7310	-0.9913	-11.9031	-0.9204
a_{ji}	80.0000	-2.3469	12.0458	2.2626
b_{ij}	920.1935	430.6393	2903.3017	2457.8009
b_{ji}	22.6499	363.5577	-3118.7686	-1664.9759
c_{ij}	0	0.7060	0.3	0.3
d_{ij}	-0.0024	-0.0048	-0.0029	0.0058
e_{ij}	-7.0775	0	0	-0.6979
e_{ji}	-14.6824	0	0	0.6749
f_{ij}	0.0268	0	0	0.0015
f_{ji}	0.0224	0	0	-0.0071
Parameters	Ionic liquids (2)			
	[emim][NTf$_2$]	[hmim][Cl]	[emim][SCN]	[DMEA][Ac]
a_{ij}	-0.0628	-1.4354	-0.0545	-4.7986
a_{ji}	-0.0383	0.0363	-0.8702	-6.1697
b_{ij}	25.5290	1126.5169	178.4180	1664.0412
b_{ji}	-212.1376	-475.9309	-516.4417	1133.0704
c_{ij}	0.3	0.3	-0.2655	0.4199
d_{ij}	0.0566	0.0074	0.0004	-0.0036
e_{ij}	-0.0044	-0.3018	0	0
e_{ji}	0.0019	0.0985	0	0
f_{ij}	0.0004	0	0	0
f_{ji}	0.0007	0	0	0

Vapor-Liquid Equilibrium of Ammonia and Ionic Liquid Mixtures

After obtaining the NRTL parameters of ammonia/ionic liquid mixtures, the next sequence was to analyse and study the ability of NRTL model to calculate the

vapor-liquid equilibrium of ammonia and ionic liquid mixture. In this subsection, the vapor-liquid equilibrium calculation of some [bmim] based ionic liquid and ammonia mixtures and [emim] based ionic liquid and ammonia mixtures were studied. In addition, the vapor-liquid equilibrium calculations of [hmim][Cl] and [DMEA][Ac] were also studied

The results of vapor-liquid equilibrium of ammonia and [bmim] based ionic liquid mixtures with NRTL model are presented in Figure 3.1. The vapor-liquid equilibrium of binary mixtures of ammonia with two ionic liquids, [bmim][BF$_4$] and [bmim][PF$_6$] were studied.

Figure 3.1(a) shows the results of the vapor-liquid equilibrium of [bmim][BF$_4$] and ammonia mixture at several temperatures. From that figure it can be seen that the results were in good agreement as compared with the experimental data. The results indicate that the average absolute deviation for calculated vapor-liquid equilibrium of ammonia/[bmim][BF$_4$] mixture at all temperature range was 3.9%.

The results of the vapor-liquid equilibrium of [bmim][PF$_6$] and ammonia mixture at several temperatures are shown in Figure 3.1(b). Similar with those of [bmim][BF$_4$] and ammonia mixture, it is interested to see at the figure that the results have good agreement with the experimental data. The average absolute deviation for calculated vapor-liquid equilibrium of [bmim][PF$_6$] and ammonia mixture at all temperature ranges was 2.3%. However, different with those of [bmim][BF$_4$] and ammonia mixture, it is observed that the average absolute deviations have slightly higher values at temperature of 298 K. At temperature of 298 K the average absolute deviation for calculated vapor-liquid equilibrium of [bmim][PF$_6$] was 4.7%. Generally, the results of the vapor-liquid equilibrium of [bmim][PF$_6$] and ammonia mixture have better agreement with the experimental data as compared with those [bmim][BF$_4$] and ammonia mixture.
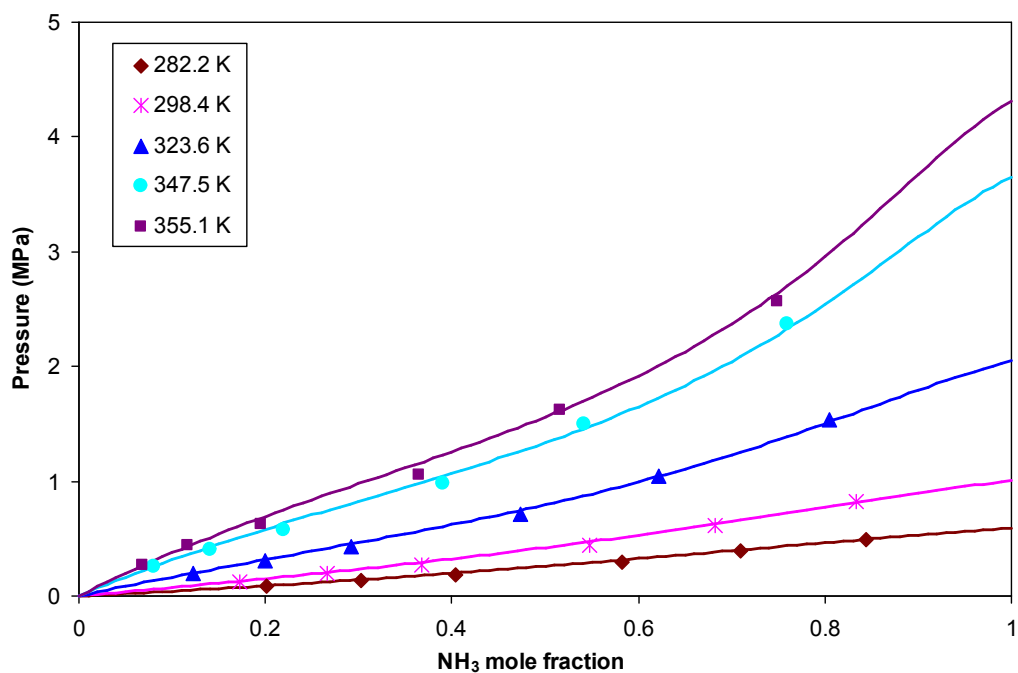
(a)
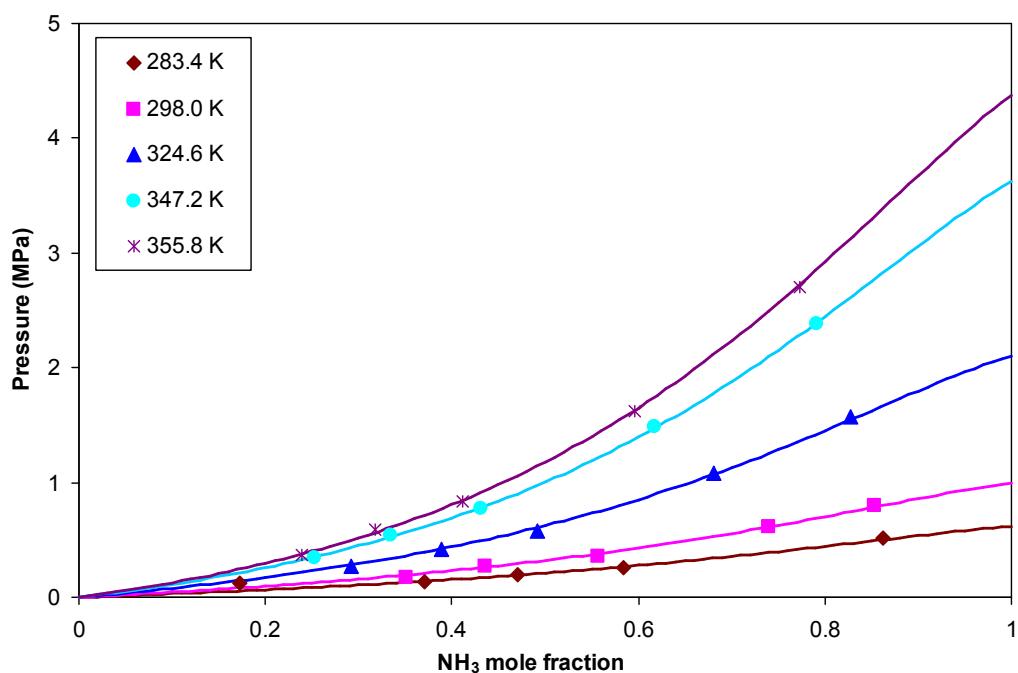
(b)

Figure 3.1. Vapor-liquid equilibrium of ammonia and [bmim] based ionic liquid mixtures at different temperatures (a) [bmim][BF_4] and (b) [bmim][PF_6].

Figures 3.2 present the calculate results of vapor-liquid equilibrium of [emim] based ionic liquid and ammonia mixture with NRTL model. The vapor-liquid

equilibrium of two ionic liquid and ammonia mixtures, [emim][EtSO$_4$] and [emim][Ac], are studied.

Figure 3.2(a) shows the results of the vapor-liquid equilibrium of [emim][EtSO$_4$] and ammonia mixture at several temperatures. From this figure it can be seen that the results at several temperatures have good agreement with the experimental data. The results indicate that the average absolute deviation for calculated vapor-liquid equilibrium for [emim][EtSO4] and ammonia mixture at all temperature range is 3.8%. It was also observed that the average absolute deviations have slightly higher values at temperature of 297.6 K and 322.3 K. The average absolute deviation for calculated vapor-liquid equilibrium of [emim][EtSO4] at temperature of 298 K was quite high, 9.2% and the average absolute deviation for calculated vapor-liquid equilibrium of [emim][EtSO4] at temperature of 322.3 K was 4.0%. In addition, the results present high deviations at higher temperature and low ammonia composition. However the high deviations at higher temperature and low ammonia composition were acceptable considering the deviation was less than 10% and the experimental data at higher temperature and low ammonia composition present high uncertainties. The results show that the average absolute deviation for calculated vapor-liquid equilibrium for [emim][EtSO4] and ammonia mixture at temperature 282.7 K, 347.5 K and 372.3 K were 2.1%, 1.2% and 2.0%, respectively.

The results of the vapor-liquid equilibrium of [emim][Ac] and ammonia mixture at several temperatures are shown in Figure 3.2(b). Similar with those ammonia/[emim][EtSO4] mixture, the results of vapor-liquid equilibrium of ammonia/[emim][Ac] have good agreement with the experimental data at several temperatures. Moreover the results also present high deviations at higher temperature and low ammonia composition. The results indicate that the average absolute deviation for calculated vapor-liquid equilibrium for ammonia/[emim][Ac] mixture at all temperature range is 4.1%.

(a)
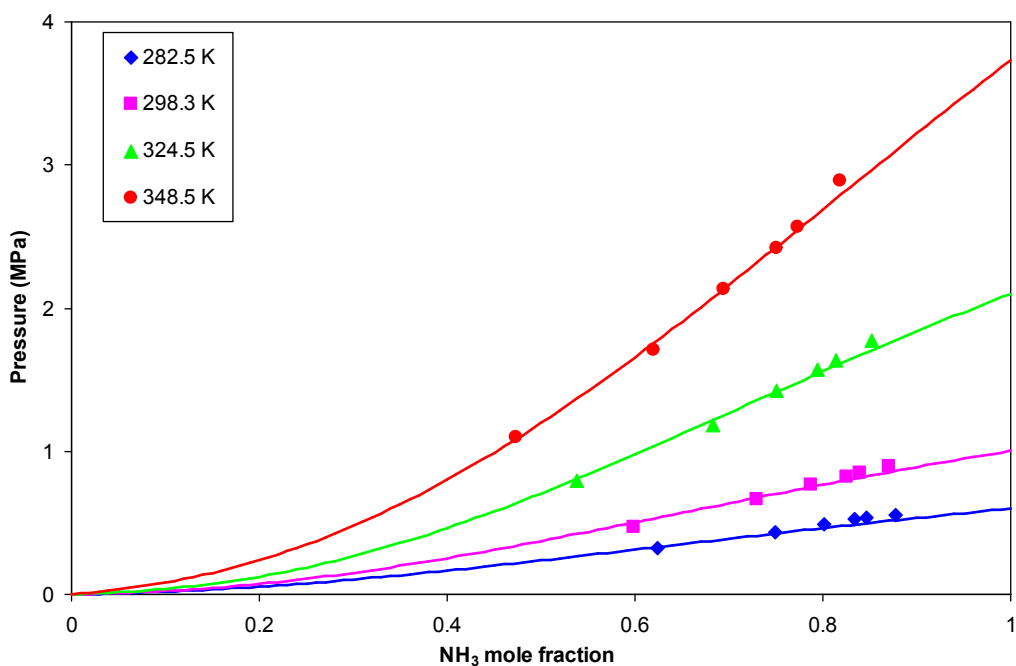
(b)

Figure 3.2. Vapor-liquid equilibrium of ammonia and [emim] based ionic liquid mixtures at different temperatures. (a) [emim][EtSO$_4$] and (b) [emim][Ac]

Figures 3.3 present the calculate results of vapor-liquid equilibrium of other [emim] based ionic liquid with ammonia using NRTL model. The vapor-liquid

equilibrium of two ionic liquid and ammonia mixtures, [emim][NTf$_2$] and [emim][SCN], are presented in Figure 3.3(a) and 3.3(b), respectively.

Figure 3.3(a) shows the results of the vapor-liquid equilibrium of [emim][NTf$_2$] and ammonia mixture at several temperatures. From this figure it can be seen that the results at several temperatures have good agreement with the experimental data. The results indicate that the average absolute deviation for calculated vapor-liquid equilibrium for [emim][NTf$_2$] and ammonia mixture at all temperature range was 8.9%, which was relatively higher than other ammonia/ionic liquid mixtures. This relatively high deviation was due to high deviation that occurs particularly in low ammonia composition and high temperature. It was also observed that the average absolute deviations have slightly higher values at temperature of 347.6 K, which presented the average deviation of 11.5%. However the high deviations at higher temperature and low ammonia composition were also acceptable considering the overall average deviation was less than 10% and the experimental data at higher temperature and low ammonia composition present high uncertainties (in this case the uncertainty was up to 18% for some data). The results show that the average absolute deviation for calculated vapor-liquid equilibrium for ammonia/[emim][NTf$_2$] mixture at temperature 283.3 K, 299.4 K and 323.4 K were 7.9%, 6.9% and 9.1%, respectively.

The results of the vapor-liquid equilibrium of ammonia/[emim][SCN] mixture at several temperatures are shown in Figure 3.3(b). Similar with other ammonia/ionic liquid mixture, the results of vapor-liquid equilibrium of ammonia/[emim][SCN] have good agreement with the experimental data at several temperatures. The results indicate that the average absolute deviation for calculated vapor-liquid equilibrium for ammonia/[emim][SCN] mixture at all temperature range is 5.0%.Moreover the results also present high deviations particularly at low ammonia composition, where the uncertainty of the experimental data was quite high.
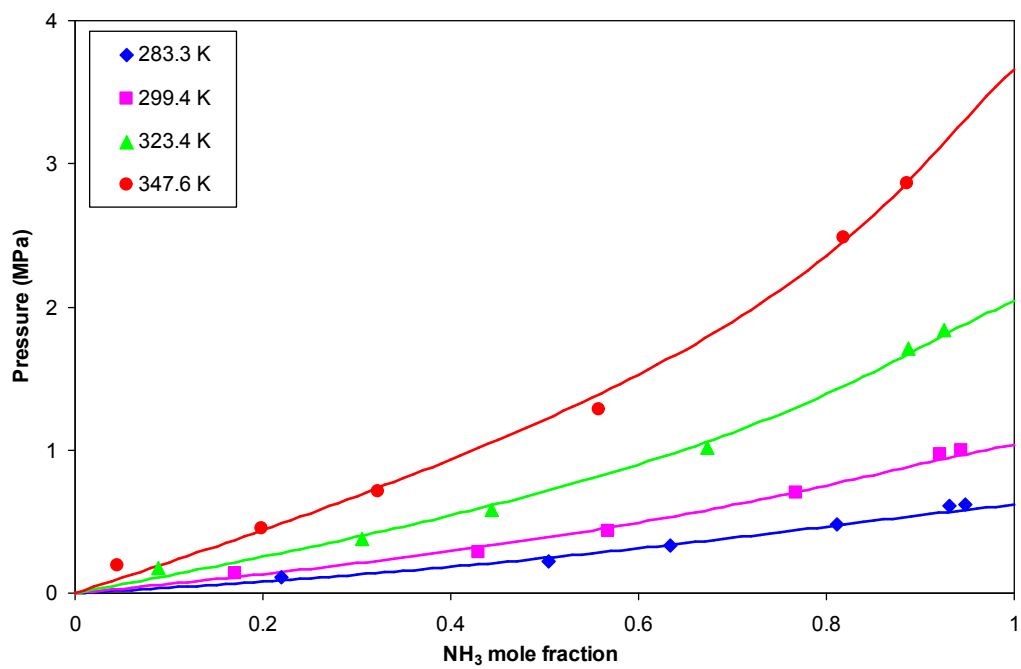
(a)
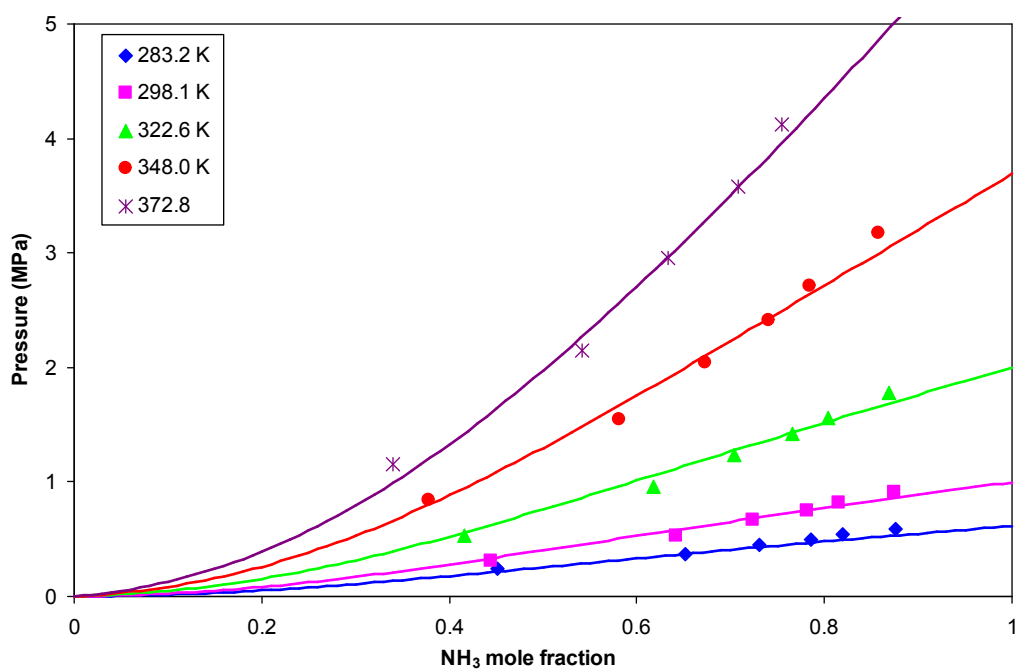
(b)

Figure 3.3. Vapor-liquid equilibrium of ammonia and [emim] based ionic liquid mixtures at different temperature. (a) [emim][NTf$_2$] and (b) [emim][SCN]

Finally, the results of the vapor-liquid equilibrium of ammonia/[hmim][Cl] and ammonia/[DMEA][Ac] mixtures at several temperatures are shown in Figure 3.4.

Figure 3.4(a) shows the results of the vapor-liquid equilibrium of ammonia/[hmim][Cl] mixture at several temperatures. The results indicate that the average absolute deviation for calculated vapor-liquid equilibrium of ammonia/[hmim][Cl] mixture at all temperature range was 8.0%, which can be considered in good agreement as compared with the experimental data. Again, the relatively high deviation was observed particularly in low ammonia composition and high temperature. It was also observed that the average absolute deviations have slightly higher values at temperature of 324.3 K, which presented the average deviation of 11.66%. The average absolute deviation for calculated vapor-liquid equilibrium for ammonia/[hmim][Cl] mixture at temperature 283.3 K, 299.4 K and 323.4 K were 7.8%, 6.7% and 5.7%, respectively.

The results of the vapor-liquid equilibrium of ammonia/[DMEA][Ac] mixture at several temperatures are shown in Figure 3.4(b). Similar with those of ammonia/[hmim][Cl] mixture, it is interested to see at the figure that the results have good agreement with the experimental data. The average absolute deviation for calculated vapor-liquid equilibrium of ammonia/[DMEA][Ac] mixture at all temperature ranges was 4.9%. Generally, the results of the vapor-liquid equilibrium of ammonia/[DMEA][Ac] mixture have better agreement with the experimental data as compared with those [bmim][BF_4] and ammonia mixture.
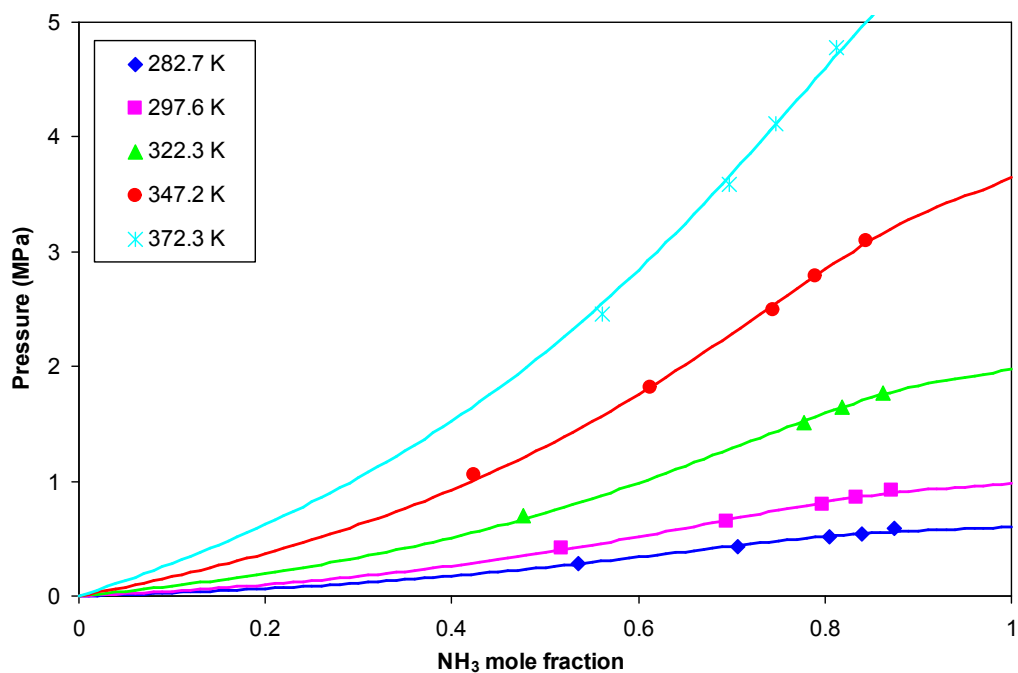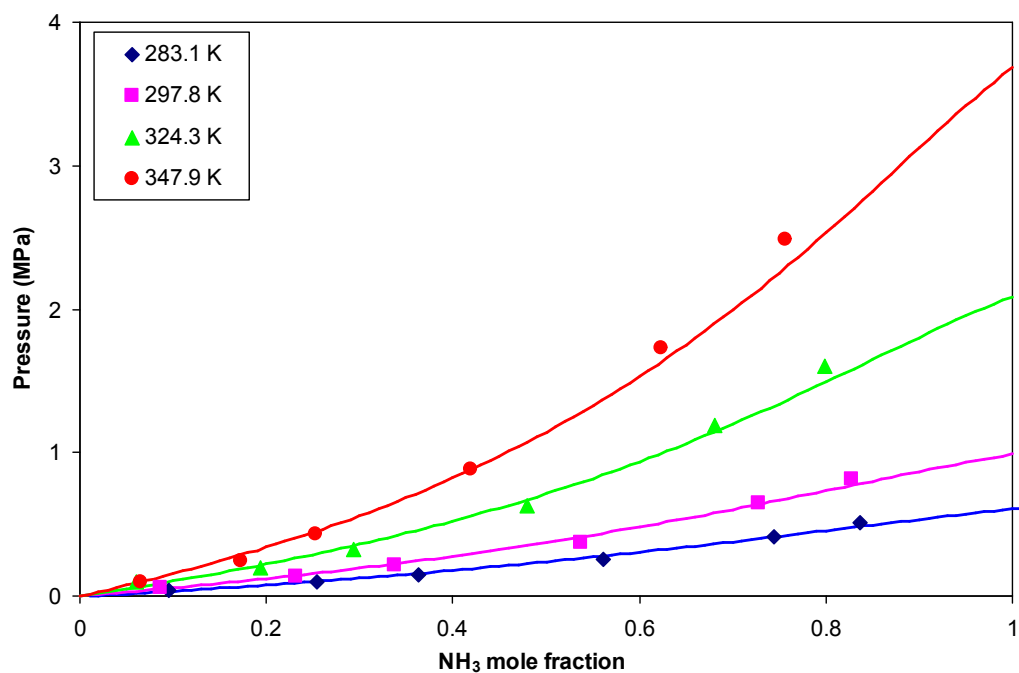
(a)
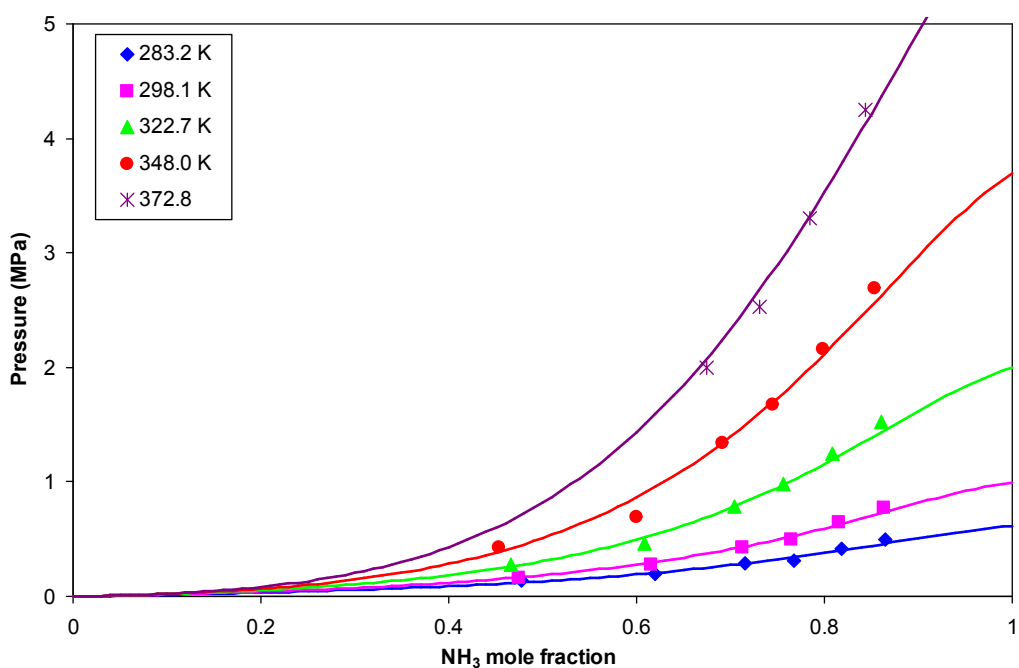
(b)

Figure 3.4. Vapor-liquid equilibrium of ammonia and [hmim] and [DMEA] based ionic liquid mixtures at different temperature. (a) [hmim][Cl] and (b) [DMEA][Ac]

3.2.2.2. Excess Properties of Ammonia/Ionic Liquid Mixtures

The calculated molar excess enthalpy, entropy, and Gibbs energy for the investigated working mixtures at temperature of 298.15 K are shown on Figure 3.5 up to Figure 3.8. From these figures it can be seen that the excess enthalpy for all studied mixture were negative. Such bonding is so strong or so numerous that H^E is more negative than TS^E, and thus G^E is negative; these mixtures are stable and do not form two liquid phases [6].
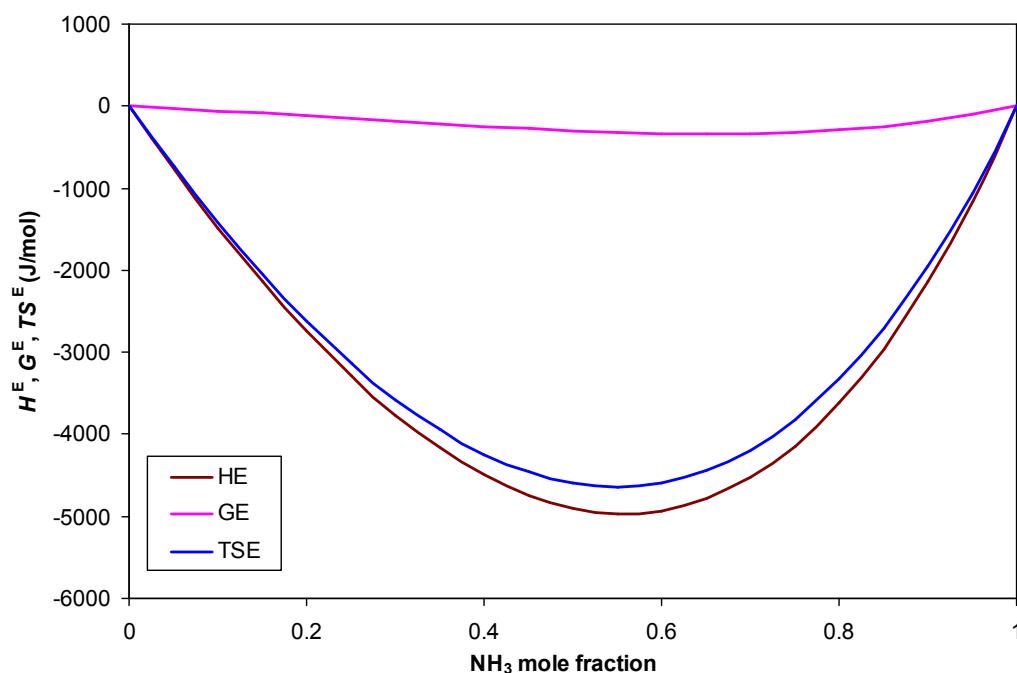
Figure 3.5. Excess enthalpy, free Gibbs energy, and entropy of ammonia and [bmim][BF$_4$] mixtures at temperature of 298.15 K

The results of calculated excess enthalpy, entropy, and Gibbs energy of ammonia and [bmim] based ionic liquid mixtures with NRTL model are presented in Figure 3.5 and Figure 3.6. Figure 3.5 shows the results of calculated excess enthalpy, entropy, and Gibbs energy of [bmim][BF$_4$] and ammonia mixture at temperature of 298.15 K. From that figure it can be seen that the minimum excess enthalpy was about 5 kJ/mole. The results of calculated excess enthalpy, entropy, and Gibbs energy of [bmim][PF$_6$] and ammonia mixture at at temperature of 298.15 K are shown in Figure 3.6. Lower than those of [bmim][BF$_4$] and ammonia mixture, from that figure it can be seen that the minimum excess enthalpy was about 2 kJ/mole.
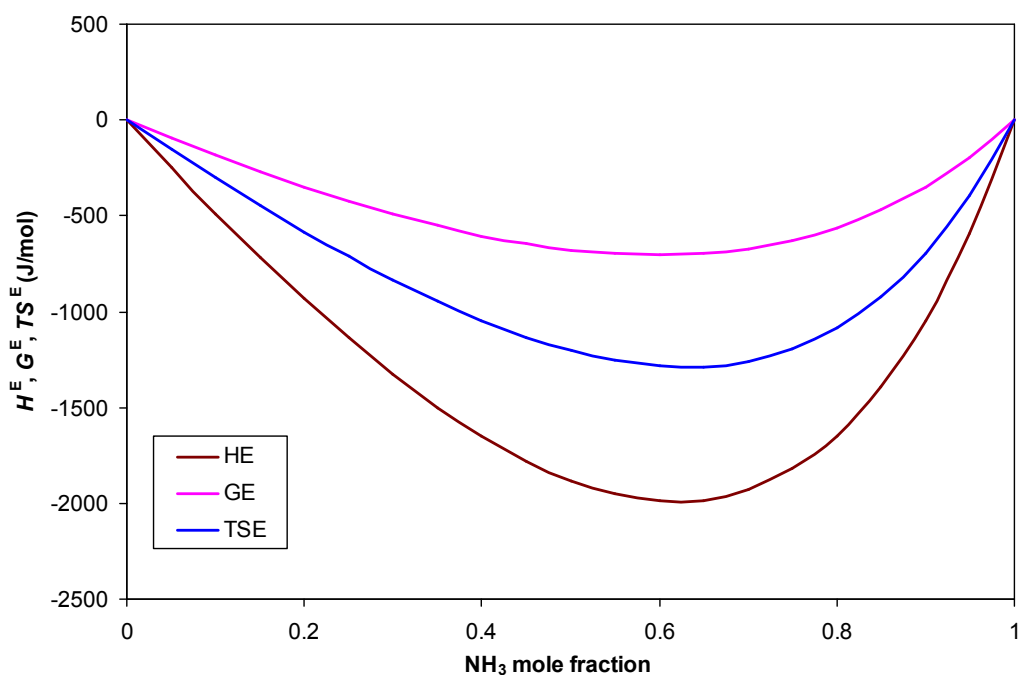
Figure 3.6. Excess enthalpy, free Gibbs energy, and entropy of ammonia and [bmim][PF$_6$] mixtures at temperature of 298.15 K

Figure 3.7 presents the results of calculated excess enthalpy, entropy, and Gibbs energy of ammonia and [emim] based ionic liquid mixtures using NRTL model. Figure 3.7(a) shows the results of calculated excess enthalpy, entropy, and Gibbs energy of [emim][EtSO$_4$] and ammonia mixture at temperature of 298.15 K. From these figures, it can be seen that the trends for excess properties are quite similar with those of [bmim] based ionic liquid mixtures. The maximum excess enthalpy was about 6.7 kJ/mole. The results of calculated excess enthalpy, entropy, and Gibbs energy of [emim][Ac] and ammonia mixture at at temperature of 298.15 K are shown in Figure 3.7(b). Lower than those of [emim][Ac] and ammonia mixture, from that figure it can be seen that the maximum excess enthalpy was about 5 kJ/mole.
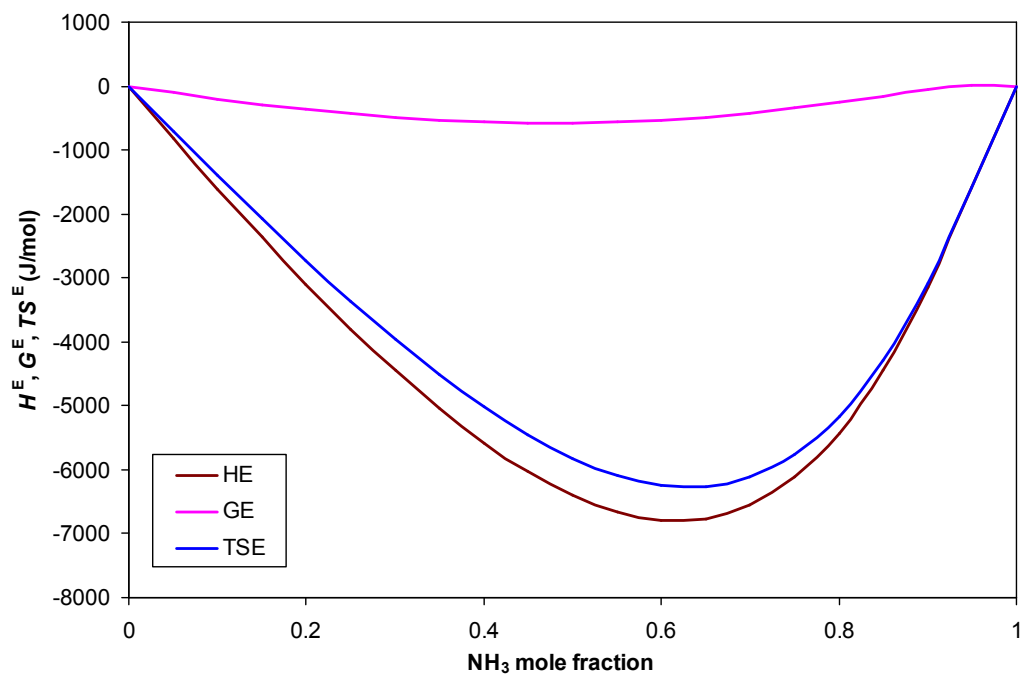
(a)
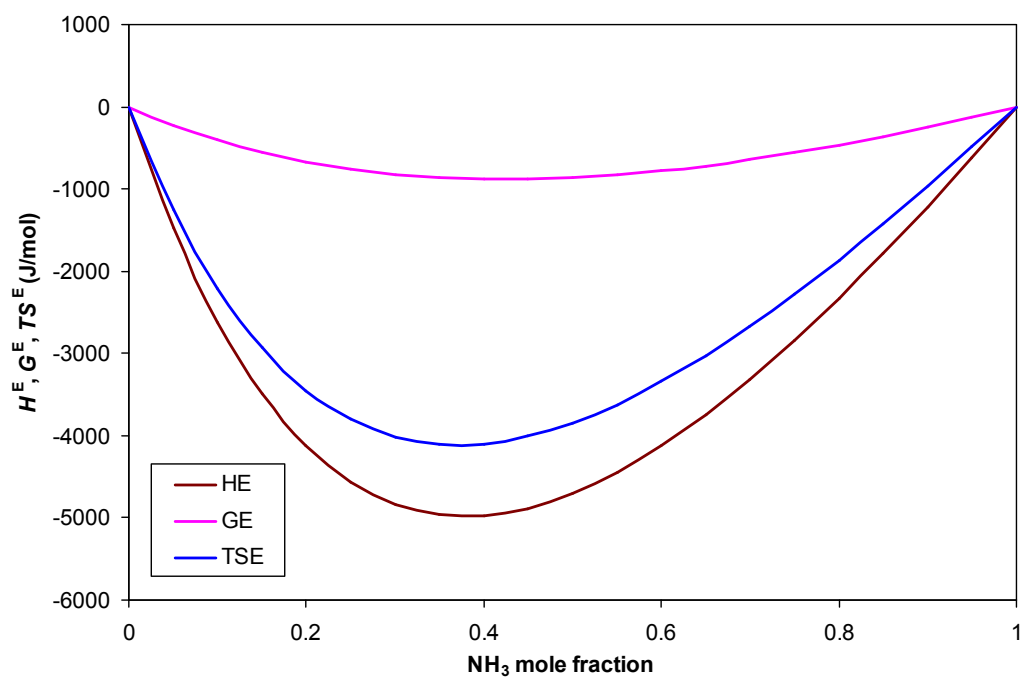
(b)

Figure 3.7. Excess enthalpy, free Gibbs energy, and entropy of ammonia and [emim] based ionic liquid mixtures at temperature of 298.15 K. (a) [emim][EtSO4] and (b) [emim][Ac]

Figure 3.8 and 3.9 present the results of calculated excess enthalpy, entropy, and Gibbs energy of other two ammonia and [emim] based ionic liquid mixtures using NRTL model. Figure 3.8 shows the results of calculated excess enthalpy, entropy, and Gibbs energy of [emim][NTf$_2$] and ammonia mixture at temperature of 298.15 K. From these figures, it can be seen that the maximum excess enthalpy was about 0.9 kJ/mole.
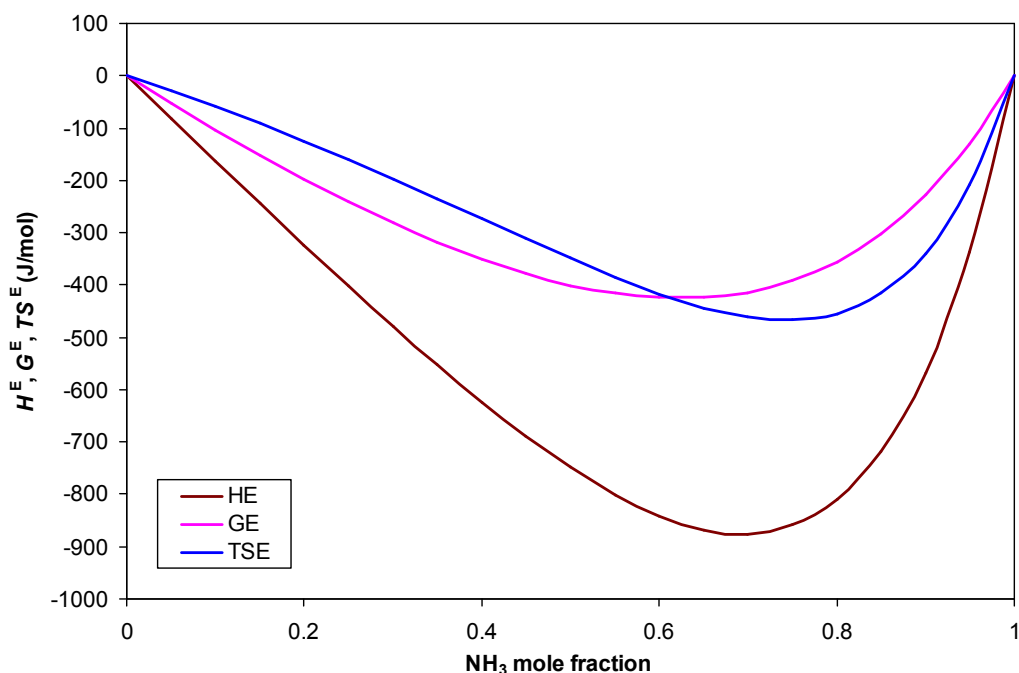
Figure 3.8. Excess enthalpy, free Gibbs energy, and entropy of ammonia and [emim][NTf$_2$] mixtures at temperature of 298.15 K

The results of calculated excess enthalpy, entropy, and Gibbs energy of [emim][SCN] and ammonia mixture at at temperature of 298.15 K are shown in Figure 3.9. It is interesting to observe that at lower ammonia composition, (i.e ammonia mole fraction < 0.5) the excess enthalpy was negative which means that the mixing process is exothermic. On contrary, at higher ammonia composition, (i.e ammonia mole fraction > 0.5) the excess enthalpy was positive which means that the mixing process is endothermic. Different than other of [emim] based ionic liquid mixtures, from that figure it can be seen that the excess enthalpy was ranged between -0.2 kJ/mole and 0.05 kJ/mole.
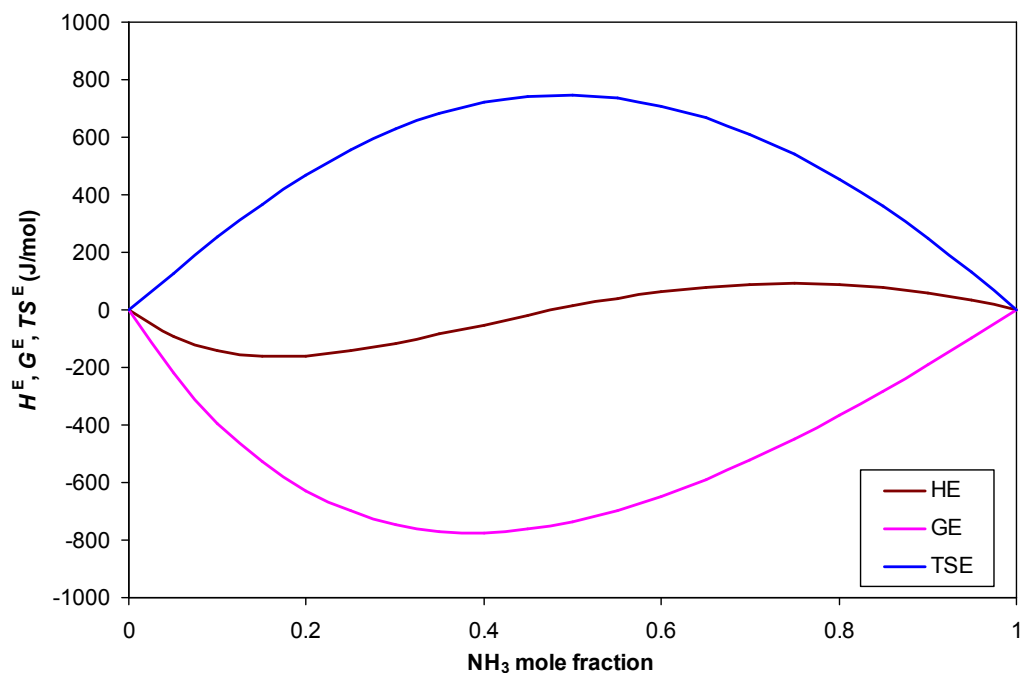
Figure 3.9. Excess enthalpy, free Gibbs energy, and entropy of ammonia and [emim][SCN] mixtures at temperature of 298.15 K

The results of calculated excess enthalpy, entropy, and Gibbs energy of ammonia and [hmim] and [DMEA] based ionic liquid mixtures with NRTL model are presented in Figure 3.10. Figure 3.10(a) shows the results of calculated excess enthalpy, entropy, and Gibbs energy of [hmim][Cl] and ammonia mixture at temperature of 298.15 K. From that figure it can be seen that the minimum excess enthalpy was about 2.1 kJ/mole. The results of calculated excess enthalpy, entropy, and Gibbs energy of [DMEA][Ac] and ammonia mixture at at temperature of 298.15 K are shown in Figure 3.10(b). Lower than those of [hmim][Cl] and ammonia mixture, from that figure it can be seen that the minimum excess enthalpy was about 7.2 kJ/mole.
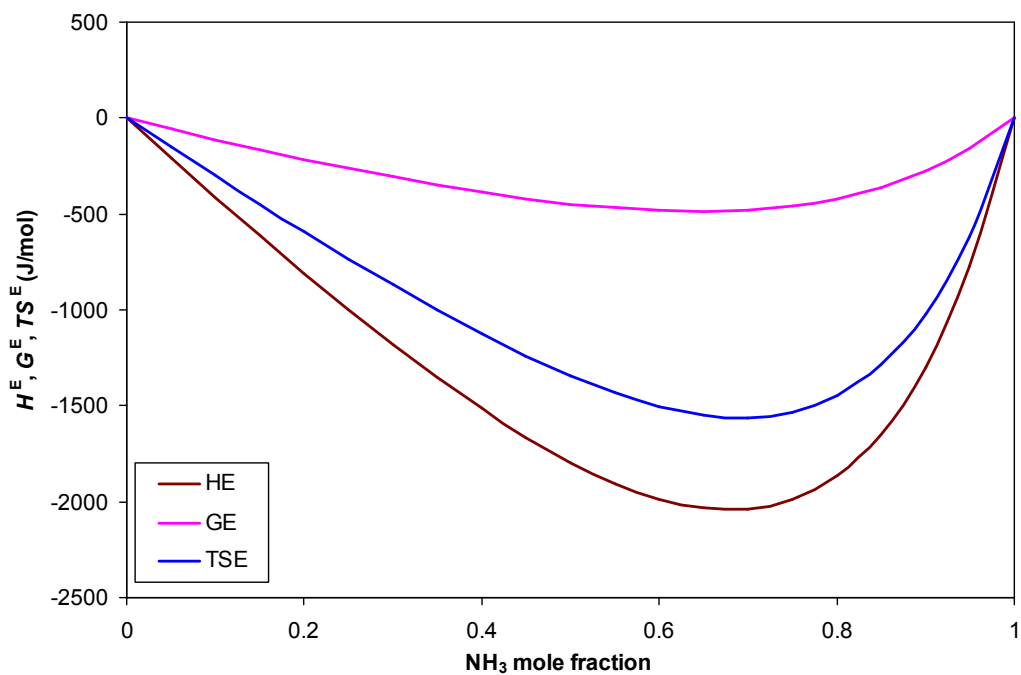
(a)
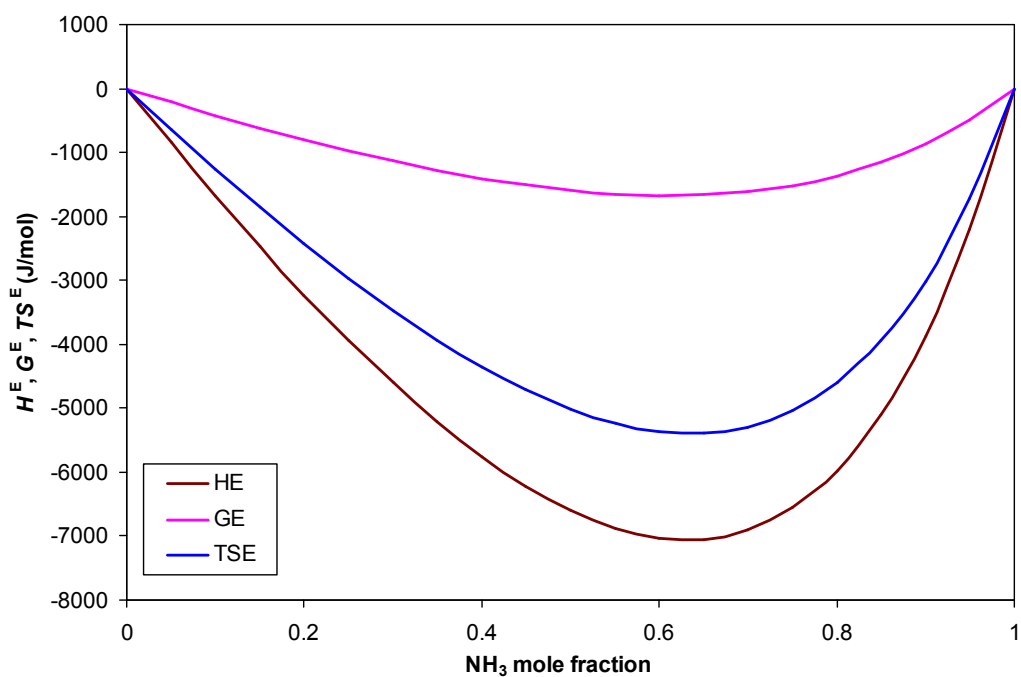
(b)

Figure 3.10. Excess enthalpy, free Gibbs energy, and entropy of ammonia and [emim] based ionic liquid mixtures at temperature of 298.15 K. (a) [hmim][Cl] and (b) [DMEA][Ac]

3.3. Reidlich-Kwong-Soave Equation of State

3.3.1. RK-Soave EOS and Its Parameters

Redlich-Kwong-Soave Equation of State (RKS-EOS) model is an equation of states based on modification of Redlich-Kwong Equation of State (RK-EOS) [8]. equation of state can be mathematically described as [9]

$$P = \frac{RT}{V_m - b} - \frac{a}{V_m(V_m + b)}$$

(3.13)

where parameters a and b are expressed in Equation (3.14).

$$a = a_0 + a_1$$

$$b = \sum_i x_i b_i$$

(3.14)

Parameters a_0 is the standard quadratic mixing term and a_1 is an additional asymmetric (polar) term, both are expressed in Equation (3.15).

$$a_0 = \sum_{i=1}^{n} \sum_{j=1}^{n} x_i x_j \sqrt{a_i a_j}\left(1 - k_{ij}\right)$$

(3.15)

$$a_1 = \sum_{i=1}^{n} x_i \left(\sum_{j=1}^{n} x_j \left((a_i a_j)^{1/2} l_{ji}\right)^{1/3} \right)^3$$

The parameter a_i in Equation (3.15) an b_i in Equation (3.14) are pure component parameters based on critical properties of each pure component and are given by eq. (3.16)

$$a_i = 0.42747 \frac{R^2 T_{ci}^{\ 2}}{P_{ci}} \alpha_i$$

$$\alpha_i = 1$$

(3.16)

$$b_i = 0.08664 \frac{RT_{ci}}{P_{ci}}$$

In addition, the parameter k_{ij} in Equation (3.15) and l_{ij} in Equation (3.14) are optimum binary interaction parameters, which can be described in Equation (3.17) and (3.18)

$$k_{ij} = k_{ij}^{(1)} + k_{ij}^{(2)}T + k_{ij}^{(2)}/T$$

$$\text{and}$$

$$k_{ij} = k_{ji} \qquad k_{ii} = 0$$

(3.17)

$$l_{ij} = l_{ij}^{(1)} + l_{ij}^{(2)}T + l_{ij}^{(2)}/T$$

$$\text{and}$$

$$l_{ij} \neq l_{ji} \qquad l_{ii} = 0$$

(3.18)

Equation (3.16) shows that to be able to model a mixture using RK-Soave EOS, it is necessary to provide critical properties of each component. However, as several authors have indicated, most ionic liquids start to decompose at low temperature and in many cases at temperatures approaching the normal boiling point [10-11]. Therefore, critical properties cannot be measured [10]. Since experimental data do not exist, the "fictional" critical properties are then necessary to fulfill the missing critical parameters for ionic liquids. These fictional critical properties are estimated using group contribution method as proposed by Valderrama et al [10].

Moreover, in order calculate derived properties from equation of states, such excess properties and the property changes, the residual properties equation are used. The residual property is the difference values between ideal gas properties and real gas properties which may be mathematically written in Equation (3.19).

$$\Delta M' = M^{ig} - M$$

(3.19)

The residual enthalpy and entropy can be derived from RK-Soave EOS using Equation (3.20) and (3.21) [6, 12].

$$\Delta H' = \left(\frac{T}{b} \frac{da}{dT} - \frac{a}{b} \right) \ln \frac{V}{V+b} + RT(1-Z)$$

(3.20)

$$\Delta S' = \frac{1}{b} \frac{da}{dT} \ln \frac{V}{V+b} + RT \ln \frac{RT}{P(V-b)}$$

(3.21)

The temperature derivative of the a parameter can be written in Equation (3.22).

$$\frac{da}{dT} = \sum_{i=1}^{N} \sum_{j=1}^{N} (0.5 A_1 A_2 A_3)(1 - k_{ij}) x_i x_j$$

(3.22)

The symbols $A_1 - A_3$ are defined in Equation (3.23) – (3.25).

$$A_1 \equiv (a_i a_j)^{-0.5} \qquad (3.23)$$

$$A_2 \equiv a_j \frac{da_i}{dT} + a_i \frac{da_j}{dT} \qquad (3.24)$$

$$A_3 \equiv 1 \qquad (3.25)$$

The terms $\frac{da_i}{dT}$ (i=i or j) in Equation (3.24) is given by Equation (3.26)

$$\frac{da_i}{dT} = 0.42747 \frac{R^2 T_{ci}^2}{P_{ci}} \qquad (3.26)$$

Hence the excess properties and be written using the residual properties obtained above, using Equation (3.27) – (3.29).

$$\frac{H^E}{RT} = \sum_{i=1}^{N} x_i \frac{\Delta H_i'}{RT} - \frac{\Delta H'}{RT} \qquad (3.27)$$

$$\frac{S^E}{R} = \sum_{i=1}^{N} x_i \frac{\Delta S_i'}{R} - \frac{\Delta S'}{R} \qquad (3.28)$$

$$\frac{G^E}{RT} = \frac{H^E}{RT} - \frac{S^E}{R} \qquad (3.29)$$

The absolute average deviation is calculated using Equation (3.12).

3.3.2. Results and Discussion

3.3.2.1 RK-Soave Parameters

The RK-Soave EOS parameters were obtained from experimental VLE data regression. The detail results of critical parameters of pure ionic liquids and pure ammonia are given in the Table 3.2.

Table 3.2. Critical properties of ionic liquids and ammonia [Ref]

Compound	*MW*	P_c (bar)	T_c (K)	ω
[bmim][BF$_4$]	226.0	20.38	643.2	0.8877
[bmim][PF$_6$]	284.2	17.28	719.4	0.7917
[emim][NTf$_2$]	391.3	32.65	1249.3	0.2157
[hmim][Cl]	202.7	23.50	829.2	0.5725
[emim][EtSO$_4$]	236.3	40.46	1067.5	0.3744
[emim][Ac]	170.2	29.19	807.1	0.5889
[emim][SCN]	169.3	22.26	1013.6	0.3931
[DMEA][Ac]	149.2	32.93	724.4	0.8619
ammonia	17.0	112.80	405.7	0.2526

The optimimum binary parameter of k_{ij} obtained from vapor-liquid equilibrium data regression are presented in Table 3.3.

Table 3.3. Binary parameter of k_{ij} for present EOS

Compound	$k_{ij}^{(1)}$	$k_{ij}^{(2)}$	$k_{ij}^{(3)}$
[bmim][BF$_4$]	-1.6777	0.0027	230.1002
[bmim][PF$_6$]	-4.9642	0.0070	800.3859
[emim][Ac]	-1.2196	0.0017	179.1004
[emim][EtSO$_4$]	-0.0471	-0.0002	10.4112
[emim][SCN]	1.6230	-0.0027	-282.2980
[emim][Tf2N]	-0.5664	0.0008	64.2152
[hmim][Cl]	-3.5871	0.0053	553.2724
[DMEA][Ac]	-3.2504	0.0041	537.6193

Moreover, the optimimum binary parameter of l_{ij} obtained from vapor-liquid equilibrium data regression are presented in Table 3.4.

Table 3.4. Binary parameter of l_{ij} for present EOS

Compound	$l_{ij}^{(1)}$	$l_{ji}^{(1)}$	$l_{ij}^{(2)}$	$l_{ji}^{(2)}$	$l_{ij}^{(3)}$	$l_{ji}^{(3)}$
[bmim][BF$_4$]	4.0660	-2.3550	-0.0077	0.0038	-560.79	338.89
[bmim][PF$_6$]	-47.4068	-14.3529	0.0736	0.0207	7473.16	2366.58
[emim][Ac]	-0.3595	-0.2162	0	0	0	0
[emim][EtSO$_4$]	-0.3115	-0.1787	0	0	0	0
[emim][SCN]	19.4296	6.9755	-0.0288	-0.0115	-3382.49	-1123.56
[emim][N Tf$_2$]	-0.8930	5.8574	0.0020	-0.0089	43.03	-1055.35
[hmim][Cl]	-8.5509	-9.3684	0.0126	0.0157	1366.84	1350.94
[DMEA][Ac]	-0.7007	-0.3135	0	0	0	0

3.3.2.2 Vapor-Liquid Equilibrium of Ammonia and Ionic Liquid Mixtures

After obtaining the all parameters of ammonia/ionic liquid mixtures for present cubic equation of state, the next sequence is to analyse and study the ability of RK-Soave EOS model to calculat the vapor-liquid equilibrium of ammonia and ionic liquid mixture. In this subsection, the vapor-liquid equilibrium of some [bmim] based ionic liquid and ammonia mixtures and [emim] based ionic liquid and ammonia mixtures were studied and calculated using RK-Soave EOS. In addition, the vapor-liquid equilibrium calculation of [hmim][Cl] and [DMEA][Ac] was also studied

The results of vapor-liquid equilibrium calculation of ammonia and [bmim] based ionic liquid mixtures with RK-Soave EOS model are presented in Figure 3.11. The vapor-liquid equilibrium of binary mixtures of ammonia with two ionic liquids, [bmim][BF$_4$] and [bmim][PF$_6$] were studied.

Figure 3.11(a) shows the results of the vapor-liquid equilibrium of [bmim][BF$_4$] and ammonia mixture at several temperatures. From that figure it can be seen that the results were in good agreement as compared with the experimental data. The results indicate that the average absolute deviation for calculated vapor-liquid equilibrium of ammonia/[bmim][BF$_4$] mixture at all temperature range was 1.6%.

The results of the vapor-liquid equilibrium of [bmim][PF$_6$] and ammonia mixture at several temperatures are shown in Figure 3.11(b). Similar with those of [bmim][BF$_4$] and ammonia mixture, it is interested to see at the figure that the results have good agreement with the experimental data. The average absolute deviation for calculated vapor-liquid equilibrium of [bmim][PF$_6$] and ammonia mixture at all temperature ranges was 4.3%. However, different with those of [bmim][BF$_4$] and ammonia mixture, it was observed that generally the average absolute deviations are slightly higher when compared with those [bmim][BF$_4$] and ammonia mixture.
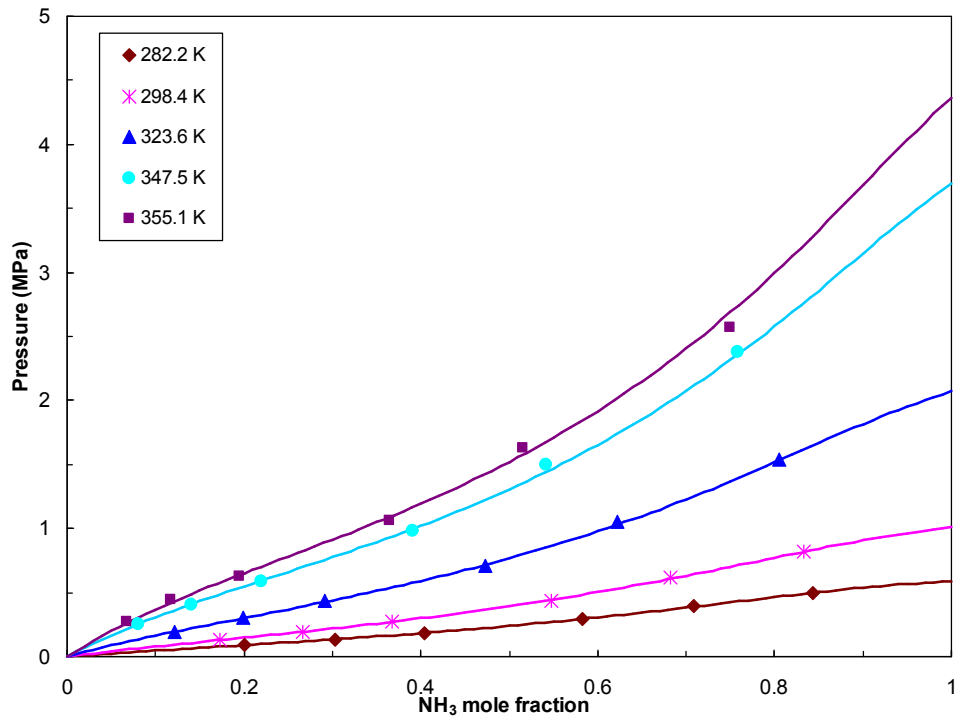
(a)
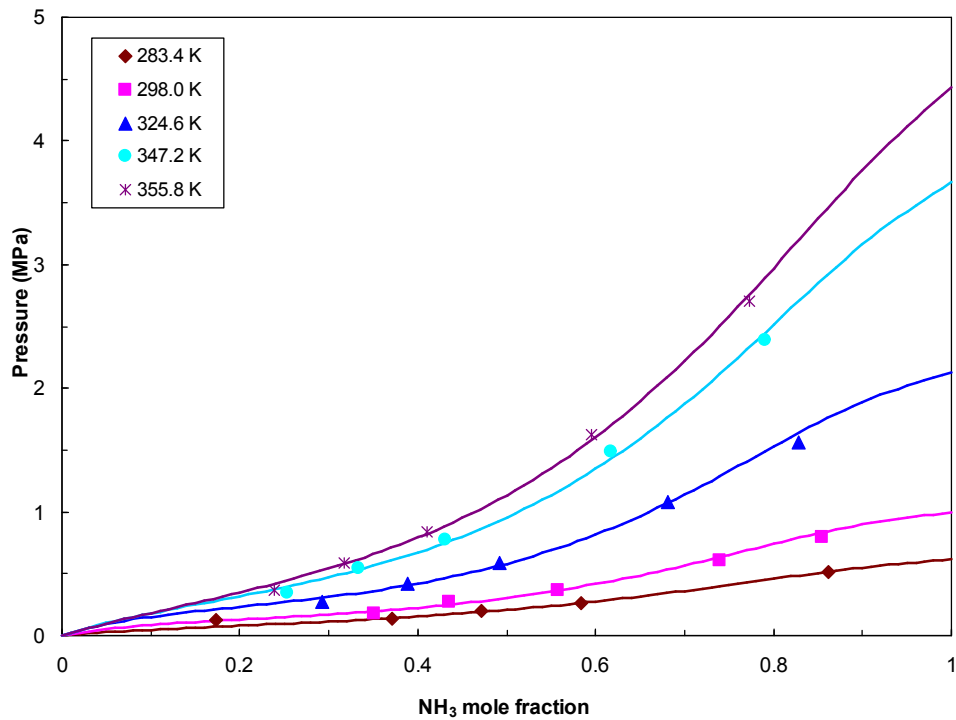
(b)

Figure 3.11. Vapor-liquid equilibrium of ammonia and [bmim] based ionic liquid mixtures at different temperatures (a) [bmim][BF$_4$] and (b) [bmim][PF$_6$].

Figures 3.12 present the results of vapor-liquid equilibrium of [emim] based ionic liquid and ammonia mixture with RK-Soave EOS model. The vapor-liquid equilibrium of two ionic liquid and ammonia mixtures, [emim][EtSO$_4$] and [emim][Ac], are studied.

Figure 3.12(a) shows the results of the vapor-liquid equilibrium of [emim][EtSO$_4$] and ammonia mixture at several temperatures. From this figure it can be seen that the results at several temperatures have good agreement with the experimental data. The results indicate that the average absolute deviation for calculated vapor-liquid equilibrium for [emim][EtSO$_4$] and ammonia mixture at all temperature range is 0.9%. It was also observed that the average absolute deviations have slightly higher values particularly at lower temperature and lower ammonia composition, such as at temperature of 282.7 K and 297.6 K. The average absolute deviation for calculated vapor-liquid equilibrium of [emim][EtSO$_4$] at temperature of 282.7 K was 1.8% and the average absolute deviation for calculated vapor-liquid equilibrium of [emim][EtSO$_4$] at temperature of 297.6 K was 1.2%. However the high deviations at higher temperature and low ammonia composition were acceptable considering the deviation was less than 10% and the experimental data at higher temperature and low ammonia composition present high uncertainties. The results show that the average absolute deviation for calculated vapor-liquid equilibrium for [emim][EtSO$_4$] and ammonia mixture at temperature 322.7 K, 347.5 K and 372.3 K were 0. 6%, 0.6% and 0.3%, respectively.
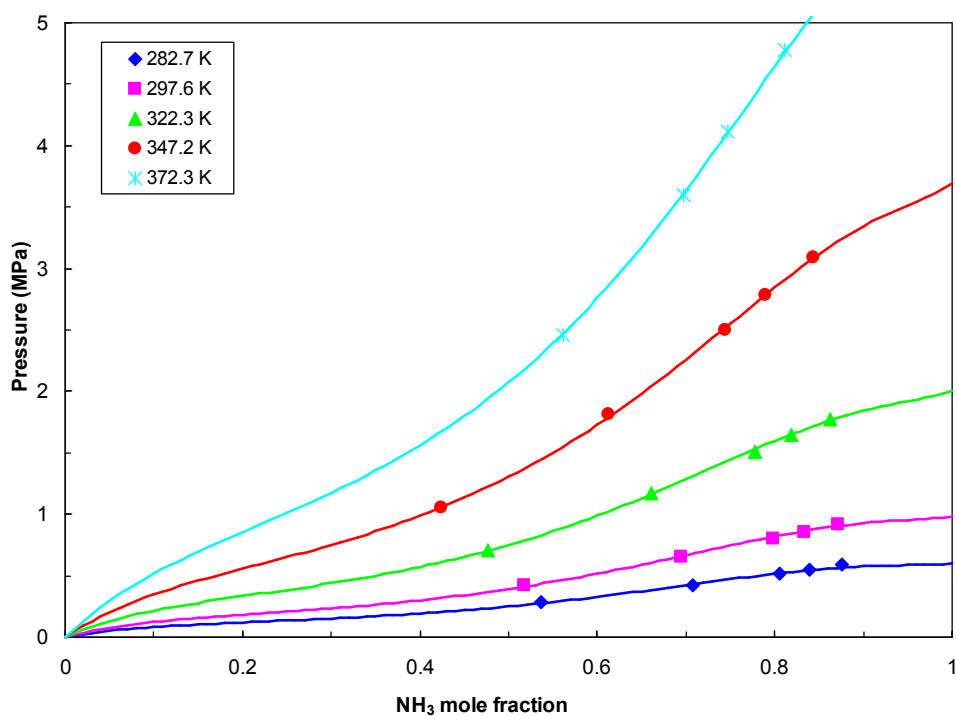
(a)
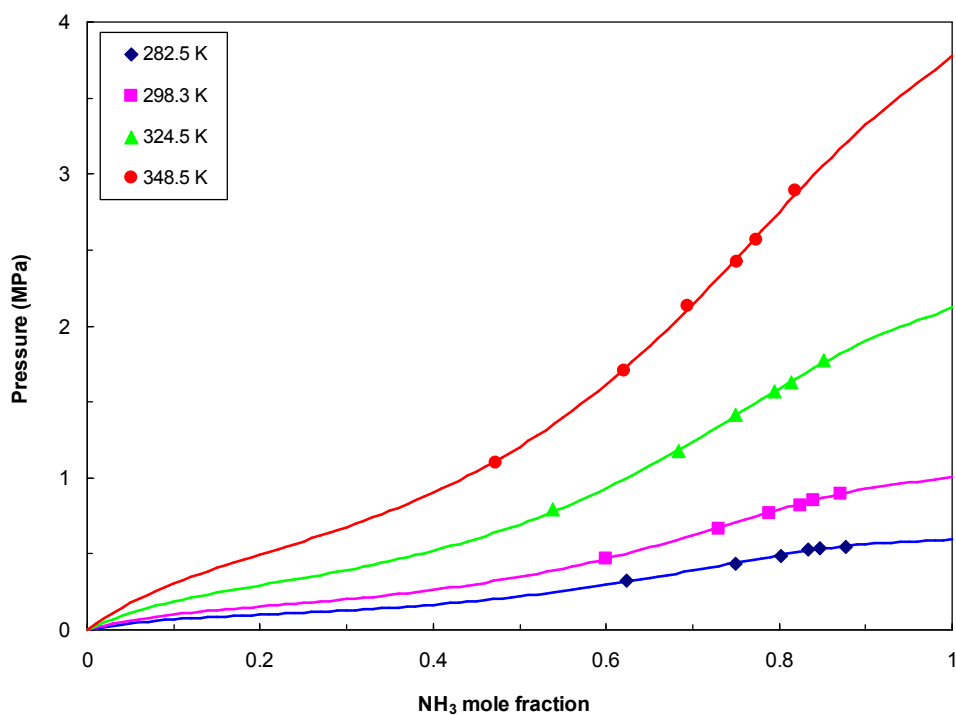
(b)

Figure 3.12. Vapor-liquid equilibrium of ammonia and [emim] based ionic liquid mixtures at different temperatures. (a) [emim][EtSO$_4$] and (b) [emim][Ac]

The results of the vapor-liquid equilibrium of [emim][Ac] and ammonia mixture at several temperatures are shown in Figure 3.12(b). Similar with those ammonia/[emim][EtSO4] mixture, the results of vapor-liquid equilibrium of ammonia/[emim][Ac] have good agreement with the experimental data at several temperatures. Moreover the results also present high deviations at lower temperature and low ammonia composition. The results indicate that the average absolute deviation for calculated vapor-liquid equilibrium for ammonia/[emim][Ac] mixture at all temperature range is 0.8%.

Figures 3.13 present the results of vapor-liquid equilibrium of other [emim] based ionic liquid with ammonia using RK-Soave EOS model. The vapor-liquid equilibrium of two ionic liquid and ammonia mixtures, [emim][NTf$_2$] and [emim][SCN], are presented in Figure 3.13(a) and 3.13(b), respectively.

Figure 3.13(a) shows the results of the vapor-liquid equilibrium of [emim][NTf$_2$] and ammonia mixture at several temperatures. From this figure it can be seen that the results at several temperatures have good agreement with the experimental data. The results indicate that the average absolute deviation for calculated vapor-liquid equilibrium for [emim][NTf$_2$] and ammonia mixture at all temperature range was 6.2%, which was relatively higher than other ammonia/ionic liquid mixtures. This relatively high deviation was due to high deviation that occurs particularly in low ammonia composition and high temperature. It was also observed that the average absolute deviations have slightly higher values at temperature of 347.6 K, which presented the average deviation of 16.4%. However the high deviations at higher temperature and low ammonia composition were also acceptable considering the overall average deviation was less than 10% and the experimental data at higher temperature and low ammonia composition present high uncertainties (in this case the uncertainty was up to 18% for some data). The results show that the average absolute deviation for calculated vapor-liquid equilibrium for ammonia/[emim][NTf$_2$] mixture at temperature 283.3 K, 299.4 K and 323.4 K were 2.9%, 3.7% and 1.8%, respectively.
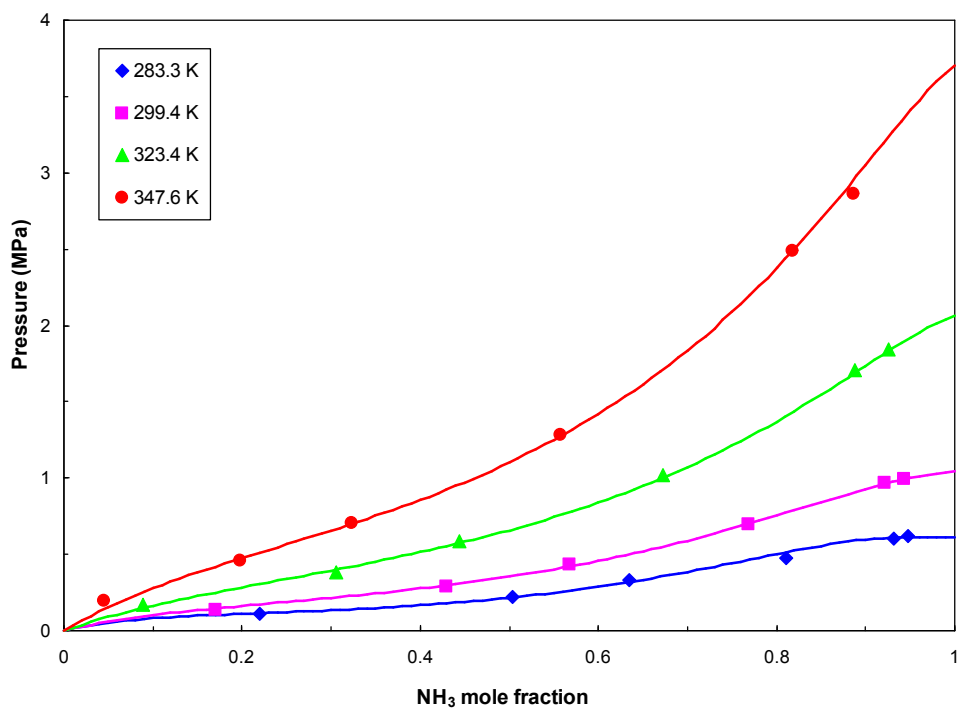
(a)
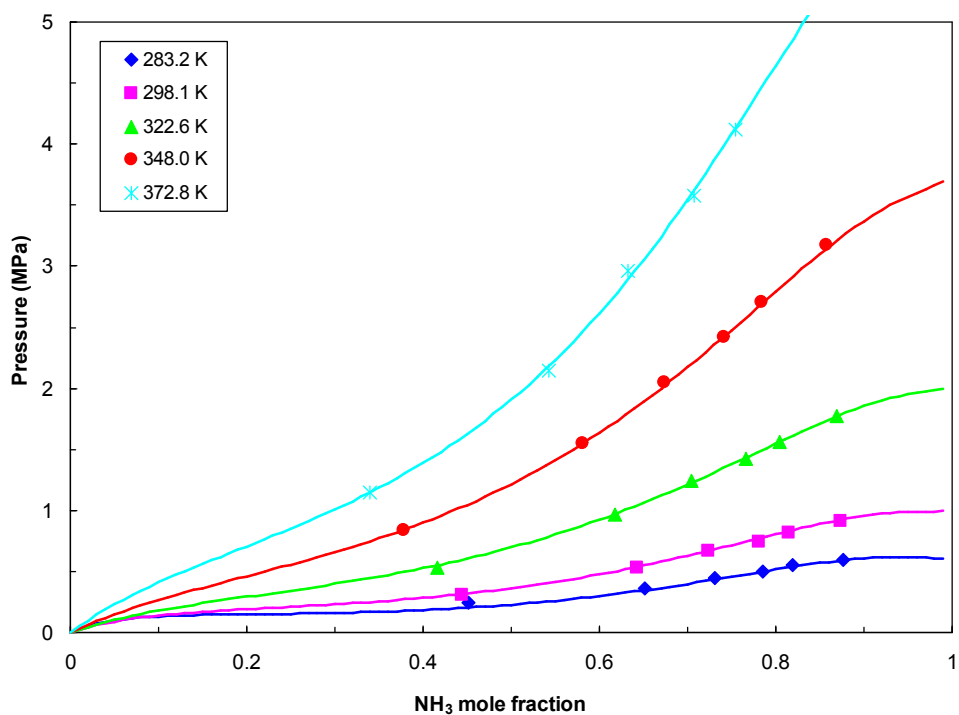
(b)

Figure 3.13. Vapor-liquid equilibrium of ammonia and [emim] based ionic liquid mixtures at different temperature. (a) [emim][NTf$_2$] and (b) [emim][SCN]

The results of the vapor-liquid equilibrium of ammonia/[emim][SCN] mixture at several temperatures are shown in Figure 3.13(b). Similar with other ammonia/ionic liquid mixture, the results of vapor-liquid equilibrium of ammonia/[emim][SCN] have good agreement with the experimental data at several temperatures. The results indicate that the average absolute deviation for calculated vapor-liquid equilibrium for ammonia/[emim][SCN] mixture at all temperature range is 1.8%.Moreover the results also present high deviations particularly at low ammonia composition, where the uncertainty of the experimental data was quite high.

Finally, the results of the vapor-liquid equilibrium of ammonia/[hmim][Cl] and ammonia/[DMEA][Ac] mixtures at several temperatures are shown in Figure 3.14. Figure 3.14(a) shows the results of the vapor-liquid equilibrium of ammonia/[hmim][Cl] mixture at several temperatures. The results indicate that the average absolute deviation for calculated vapor-liquid equilibrium of ammonia/[hmim][Cl] mixture at all temperature range was 5.2%, which can be considered in good agreement as compared with the experimental data. Again, the relatively high deviation was observed particularly in low ammonia composition. It was also observed that the average absolute deviations have slightly higher values at temperature of 324.3 K, which presented the average deviation of 8.2%. The average absolute deviation for calculated vapor-liquid equilibrium for ammonia/[hmim][Cl] mixture at temperature 283.3 K, 299.4 K and 323.4 K were 4.1%, 5.4% and 3.1%, respectively.
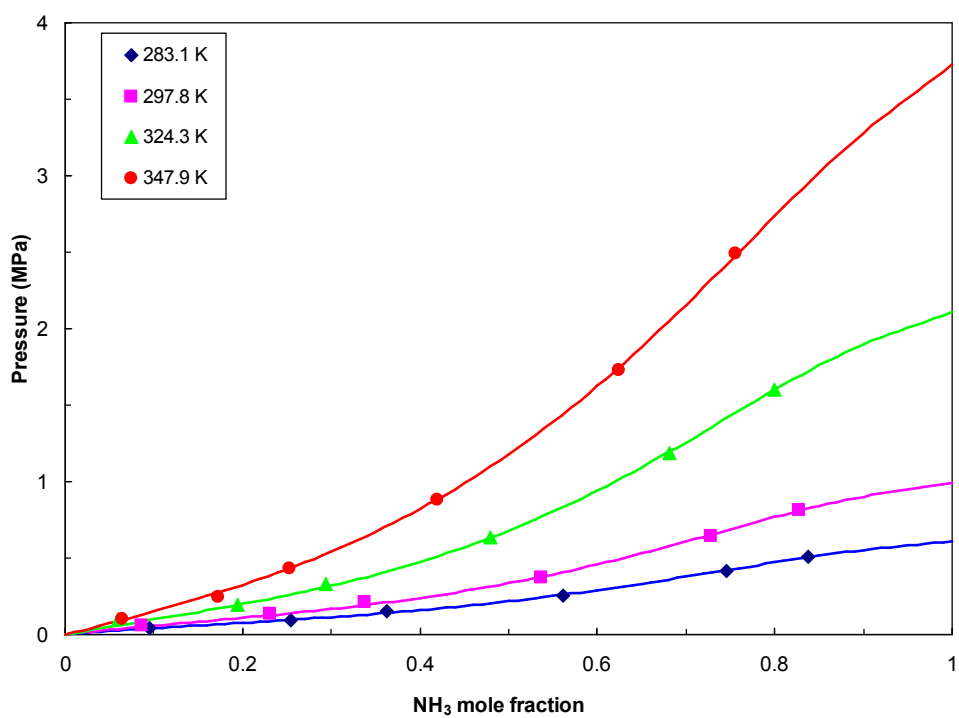
(a)
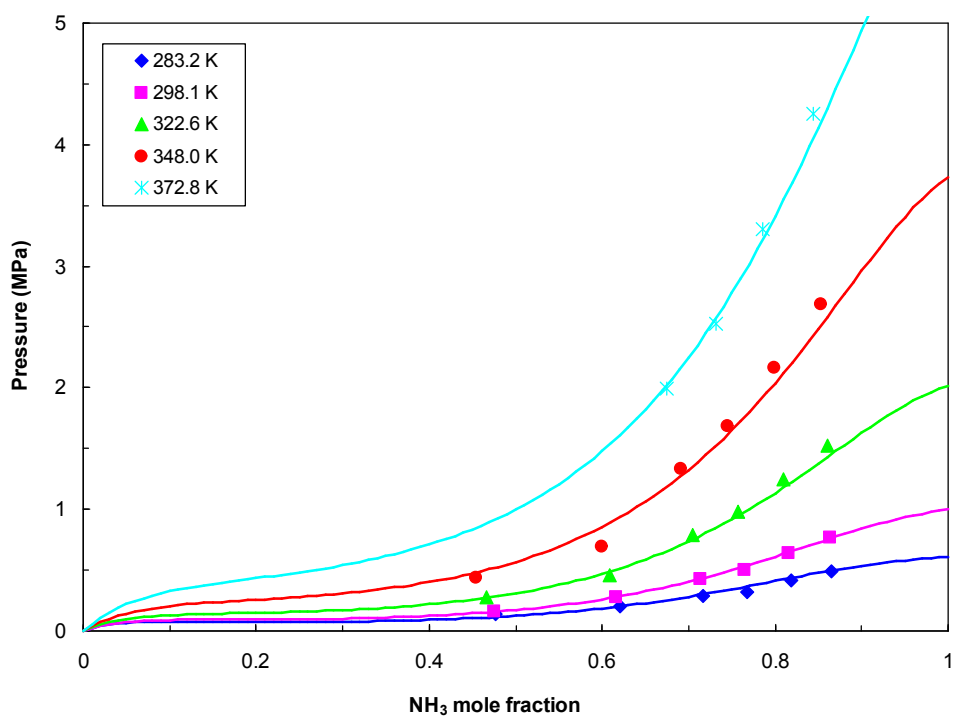
(b)

Figure 3.14. Vapor-liquid equilibrium of ammonia and [hmim] and [DMEA] based ionic liquid mixtures at different temperature. (a) [hmim][Cl] and (b) [DMEA][Ac]

The results of the vapor-liquid equilibrium of ammonia/[DMEA][Ac] mixture at several temperatures are shown in Figure 3.14(b). Similar with those of ammonia/[hmim][Cl] mixture, it is interested to see at the figure that the results have good agreement with the experimental data. The average absolute deviation for calculated vapor-liquid equilibrium of ammonia/[DMEA][Ac] mixture at all temperature ranges was 5.4%. Generally, the results of the vapor-liquid equilibrium of ammonia/[DMEA][Ac] mixture have better agreement with the experimental data as compared with those [bmim][BF$_4$] and ammonia mixture.

3.3.2.3 Excess Properties of Ammonia/Ionic Liquid Mixtures

The calculated excess enthalpy, entropy, and Gibbs energy for the investigated working mixtures at temperature of 298.15 K are shown on Figure 3.5 up to Figure 3.8.
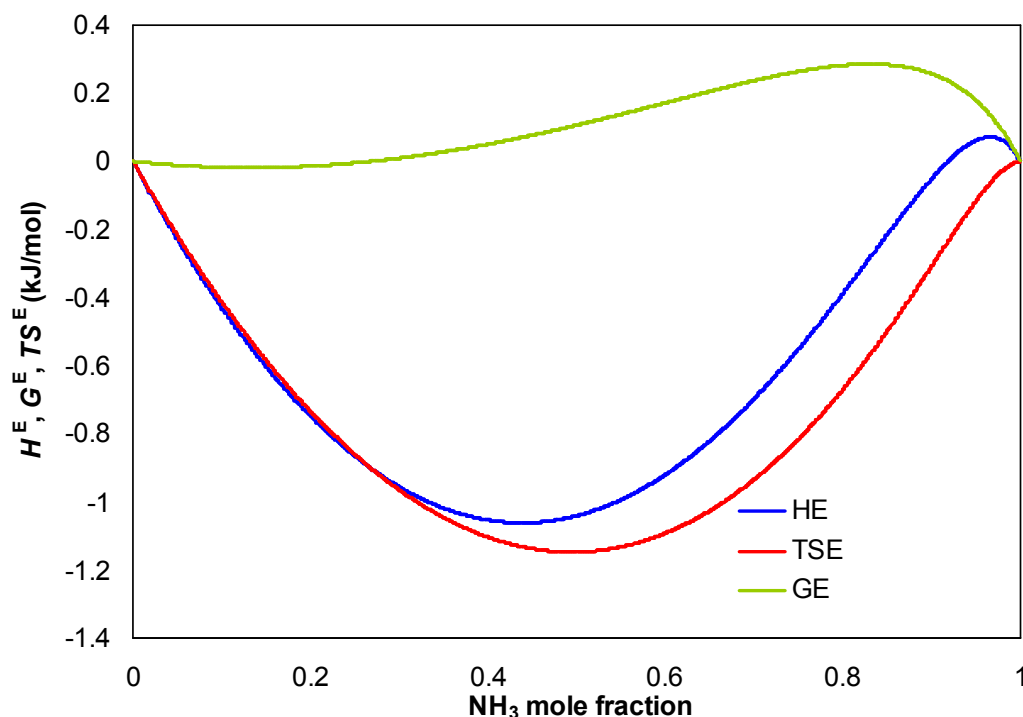
Figure 3.15. Excess enthalpy, free Gibbs energy, and entropy of ammonia and [bmim][BF$_4$] mixtures at temperature of 298.15 K

The results of calculated excess enthalpy, entropy, and Gibbs energy of ammonia and [bmim] based ionic liquid mixtures with RK-Soave EOS model are presented in Figure 3.15 and Figure 3.16. Figure 3.15 shows the results of calculated excess enthalpy, entropy, and Gibbs energy of [bmim][BF$_4$] and ammonia mixture at temperature of 298.15 K. From that figure it can be seen that the minimum excess enthalpy was about 1.18 kJ/mole. The results of calculated excess enthalpy, entropy, and Gibbs energy of [bmim][PF$_6$] and ammonia mixture at at temperature of 298.15 K are shown in Figure 3.6. Lower than those of [bmim][BF$_4$] and ammonia mixture, from that figure it can be seen that the minimum excess enthalpy was about 3 kJ/mole.
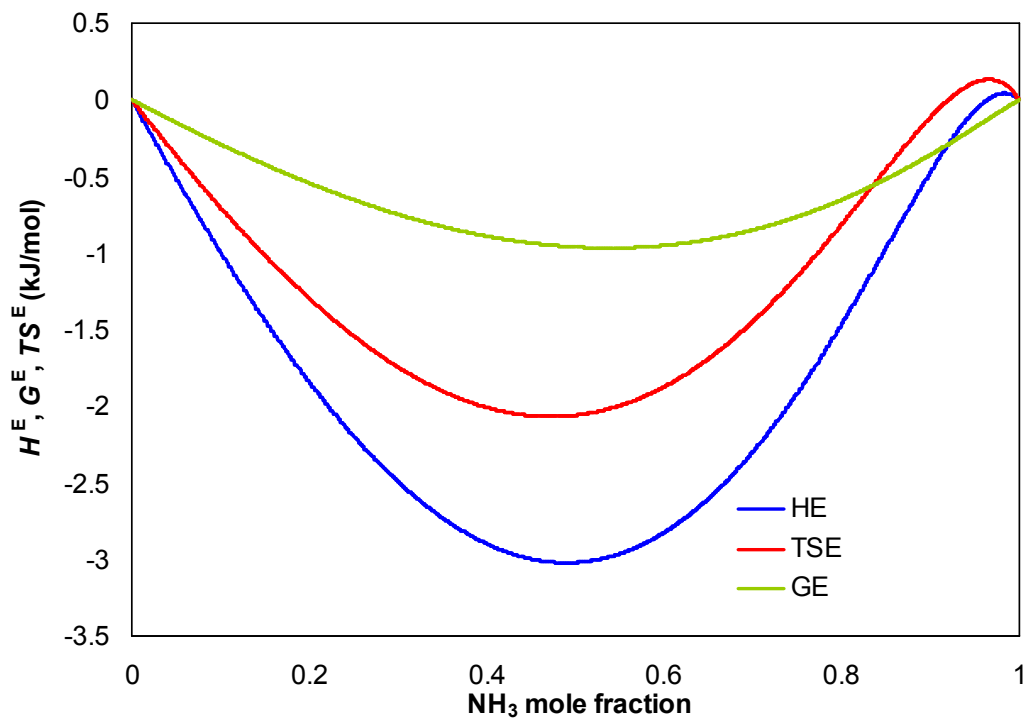
Figure 3.16. Excess enthalpy, free Gibbs energy, and entropy of ammonia and [bmim][PF$_6$] mixtures at temperature of 298.15 K
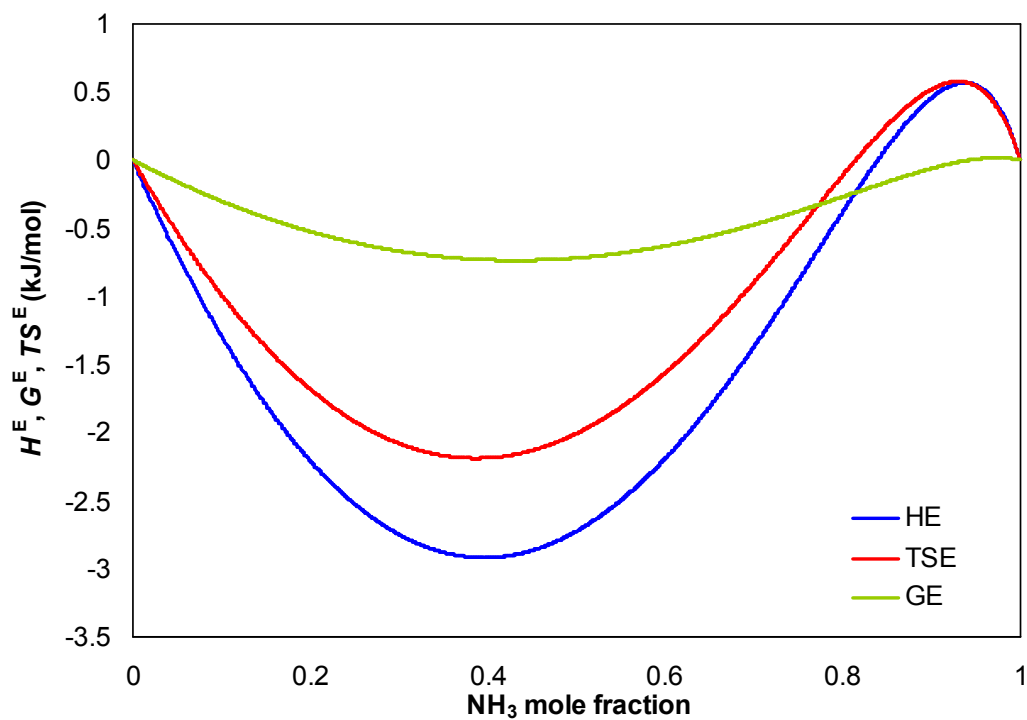
(a)
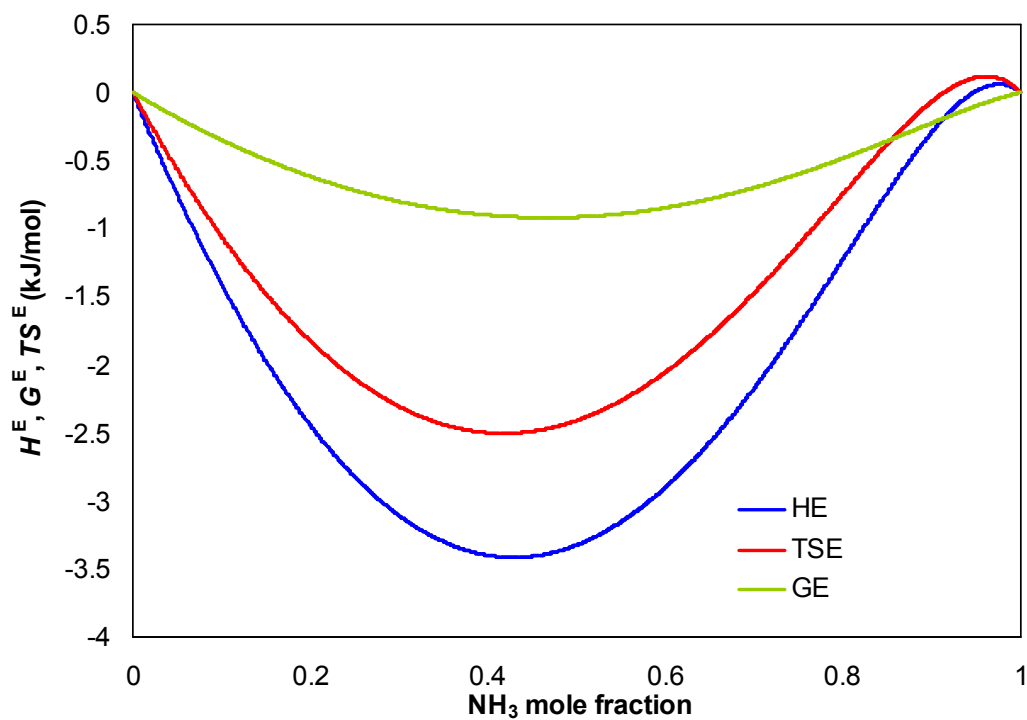
(b)

Figure 3.17. Excess enthalpy, free Gibbs energy, and entropy of ammonia and [emim] based ionic liquid mixtures at temperature of 298.15 K. (a) [emim][EtSO$_4$] and (b) [emim][Ac]

Hifni M. Ariyadi, Doctoral Thesis, Universitat Rovira i Virgili, 2016

Figure 3.17 presents the results of calculated excess enthalpy, entropy, and Gibbs energy of ammonia and [emim] based ionic liquid mixtures using RK-Soave EOS model. Figure 3.7(a) shows the results of calculated excess enthalpy, entropy, and Gibbs energy of [emim][EtSO$_4$] and ammonia mixture at temperature of 298.15 K. From these figures, it can be seen that the trends for excess properties are quite similar with those of [bmim] based ionic liquid mixtures. The maximum excess enthalpy was about 2.9 kJ/mole. The results of calculated excess enthalpy, entropy, and Gibbs energy of [emim][Ac] and ammonia mixture at at temperature of 298.15 K are shown in Figure 3.7(b). Lower than those of [emim][Ac] and ammonia mixture, from that figure it can be seen that the maximum excess enthalpy was about 3.4 kJ/mole.

Figure 3.18 and 3.19 present the results of calculated excess enthalpy, entropy, and Gibbs energy of other two ammonia and [emim] based ionic liquid mixtures using RK-Soave EOS model. Figure 3.18 shows the results of calculated excess enthalpy, entropy, and Gibbs energy of [emim][NTf$_2$] and ammonia mixture at temperature of 298.15 K. Different with other ammonia/ionic liquid mixtures, it is interesting to observe that the excess enthalpy was positive in all composition range which means that the mixing process is endothermic. In addition, there were two peaks of excess enthapy line. From these figures, it can be seen that the maximum excess enthalpy was about 1.15 kJ/mole.
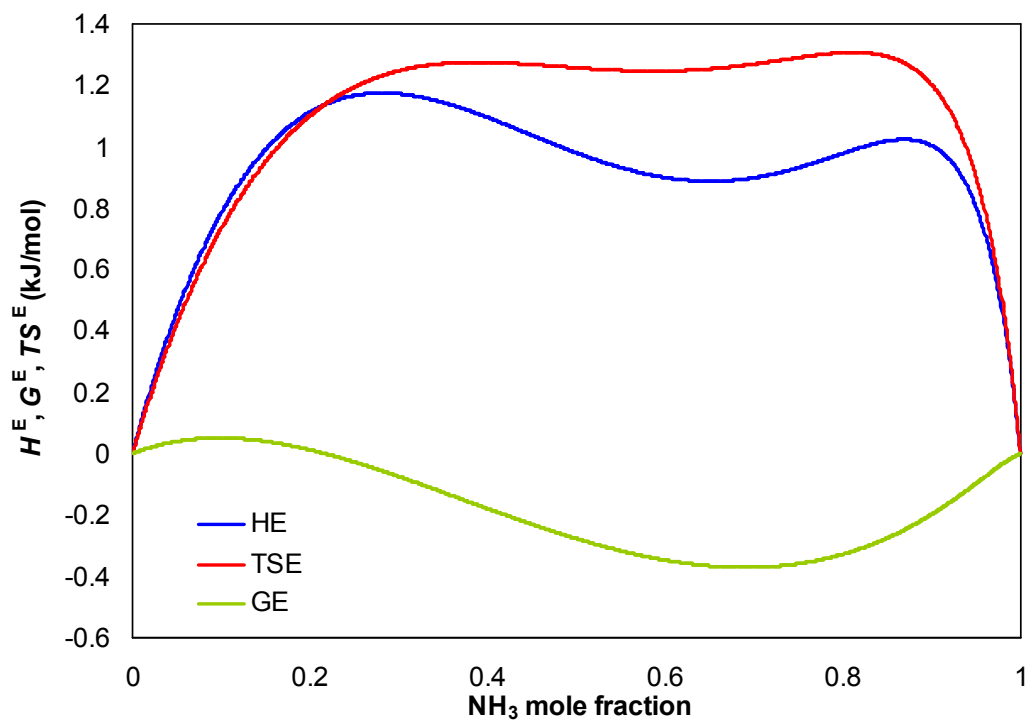
Figure 3.18. Excess enthalpy, free Gibbs energy, and entropy of ammonia and [emim][NTf$_2$] mixtures at temperature of 298.15 K

The results of calculated excess enthalpy, entropy, and Gibbs energy of [emim][SCN] and ammonia mixture at at temperature of 298.15 K are shown in Figure 3.9. Similarly with that of ammonia/[emim][NTf$_2$] mixture, it is interesting to observe that the excess enthalpy was positive in all composition range which means that the mixing process is endothermic. In addition, there were two peaks of excess enthapy line. The maximum excess enthalpy was about 0.95 kJ/mole.
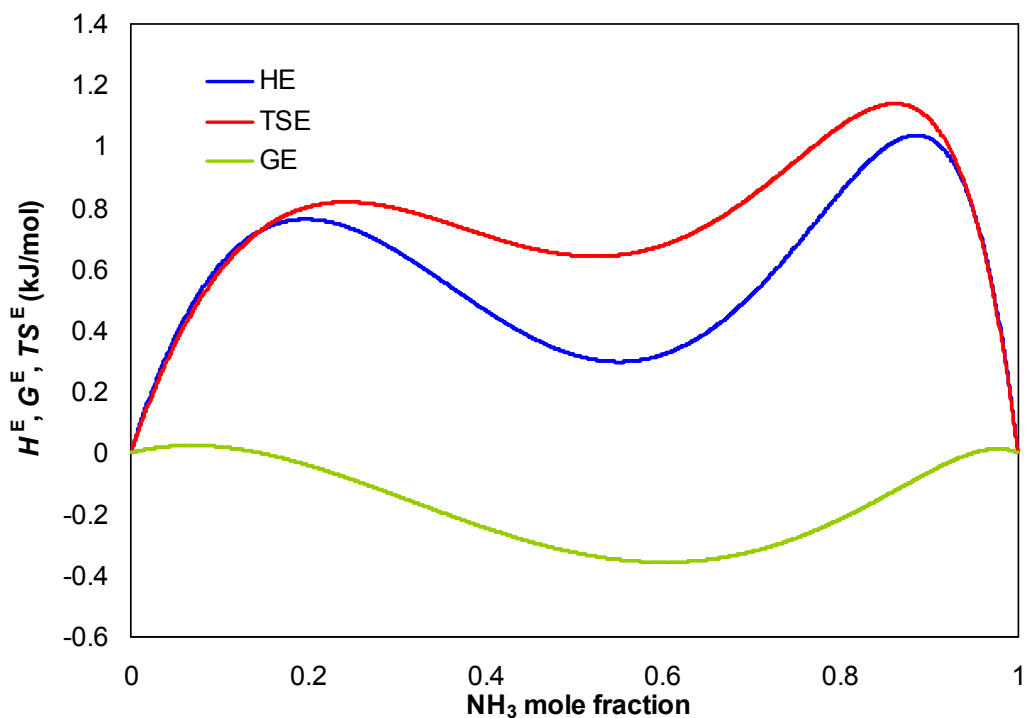
(b)

Figure 3.19. Excess enthalpy, free Gibbs energy, and entropy of ammonia and [emim][SCN] mixtures at temperature of 298.15 K

The results of calculated excess enthalpy, entropy, and Gibbs energy of ammonia and [hmim] and [DMEA] based ionic liquid mixtures with NRTL model are presented in Figure 3.10. Figure 3.10(a) shows the results of calculated excess enthalpy, entropy, and Gibbs energy of [hmim][Cl] and ammonia mixture at temperature of 298.15 K. From that figure it can be seen that the minimum excess enthalpy was about 2.2 kJ/mole. The results of calculated excess enthalpy, entropy, and Gibbs energy of [DMEA][Ac] and ammonia mixture at at temperature of 298.15 K are shown in Figure 3.10(b). It is interesting to observe that at lower ammonia composition, (i.e ammonia mole fraction < 0.45) the excess enthalpy was negative which means that the mixing process is exothermic. On contrary, at higher ammonia composition, (i.e ammonia mole fraction > 0.45) the excess enthalpy was positive which means that the mixing process is endothermic. Different than other of [emim] based ionic liquid mixtures, from that figure it can be seen that the excess enthalpy was ranged between -0.9 kJ/mole and 1 kJ/mole.
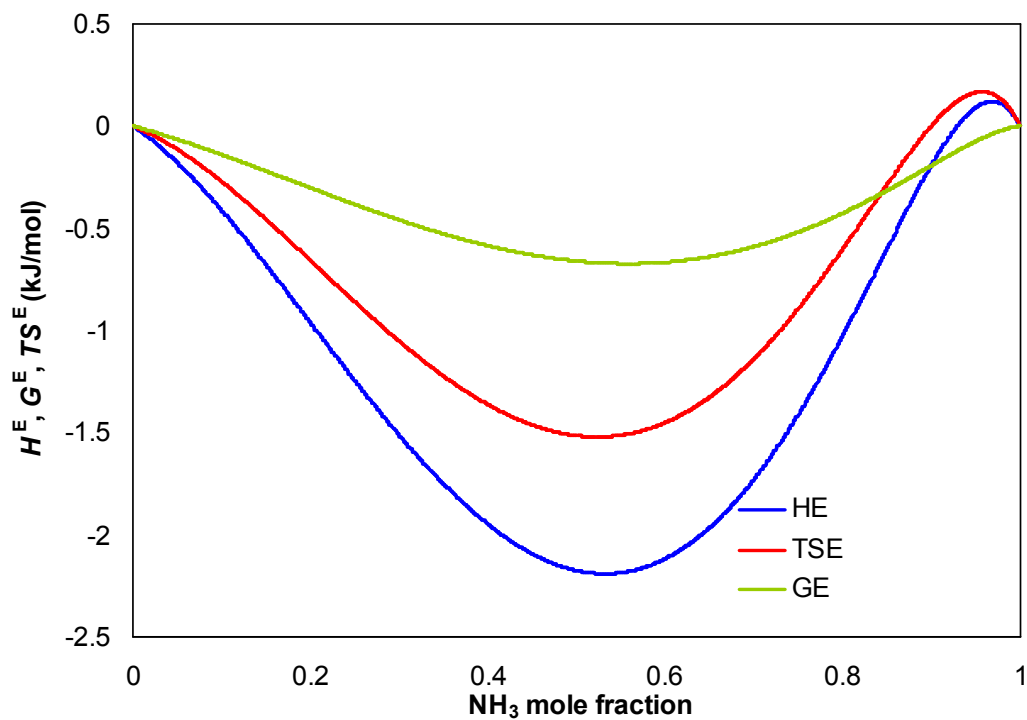
(a)
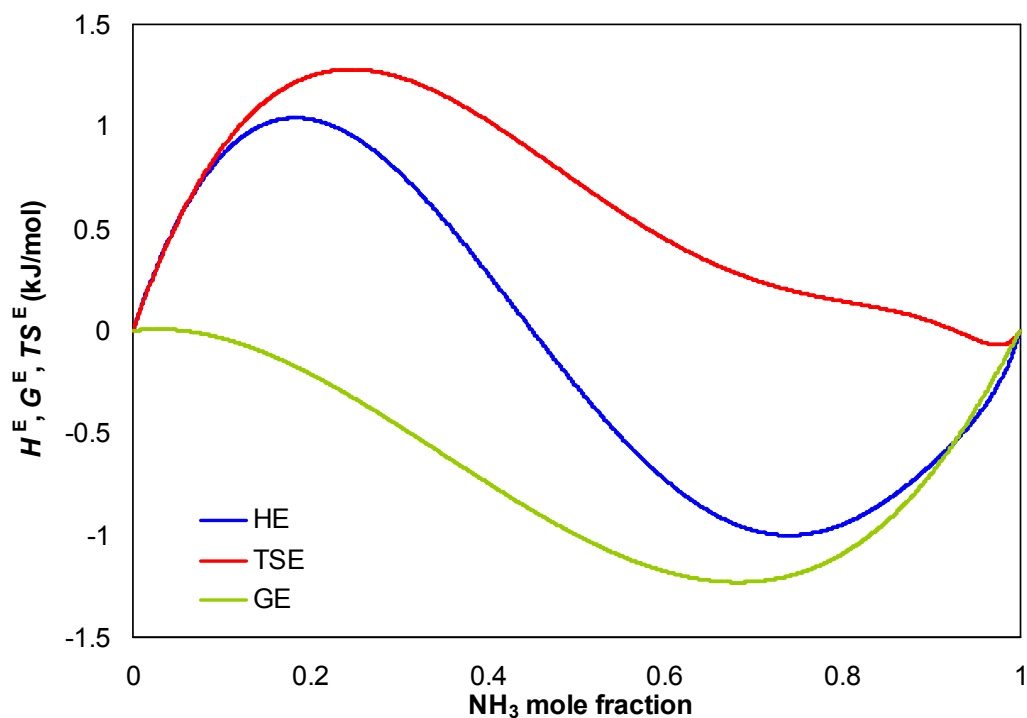
(b)

Figure 3.20. Excess enthalpy, free Gibbs energy, and entropy of ammonia and [emim] based ionic liquid mixtures at temperature of 298.15 K. (a) [hmim][Cl] and (b) [DMEA][Ac]

3.4. PC-SAFT Equation of State

3.4.1. Parameters and Data Regression

The perturbed-chain statistical associating fluid theory (PC-SAFT) equation of state was developed by Gross and Sadowski [13–14] by applying the perturbation theory of Barker and Henderson to a hard-chain reference fluid. The PC-SAFT was a development of the SAFT equation of state developed by Huang and Radosz [15–16], with some modifications on the expressions for the dispersion forces.

Similarly to SAFT, there are three pure-component parameters for pure ionic liquids. These three pure-component parameters and their names are shown in Table 3.5.

Table 3.5. Three PC-SAFT parameters of pure ionic liquids considered as non-associating fluids.

Parameter	Symbol	Unit
segment number	m	-
segment diameter	σ	Å
segment energy	ε/κ_B	K
binary parameter	k_{ij}	-

To be able to model the vapor-liquid equilibrium of ionic liquids and ammonia mixtures using PC-SAFT, the molecular parameters of pure ionic liquids and ammonia must be determined. In addition, the binary parameter of ionic liquids and ammonia mixture also must be determined.

Before applying PC-SAFT equation of state to the mixture, it is important to calculate the molecular parameters of pure compounds. In this work, the ionic liquids are treated as non-associating fluids, therefore the ionic liquids are represented by three parameters m, σ (Å) and ε/κ_B (K). The PC-SAFT parameters of pure ionic liquids are calculated using experimental density data at atmospheric pressure and several temperatures. The experimental density data of ionic liquids are extracted from Thermo Data Engine [17].

In addition to the PC-SAFT parameters of ionic liquids, the PC-SAFT parameters of pure ammonia are taken from literature [18] with considering the ammonia molecule as non-associating substance. Therefore, the ammonia molecule is also represented by three parameters.

The PC-SAFT binary interaction parameter k_{ij} of ammonia and ionic liquid mixture requires experimental vapor-liquid equilibrium data to be fitted. By default, the binary interaction parameter k_{ij} is set as zero (k_{ij}=0). The PC-SAFT binary interaction parameter k_{ij} of ammonia and ionic liquid mixtures are obtained by regressing the experimental vapor-liquid equilibrium data of ammonia and ionic liquids mixtures.

3.4.2. Results and Discussion

3.4.2.1 PC-SAFT Parameters of Pure Ionic Liquids and Ammonia

The detail results of PC-SAFT parameters of pure ionic liquids and pure ammonia regressed from experimental data are given in the table 3.6.

Table 3.6. Molecular parameters of pure ionic liquids considered as non-associating fluids

Ionic liquids	M_w (g/mol)	m	σ (Å)	ε/κ_B (K)	AAD (%)
[bmim][BF$_4$]	226.03	1.9419	5.2884	568.493	0.16
[bmim][PF$_6$]	284.18	2.6285	4.9672	534.511	0.11
[emim][Ac]	170.21	3.2232	4.3499	854.279	0.03
[emim][BF$_4$]	197.97	3.1402	4.4106	958.967	0.19
[emim][EtSO$_4$]	236.29	2.7418	4.8383	688.892	0.09
[emim][Tf$_2$N]	391.32	1.6869	3.6848	525.058	0.05
[hmim][Cl]	202.73	3.1017	4.7048	713.408	0.01
refrigerant					
NH$_3$ - ammonia	17.03	2.4507	2.3841	212.86	

3.4.2.2 *Density of Pure Ionic Liquids*

To check the validity of the calculated pure parameters of ionic liquids, it is necessary to estimate the density of pure ionic liquids using PC-SAFT pure parameters obtained from data regression. The estimated densities of pure ionic liquids then are compared with the experimental data. The densities are estimated at atmospheric pressure and various temperatures. The ionic liquids are considered as non-associating molecules, and the values of the three molecular parameters m, σ (Å) and ε/κ_B (K) obtained after data regression are given in table 3.6. The results of estimation of density of pure ionic liquids are presented in figures 1.

Figure 3.21 (a) shows the comparison of estimated densities of two [bmim] based ionic liquids with the experimental density data using PC-SAFT model. The two [bmim] based ionic liquids studied here are [bmim][BF$_4$] and [bmim][PF$_6$]. The results show that the PC-SAFT model with molecular paramaters obtain from data regression and considering the ionic liquids as non-associating fluids can estimate the densities of pure ionic liquids with high accuracy. The results show that the average absolute deviaton of estimated densities for [bmim][BF$_4$] and [bmim][PF$_6$] are 0.16% and 0.11%, respectively.

The estimated densities of four pure [emim] based ionic liquids are shown in figures 3.21 (b) and 3.22 (a). The four [emim] based ionic liquids studied here are [emim][Ac], [emim][EtSO4], [emim][BF4] and [emim][Tf2N]. Figure 3.21 (b) shows the comparison of estimated densities of [emim][Ac] and [emim][EtSO4] with the experimental density data using PC-SAFT model. In addition, the comparison of estimated densities of [emim][BF4] and [emim][Tf2N] with the experimental density data is presented in figure 3.22 (a). Similar with those of [bmim] based ionic liquids, the results show that the PC-SAFT model with molecular paramaters obtain from data regression and considering ionic liquids as non-associating fluids can estimate the densities of pure ionic liquids with high accuracy. The average absolute deviaton of estimated densities of [emim][Ac] and [emim][EtSO4] are 0.03% and 0.09%, respectively. Slightly similar with those of [emim][Ac] and [emim][EtSO4], the average absolut deviations were shown by the density estimation of [emim][BF4] and [emim][Tf2N], which are 0.19% and 0.05%, respectively.
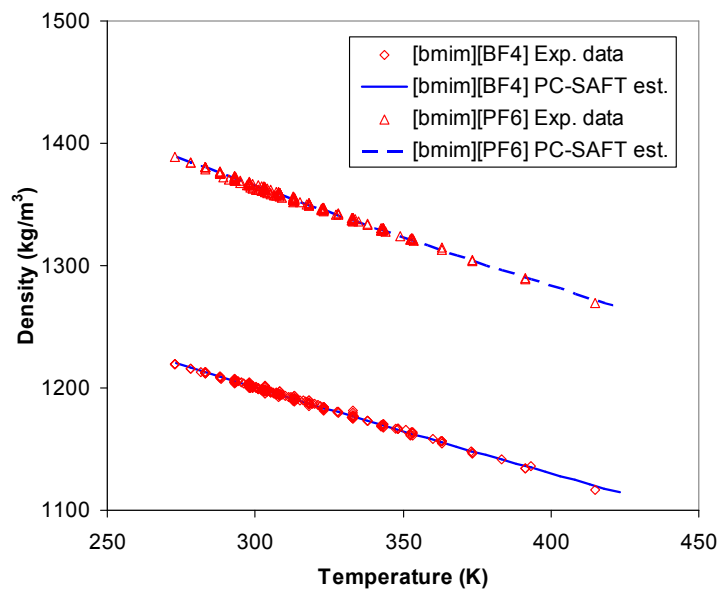
(a)
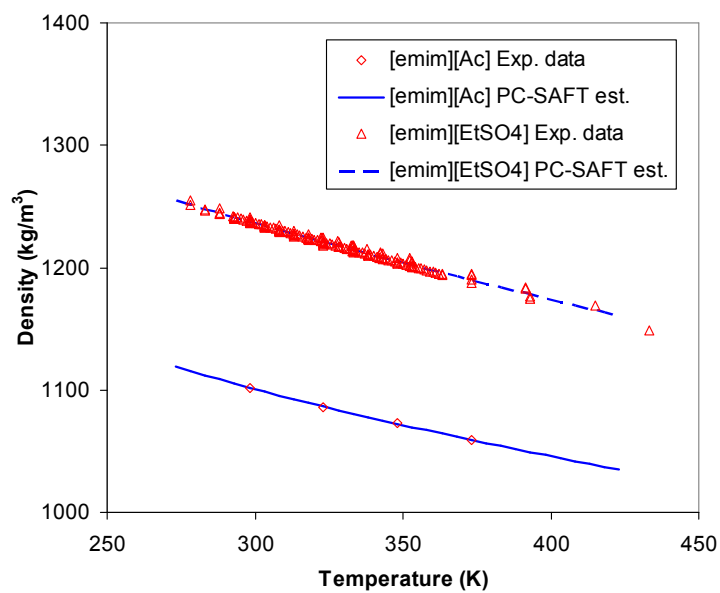
(b)

Figure 3.21. Temperature-density chart for pure ionic liquids considered as non-associating fluids. (a) [bmim][BF$_4$] and [bmim][PF$_6$], (b) [emim][Ac] and [emim][EtSO$_4$]

Figure 3.22 (b) shows the estimated densities of [hmim] based ionic liquids as compared with experimental dendsity data. However, only one ionic liquids, [hmim][Cl] is studied, due to the limits of experimental data. The average absolute deviaton of estimated densities of [hmim][Cl] is 0.01%.
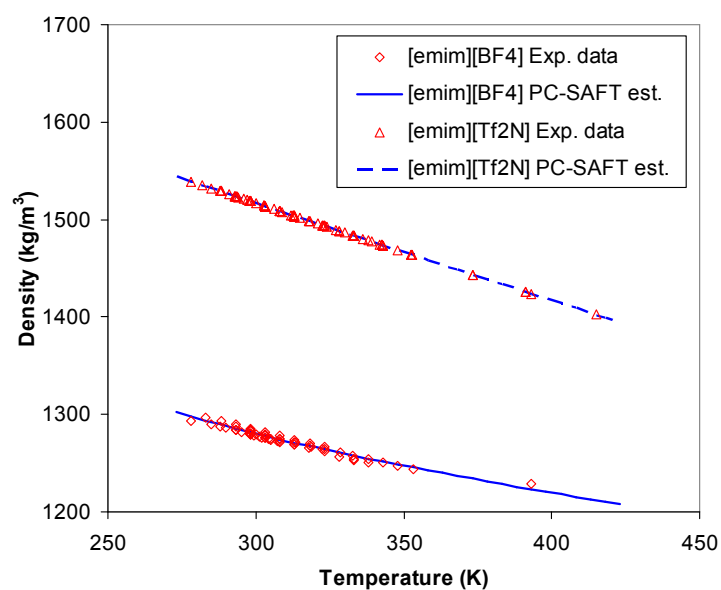
(a)
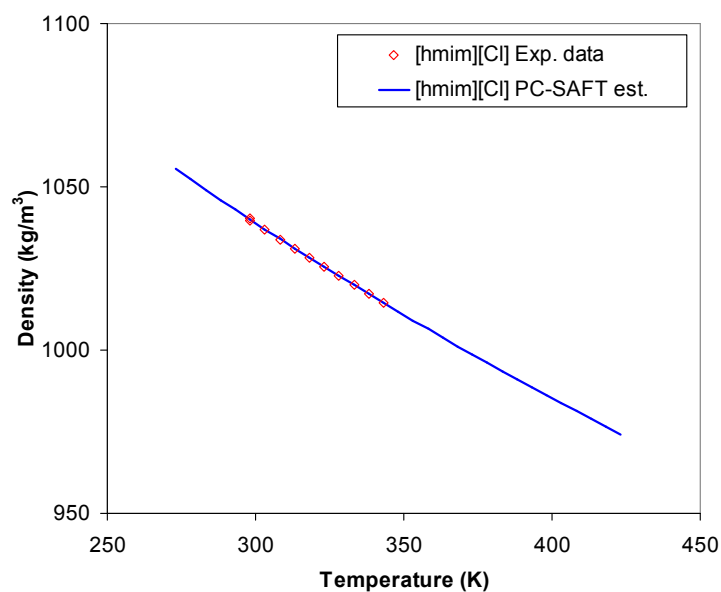
(b)

Figure 3.22. Temperature-density chart for pure ionic liquids considered as non-associating fluids. [emim][EtSO$_4$], (c) [emim][BF$_4$] and [emim][Tf$_2$N], and (d) [hmim][Cl]

3.4.2.3 *PC-SAFT Binary Interaction Parameters of Ionic Liquid and Ammonia Mixtures*

The use of PC-SAFT model for ammonia and ionic liquid mixtures requires the binary interaction parameter k_{ij} value. As mentioned above, it is necessary to fit

the value of the binary parameter k_{ij} from the experimetal VLE data. Otherwise the PC-SAFT thermodynamic model will use the binary interaction parameter value k_{ij}=0 as default value.
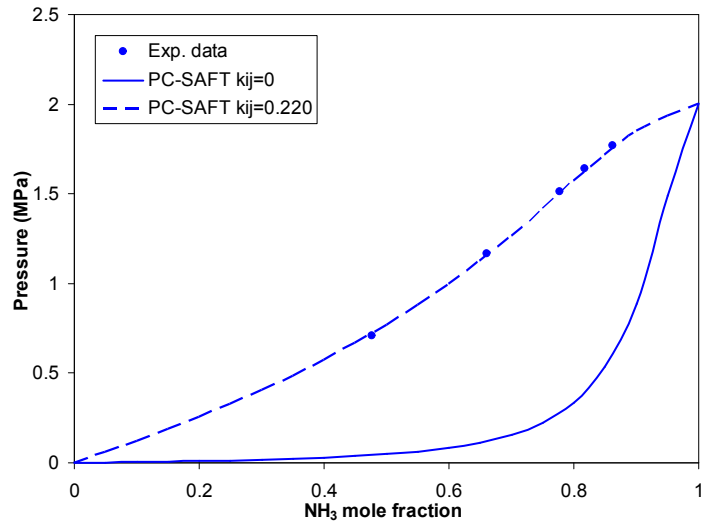
(a)
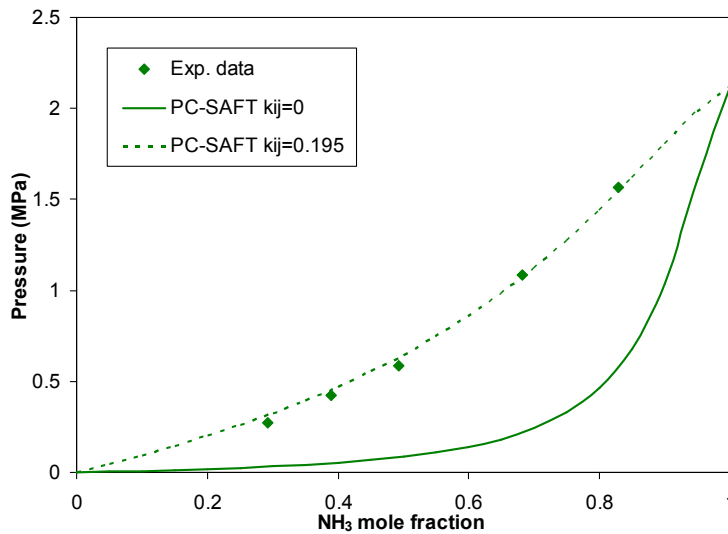
(b)

Figure 3.23. Solubility calculation of ammonia in (a) [emim][Ac] at T= 322.3 K using PC-SAFT model with k_{ij}=0 and k_{ij}=0.220 and (b) [bmim][PF$_6$] at T=324.6 K using PC-SAFT model with $k$ij=0 and $k$ij=0.195

It is necessary to understand the difference of ammonia and ionic liquids mixture vapor-liquid equilibrium calculated using default binary interaction parameter k_{ij}=0 and using binary interaction parameter k_{ij} value obtained by

regression from experimental VLE data. Figure 3.23 show the difference of the solubility calculation of ammonia in [emim][Ac] at temperature 322.3 K using PC-SAFT model with $k_{ij}=0$ and k_{ij} value obtained by regression from experimental VLE data (k_{ij}=0.220) and the solubility calculation of ammonia in [bmim][PF6] at T=324.6 K using PC-SAFT model with $k$ij=0 and $k$ij=0.195.

From figure 3.23 it can be seen that the results of ammonia and [emim][Ac] mixture at temperature 322.3 K with k_{ij} constant (k_{ij}=0) have high deviation as compared to the experimental data. The better results are shown by the k_{ij} fitted from experimental data (k_{ij}=0.220), which have absolute average deviation about 1.03%. In addition, From figure 3.23 it also can be seen that the results of ammonia and [bmim][PF6] mixture at temperature 324.6 K with k_{ij} constant (k_{ij}=0) have high deviation as compared to the experimental data. The better results are shown by the k_{ij} fitted from experimental data (k_{ij}=0.195), which have absolute average deviation about 1.03%

From this analysis, it can be concluded that the use of default binary interaction parameter k_{ij}=0 is not be able to calculate the vapor-liquid equilibrium of ammonia and ionic liquid mixture with high accuracy. Therefore, in this work, the binary parameter k_{ij} of some ammonia-ionic liquids mixture are determined by regressing the experimental VLE data.

The values of binary interaction parameter k_{ij} for some ammonia and ionic liquid mixtures obtained from data regression using experimental VLE data at different temperatures are shown in figure 3.24. As shown in figure 3.24 (a), the values of binary parameters k_{ij} of ammonia and [bmim] based ionic liquid mixtures slightly increase with the temperature. Opposite with those of ammonia and [bmim] based ionic liquid mixtures, the values of binary parameters k_{ij} of ammonia and [emim] based ionic liquid mixtures slightly decrease with the temperature, as presented in figure 3.24 (b).
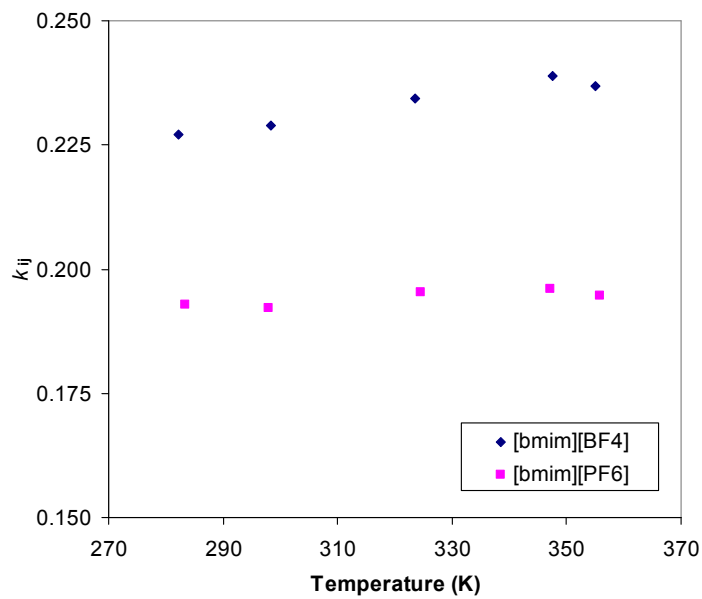
(a)
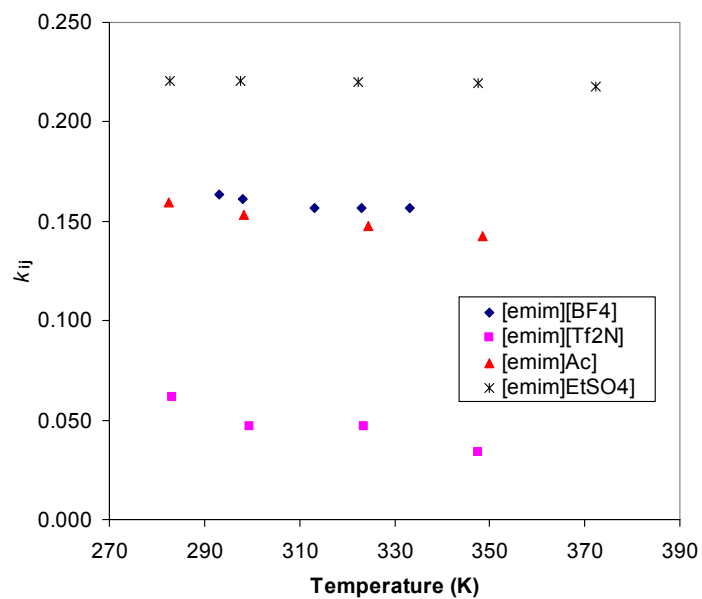
(b)

Figure 3.24. Binary interaction parameter k_{ij} value of ammonia and ionic liquid mixtures at several temperatures. (a) [bmim] based ionic liquids, and (b) [emim] based ionic liquids

3.4.2.4 *Vapor-liquid equilibrium of Ammonia and Ionic Liquid Mixtures*

After calculating the PC-SAFT parameters of pure ionic liquids and single binary interaction parameter k_{ij} of ammonia and ionic liquid mixtures, the next

sequence is to analyse and study the ability of PC-SAFT model to calculate the vapor-liquid equilibrium of ammonia and ionic liquid mixture. In this subsection, the vapor-liquid equilibrium calculation of some [bmim] based ionic liquid and ammonia mixtures and [emim] based ionic liquid and ammonia mixtures was studied. In addition, the vapor-liquid equilibrium calculation of [hmim][Cl] was also studied

The results of vapor-liquid equilibrium of ammonia and [bmim] based ionic liquid mixtures with PC-SAFT model are presented in figures 4. The vapor-liquid equilibrium of two ionic liquids, [bmim][BF$_4$] and [bmim][PF$_6$], are studied.

Figure 3.25(a) shows the results of the vapor-liquid equilibrium of [bmim][BF$_4$] and ammonia mixture at several temperatures. From that figure it is interesting to see that the results at low temperature (i.e. 282.2 K and 296.4 K) have good agreement as compared with the experimental data. The results indicate that the average absolute deviation for calculated vapor-liquid equilibrium of [bmim][BF$_4$] and ammonia mixture at temperature 282.2 K and 296.4 K is 5.5% and 6.4% respectively. However, the model has difficulty to calculate the vapor-liquid equilibrium with high accuracy at higher temperature and low ammonia composition. The higher average absolute deviations appear at higher temperature. For instance, at temperature of 323.6 K the results have the average absolute deviation of 10.9%. At this temperature, it is also can be seen that the higher deviation appear at lower ammonia mole fraction. At higher ammonia mole fraction (i.e higher than 0.4 ammonia mole fraction) at 323.6 K, the calculation result is in good agreement with the experimental data with deviation lower than 3%. However, at lower ammonia mole fraction (i.e lower than 0.4 ammonia mole fraction) at same temperature, the deviation is around 12–28%. The higher average absolut deviation is shown at temperature of 347.5 K and 355.1 K, which the average absolut deviation is 17.2% and 23.7%, respectively. At these temperatures, the higher deviation also appear at lower ammonia mole fraction.
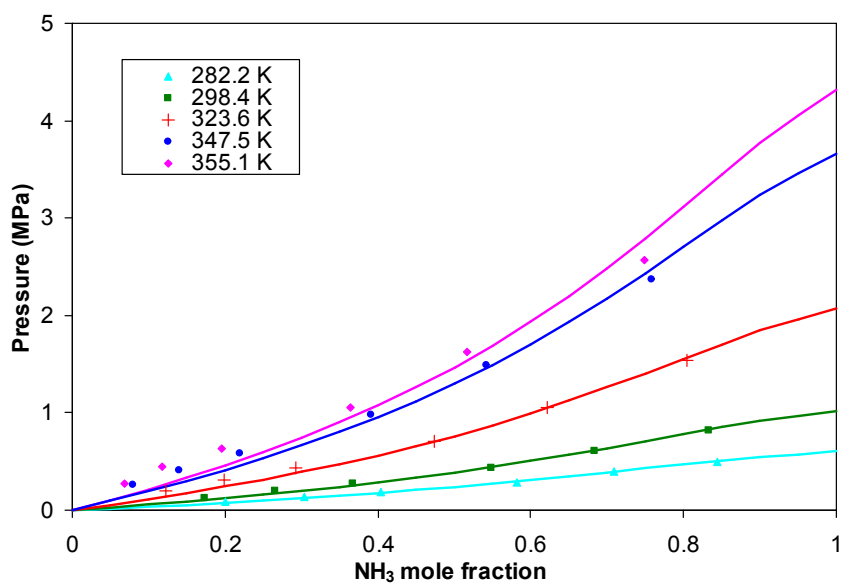
(a)
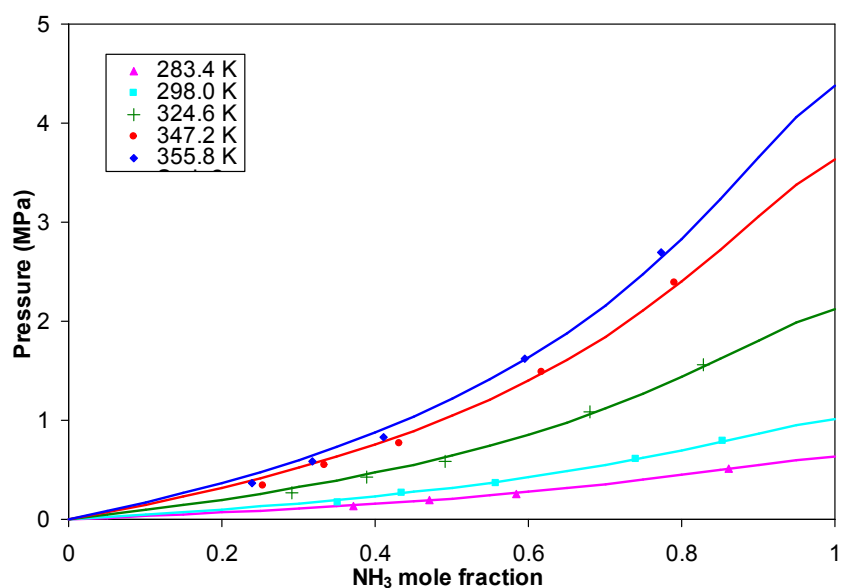
(b)

Figure 3.25. Vapor-liquid equilibrium of ammonia and [bmim] based ionic liquid mixtures at different temperatures with a temperature-dependent binary parameter k_{ij}. (a) [bmim][BF$_4$] and (b) [bmim][PF$_6$].

The results of the vapor-liquid equilibrium of [bmim][PF$_6$] and ammonia mixture at several temperatures are shown in figure 3.25(b). Similar with those of [bmim][BF$_4$] and ammonia mixture, it is interested to see at the figure that the results at low temperature (283.4 K and 298 K) have good agreement with the experimental

data. The average absolute deviation for calculated vapor-liquid equilibrium of [bmim][PF$_6$] and ammonia mixture at temperature 283.4 K and 298 K is 1.5% and 4.6% respectively. However, different with those of [bmim][BF$_4$] and ammonia mixture, the average absolute deviations have slightly higher values at higher temperature. As an example, at temperature of 324.6 K the results have the average absolute deviation of 6.8%. At this temperature, it is also can be seen that the higher deviation appear at lower ammonia mole fraction. The higher average absolut deviation appear at temperature of 347.2 K and 355.8 K, which has value 8.8% and 9.1%, respectively. At these temperatures, the higher deviation also appear at lower ammonia mole fraction. Generally, the results of the vapor-liquid equilibrium of [bmim][PF$_6$] and ammonia mixture have better agreement with the experimental data as compared with those [bmim][BF$_4$] and ammonia mixture.

Figures 3.26 present the results of vapor-liquid equilibrium of [emim] based ionic liquid and ammonia mixture with PC-SAFT model. The vapor-liquid equilibrium of two ionic liquid and ammonia mixtures, [emim][EtSO$_4$] and [emim][Ac], are studied.

Figure 3.26(a) shows the results of the vapor-liquid equilibrium of [emim][EtSO$_4$] and ammonia mixture at several temperatures. From this figure it can be seen that the results at several temperatures have good agreement with the experimental data. The results indicate that the average absolute deviation for calculated vapor-liquid equilibrium for [emim][EtSO$_4$] and ammonia mixture at temperature 282.7 K and 297.6 K is 2.3% and 1.3%, respectively. Unlike with those of ammonia and [bmim] based ionic liquid mixture, The PC-SAFT model can calculate the vapor-liquid equilibrium of [emim][EtSO$_4$] and ammonia mixture with high accuracy higher temperature. The results show that the average absolute deviation for calculated vapor-liquid equilibrium for [emim][EtSO$_4$] and ammonia mixture at temperature 322.3 K, 347.5 K and 372.3 K is 1.0%, 0.5% and 0.6% respectively.
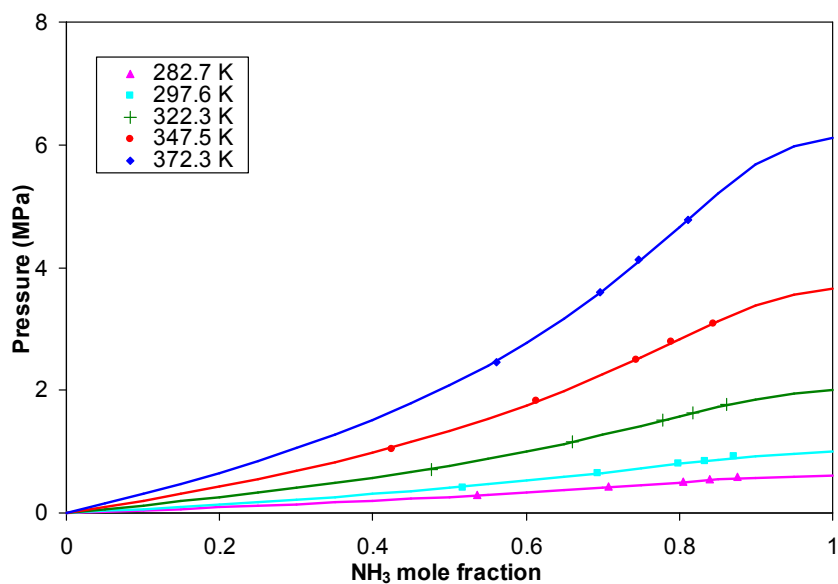
(a)
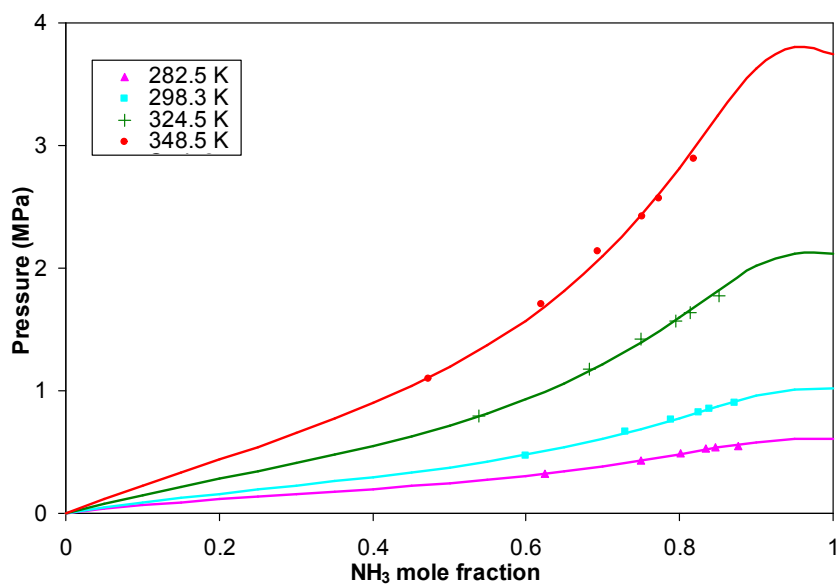
(b)

Figure 3.26. Vapor-liquid equilibrium of ammonia and [emim] based ionic liquid mixtures at different temperatures with a temperature-dependent binary parameter k_{ij}. (a) [emim][EtSO$_4$] and (b) [emim][Ac]

The results of the vapor-liquid equilibrium of [emim][Ac] and ammonia mixture at several temperatures are shown in figure 3.26(b). Similar with those [emim][EtSO4] and ammonia mixture, it is interesting to see from the figure that the results have good agreement with the experimental data at several temperatures. The

average absolute deviation lies between 0.5% and 2.3% for temperature range from 283.2 K to 372.8 K.

Finally, the results of the vapor-liquid equilibrium of [hmim][Cl] and ammonia mixture at several temperatures are shown in Figure 3.27.
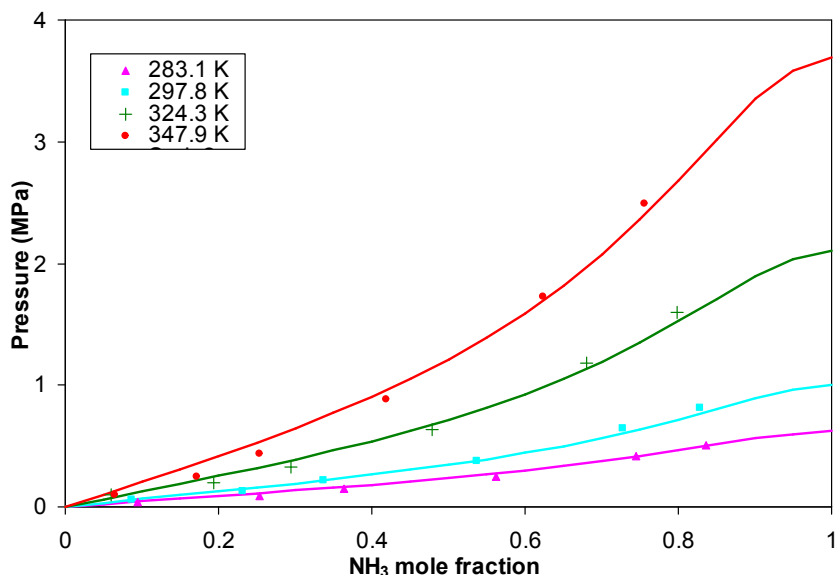
Figure 3.27. Vapor-liquid equilibrium of ammonia and [hmim][Cl] mixture at different temperatures with a temperature-dependent binary parameter k_{ij}.

Similar with those of [bmim][BF$_4$] and ammonia mixture, it can be seen that the PC-SAFT equation of state can calculate the vapor-liquid equilibrium with high accuracy at low temperature, but has difficulty to predit the vapor-liquid equilibrium at higher temperature. The results have good agreement with the experimental data at low temperatures. The average absolute deviation is 7.0% and 5.1% for temperature of 283.1 K and 297.8 K. The higher average absolut deviation is shown at temperature of 324.3 K and 347.8 K, which the average absolut deviation is 13.9% and 18.5%, respectively.

3.5. UNIFAC Model

3.5.1. UNIFAC Equations and Parameters

UNIFAC model (UNIQUAC Functional-group Activity Coefficients) is a predictive thermodynamic model, which is used to calculate the vapor-liquid equilibrium of mixtures [19]. This model was built based on group contribution method to calculate activity coefficient. The equation of activity coefficient in UNIFAC can be written in Equation (3.31) as a summation of combinatorial contribution and residual contribution to the activity coefficient [20].

$$\ln \gamma = \ln \gamma_i^C + \ln \gamma_i^R \qquad (3.31)$$

The combinational part, $\ln \gamma_i^C$, is essentially due to differences in shape and size of the molecules, can be expressed mathematically as

$$\ln \gamma_i^C = 1 - \Phi_i + \ln \Phi_i - 5q_i \left[1 - \frac{\Phi_i}{\theta_i} + \ln \frac{\Phi_i}{\theta_i} \right] \qquad (3.32)$$

where

$$\Phi_i = \frac{r_i}{\sum_j x_j r_j} \qquad (3.33)$$

$$\theta_i = \frac{q_i}{\sum_j x_j q_j} \qquad (3.34)$$

The parameters r_i and q_i are pure components parameters which are relative to molecular van der Waals volumes and molecular surface area, respectively. These parameters are calculated using Equation (3.35) and (3.36) as the summation of the group volume (R_k) and group area parameters (Q_k), respectively.

$$r_i = \sum_k v_k^{(i)} R_k \qquad (3.35)$$

$$q_i = \sum_k v_k^{(i)} Q_k \qquad (3.36)$$

The residual part $\ln \gamma_i^R$, is essentially due to energetic interactions, can be expressed as

$$\ln \gamma_i^R = \sum_k v_k^{(i)} \left[\ln \Gamma_k - \ln \Gamma_k^{(i)} \right]$$

(3.37)

where Γ_k is the activity coefficient of a group at mixture composition, and Γ_k^i is the activity coefficient of group k in a mixture of groups corresponding to pure i. The parameters Γ_k and Γ_k^i are defined by Equation (3.38).

$$\ln \Gamma_k = Q_k \left(1 - \ln \sum_m \theta_m \tau_{mk} - \sum_m \left(\frac{\theta_m \tau_{km}}{\sum_n \theta_n \tau_{nm}} \right) \right)$$

(3.38)

The parameter θ_m is the surface area fraction in group m in the mixture which can be expressed in Equation (3.39) and X_m is the fraction group m in the mixture which can be expressed in Equation (3.40)

$$\theta_m = \frac{Q_m X_m}{\sum_n Q_n X_n}$$

(3.39)

$$X_m = \frac{\sum_i v_m^{(i)} x_i}{\sum_i \sum_k v_k^{(i)} x_i}$$

(3.40)

The parameter τ_{nm} is the group interaction parameter and a function of adjustable group interaction parameter between group n and m. This parameter is defined in Equation (3.41).

$$\tau_{nm} = \exp\left(-\left(a_{nm}/T\right)\right)$$

(3.41)

The functional groups for ionic liquids and ammonia used in this UNIFAC model were following the division method of Kim et al [21]. The group divisions for ionic liquids are presented in Table 3.7.

Table 3.7. Group divisions of ionic liquids for UNIFAC model

Ionic liquids	Group division
[emim][BF$_4$]	[mim]BF$_4$ + CH$_2$ + CH$_3$
[bmim][BF$_4$]	[mim]BF$_4$ + 3 CH$_2$ + CH$_3$
[hmim][BF$_4$]	[mim]BF$_4$ + 5 CH$_2$ + CH$_3$
[omim][BF$_4$]	[mim]BF$_4$ + 7 CH$_2$ + CH$_3$
[emim][EtSO$_4$]	[mim][EtSO$_4$] + CH$_2$ + CH$_3$
[emim][Ac]	[mim][Ac] + CH$_2$ + CH$_3$

The group volume (R_k) and group area parameters (Q_k) values of each group were taken from reference [22-24] and are presented in Table 3.8.

Table 3.8. Values of group volume (R_k) and group area (Q_k) parameters

Group	R_k	Q_k	Ref.
NH$_3$	1.4397	2.0918	[22]
CH$_3$	0.9011	0.8480	[23]
CH$_2$	0.6744	0.5400	[23]
[mim][BF$_4$]	6.5669	4.0050	[23]
[mim][EtSO$_4$]	4.4225	3.6114	[24]
[mim][Ac]	5.8595	2.7783	[24]

Moreover, the values of group interaction parameter between group n and m, a_{mn} and a_{nm}, were taken from reference [19,24] and are presented in Table 3.9.

Table 3.9. Values of group interaction parameter a_{mn}

m	n	a_{mn}	a_{nm}	Ref.
NH$_3$	CH$_2$	914.100	-423.600	[19]
NH$_3$	[mim][BF$_4$]	320.400	-404.700	[19]
NH$_3$	[mim][EtSO$_4$]	2.849	-89.590	[19]
NH$_3$	[mim][Ac]	-216.100	-388.000	[19]
CH$_2$	[mim][BF$_4$]	1108.510	588.740	[24]
CH$_2$	[mim][EtSO$_4$]	225.992	332.837	[19]
CH$_2$	[mim][Ac]	680.000	1244.000	[19]

The experimental VLE data of ammonia/[emim][BF$_4$] and ammonia/[emim][EtSO$_4$]mixtures are taken from Yokozeki and Shiflett [5-6]. In addition to the experimental VLE data from these author, the experimental VLE data of ammonia/[C$_n$mim][BF$_4$] mixtures (n=2,4,6,8) were taken from Li et al. [7]. The absolute average deviation is calculated using Equation (3.12).

3.5.2. Results and Discussion

3.5.2.1 *Vapor-liquid equilibrium of Ammonia and Ionic Liquid Mixtures*

Due to limited UNIFAC parameters available in the database, only several ammonia/ionic liquid mixtures were studied using this methods. In this subsection, the vapor liquid eqilibrium of binary ammonia and $[C_nmim][BF_4]$, $[emim][EtSO_4]$, and $[emim][Ac]$ mixture were analysed using UNIFAC method.

The results of vapor-liquid equilibrium calculation of ammonia/$[C_nmim][BF_4]$ mixtures (n=2,4,6,8) with UNIFAC model are presented in Figure 3.21 and Figure 3.22.

Figure 3.28 shows the results of the vapor-liquid equilibrium of $[emim][BF_4]$ and ammonia mixture at several temperatures. Different with the results of other thermodynamic model, from that figure it can be seen that the average absolute deviation were slightly higher compared with the experimental data. The results indicate that the average absolute deviation for calculated vapor-liquid equilibrium of ammonia/$[emim][BF_4]$ mixture at all temperature range was 17.3%.
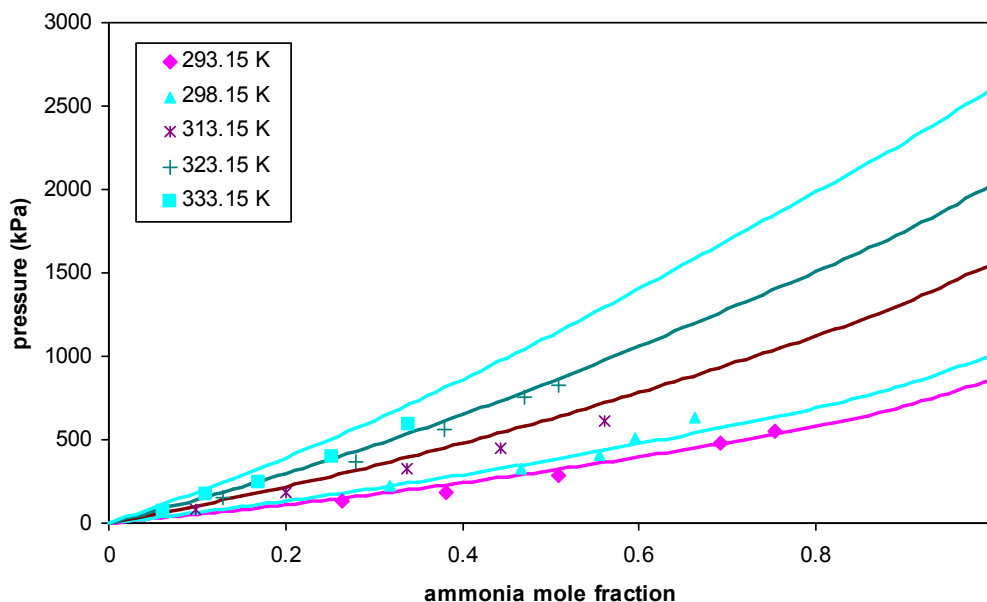
Figure 3.28. Vapor-liquid equilibrium of ammonia $[emim][BF_4]$

The results of the vapor-liquid equilibrium of [bmim][BF$_4$] and ammonia mixture at several temperatures are shown in Figure 3.29. Similar with those of ammonia and [emim][BF$_4$] mixture, that the average absolute deviation were slightly higher compared with the experimental data although the overall absolute deviation were slightly lower than that of ammonia/[emim][BF$_4$]. The average absolute deviation for calculated vapor-liquid equilibrium of [bmim][BF$_4$] and ammonia mixture at all temperature ranges was 15.8%. In addition, it was observed that the average absolute deviations have higher values at higher temperature.
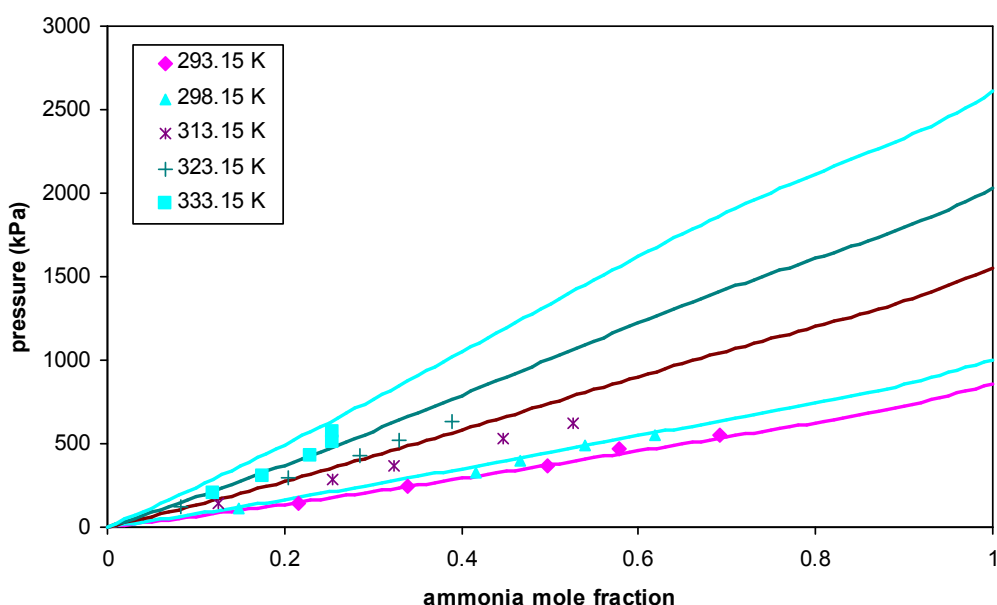
Figure 3.29. Vapor-liquid equilibrium of ammonia/[bmim][BF4] mixture

Figure 3.30(a) shows the results of the vapor-liquid equilibrium of [hmim][BF$_4$] and ammonia mixture at several temperatures. From this figure it can be seen that the results at several temperatures have higher deviation when compared with those of [emim][BF$_4$] and [bmim][BF$_4$] . The results indicate that the average absolute deviation for calculated vapor-liquid equilibrium for [hmim][BF$_4$] and ammonia mixture at all temperature range is 17.4%. It was also observed that the average absolute deviations have slightly higher values particularly at higher temperature such as at temperature of 333.15 K with the average absolute deviation

of 44.9%. However at lower temperature (i.e. at 298.15 k) the deviations were acceptable considering the deviation was less than 10%.
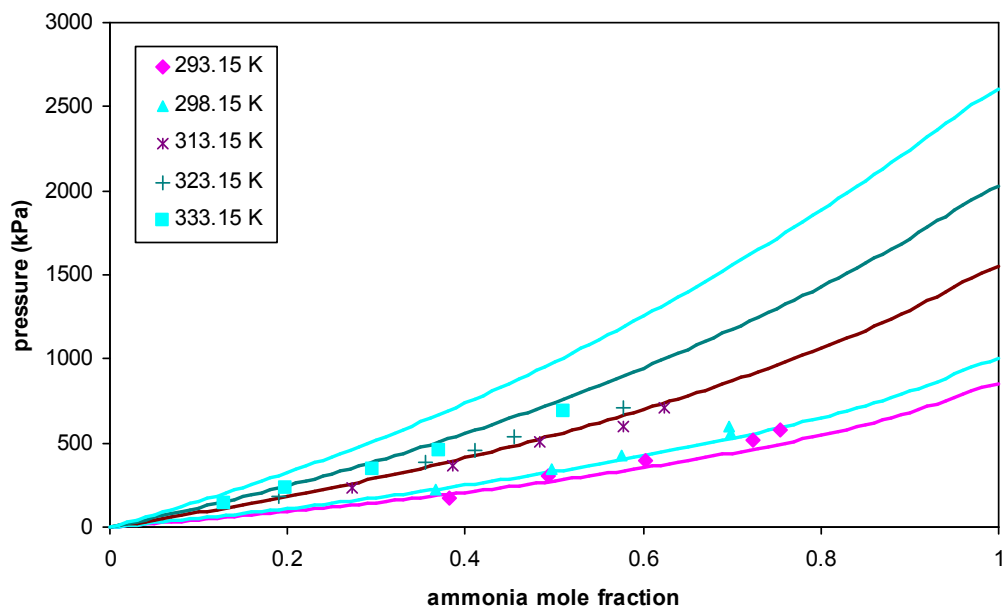
(a)
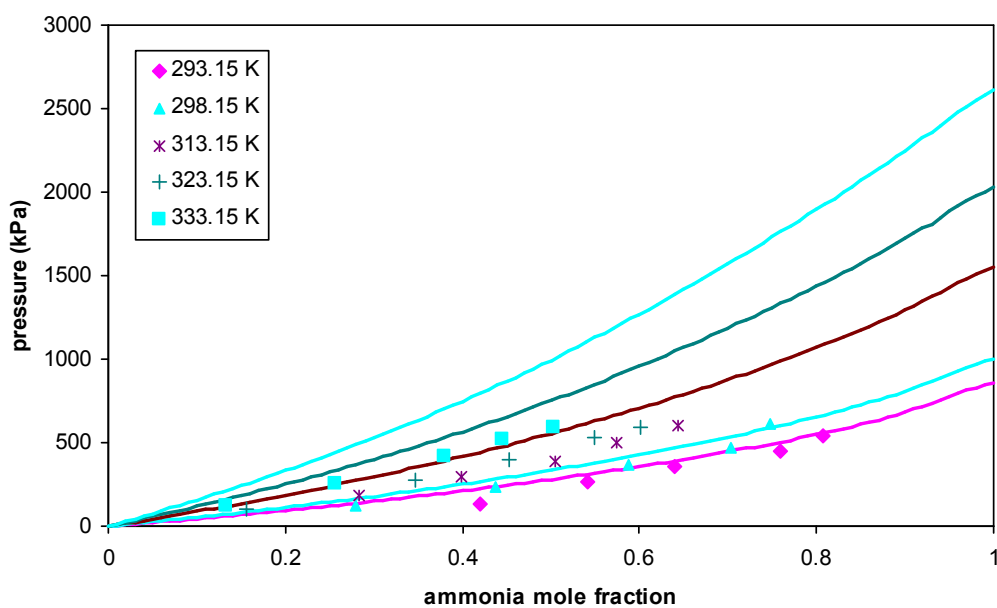
(b)

Figure 3.30. Vapor-liquid equilibrium of ammonia and (a) [hmim][BF$_4$] and (b) [omim][BF$_4$].

The results of the vapor-liquid equilibrium of [omim][BF$_4$] and ammonia mixture at several temperatures are shown in Figure 3.30(b). Similar with those ammonia/[hmim][BF$_4$] mixture, the results of vapor-liquid equilibrium of ammonia/[omim][BF$_4$] at several temperatures have higher deviation when compared with those of [C$_n$mim][BF$_4$] with shorther alkyl chain. The results indicate that the average absolute deviation for calculated vapor-liquid equilibrium for [omim][BF$_4$] and ammonia mixture at all temperature range is 41.1%.

Finally, Figure 3.31(a) shows the results of the vapor-liquid equilibrium of [emim][EtSO$_4$] and ammonia mixture at several temperatures. From this figure it can be seen that the results at several temperatures have good agreement with the experimental data. In addition, the UNIFAC model was able to calculate the vapor pressure of ammonia/[emim][EtSO$_4$] mixture with higher accuracy in comparison with those of ammonia/[C$_n$mim][BF$_4$] mixtures. The results indicate that the average absolute deviation for calculated vapor-liquid equilibrium for [emim][EtSO$_4$] and ammonia mixture at all temperature range is 5.4%. It was also observed that the average absolute deviations have slightly higher values particularly at lower temperature and lower ammonia composition, such as at temperature of 282.7 K. The average absolute deviation for calculated vapor-liquid equilibrium of [emim][EtSO$_4$] at temperature of 282.7 K was 9.4%. However the high deviations at higher temperature and low ammonia composition were acceptable considering the deviation was less than 10% and the experimental data at higher temperature and low ammonia composition present high uncertainties.

The results of the vapor-liquid equilibrium of [emim][Ac] and ammonia mixture at several temperatures are shown in Figure 3.31(b). Similar with those ammonia/[emim][EtSO$_4$] mixture, the results of vapor-liquid equilibrium of ammonia/[emim][Ac] have good agreement with the experimental data at several temperatures, although with higher deviation. Moreover the results also present high deviations at higher temperature and low ammonia composition. The results indicate that the average absolute deviation for calculated vapor-liquid equilibrium for ammonia/[emim][Ac] mixture at all temperature range is 13.4%.
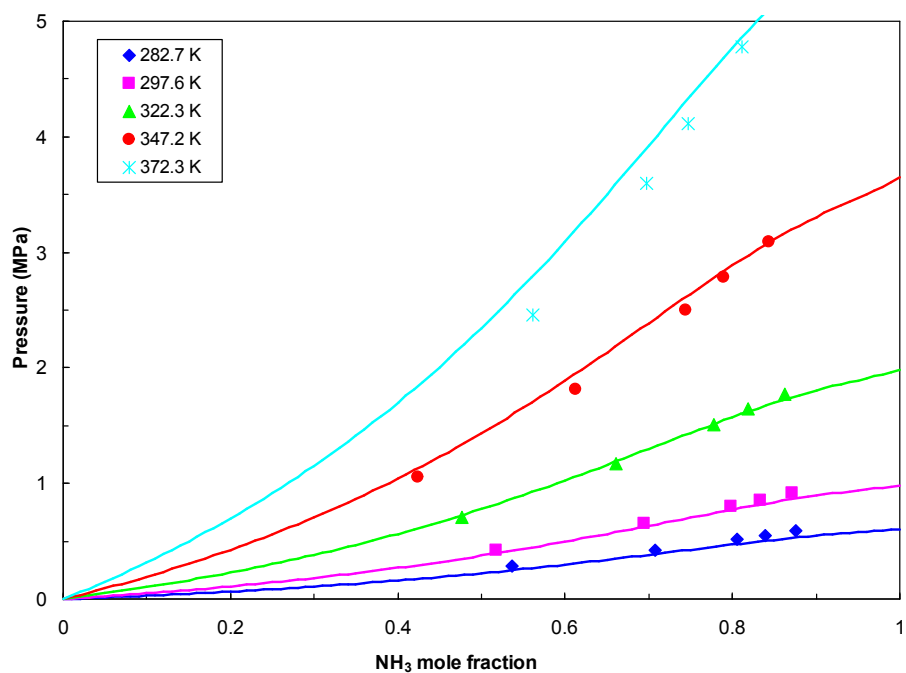
(a)
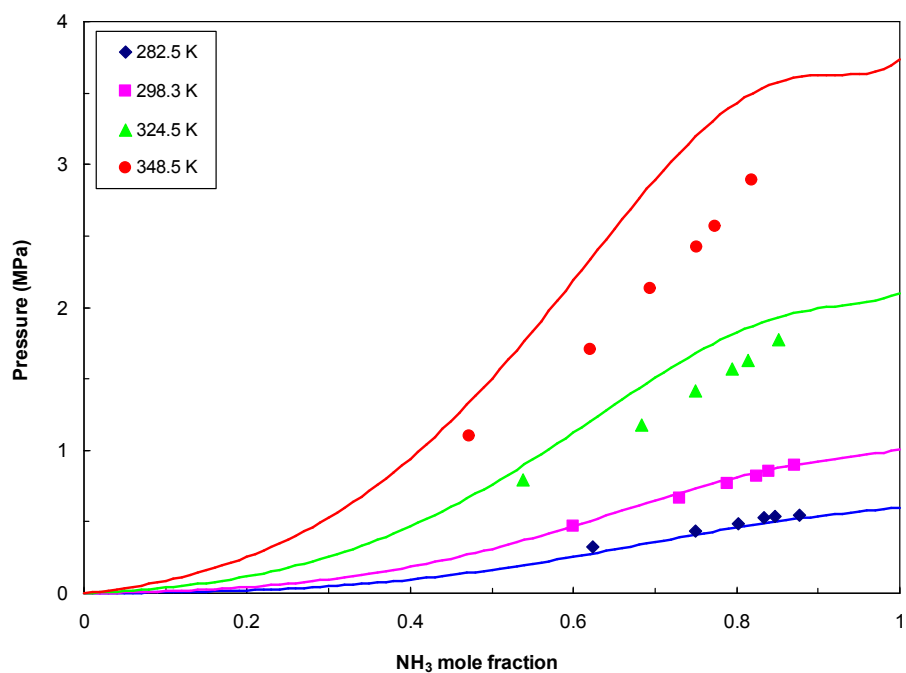
(b)

Figure 3.31. Vapor-liquid equilibrium of ammonia and [emim] based ionic liquid mixtures at different temperature. (a) [emim][EtSO$_4$] and (b) [emim][Ac]

3.6. Comparative Analysis

In this chapter, the ability of different model to calculate the vapor-liquid equilibrium of ammonia/ionic liquid mixtures was investigated. Four different

thermodynamic models used to calculate the vapor-liquid equilibrium of ammonia/ionic liquid mixtures, namely Non-Random Two Liquid (NRTL) model, Reidlich-Kwong-Soave Equation of State (RK-Soave EOS), are studied and analyzed. The study is carried out by firstly reviewing different thermodynamic models. Then, some experimental vapour-liquid-equilibrium data from literature of ammonia/ionic liquid mixtures are fitted with different models. The fitted interaction parameters and fitting quality of each model are listed for comparison. In the case of UNIFAC model, both group parameters of pure fluid and binary group interaction parameters were obtained from literature. Finally after both pure parameters and binary interaction are obtained, the vapor-liquid equilibrium calculation of ammonia and ionic liquid mixture is studied and analyzed the applicability of each model is estimated by taking into account both its precision and its simplicity.

The first thermodynamic model studied in this chapter, NRTL, shows its ability to model the vapor-liquid equilibrium of ammonia/ionic liquid mixtures with high accuracy. All results of the vapor liquid equilibrium using NRTL method were in good agreement for all ammonia/ionic liquid mixtures when compared with the experimental data. The NRTL model is able to calculate the vapor-liquid equilibrium of ammonia and ionic liquid mixtures in a wide range of temperatures and pressures. The overall average absolute deviations for calculated vapor-liquid equilibrium of ammonia/ionic liquids mixture were between 2.25% and 8.87%. In addition, the NRTL model is also able to calculate the excess properties of the mixtures. The results show that the excess enthalpy for all studied mixture were negative, except in the case of ammonia/[emim][SCN] mixture at high ammonia compositions. It means that the mixing process of studied ammonia/ionic liquid are exothermic. However, as there are no excess enthalpy data available in the literature, these results could not be compared and confirmed. In terms of simplicity, the NRTL model was considered as the simplest model in comparison with other three thermodynamic model. To be able to use this model, one only need at least vapor-liquid equilibrium data. The addition excess enthalpy data may improve the optimization of the binary interaction parameters, thus improve the quality of the model.

The Reidlich-Kwong-Soave Equation of State (RK-Soave EOS) also shows its ability to model the vapor-liquid equilibrium of ammonia/ionic liquid mixtures

with high accuracy. All results of the vapor liquid equilibrium using RK-Soave EOS method were in good agreement for all ammonia/ionic liquid mixtures when compared with the experimental data. The overall average absolute deviations for calculated vapor-liquid equilibrium of ammonia/ionic liquids mixture were between 0.77% and 6.21%. In addition, the RK-Soave EOS is also able to calculate the excess properties of the mixtures. However, different with that the NRTL model, the results of the excess enthalpy calculation using RK-Soave model show that the excess enthalpy for some studied mixture were positive, such as in the case of ammonia/[emim][NTf$_2$] and ammonia/[emim][SCN], also ammonia/[DMEA][ac] mixture at low ammonia compositions. Thus, it is important to confirm the results with the experimental data which are not available in the literature. In terms of simplicity, the RK-Soave EOS model was considered as less simple when compared with NRTL model. This is because the RK-Soave EOS model needs crtitical properties in addition to vapor-liquid equilibrium data. However, as several authors have indicated, most ionic liquids start to decompose at low temperature and in many cases at temperatures approaching the normal boiling point [10-11]. Therefore, critical properties cannot be measured [10]. Since experimental data do not exist, the "fictional" critical properties are then necessary to fulfill the missing critical parameters for ionic liquids. These "fictional" critical properties are sometimes estimated using group contribution such as proposed by Valderrama et al [10] or estimated using Vetere's method [6,25]. Obviously, as the critical properties of ionic liquid do not exist, the estimation results are not able to be confirmed and therefore may affect the accuracy of the model.

The third thermodynamic model studied in this chapter, perturbed-chain statistical associating fluid theory (PC-SAFT), also shows its ability to model the vapor-liquid equilibrium of ammonia/ionic liquid mixtures with high accuracy. All results of the vapor liquid equilibrium using PC-SAFT method were in good agreement for all ammonia/ionic liquid mixtures when compared with the experimental data. The overall average absolute deviations for calculated vapor-liquid equilibrium of ammonia/ionic liquids mixture were between 1.18% and 12.65%. In comparison with The PC-SAFT model can also be considered simple as it needs at least density data of pure fluid to obtained PC-SAFT pure parameters. An

advantage of this model is that this model enable to calculate whether two compound are soluble by only using PC-SAFT parameters of pure compounds. However, to be able to calculate the vapor-liquid equilibrium of a mixture with good accuracy, it is necessary to fit the value of the binary parameter k_{ij} from the experimetal VLE data.

The last thermodynamic model studied in this chapter is UNIFAC model. Our results shows that UNIFAC model shows its ability to model the vapor-liquid equilibrium of ammonia/ionic liquid mixtures with less accuracy in comparison with other three thermodynamic models. The overall average absolute deviations for calculated vapor-liquid equilibrium of ammonia/ionic liquids mixture were between 5.44% and 43.57%. The limited group parameters and binary group interaction parameters for ionic liquids available in the literature made the UNIFAC model is unable to calculate the vapor-liquid eqilibrium and its related properties with high accuracy.

Table 3.10 shows the summary *AAD* of ammonia/ionic liquid solubility calculation using four different models.

Table 3.10. Summary of *AAD* of ammonia/ionic liquid solubility calculation using different models.

Ionic Liquid	AAD (%)			
	NRTL Model	RK-Soave EOS	PC-SAFT EOS	UNIFAC Model
[bmim][BF$_4$]	3.9	1.6	11.8	15.8
[bmim][PF$_6$]	2.3	4.3	5.9	-
[emim][Ac]	4.1	0.8	1.4	13.4
[emim][EtSO$_4$]	3.8	0.9	1.2	5.4
[emim][SCN]	5.0	1.8	3.1	-
[emim][Tf2N]	8.9	6.2	12.7	-
[hmim][Cl]	8.9	5.2	11.2	-
[DMEA][Ac]	4.9	5.4	-	-

From table 3.10 and above analysis, it can be concluded that both NRTL and RK-Soave model show their ability to calculate the vapor-liquid equilibrium of ammonia/ionic liquid mixtures with high accuracy. Although the results using NRTL model were slightly less accurate than those of RK-Soave model, NRTL model is

considered as the simplest model in comparison with other thermodynamic models studied in this chapter. If the critical properties of ionic liquids are available or can be calculated, the cubic EOS also can be used, such as have been done by some authors [6-7]. PC-SAFT model, although it is not as simple as NRTL model and RK-Soave model, this model is able to calculate whether two pure compounds are soluble or not. Finally, UNIFAC model is so far not recommended to be used to calculate the phase-equilibrium of ammonia/ionic liquid mixtures due to its limitation in group parameters available in the database.

3.7. COP Estimation of Absorption Refrigeration Cycle Working with Ammonia/Ionic Liquid Mixtures

Using vapor-liquid equilibrium model described in this Chapter, it is possible to create *PTx* diagram of ammonia/ionic liquid mixtures and draw the solution cycle of ammonia/ionic liquid working pairs in the absorption system on the *PTx* diagram. In addition, the heat of mixing of the solution also can be estimated either using *PTx* diagram or using a thermodynamic model described in previous section. Therefore the *COP* of the absorption refrigeration system using ammonia/ionic liquid working fluids can be estimated using Equation (2.10)-(2.15) as described in Chapter 2.

Figure 3.32. shows the Duhring diagram (ln *P*-(1/*T*)-*x*) of ammonia/[bmim][BF$_4$] and ammonia/[emim][NTf$_2$] mixtures with the working fluid cycle of absorption refrigeration system. This diagram were built using NRTL model described in previous section. The working fluid cycle in the diagram was drawn based on operation condition of T_{EVAP}=10ºC, T_{COND}=40ºC, T_{ABS}=30ºC, and T_{GEN}=100ºC.
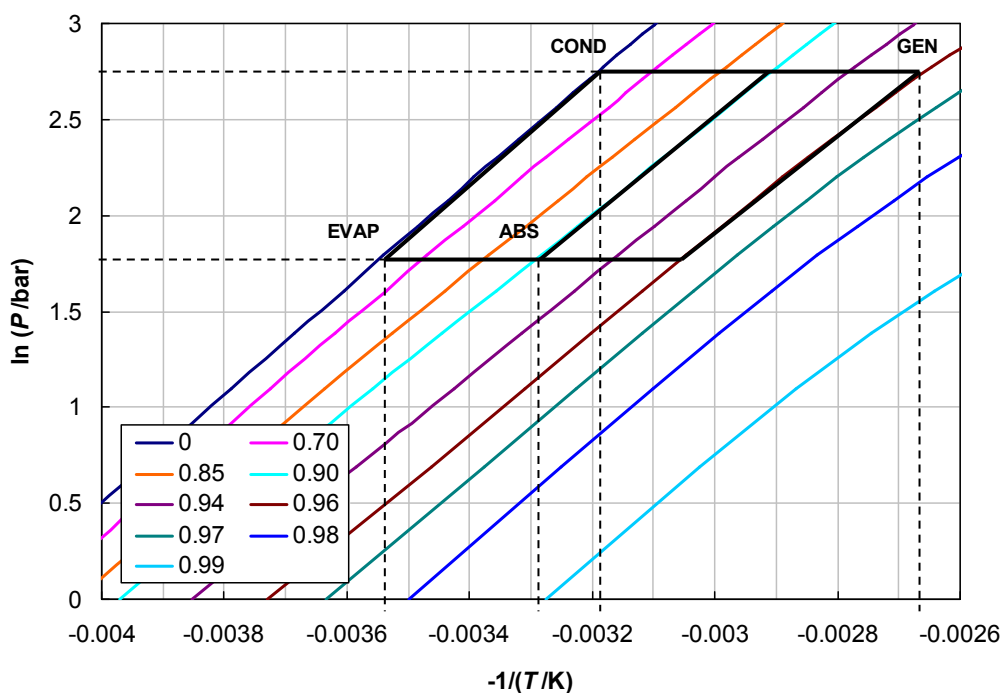
(a) ammonia/[bmim][BF$_4$]
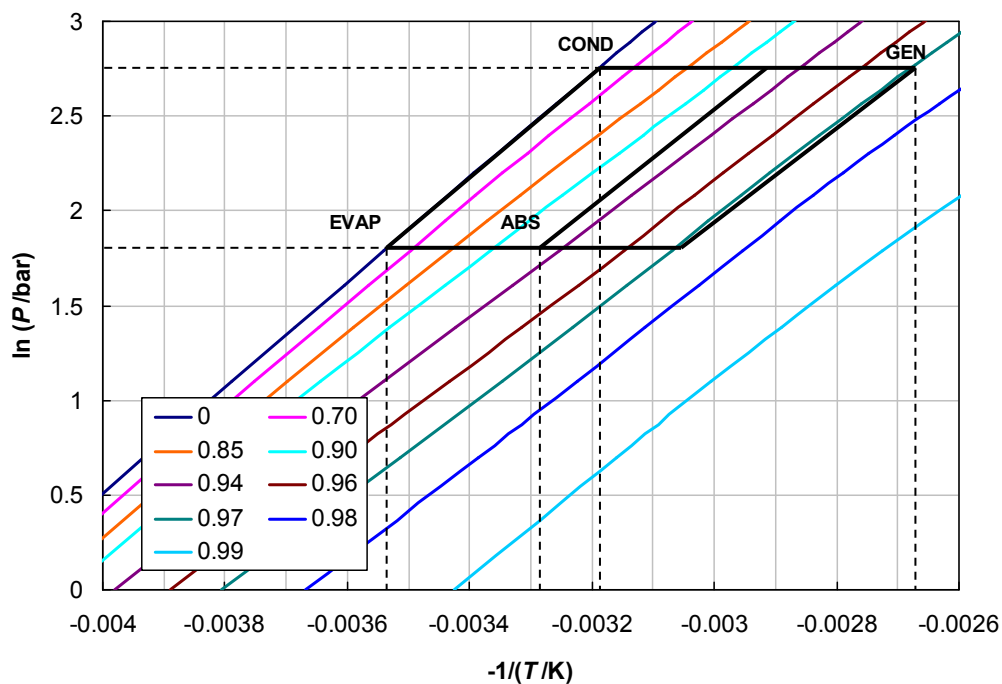
(b) ammonia/[emim][NTf$_2$]

Figure 3.32. Dühring diagram (ln P-(1/T)-x) of (a) ammonia/[bmim][BF$_4$] and (b) ammonia/[emim][NTf$_2$] mixture with the cycle colution of absorption refrigeration system. Color lines: ionic liquid mass fraction; black lines: working fluid cycle

From Figure 3.32. it can be noted that for this operation condition, the ammonia/ionic liquid solution works at high concentration (in absorbent). The concentration of the solution at rich solution (in refrigerant) was more than 0.80 (wt. of absorbent) as the concentration lines were not distributed uniformly between pure refrigerant line and pure absorbent line. The *PTx* diagram of other ammonia/ionic liquid mixtures studied in this chapter also show similar behavior.

Table 3.11. *COP* estimation of absorption refrigeration cycle with ammonia/ionic liquid working fluids

Parameters	Absorbent				
	[bmim]-[BF$_4$]	[bmim]-[PF$_6$]	[emim]-[NTf$_2$]	[emim]-[EtSO$_4$]	[emim]-[SCN]
T_{EVAP} (°C)	10	10	10	10	10
T_{COND} (°C)	40	40	40	40	40
T_{ABS} (°C)	30	30	30	30	30
T_{GEN} (°C)	100	100	100	100	100
Δh_v (kJ/kg)	1323	1323	1323	1323	1323
Δh_{mix} (kJ/kg)	137.39	142.35	132.76	69.81	251.96
$C_{p,r,l}$ (kJ/kg)	4.87	4.87	4.87	4.87	4.87
X_{ABS} (%wt. IL)	88.9	91.1	92.4	89.9	86.8
X_{GEN} (%wt. IL)	95.8	95.7	97.1	95.4	92.8
f	13.96	20.94	21.00	17.52	15.37
COP	0.715	0.588	0.657	0.612	0.648
COP from literature [5-6]	0.557	0.575	0.589	0.485	0.557

The *COP* estimation for absorption cycle using ammonia/ionic mixtures using Equation (2.15) were presented in Table 3.11. For comparison purpose, this evaluation was based on the operation condition similar to those published by Yokozeki and Shiflett [32] with heat exchanger effectiveness of 1 and refrigerant mass flowrate of 1 kg/s.

From Table 3.11 it can be seen that using solubility data and properties of pure refrigerant, the estimated *COP* values of the cycle with new working fluids

were close to the theoretical evaluation using detail parameters obtained from literature [5-6], although these values were generally slightly higher. The difference of these results was acceptable as this evaluation was only approximation using limited data.

Therefore to be able to obtain more detail results, detail calculation and simulation need to be carried out. Detail simulation allows us to have better results and understanding not only about *COP*, solution concentration and solution flow ratio, but also detail about other performance parameters such as thermal load of each components, solution pump's mechanical works, etc.

3.8. Conclusions

In this chapter, the ability of four different models to calculate the vapor-liquid equilibrium calculation of ammonia/ionic liquid mixtures, namely Non-Random Two Liquid (NRTL) model, Reidlich-Kwong-Soave Equation of State (RK-Soave EOS), Perturbed-chain statistical associating fluid theory (PC-SAFT) Equation of State, and UNIFAC model were studied and analyzed. Using selected thermodynamic model, the *PTx* diagram can be drawn and the heat of mixing of the working fluids can be estimated. Finally the COP of the absorption cycle using ammonia/ionic liquid can be estimated.

Both NRTL and RK-Soave model show their ability to calculate the vapor-liquid equilibrium of ammonia/ionic liquid mixtures with high accuracy. Although the results using NRTL model were slightly less accurate than those of RK-Soave model, NRTL model is considered as the simplest model in comparison with other thermodynamic models studied in this chapter. If the critical properties of ionic liquids are available or can be calculated, the cubic EOS also can be used, such as have been done by some authors [6-7]. PC-SAFT model, although it is not as simple as NRTL model and RK-Soave model, this model is able to calculate whether two pure compounds are soluble or not. Finally, UNIFAC model is so far not recommended to be used to calculate the phase-equilibrium of ammonia/ionic liquid mixtures due to its limitation in group parameters available in the database.

Using selected thermodynamic model, the PTx diagram has been drawn and the heat of mixing of the working fluids has been estimated. Finally the COP of the absorption cycle using ammonia/ionic liquid can be estimated. For specific operation condition, the ammonia/ionic liquid solution works at high concentration (in absorbent) as the concentration lines were not distributed uniformly between pure refrigerant line and pure absorbent line. In addition, the estimated *COP* values of the cycle with new working fluids were close to the theoretical evaluation using detail parameters obtained from literature [5-6].

Based above analysis, it can be concluded that NRTL and cubic Equation of State are the most appropriate model to be used to calculate the vapor-liquid equilibrium of ammonia/ionic liquid mixture due to their simplicity and their accuracy. Moreover, to be able to obtain more detail results, detail calculation and simulation need to be carried out. Detail simulation allows us to have better results and understanding not only about *COP*, solution concentration and solution flow ratio, but also detail about other performance parameters at different operation conditions.

Therefore, in the next chapter, the NRTL model would be used to perform the thermodynamic performance simulation of absorption refrigeration systems using ammonia/ionic liquid mixtures as working fluid.

3.9. References

[1] Chen, Y., Mutelet, F., and J Jaubert, J. N., Modeling the Solubility of Carbon Dioxide in Imidazolium-Based Ionic Liquids with the PC-SAFT Equation of State, *J. Phys. Chem. B,* 2012, 116, 14375−14388

[2] Renon, H., and Prausnitz, J. M., Local Compositions in Thermodynamic Excess Functions for Liquid Mixtures, *AIChE Journal,* 1968, 14 (1), 135-144

[3] Schmidt, K.A.G., Maham, Y., Mather, A.E., Use of the NRTL equation for simultaneous correlation of vapour-liquid equilibrium and excess enthalpy: Applications to aqueous alkanolamine systems. *J. Thermal Analysis and Calorimetry*, 2007, 89 (1), 61-72

[4] Kim, Y. J., Kim, S., Joshi, Y. K., Fedorov, A. G., and Paul, A., Kohl, P. A., Thermodynamic analysis of an absorption refrigeration system with ionic-liquid/refrigerant mixture as a working fluid. *Energy.* 2012; 44; 1005-1016

[5] Yokozeki, A., Shiflett, M.B., Ammonia solubilities in room-temperature ionic

liquids, ammonia solubilities in room-temperature ionic liquids. *Ind. Eng. Chem. Res*. 2007; 46; 1605-1610

[6] Yokozeki, A., Shiflett, M. B., Vapor–liquid equilibrium of ammonia + ionic liquid mixtures, *Applied Energy*, 84, 1258-1273, (2007).

[7] Li, G., Zhou, Q., Zhang, X., Wang, L., Zhang, S., Lia, J., Solubilities of ammonia in basic imidazolium ionic liquids. *Fluid Vapor-liquid equilibrium*. 2010 ;297(1); 34–39

[8] Soave, G., Equilibrium Constants for Modified Redlich-Kwong Equation-of-state, *Chem. Eng. Sci.*, Vol. 27, (1972), pp. 1196 – 1203

[9] Aspen Plus (Version 7.3): Aspen technology Inc. (2012)

[10] Valderrama, J.O., and Rojas, R.E., Critical Properties of Ionic Liquids. Revisited, *Ind. Eng. Chem. Res*., 2009, 48, 6890–6900

[11] Rebelo, L. P., Canongia, J. N., Esperanca, J. M., Filipe, E., On the Critical Temperature, Normal Boiling Point, and Vapor Pressure of Ionic Liquids. *J. Phys. Chem. B*., 2005, 109 (13), 6040–6043.

[12] VanNess, H.C., Abbott, M.M., Classical thermodynamics of nonelectrolyte solutions. New York: MacGraw-Hill; 1982

[13] Gross, J., and Sadowski, G., Perturbed-Chain SAFT: An Equation of State Based on a Perturbation Theory for Chain Molecules, *Ind. Eng. Chem. Res*., 2001, 40, 1244-1260

[14] Gross, J., and Sadowski, G., Application of the Perturbed-Chain SAFT Equation of State to Associating Systems, *Ind. Eng. Chem. Res*., 2002, 41, 5510-5515

[15] Huang, S.H., and Radosz, M., Equation of state for small, large, polydisperse, and associating molecules, *Ind. Eng. Chem. Res*., 1990, 29, 2284-2294

[16] Huang, S.H., and Radosz, M., Equation of state for small, large, polydisperse, and associating molecules: extension to fluid mixtures, *Ind. Eng. Chem. Res*., 1991, 30, 1994-2005

[17] NIST Thermo Data Engine (TDE), ASPEN Plus v.7.3, Aspen Technology, Inc.

[18] K.R. Patil, C. Nieto de Castro, Anil Kumar, Ramesh Gardas, A. Coronas, Report on the energy-related parameters for cations and anions of Ionic Liquids and molecular solvents, Narilar Project Report, 2013

[19] Sun G., Huang W., Zheng D., Dong L., and Wu X., Vapor-Liquid Equilibrium Prediction of Ammonia-Ionic Liquid Working Pairs of Absorption Cycle Using UNIFAC Model, *Chin. J. Chem. Eng.*, 2014, 22 (1), 72-78

[20] Lei, Z., Zhang, J., Li, Q., and Chen, B., UNIFAC Model for Ionic Liquids, *Ind. Eng. Chem. Res.*, 2009, 48, 2697–2704

[21] Kim, Y.S., Choi, W.Y., Jang, J.H., Yoo, K.P., Lee, C.S., "Solubility measurement and calculation of carbon dioxide in ionic liquids", *Fluid Phase Equilib.*, 2005, 228-229, 439-445

[22] Thomsen, K., Rasmussen, P., "Modeling of vapor-liquid-solid equilibrium in gas-aqueous electrolyte systems", *Chem. Eng. Sci.*, 1999, 54 (12), 1787-1802

[23] Wang, J.F., Sun, W., Li, C.X. Wang, Z.H., "Correlation of infinite dilution activity coefficient of solute in ionic liquid using UNIFAC model", *Fluid Phase Equilib.*, 264 (1-2), 235-241 (2008).

[24] Lei, Z.G., Zhang, J.G., Li, Q.S., Chen, B.H., "UNIFAC model for ionic liquids", *Ind. Eng. Chem. Res.*, 2009, 48 (5), 2697-2704

[25] Vetere A. Again the rackett equation. Chem Eng J 1992;49:27–33

[26] Kotenko. O., Moser, H., and Rieberer, R., Thermodynamic Analysis Of Ammonia/Ionic Liquid Absorption Heat Pumping Processes. *Proc. Int. Sorption Heat Pump Conf.*, 2011; 89-796

[27] Swarnkar, S. K., Srinivasa Murthy, S. S., Gardas, R. L., Venkatarathnam, G., Performance of a vapour absorption refrigeration system operating with ionic liquid-ammonia combination with water as cosolvent, *Applied Thermal Engineering*, 2014, 72 (2), 250-257

Chapter 4

Performance of Absorption Refrigeration Systems with Ammonia/Ionic Liquid as Working Fluids using ASPEN Plus

4.1. Introduction

Using solubility data, the COP of the absorption cycle using ammonia/ionic liquid can be estimated. However, to be able to obtain more detail results, detail calculation and simulation need to be carried out. Detail simulation allows us to have better results and understanding not only about *COP*, solution concentration and solution flow ratio, but also detail about other performance parameters at different operation conditions.

In this chapter, the detail performances of absorption refrigeration systems using ammonia/ionic liquid mixtures working pair were theoretically studied and analysed. The 1-ethyl-3-methylimidazolium ethylsulfate ([emim][EtSO$_4$]), (1-ethyl-3-methylimidazolium thiocyanate ([emim][SCN]), -butyl-3-methylimidazolium hexafluorophosphate ([bmim][PF$_6$]), 1-ethyl-3-methylimidazolium bis(trifluoromethyl-sulfonyl)imide ([emim][NTf$_2$]), 1-butyl-3-methylimidazolium tetrafluoroborate ([bmim][BF$_4$]) have been selected as absorbent for ammonia absorption applications. The thermodynamic properties correlation of ammonia/ionic liquid mixture were built using activity coefficient based model non-random two-liquid (NRTL) based on experimental vapor-liquid equilibrium data. Other thermophysical properties necessary for the investigation were correlated from

experimental data obtained from literature. The thermodynamic performance of absorption refrigeration systems with these new proposed ammonia/ionic liquid working fluids were analysed and discussed based on key parameters of coefficient of performance (*COP*), solution mass flow ratio (*f*) solution mass flowrate per unit of cooling load (*R*).

4.2. Thermodynamic Properties

As it has been conclude in previous chapter that NRTL and cubic Equation of State are the most appropriate model to be used to calculate the phase equilibria of ammonia/ionic liquid mixture due to their simplicity and their accuracy, therefore the thermodynamic properties correlation of ammonia/ionic liquid mixture were built based on activity coefficient based model non-random two-liquid (NRTL). NRTL model is an empirical equation proposed by Renon and Prausnitz [1] based on the local composition representation of the excess Gibbs energy, G^E, of liquid mixtures. The detail of NRTL model has been previously described in Chapter 3.

All thermodynamics calculations of ammonia/ionic liquid working fluids were carried out using ASPEN Plus [2]. To calculate the thermodynamic properties of ammonia/ionic liquid mixtures, the experimental properties data of pure ionic liquids were extracted from the literature as well as experimental VLE data of ammonia/IL mixtures. The experimental properties data of pure IL liquids extracted for the simulation are heat capacity, density/molar volume and viscosity. The properties data sets and property data correlations used to calculate thermodynamics properties of ammonia/ionic liquid mixtures were extracted from NIST Thermo Data Engine available in ASPEN Plus [3].

In addition, the experimental vapor-liquid eqilibrium data for ammonia/ionic liquid mixtures were taken from Yokozeki and Shiflett [4–5] as they were not available in NIST database in ASPEN Plus. Similarly, the density and heat capacity data of pure [emim][SCN] were taken from Ficke et al [6].

The NRTL binary parameters were obtained from vapor liquid equilibrium data [2] regression and have been discussed in Chapter 3.

The isobaric heat capacities of pure ionic liquids necessary to calculate the enthalpy of the working fluids were correlated using ThermoML polynomial equation which can be expressed as [2]

$$C_{p,m} = \sum_{n=1}^{5} C_n (T + 273.15)^{n-1} \qquad (4.1)$$

where $C_{p,m}$ is molar isobaric heat capacity (J/mol) and C_n are parameters number n which are presented in Table 4.1.

Tabel 4.1. Parameters for Equation (4.1)

Parameter (C_n)	[bmim][BF$_4$]	[bmim][PF$_6$]	[emim][EtSO$_4$]	[emim][NTf$_2$]
C_1	208224.4	455384.2	304135.8	-682954.7
C_2	732.769	-1901.677	-57.854	14096.040
C_3	-0.6487	10.0087	2.6008	-66.1577
C_4	0	-0.0167	-0.0073	0.1422
C_5	0	0	0	-0.0001

For [emim][SCN], the isobaric heat capacity was calculated using [6]

$$C_{p,m} = a + \frac{b}{(T + 273.15)} \qquad (4.2)$$

where $C_{p,m}$ is molar isobaric heat capacity (kJ/kmol) and parameters a and b are set to 363.5 and $-2.256 \cdot 10^4$, respectively.

Similarly, the densities of pure ionic liquids necessary to calculate the solution pump work were correlated using ThermoML polynomial equation which can be expressed as [2]

$$\rho_m = \sum_{n=1}^{3} D_n (T + 273.15)^{n-1} \qquad (4.3)$$

where ρ_m is molar density (kmol/m^3) and D_n are parameters number n which are presented in Table 4.2.

Tabel 4.2. Parameters for Equation (4.3)

Ionic Liquids	Parameter (D_n)		
	D_1	$D_2 \cdot 10^3$	$D_3 \cdot 10^6$
[bmim][BF$_4$]	6.2656	-3.1961	0
[bmim][PF$_6$]	5.6724	-2.9026	0
[emim][EtSO$_4$]	6.0024	-2.5775	0
[emim][NTf$_2$]	4.6352	-2.5374	0
[emim][SCN]	6.6852	-3.7115	1.8845

In addition, the thermophysical properties of ammonia refrigerant vapor were correlated by means of Reidlich-Kwong Equation of State and its parameters wew already available in Aspen Plus.

4.3. Mathematical Model and Cycle Configuration

The absorption cycle was modeled in ASPEN Plus based on basic single effect absorption cycle configuration. As mentioned above, due to very low vapor pressure of the ionic liquid there is no necessary to add rectification process in the ammonia/ionic liquid absorption refrigeration cycle for the generation of refrigerant vapor with sufficient purity.

Because ASPEN uses a sequential solver, it is necessary to model a "break" in closed cycles to give inputs to the model. In the present work the outlet of the absorber was not connected to the inlet of the solution pump, therefore the streams at absorber outlet and solution pump inlet were defined as stream 1A and stream 1, respectively. The model is considered to be well converged if these two fluid streams give the same results. The break in stream 1 allows for inputs to be given for the model. These inputs were the absorber temperature, a vapour fraction of zero, the solution mass flow rate, and the mass fraction of ammonia and ionic liquid.

The flowsheet diagram of the single stage absorption refrigeration cycle using ammonia/ionic liquid mixtures is shown in Figure 4.1. The cycle components and the assumptions given in each component are specified below:

- Absorber: consist of ASPEN models 'mixer' (MIX) and 'heater' (ABS). The mixer is specified as an adiabatic mixer and the rich solution at the absorber outlet is at saturated-liquid condition.

- Generator: consist of ASPEN model 'flash' for vapor-liquid phase. The vapor refrigerant is generated by supplying heat at high temperature.

- Condenser: consist of ASPEN model 'heater' (COND). The refrigerant at the condenser outlet is at saturated-liquid condition.

- Evaporator: consist of ASPEN model 'heater' (EVAP). The refrigerant at the evaporator outlet has temperature of 5°C (corresponds to the low pressure level 5.15 bar).

- Solution heat exchanger: consist of two ASPEN models 'heater' (COLDSHX and HOTSHX). The heat is transferred from stream 4 (hot side inlet) to stream 2 (cold side inlet), resulting in stream 5 (hot side outlet) and stream 3 (cold side outlet). The heat exchanger effectiveness is equal to 0.8. The correlation between heat exchanger effectiveness and each stream temperature was implemented in ASPEN Plus using calculator block.

- Solution pump: consist of ASPEN model 'pump' (SPUMP). The discharge pressure of the solution pump is equal to the high pressure level (e.g. 11.63 bar), and isentropic pump efficiency is equal to 50%.

- Refrigerant valve and solution valve: consist of ASPEN model 'valve' (RVL and SVL, respectively). The discharge pressure of the valves is equal to the low pressure level.

In addition, following assumptions were applied to perform the simulation of single stage absorption refrigeration cycle using ammonia/ionic liquid mixtures:

- The cycles are in steady-state condition.

- The thermal and pressure losses during the whole processes are negligible

- Solution and refrigerant valves are isenthalpic.

As the vapour pressure of pure ionic liquids is negligible, there is no necessary to add rectification column at the refrigerant outlet of the generator and the vapour at the outlet of generator is pure refrigerant vapour.

The solution heat exchanger effectiveness was set in Aspen Plus using Calculator Block. The solution heat exchanger effectiveness can be formulated using Equation (4.4)

$$\varepsilon_{SHX} = \frac{(T_4 - T_5)}{(T_4 - T_2)} \tag{4.4}$$

Figure 4.1. Flowsheet diagram of absorption refrigeration cycle in ASPEN Plus

Moreover, some key parameters were used to evaluate the performance of absorption refrigeration cycle. These key parameters were also applied in Aspen Plus using Calculator Block. Coefficient of performance (*COP*) is defined as the ratio of

available useful cooling output of the system to the total power supplied to the system. The *COP* can be mathematically written as

$$COP = \frac{Q_{EVAP}}{Q_{GEN} + W_p} \tag{4.5}$$

where Q_{EVAP} and Q_{GEN} are the cooling output of the evaporator and the heat input of the generator, respectively and W_p is the working input of the solution pump.

The work input of the solution pump W_p is negligible relative to the heat input in the generator therefore the pump work is usually neglected for the purposes of analysis.

Solution mass flow ratio (*f*) is defined as the ratio of mass flow rates of weak solution to produced refrigerant vapour. Thus, the *f* can be mathematically written in Equation (4.6).

$$f = \frac{m_s}{m_r} \tag{4.6}$$

Another important parameter to evaluate the performance of absorption cycle is solution mass flowrate per unit of cooling load (*R*) which is defined as weak solution mass flow rate needed to produce a unit cooling thermal load of refrigeration. This parameter can be written in Equation (4.7).

$$R = \frac{m_s}{Q_{EVAP}} \tag{4.7}$$

4.4. Model Validations

Before applying the model in the absorption refrigeration systems using new proposed working fluids the model was first validated by comparing the results with the simulation data from literature [4-5,7]. As discussed in the previous chapter, the experimental investigation of the performance of ammonia/ionic liquid working fluids for absorption refrigeration applications are still not available in open literature. Therefore the the results of the performance of absorption refrigeration

systems working with ammonia/ionic liquid mixtures using NRTL model were validated with the simulation results of Yokozeki and Shiflett [4-5] and Ruiz et al [7]. For validation purpose, the absorption refrigeration system was set at same operation conditions (T_{GEN}=100ºC, T_{ABS}=30ºC, T_{COND}=40ºC, T_{EVAP}=10ºC, and ε_{SHX}=1). The comparison of present results with the simulation results from Yokozeki and Shiflett and Ruiz et al [4-5,7] are presented in Table 4.3.

Table 4.3. Comparison of present work with literature [4-5]

Ionic Liquid	*f*			*COP*		
	Present Work	Yokozeki and Shifflet [4-5]	Ruiz et al. [7]	Present Work	Yokozeki and Shifflet [4-5]	Ruiz et al. [7]
[bmim][BF$_4$]	13.96	12.98	-	0.612	0.557	-
[bmim][PF$_6$]	20.94	17.27	-	0.545	0.575	-
[emim][NTf$_2$]	21.00	24.57	-	0.446	0.589	-
[emim][EtSO$_4$]	17.52	17.55	21.24	0.612	0.485	0.540
[emim][SCN]	15.37	12.42	12.79	0.497	0.557	0.592
Ionic Liquid	X_{GEN} (% wt. IL)			X_{ABS} (% wt. IL)		
	Present Work	Yokozeki and Shifflet [4-5]	Ruiz et al. [7]	Present Work	Yokozeki and Shifflet [4-5]	Ruiz et al. [7]
[bmim][BF$_4$]	95.8	95.7	-	88.9	88.3	-
[bmim][PF$_6$]	95.7	94.5	-	91.1	89.0	-
[emim][NTf$_2$]	97.1	96.3	-	92.4	92.4	-
[emim][EtSO$_4$]	95.4	95.2	93.70	89.9	89.8	89.80
[emim][SCN]	92.8	92.7	92.40	86.8	85.2	85.20

From this comparison, it can be seen that our results were all in good agreement with the simulation results taken from reference [1,4]. The small discrepancies between our results and those of reference were quite acceptable considering different thermodynamic methods and parameters used in the simulations.

4.5. Results And Discussions

In this chapter, the thermodynamic performance of absorption refrigeration cycle using five different ionic liquids as absorbents were evaluated. The ammonia/ionic liquid working mixtures available in the literature, namely ammonia/[bmim][BF$_4$], ammonia/[bmim][PF$_6$], ammonia/[emim][NTf$_2$], ammonia/[emim][EtSO$_4$], and ammonia/[emim][SCN], were investigated.

4.5.1. Performance of Absorption Refrigeration Cycle

The performance of absorption refrigeration cycle working with ammonia/ionic liquid working fluids were evaluated at typical operation conditions for refrigeration applications. In this chapter, the analyses were carried out with ionic liquid mass flow rate of 1 kg/s. Table 4.4 shows the performance and thermal load of absorption refrigeration cycle at T_{GEN}=100ºC, T_{ABS}=30ºC, T_{COND}=30ºC, T_{EVAP}=5ºC, and ε_{SHX}=0.8 for absorbent (ionic liquid) mass flow rate of 1 kg/s. As it can be observed in this table the coefficient of performance (*COP*) of the systems working with ammonia/ionic liquid fluid mixtures lies between 0.65 and 0.87 Among all of ammonia/ionic liquid working fluids studied in this chapter, the ammonia/[emim][NTf$_2$] working fluid presented the highest COP than that of other ammonia/ionic liquid mixtures. The *COP* of the systems with ionic liquids as absorbents follows an order of [emim][NTf$_2$] > [emim][SCN] > [bmim][PF$_6$] > [bmim][BF$_4$] > [emim][EtSO$_4$].

In terms of circulation ratio, it can be seen from Table 4.4 that the circulation ratios (*f*) of the absorption systems working with ammonia/ionic liquid working fluids at same ionic liquid mass flow rate and operation conditions were quite high due to low solubility of ammonia into ionic liquids. The *f* of the systems working with ammonia/ionic liquid fluid mixtures lies between 16.37 and 24.55. The lowest *f* among all of studied ammonia/ionic liquid working fluids was shown by ammonia/[emim][BF$_4$] where as the highest one is shown by ammonia/ [emim][NTf$_2$].

In addition, although the *COP* of the system working with ammonia ammonia/[emim][NTf$_2$] was higher than the systems with other working fluids, it is also interesting to see that its circulation ratio was the highest among other working fluids. On contrary, although the *COP* of the system working with ammonia ammonia/[bmim][BF$_4$] was lower than the systems with other working fluids, its circulation ratio was the lowest among other working fluids.

Table 4.4. Performance and thermal load of absorption refrigeration cycle

Parameter	Absorbent				
	[bmim]-[BF$_4$]	[emim]-[EtSO$_4$]	[emim]-[NTf$_2$]	[bmim]-[PF$_6$]	[emim]-[SCN]
Performance					
COP	0.6708	0.6574	0.8723	0.6959	0.8192
f (kg/kg)	18.1883	20.5227	27.2611	21.0873	19.7217
R (kg/MW s)	16.3772	18.4791	24.5466	18.9875	17.7579
Thermal load					
Q_{EVAP} (kW)	66.5531	58.8556	43.1471	57.6938	62.8347
Q_{GEN} (kW)	99.2126	89.5330	49.4642	82.9108	76.7055
Q_{ABS} (kW)	88.1471	80.4745	42.2876	73.3056	66.8058
Q_{COND} (kW)	78.3059	69.2489	50.7665	67.8820	73.9307
Q_{SHX} (kW)	96.2195	110.50972	7.7107	83.5164	25.4209
W_p (kW)	0.6873	0.6652	0.4427	0.5830	1.19637
Solution concentration					
X_{ABS} (%wt. absorbent)	91.75	91.95	94.42	91.29	89.62
X_{GEN} (%wt. absorbent)	97.08	96.66	98.01	95.83	94.41

The higher circulation ratio of ammonia/ionic liquid working fluids also affects the solution mass flowrate per unit of cooling load (*R*). It is interesting to see

that although the *COP* of the system working with ammonia/[emim][NTf$_2$] mixture was higher than the systems with other working fluids, its *R* was the lowest among other working fluids. It means that at the same ionic liquid mass flow rate and at the same operation conditions, the systems working with ammonia/[emim][NTf$_2$] mixture can produce lower cooling capacity. In contrary, although the *COP* of the system working with ammonia ammonia/[bmim][BF$_4$] mixture was lower than the systems with other working fluids, on contrary its *R* value was the highest among other working fluids, which means that at the same ionic liquid mass flow rate and at the same operation conditions, the systems working with ammonia/[bmim][BF$_4$] mixture can produce higher cooling capacity. The *R* of the systems working with ammonia/ionic liquid fluid mixtures lies between 8.2 kg/MW·s and 22.8 kg/MW·s. The lowest *R* among all of studied ammonia/ionic liquid working fluids was shown by ammonia/[bmim][BF$_4$] mixture where as the highest one was shown by ammonia/ [emim][NTf$_2$] mixture. To produce cooling load of 1 MW, the absorption systems working with ammonia/[bmim][BF$_4$] only needs 16.38 kg/s of solution mass flowrate and to produce cooling load of 1 MW, the absorption systems working with ammonia/[emim][NTf$_2$] needs as much as 24.55 kg/s of solution mass flowrate. It implies that generally an absorption system working with ammonia/ionic liquids needs more solution to produce cooling than other conventional working fluids.

In addition, it is also interesting to see from Table 4.4 that the energy consumption needed to operate the absorption cycle mainly occurs at the generator, and that the mechanical work required for the solution pump is very small in comparison with energy input of the generator (less than 1% in the case of the highest solution pump's work) and thus can be neglected for general calculations or when information on solution density is not available [8].

4.5.1.1. *Effect of Generator Temperature*

Figure 4.2 shows the effects of generator temperatures on the *COP* of the absorption refrigeration cycles with various working fluids. As illustrated in Figure 4.2, the *COP* increases when the generator increases and then slightly decreases when the generator temperature is kept increase. For all systems, it also can be

observed that there is a low generator temperature limit for each cycle. Each cycle cannot be operated at generator temperatures lower than its limit. The generator temperature limit of all working fluid systems is around $62-65°C$.
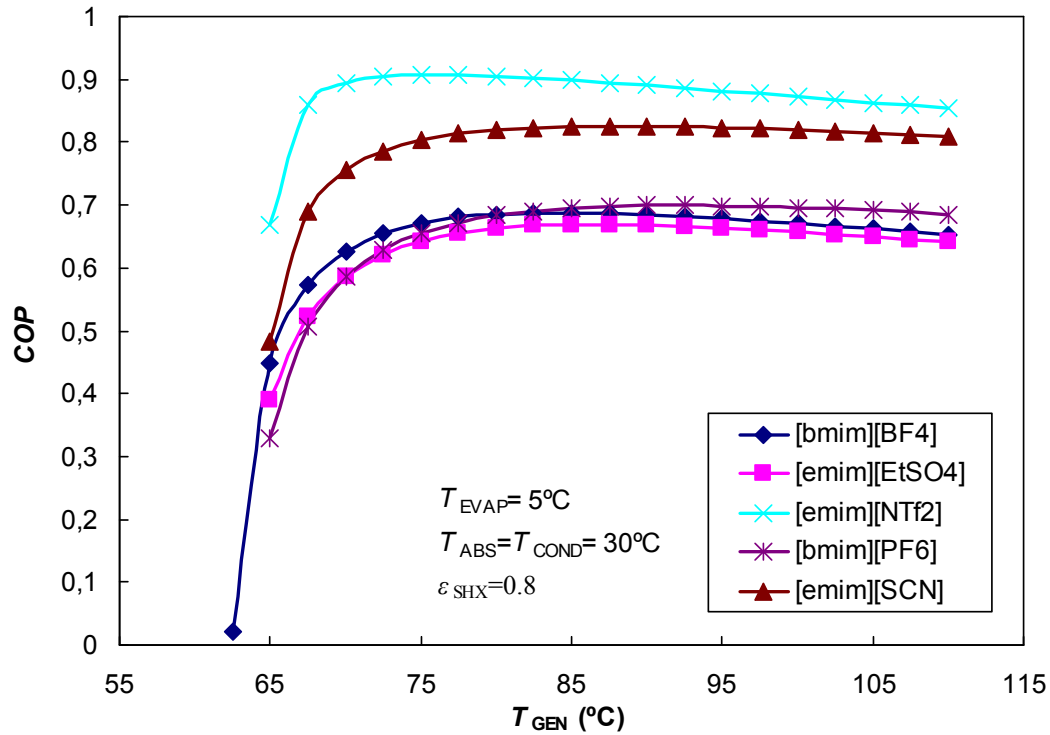
Figure 4.2. Effect of generator temperature on *COP* of the absorption systems

Among all ammonia/ionic liquid mixtures studied working fluid, the highest *COP* was reached by the cycle with ammonia/[emim][NTf$_2$] working fluids. The maximum *COP* of the absorption refrigeration cycle with this working fluid reaches at generator temperature of 75°C and decreases gradually when the generator temperature was operated above 75°C. On the other hand, other four ionic liquid-based working fluids have similar *COP* behaviour however, their maximum COP were reached at the generator temperature of 85°C. The *COP* among these four ionic liquid-based working fluid follow an order of [emim][SCN] > [bmim] [PF$_6$] > [bmim][BF$_4$] > [emim][EtSO$_4$] for generator temperature above 85°C. The highest *COP* of each cycle working with ammonia/ionic liquid mixtures were lies between 0.67 and 0.89.
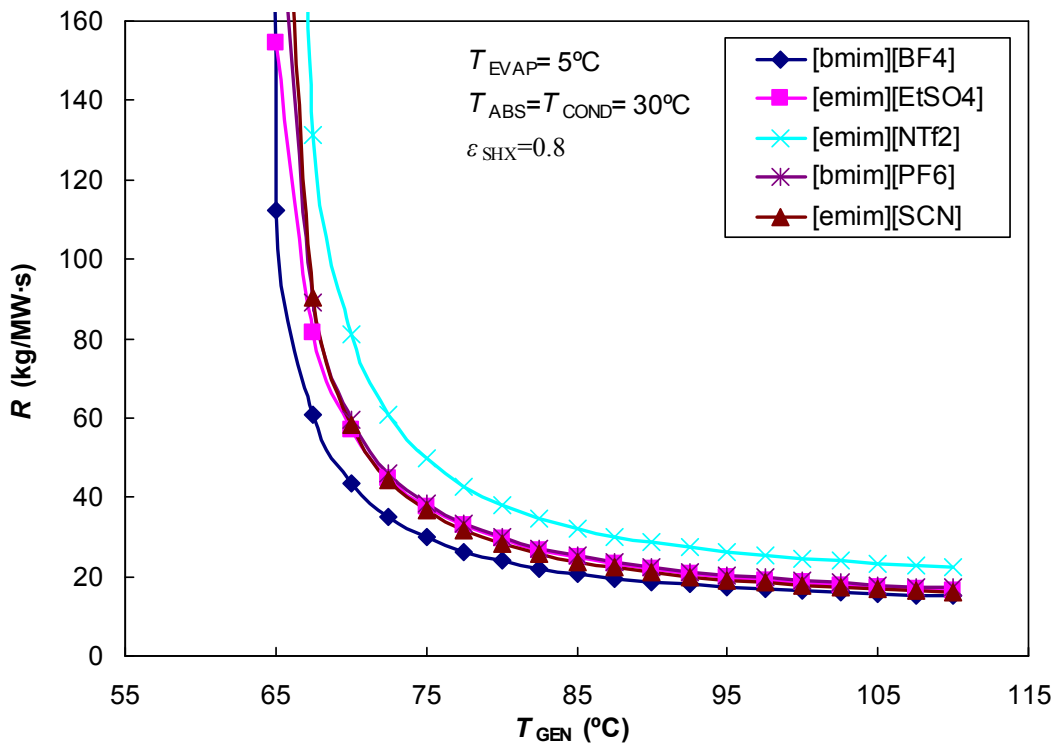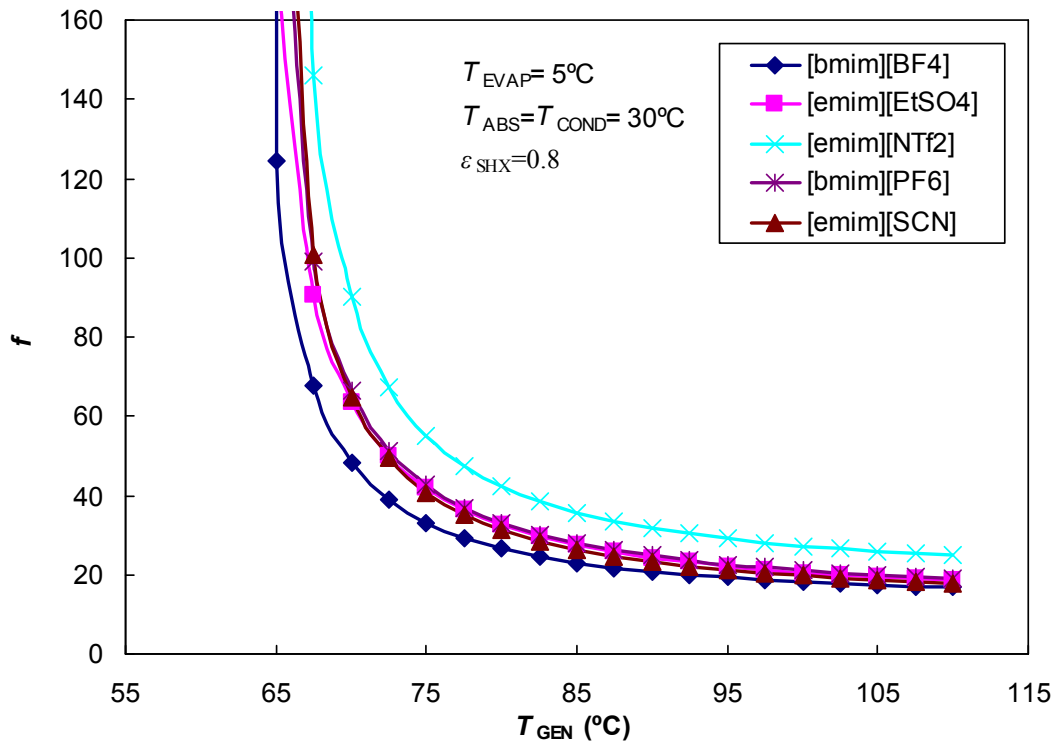
Figure 4.3. Effect of generator temperature on f (a) and R (b) of the absorption systems

The effects of generator temperature on the solution circulation ratio (f) and solution mass flowrate per unit of cooling load (R) of the absorption refrigeration cycles with various working fluids are shown in Figure 4.3. As it has been mentioned before, the amount of solution needed to operate the absorption refrigeration cycle at same cooling capacity is different due to their solubility with ammonia. For all studied working fluids, the solution circulation ratio of the absorption cycle decreases when the generator temperature increases as at higher generator temperature the systems are able to produce more refrigerant vapour. The solution circulation ratio increases significantly when the generator temperature decreases near to its generator temperature limits. The ammonia/[bmim][BF$_4$] working fluid was the lowest among all four ionic liquids base working fluid and the f values of the ammonia/[emim][NTf$_2$] was the highest. The solution ratios of the systems with other three ammonia/ionic liquids mixtures were almost similar at all generator temperature ranges. At generator temperature of 85ºC, corresponds to the optimum generator temperature, the solution circulation ratio of the systems with ammonia/[bmim][BF$_4$] working fluid was 23.00 and the solution circulation ratio of the systems with ammonia/[emim][NTf$_2$] working fluid was 35.78. For other three ammonia/ionic liquid mixtures, at generator temperature of 85ºC, solution circulation ratios of the systems were quite similar, between 26 and 28.

Regarding to the solution mass flowrate per unit of cooling load (R), the R values of the absorption systems working with ammonia/ionic liquid working fluids at same solution mass flow rate and operation conditions were relatively high. The trends of R values are similar to the f values as at the same cooling capacity and operation conditions the circulation ratio was related to the solution mass flowrate per unit of cooling load. The ammonia/[bmim][BF$_4$] working fluid was the lowest among all four ionic liquids base working fluid and the f values of the ammonia/[emim][NTf$_2$] was the highest. The solution ratios of the systems with other three ammonia/ionic liquids mixtures were almost similar at all generator temperature ranges. At generator temperature of 85ºC, corresponds to the optimum generator temperature, the solution circulation ratio of the systems with ammonia/[bmim][BF$_4$] working fluid was 20.71 kg/MW.s and the solution circulation ratio of the systems with ammonia/[emim][NTf$_2$] working fluid was 32.18

kg/MW.s. For other three ammonia/ionic liquid mixtures, at generator temperature of 85ºC, solution circulation ratios of the systems were quite similar, with R values around 22.99 – 25.20 kg/MW.s.

4.5.1.2.   *Effect of Cooling Temperature*

The effects of cooling temperature on the performance of the absorption refrigeration systems with different ammonia/ionic liquid working fluids are shown in Figure 4.4. It can be seen in Figure 4.4, the *COP* of the system increases with the increase of the evaporator temperature. Again, the *COP* of the systems working with ammonia/[emim][NTf$_2$] was the highest when compared with the systems with other working fluids for cooling temperature range of 5ºC - 10ºC, followed by the systems with ammonia/[emim][SCN] working fluid. For other ammonia/ionic liquid working fluids, the *COP* values follow an order of [bmim][PF$_6$] > [bmim] [BF$_4$] > [emim][EtSO$_4$] for a range of cooling temperature from -5ºC to 10ºC, although the values for these three working fluids were not significantly differrent. For cooling temperature below -2ºC, which is the refrigeration temperature, the system with ammonia/[bmim][PF$_6$] working fluid shows lower *COP* in comparison with those of ammonia/[bmim][BF$_4$] and ammonia/[emim][EtSO$_4$] working fluids. Moreover, at cooling temperature higher than -2ºC, the system with ammonia/[emim][EtSO$_4$] working fluid shows lower *COP* in comparison with those of ammonia/[bmim][PF$_6$] and ammonia/[bmim][BF$_4$] working fluids.
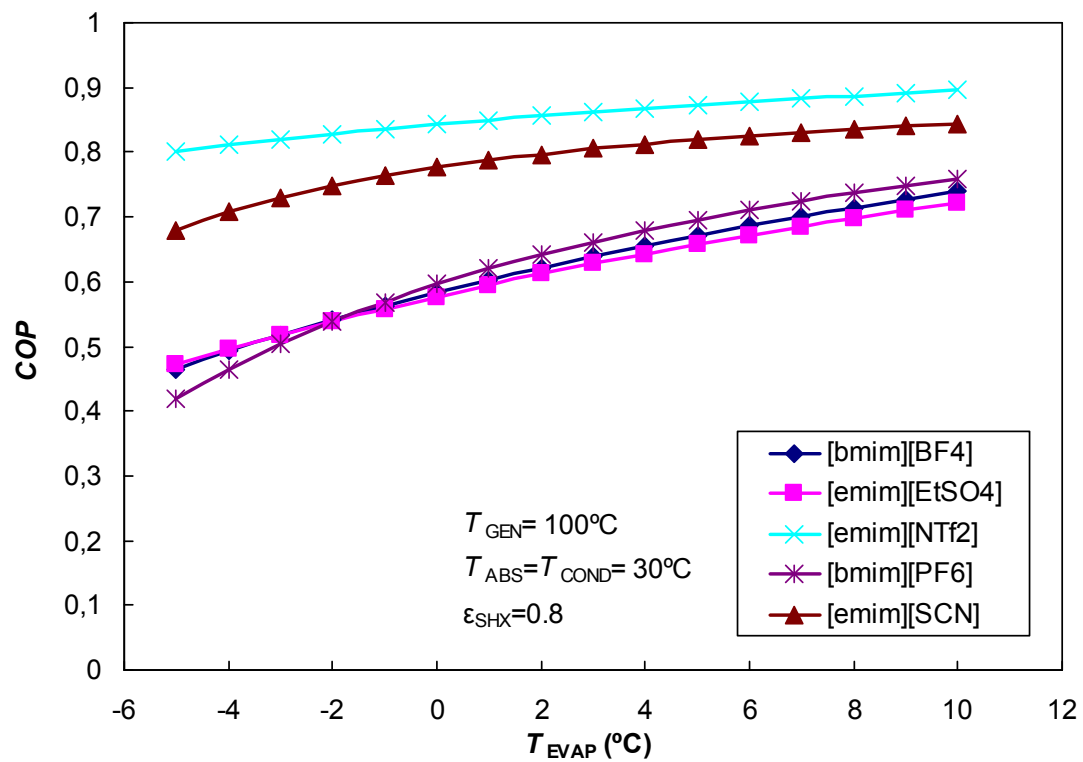
Figure 4.4. Effect of cooling temperature on *COP* of the absorption systems

In terms of solution circulation ratio (*f*) and solution mass flowrate per unit of cooling load (*R*), the increase in cooling temperature will decrease both the circulation ratio (*f*) and solution mass flowrate per unit of cooling load (*R*) as it shown in Figure 4.5. Similarly, the trends of the cooling temperature versus *R* values were identical with those of the *f* values.
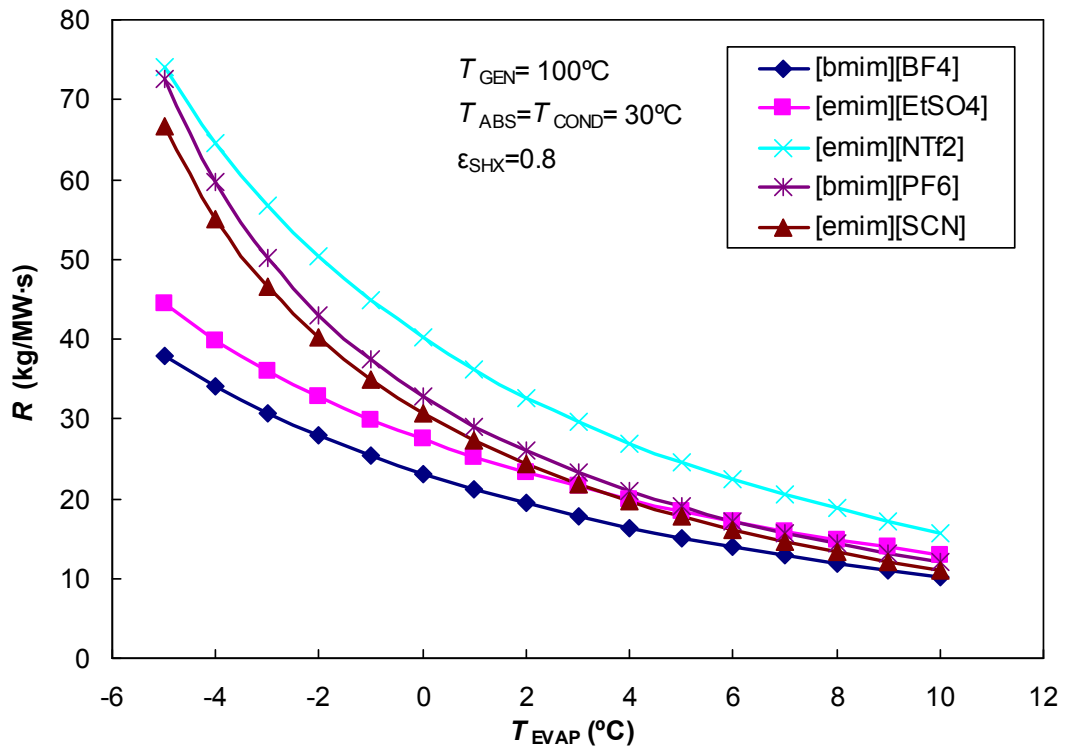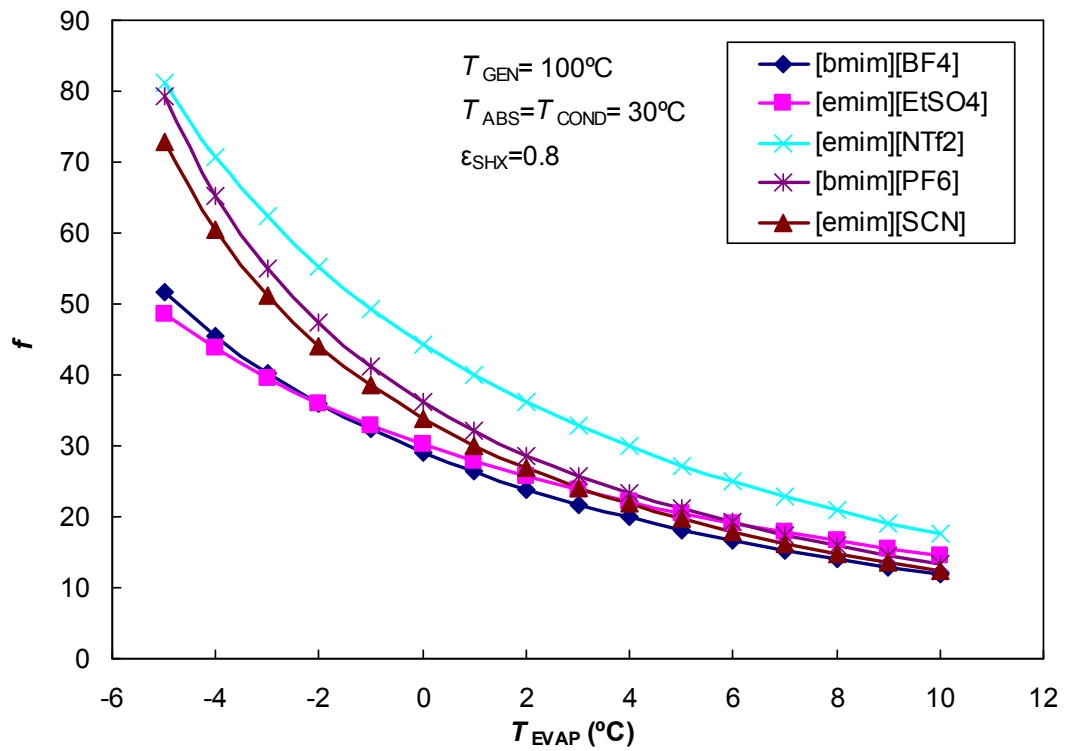
Figure 4.5. Effect of cooling temperature on f (a) and R (b) of the absorption systems

Among all ionic liquids studied here, again the R and f values of ammonia/[emim][NTf$_2$] working fluid is the highest when compared with other

systems followed by the ammonia/[bmim][PF$_6$], ammonia/[emim][SCN] and ammonia/[emim][EtSO$_4$] working fluid, being that of the ammonia/[bmim][BF$_4$] the highest in R and f.

4.5.1.3. Effect of Absorber and Condenser Temperature

The effects of absorber and condenser temperature on the performance of the absorption refrigeration systems with different ammonia/ionic liquid working fluids are shown in Figure 4.6. In this case, the absorber and condenser temperature were set at same level, as the condenser and absorber temperatures are usually set at a similar level. From this figure one can observe that the COP of the systems decreases with the increase in absorber/condenser temperature. The COP of the systems working with ammonia/[emim][NTf$_2$] was the highest when compared with the systems with other working fluids for absorber/condenser temperature range of 25ºC - 40ºC, followed by the systems with ammonia/ [emim][SCN] working fluid. For other ammonia/ionic liquid working fluids, the COP values follow an order of [bmim][PF$_6$] > [bmim] [BF$_4$] > [emim][EtSO$_4$] for a range of cooling temperature from 25ºC - 40ºC, although the values for these three working fluids were not significantly differrent. For absorber/condenser temperature below 35ºC, the system working with ammonia/[bmim][PF$_6$] working fluid shows higher COP in comparison with those of ammonia/[bmim][BF$_4$] and ammonia/[emim][EtSO$_4$] working fluids. Moreover, at cooling temperature higher than 35ºC, the system with ammonia/[emim][EtSO$_4$] working fluid shows lower COP in comparison with those of ammonia/[bmim][PF$_6$] and ammonia/[bmim][BF$_4$] working fluids.
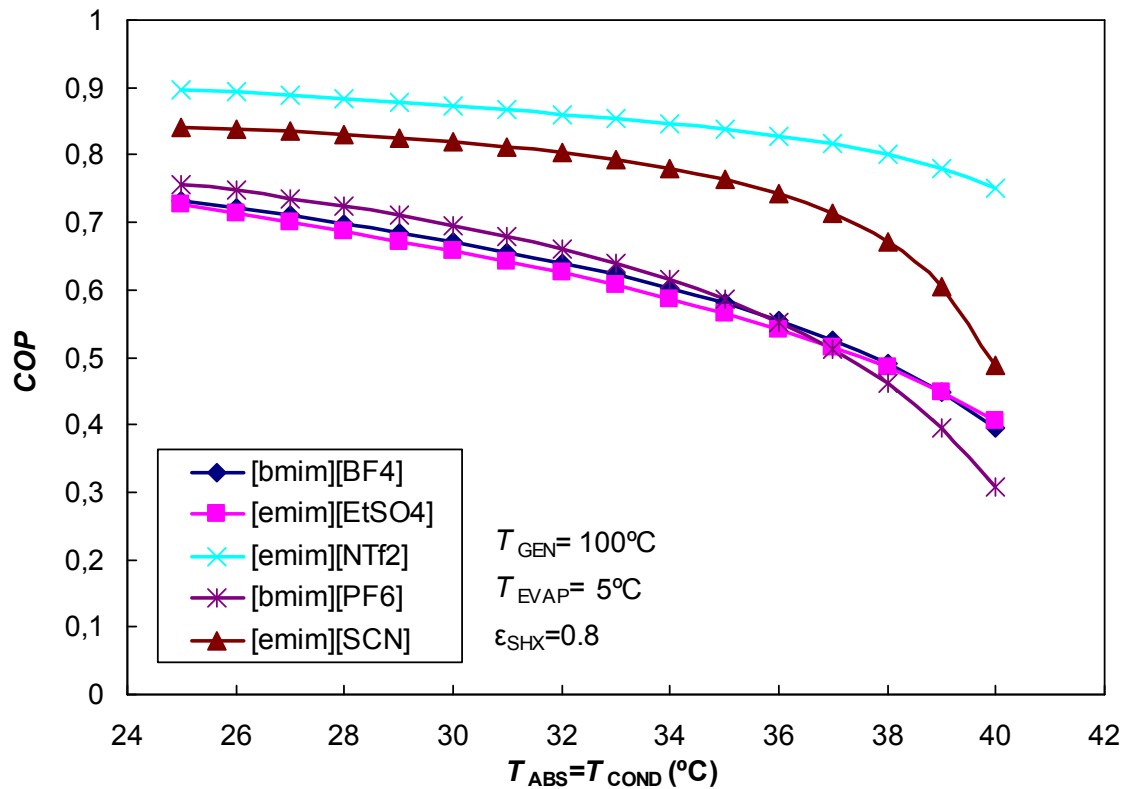
Figure 4.6. Effect of absorber and condenser temperature on *COP* of the absorption systems

The effects of absorber/condenser temperature on the solution circulation ratio (*f*) and solution mass flowrate per unit of cooling load (*R*) are shown in Figure 4.7. The increase in absorber/condenser temperature will increase both the circulation ratio (*f*) and solution mass flowrate per unit of cooling load (*R*).

Among all ionic liquids studied here, the *R* and *f* values of ammonia/[bmim][BF$_4$], ammonia/[emim][EtSO$_4$], ammonia/[bmim][PF$_6$], and ammonia/[emim][SCN] working fluid presented the lowest in R and f values, although their values are quite similar, , being that of the ammonia/[emim][NTf$_2$] the highest in *R* and *f*. The *R* and *f* values of for all the systems with ammonia/ionic liquid working fluid increase dramatically when the absorber/condenser temperatures are higher than 35ºC.
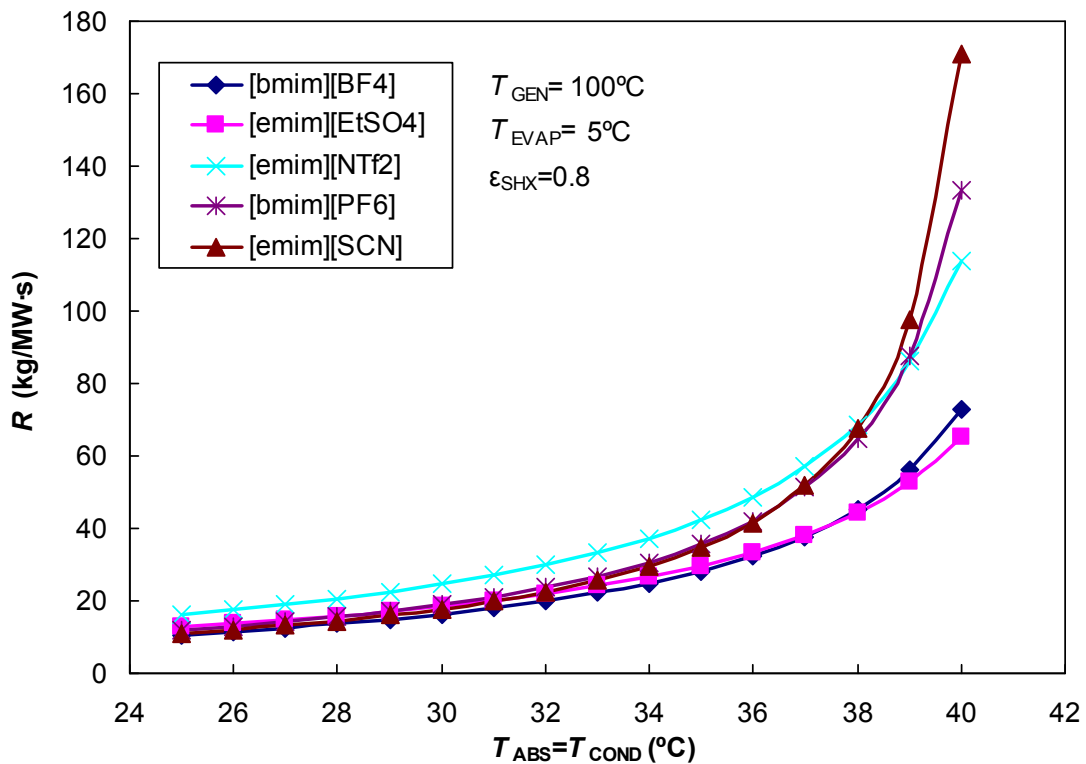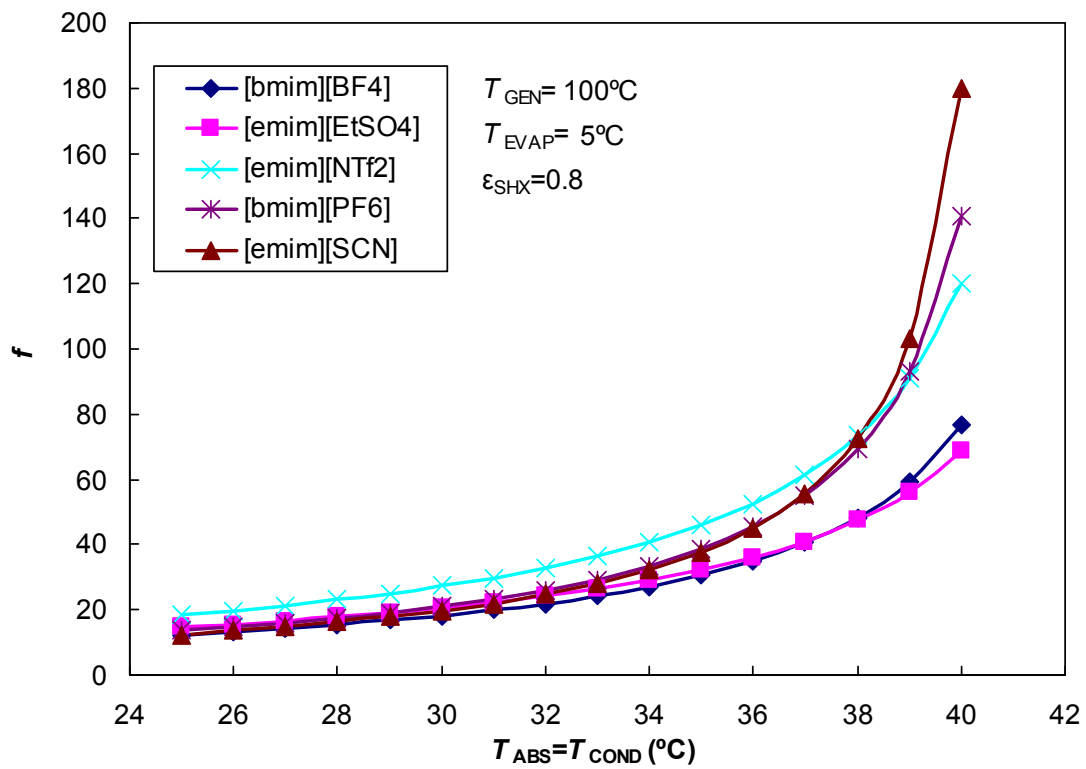
Figure 4.7. Effect of absorber and condenser temperature on f (a) and R (b) of the absorption systems

4.6. Conclusions

In this chapter, the performances of five ammonia/ionic liquid mixtures working pair for absorption refrigeration applications are theoretically studied and analysed. The 1-ethyl-3-methylimidazolium ethylsulfate ([emim][EtSO$_4$]), (1-ethyl-3-methylimidazolium thiocyanate ([emim][SCN]), -butyl-3-methylimidazolium hexafluorophosphate ([bmim][PF$_6$]), 1-ethyl-3-methylimidazolium bis(trifluoromethyl-sulfonyl)imide ([emim][NTf$_2$]), 1-butyl-3-methylimidazolium tetrafluoroborate ([bmim][BF$_4$]) have been selected as new absorbent for ammonia absorption applications. The selection was mainly based on the availability of their thermodynamic property data in the literature. The performances of these ammonia/ionic liquids mixtures were analysed and evaluated. The thermodynamic properties correlation of ammonia/ionic liquid mixture were built using activity coefficient based model non-random two-liquid (NRTL) based on experimental vapor-liquid equilibrium data. Other thermophysical properties necessary for the investigation were correlated from experimental data. All the calculation and simulation works were carried out using commercial software ASPEN Plus.

Among five ammonia/ionic liquid working fluids studied in this chapter, at certain operation conditions, the ammonia/[emim][NTf$_2$] working fluid presented the highest *COP* than that of other ammonia/ionic liquid mixtures. The *COP* of the systems with ionic liquids as absorbents follows an order of [emim][NTf$_2$] > [emim][SCN] > [bmim][PF$_6$] > [bmim][BF$_4$] > [emim][EtSO$_4$]. However, although the *COP* of the system working with ammonia ammonia/[emim][NTf$_2$] was higher than the systems with other working fluids, it is also interesting to see that its circulation ratio was the highest among other working fluids. On contrary, although the *COP* of the system working with ammonia ammonia/[bmim][BF$_4$] was lower than the systems with other working fluids, its circulation ratio was the lowest among other working fluids. Similarly, although the *COP* of the system working with ammonia/[emim][NTf$_2$] mixture was higher than the systems with other working fluids, its *R* was the lowest among other working fluids. It means that at the same ionic liquid mass flow rate and at the same operation conditions, the systems working with ammonia/[emim][NTf$_2$] mixture produces lower cooling capacity. In contrary, although the *COP* of the system working with ammonia

ammonia/[bmim][BF_4] mixture was lower than the systems with other working fluids, on contrary its R value was the highest among other working fluids, which means that at the same ionic liquid mass flow rate and at the same operation conditions, the systems working with ammonia/[bmim][BF_4] mixture can produce higher cooling capacity.

From these results, it can be said that the ionic liquid has a great potential to be an alternative absorbent for ammonia refrigerant. The ammonia/ionic liquid working fluid can provide competitive performance in comparison with conventional absorbent for ammonia refrigerant. However, some drawbacks are still remains to be solved such as relatively low solubility of ammonia into ionic liquids which affects to the solution circulation mass flow ratio and relatively high viscosity of ionic liquid in comparison with other conventional absorbent which may affects to the performance of absorber and solution pump. In addition, to date the availability of the thermophysical properties of ammonia/ionic liquids mixtures are very few and limited. Therefore, it is recommended to deeply explore other ionic liquids that may be a better candidate as an absorbent for ammonia refrigerant and has thermophysical properties suitable for absorption refrigeration applications. Moreover the measurement of the thermophysical properties of ionic liquids and their mixtures with ammonia is a must to provide adequate thermophysical data to further investigate the characteristic and performance of ionic liquid as an alternative absorbent for ammonia refrigerant.

4.7.   References

[1]   Renon, H., and Prausnitz, J. M., Local Compositions in Thermodynamic Excess Functions for Liquid Mixtures, *AIChE Journal,* 1968, 14 (1), 135-144

[2]   Aspen Plus (Version 7.3): Aspen technology Inc. (2012)

[3]   NIST Thermo Data Engine. National Institute of Standards and Technology (NIST) and Aspen technology Inc. (2012)

[4]   Yokozeki, A., Shiflett, M. B., Vapor–liquid equilibria of ammonia + ionic liquid mixtures, *Applied Energy*, 84, 1258-1273, (2007).

[5]   Yokozeki, A., Shiflett, M.B., Ammonia solubilities in room-temperature ionic liquids, ammonia solubilities in room-temperature ionic liquids. *Ind. Eng. Chem. Res*. 2007; 46; 1605-1610

[6]   Ficke, L.E., Novak, R.R., and Brennecke, J.F., Thermodynamic and Thermophysical Properties of Ionic Liquid + Water Systems, *J. Chem. Eng. Data*, 2010, 55, 4946–4950

[7]   Ruiz, E, Ferro, V.R., de Riva, J., Moreno, D., Palomar, J., Evaluation of ionic liquids as absorbents for ammonia absorption refrigeration cycles using COSMO-based process simulations. *Applied Energy*. 2014; 123; 281–291

[8]   Sun, D., Comparison of the performances of NH_3-H_2O, NH_3-$LiNO_3$ and NH_3-NaSCN absorption refrigeration systems, *Energy Convers. Mgmt.,* 1998, 39 (5/6), 357-368

Chapter 5

Thermodynamic Simulation of Absorption Refrigeration Systems using Selected Ionic Liquids as Absorbents and Ammonia as Refrigerant

5.1. Introduction

New set of thermophysical properties of new ammonia/ionic liquid mixtures necessary for absorption systems investigation have been measured by our research group. These new set of thermophysical properties data allow us to study the performance of absorption refrigeration system using ammonia/ionic liquid working fluid with more reliable and accurate results. The new proposed working fluids present better properties as compared to ionic liquid studied in Chapter 4.

In this chapter, the performances of new proposed ammonia/ionic liquid mixtures working pair for absorption refrigeration applications were therefore theoretically studied and analysed. The 1-(2-Hydroxyethyl)-3-methylimidazolium tetrafluoroborate ([EtOHmim][BF$_4$]), 1-(2-Hydroxyethyl)-3-methylimidazolium bis(trifluoromethyl- sulfonyl)imide ([EtOHmim][NTf$_2$]), (2-hydroxyethyl)-N,N,N-trimethyl bis(trifluoromethylsulfonyl)imide ([N$_{111}$(2OH)][NTf$_2$]), and N-Trimethyl-N- propylammonium Bis(trifluoromethane- sulfonyl)imide ([N$_{1113}$][NTf$_2$]) have been selected as new absorbent for ammonia absorption applications. The thermodynamic properties correlation of ammonia/ionic liquid mixture were built using activity coefficient based model non-random two-liquid (NRTL) based on

experimental vapor-liquid equilibrium data. Other thermophysical properties necessary for the investigation were correlated from experimental data. The thermodynamic performance of absorption refrigeration systems with these new proposed ammonia/ionic liquid working fluids were analysed and discussed based on key parameters of coefficient of performance (*COP*), solution mass flow ratio (*f*) solution mass flowrate per unit of cooling load (*R*). In addition, the results were compared with absorption refrigeration systems using ammonia/LiNO$_3$. Moreover, the viscosities of ammonia/ionic liquid mixtures at inlet and outlet absorber which play an important role in the heat and mass transfer processes were also discussed.

5.2. Thermodynamic Properties

The thermodynamic properties correlation of ammonia/ionic liquid mixture were built based on activity coefficient based model non-random two-liquid (NRTL). NRTL model is an empirical equation proposed by Renon and Prausnitz [1] based on the local composition representation of the excess Gibbs energy, G^E, of liquid mixtures. The detail of NRTL model has been previously described in Chapter 3.

The NRTL parameters, namely a_{12}, a_{21}, b_{12}, b_{21}, c_{12} and c_{21}, were obtained from vapor liquid equilibrium data [2] regression and are shown in Table 5.1. The parameters d_{12} and d_{21} were set to 0 for all mixtures.

Tabel 5.1. NRTL parameters for ammonia (1) and ionic liquid (2) mixtures

Ionic Liquids	a_{12}	a_{21}	b_{12}	b_{21}	c_{12}
[EtOHmim][BF$_4$]	42,6348	-18,7358	-14360,90	5200,20	0,1151
[EtOHmim][NTf$_2$]	3,0815	-0,5406	-1280,67	-715,43	0,2514
[N$_{111}$(2OH)] [NTf$_2$]	5,5013	-0,2135	-1524,63	-1238,94	0,1835
[N$_{1113}$] [NTf$_2$]	0,9961	-0,6107	-321,83	21,30	3,1604

The isobaric molar heat capacity of pure ionic liquids necessary to calculate the enthalpy of the working fluids can be obtained from correlation developed by Cera-Manjarres [2] using Equation (5.1).

$$C_{p,m} = \sum_{n=1}^{3} A_{n-1}(T + 273.15)^n \tag{5.1}$$

The parameters for Equation (5.1) were presented in Table 5.2.

<p align="center">Tabel 5.2. Parameters for Equation (12)</p>

Ionic Liquids	A_0	$A_1 \cdot 10^4$	$A_2 \cdot 10^6$
[EtOHmim] [BF$_4$]	1.6679	-20.2178	5.7111
[EtOHmim] [NTf$_2$]	0.2670	108.0479	-13.3710
[N$_{111}$(2OH)] [NTf$_2$]	0.8375	31.4717	0
[N$_{1113}$] [NTf$_2$]	0.8989	28.9433	0

Similarly, the densities of pure ionic liquids necessary to calculate the solution pump work were also obtained from correlation developed by Cera-Manjarres [2] using Equation (5.2).

$$\rho = A + B \ln(T + 273.15) \tag{5.2}$$

Parameter A and B in Equation (5.2) are obtained using Equation (5.3) and Equation (5.4).

$$A = \sum_{i=0}^{5} a_i x_1^i \tag{5.3}$$

$$B = \sum_{i=0}^{2} b_i \ln(T)^i \tag{5.4}$$

Parameters for Equation (5.3) and (5.4) were presented in Table 5.3.

<p align="center">Tabel 5.3. Parameters for Equation (5.3) and (5.4)</p>

Ionic Liquids	a_0	a_1	a_2	a_3	a_4	a_5
[EtOHmim]-[BF$_4$]	671	1230	-4500	3740	3790	-5160
[EtOHmim]-[NTf$_2$]	160000	-132	-121	-158	1140	-1480
[N$_{111}$(2OH)] [NTf$_2$]	978	-313	408	-101	-452	-214
[N$_{1113}$] [NTf$_2$]	118	-214	6100	99.9	-117	-405

Tabel 5.3. Parameters for Equation (5.3) and (5.4) *(Continued)*

Ionic Liquids	b_0	b_1	b_2
[EtOHmim]-[BF$_4$]	1240	-3310	23.1
[EtOHmim]-[NTf$_2$]	84800	-14700	851600
[N$_{111}$(2OH)] [NTf$_2$]	304	2.64	-6.66
[N$_{1113}$] [NTf$_2$]	365	48.6	-12.6

In addition, the thermophysical properties of ammonia refrigerant were taken from Tillner-Roth et al [3] and have been provided in Engineering Equation Solver.

5.3. Mathematical Model

A set of mathematical model has been built for the single stage absorption refrigeration system using ammonia as refrigerant and five different ionic liquids as absorbent. The mathematical model was built based on the application of mass and energy balance equations and on following assumptions:

- The cycles are in steady-state condition.

- The thermal and pressure losses during the whole processes are negligible

- Refrigerant leaving the condenser and evaporator are in saturated liquid and saturated vapour, respectively.

- The solutions leaving the absorber and the generator are in saturation condition.

- Solution and refrigerant valves are isenthalpic.

- The solution heat exchanger effectiveness is equal to 0.8

- Isentropic efficiency of solution pump is 50%.

As the vapour pressure of pure ionic liquids is negligible, there is no necessary to add rectification column at the refrigerant outlet of the generator and the vapour at the outlet of generator is pure refrigerant vapour. Following the schematic diagram of the absorption refrigeration cycle as described in Chapter 2, the energy and mass balance equation in each component can be described as follows:

Absorber:

$$Q_{ABS} = m_6 h_6 + m_{10} h_{10} - m_1 h_1 \qquad (5.5)$$

$$m_1 = m_6 + m_{10} \qquad (5.6)$$

$$m_1 X_1 = m_6 X_6 \qquad (5.7)$$

Generator:

$$Q_{GEN} = m_4 h_4 + m_7 h_7 - m_3 h_3 \qquad (5.8)$$

$$m_3 = m_4 + m_7 \qquad (5.9)$$

$$m_3 X_3 = m_4 X_4 \qquad (5.10)$$

Condenser:

$$Q_{COND} = m_7 \left(h_7 - h_8 \right) \qquad (5.11)$$

$$m_7 = m_8 \qquad (5.12)$$

Evaporator:

$$Q_{EVAP} = m_9 \left(h_{10} - h_9 \right) \qquad (5.13)$$

$$m_9 = m_{10} \qquad (5.14)$$

The solution heat exchanger effectiveness can be formulated using Equation (5.15)

$$\varepsilon_{SHX} = \frac{\left(T_4 - T_5 \right)}{\left(T_4 - T_2 \right)} \qquad (5.15)$$

The small mechanical power only presents in the energy balance of the solution pump.

Some key parameters were used to evaluate the performance of absorption refrigeration cycle. Coefficient of performance (*COP*) is defined as the ratio of available useful cooling output of the system to the total power supplied to the system. The *COP* can be written as

$$COP = \frac{Q_{EVAP}}{Q_{GEN} + W_p} \qquad (5.16)$$

where Q_{EVAP} and Q_{GEN} are the cooling output of the evaporator and the heat input of the generator, respectively and W_p is the working input of the solution pump.

The work input of the solution pump W_p is negligible relative to the heat input in the generator therefore the pump work is usually neglected for the purposes of analysis.

Solution mass flow ratio (*f*) is defined as the ratio of mass flow rates of weak solution to produced refrigerant vapour. Thus, the *f* can be mathematically written in Equation (5.17).

$$f = \frac{m_s}{m_r} \qquad (5.17)$$

Another important parameter to evaluate the performance of absorption cycle is solution mass flowrate per unit of cooling load (*R*) which is defined as weak solution mass flow rate needed to produce a unit cooling thermal load of refrigeration. This parameter can be written in Equation (5.18).

$$R = \frac{m_s}{Q_{EVAP}} \qquad (5.18)$$

5.4. Model Validations

Before applying the model in the absorption refrigeration systems using new proposed working fluids the model was first validated by comparing the results with the simulation data from literature [4-6]. As mentioned before, the experimental investigation of the performance of ammonia/ionic liquid working fluids for absorption refrigeration applications are still not available in open literature. Therefore the ability of NRTL model to correlate the thermophysical properties of ammonia/ionic liquid mixture in absorption refrigeration systems was validated with the simulation results of Yokozeki and Shiflett [4] and Ruiz et al [5]. Eight ionic

liquids proposed by Yokozeki and Shifflet [4,6] were used for the validation of the thermophysical model applied for absorption refrigeration systems. The absorption refrigeration system was operated at same operation conditions (T_{GEN}=100ºC, T_{ABS}=30ºC, T_{COND}=40ºC, T_{EVAP}=10ºC, and ε_{SHX}=1). The comparison of present results with the simulation results from Yokozeki and Shiflett and Ruiz et al [4-5] are presented in Table 5.4.

Table 5.4. Comparison of present work with literature [4-5]

Ionic Liquid	f			COP		
	Present Work	Yokozeki and Shifflet [4]	Ruiz et al. [5]	Present Work	Yokozeki and Shifflet [4]	Ruiz et al. [5]
[bmim][BF$_4$]	13.96	12.98	-	0.612	0.557	-
[bmim][PF$_6$]	20.94	17.27	-	0.545	0.575	-
[emim][NTf$_2$]	21.00	24.57	-	0.446	0.589	-
[hmim][Cl]	15.12	14.26	15.18	0.490	0.525	0.595
[emim][EtSO$_4$]	17.52	17.55	21.24	0.612	0.485	0.540
[emim][Ac]	11.65	12.55	11.08	0.488	0.573	0.644
[emim][SCN]	15.37	12.42	12.79	0.497	0.557	0.592
[DMEA][Ac]	6.94	7.60	-	0.556	0.612	-
Ionic Liquid	X_{GEN} (% wt. IL)			X_{ABS} (% wt. IL)		
	Present Work	Yokozeki and Shifflet [4]	Ruiz et al. [5]	Present Work	Yokozeki and Shifflet [4]	Ruiz et al. [5]
[bmim][BF$_4$]	95.8	95.7	-	88.9	88.3	-
[bmim][PF$_6$]	95.7	94.5	-	91.1	89.0	-
[emim][NTf$_2$]	97.1	96.3	-	92.4	92.4	-
[hmim][Cl]	93.1	93.9	93.40	87.0	87.3	87.30
[emim][EtSO$_4$]	95.4	95.2	93.70	89.9	89.8	89.80
[emim][Ac]	93.8	92.3	93.60	85.7	85.0	85.00
[emim][SCN]	92.8	92.7	92.40	86.8	85.2	85.20
[DMEA][Ac]	84.6	84.1		72.4	73.1	

From this comparison, it can be seen that our results were all in good agreement with the simulation results taken from reference [1,4]. The small discrepancies between our results and those of reference were quite acceptable considering different thermodynamic methods and parameters used in the simulations.

In addition, our simulation model was also validated by comparing our simulation results with those from literature [7] using other working fluids proposed for ammonia refrigerant. In this case, NH_3-$LiNO_3$ and NH_3-NaSCN were chosen for comparison as absorption refrigeration systems working with these fluids have similar configuration in terms of not necessary to add rectification process.

Table 5.5 show our simulation results of absorption refrigeration system using NH_3-$LiNO_3$ and NH_3-NaSCN working fluids in comparison with the results of Sun [7] at same operation conditions (T_{GEN}=100ºC, T_{ABS}=25ºC, T_{COND}=30ºC, T_{EVAP}=-5ºC, and ε_{SHX}=0.8). Similarly with that of comparison with ammonia/ionic liquid mixture, our simulation results are in good agreement with the results of reference [7]

Table 5.5. Comparison of present work with literature [7]

Thermal flow	NH_3-$LiNO_3$		NH_3-NaSCN	
	Present work	Sun [7]	Present work	Sun [7]
Q_{GEN} (kW)	29.7435	29.7138	27.4762	29.0292
Q_{COND} (kW)	18.2478	18.4611	18.2478	18.4611
Q_{EVAP} (kW)	18.5840	18.5974	18.5840	18.5974
Q_{ABS} (kW)	30.1389	29.9067	27.8837	29.2425
W_p (kW)	0.0591	0.0566	0.0713	0.0770
COP	0.6236	0.6247	0.6746	0.6390
f	4.38	4.09	5.01	5.35

5.5. Results And Discussions

In this chapter, the thermodynamic performance of absorption refrigeration cycle using four different ionic liquids as absorbents; ammonia/[EtOHmim][BF4], ammonia/[EtOHmim][NTf2], ammonia/[N111(2OH)] [NTf2], ammonia/[N1113] [NTf2], were evaluated. In addition, their performances were compared with the performance of absorption refrigeration cycle using ammonia/LiNO$_3$ working fluid. This comparison is necessary as ammonia/LiNO$_3$ working fluid has been proposed as an alternative working fluid for ammonia refrigerant and the absorption systems working with ammonia/ LiNO$_3$ have similar configuration in terms of not necessary to add rectification process.

5.5.1. VLE and excess enthalpy

The NRTL method has been used to model the thermodynamic properties of ammonia/ionic liquid mixtures. The solubility data of ionic liquid-ammonia were regressed to obtain NRTL binary interaction parameters. Moreover, the excess enthalpy, entropy and Gibbs energy were also predicted using NRTL method.

Figure 5.1 shows the comparison of the solubility of ammonia in ionic liquid between experimental and our correlation using NRTL method. From this figure, it can be observed that our model using NRTL method was able to predict well the solubility of ammonia in all ionic liquids studied in this chapter. All the predictions were in good agreements. However, higher discrepancies appears for ammonia/[EtOHmim][BF$_4$] and ammonia/ [N$_{1113}$] [NTf$_2$] mixture at high temperature/pressure and high ammonia mole fraction. Nevertheless this discrepancy can be neglected as in this work the cycle was operated at low ammonia concentration and at pressure of lower than 20 bar.
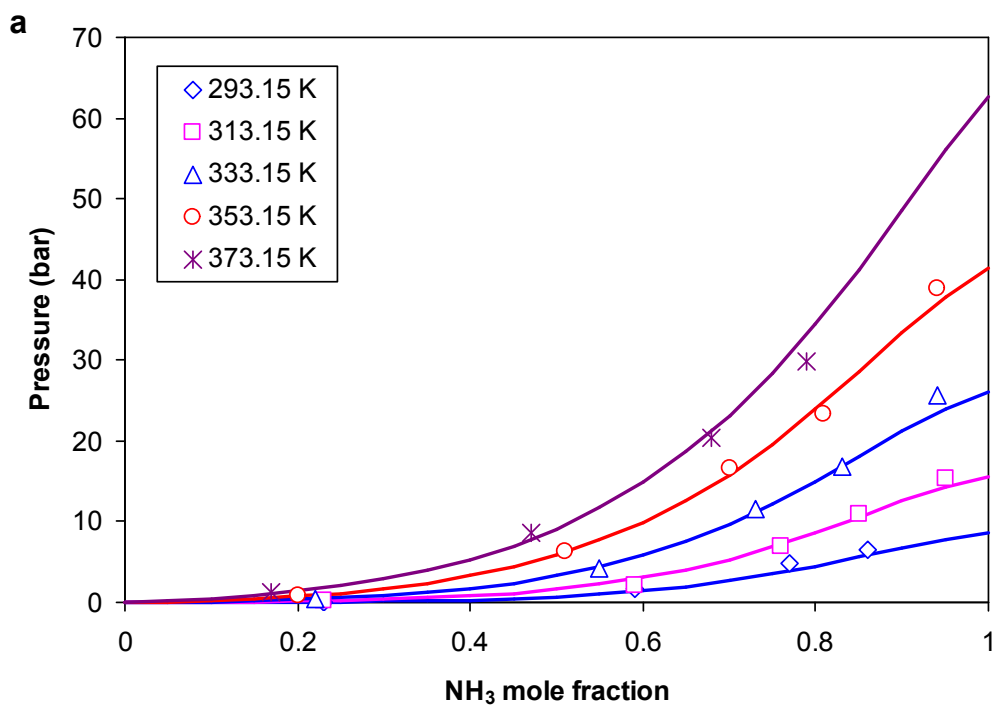
(a) ammonia/[EtOHmim][BF$_4$]

(b) ammonia/[N$_{111}$(2OH)] [NTf$_2$]

Hifni M. Ariyadi, Doctoral Thesis, Universitat Rovira i Virgili, 2016
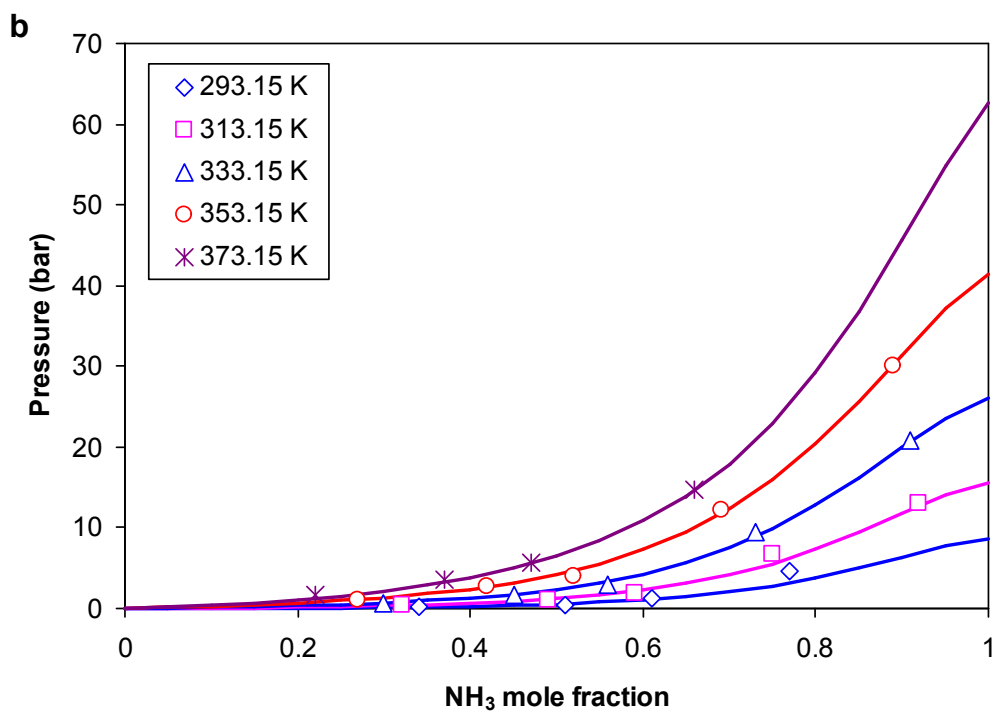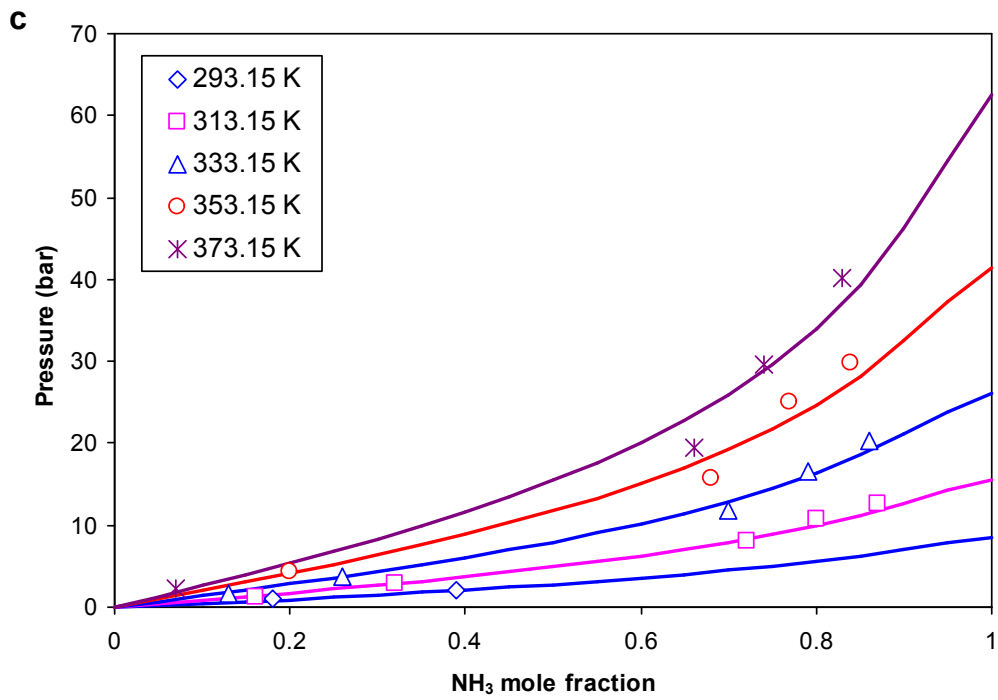
(c) ammonia/[N$_{1113}$] [NTf$_2$]
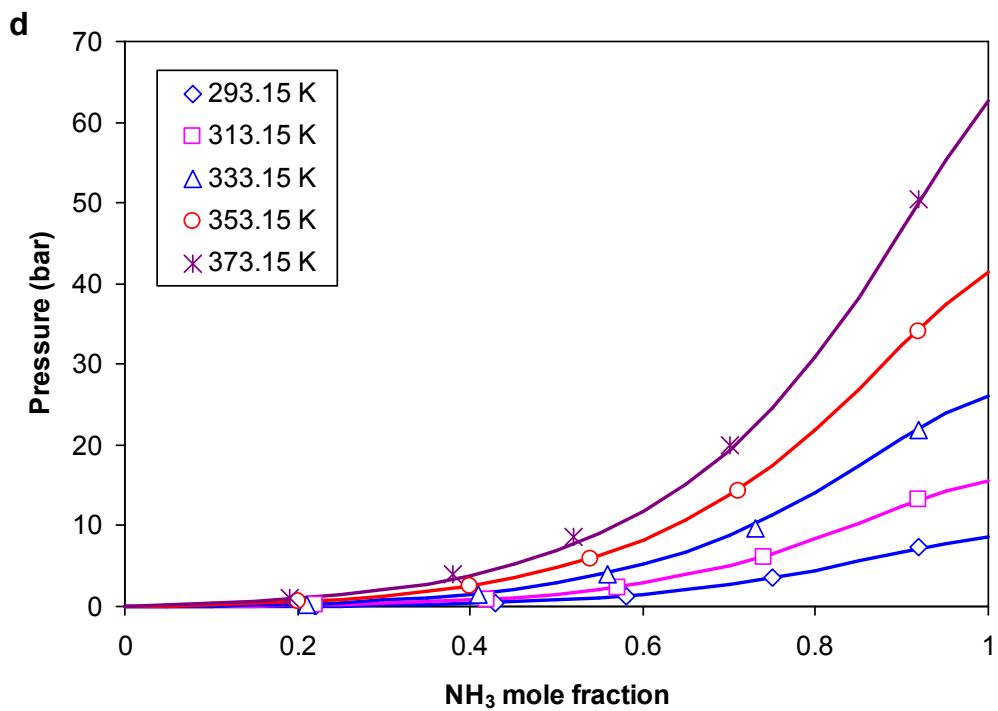
(d) ammonia/[EtOHmim][NTf$_2$]

Figure 5.1. Comparison of experimental and correlation VLE data. Symbols represent experimental data and lines represent correlation data

The predicted excess enthalpy, entropy, and Gibbs energy for the investigated working mixtures at temperature of 25ºC are shown on figure 5.2. From these figures it can be seen that the excess enthalpy for all studied mixture were negative. Such bonding is so strong or so numerous that H^E is more negative than TS^E, and thus G^E is negative; these mixtures are stable and do not form two liquid phases [4].

(a) ammonia/[EtOHmim][BF$_4$]

b
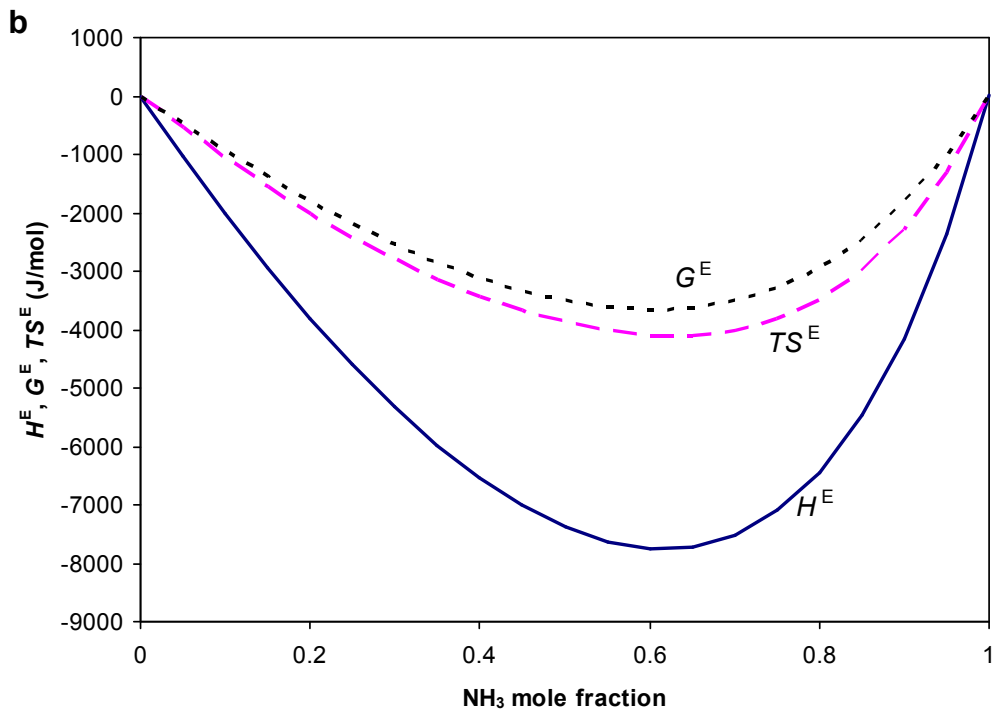
(b) ammonia/[N$_{111}$(2OH)] [NTf$_2$]

c

(c) ammonia/[N$_{1113}$] [NTf$_2$]
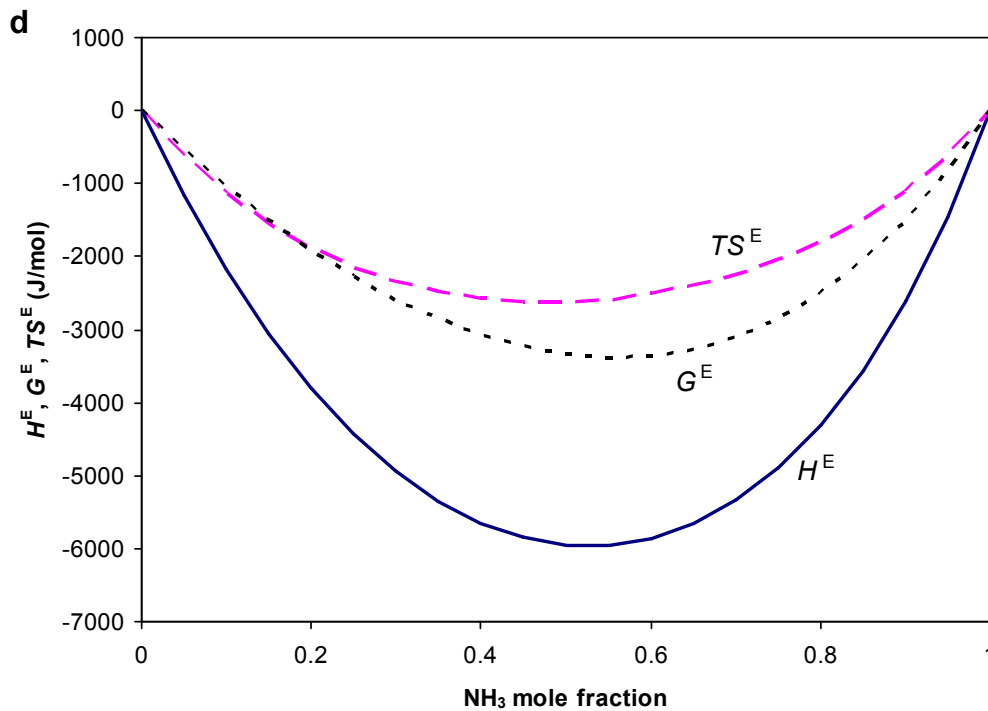
(d) ammonia/[EtOHmim][NTf$_2$]

Figure 5.2. Prediction of molar excess enthalpy, entropy, and Gibbs energy at 25ºC

5.5.2. Performance of Absorption Refrigeration Cycle

The performance of absorption refrigeration cycle working with ammonia/ionic liquid working fluids were evaluated at typical operation conditions for refrigeration applications. In this chapter, the analyses were carried out at cooling capacity of 100 kW. Table 5.6 shows the performance and thermal load of absorption refrigeration cycle at T_{GEN}=100ºC, T_{ABS}=30ºC, T_{COND}=30ºC, T_{EVAP}=5ºC, and ε_{SHX}=0.8 for cooling capacity of 100 kW. As it can be observed in this table the coefficient of performance (*CO*P) of the absorption systems working with ammonia/ionic liquid working fluids were identical when compared with ammonia/LiNO$_3$ at same cooling capacity and operation conditions. The *COP* of the systems working with ammonia/ionic liquid fluid mixtures lies between 0.54 and 0.64 whereas the *COP* of the systems working with ammonia/LiNO$_3$ fluid mixtures is 0.5850. Among all of ammonia/ionic liquid working fluids studied in this chapter, only [N$_{1113}$][NTf$_2$] presented higher COP that that of ammonia/LiNO$_3$. The *COP* of

the systems with ionic liquids as absorbents follows an order of $[N_{1113}][NTf_2] >$ $[EtOHmim][BF_4] > [N_{111}(2OH)] [NTf_2] > [EtOHmim] [NTf_2]$.

Table 5.6. Performance and thermal load of absorption refrigeration cycle

Parameter	Absorbent				
	[EtOHmim]-[BF$_4$]	[EtOHmim]-[NTf$_2$]	[N$_{111}$(2OH)]-[NTf$_2$]	[N$_{1113}$]-[NTf$_2$]	LiNO$_3$
Performance					
COP	0.5814	0.5493	0.5628	0.6393	0.5850
f (kg/kg)	8.226	16.037	11.700	22.796	3.687
R (kg/MW s)	7.307	14.245	10.393	20.250	3.275
Thermal load					
Q_{EVAP} (kW)	100.00	100.00	100.00	100.00	100.00
Q_{GEN} (kW)	171.21	183.73	176.40	154.94	170.50
Q_{ABS} (kW)	154.07	162.00	160.32	137.71	152.22
Q_{COND} (kW)	118.72	118.72	118.72	118.72	118.72
Q_{SHX} (kW)	141.45	294.41	213.92	337.09	37.70
W_p (kW)	0.7871	1.3280	1.2740	1.4800	0.4384
Solution concentration					
X_{ABS} (%wt. absorbent)	80.08	88.24	85.42	92.86	44.46
X_{GEN} (%wt. absorbent)	91.16	94.11	93.4	97.12	61.01

As the refrigerant for all systems is ammonia, the amount of refrigerant vapour needed to produce a certain nominal cooling capacity is also same for all working fluid systems. However, the amount of solution needed to operate the absorption refrigeration cycle at same cooling capacity is different due to their solubility with ammonia. Thus, in terms of circulation ratio, it can be seen from Table 5.6 that the circulation ratios (*f*) of the absorption systems working with ammonia/ionic liquid working fluids at same cooling capacity and operation

conditions were somehow higher as compared with that of ammonia/LiNO$_3$. The f of the systems working with ammonia/ionic liquid fluid mixtures lies between 7.3 and 20.3 whereas the f of the systems working with ammonia/LiNO$_3$ fluid mixtures was as low as 3.274. The lowest f among all of studied ammonia/ionic liquid working fluids was shown by ammonia/[EtOHmim][BF$_4$] where as the highest one is shown by ammonia/ [N$_{1113}$][NTf$_2$]. It is also interesting to see that although the COP of the system working with ammonia ammonia/ [N$_{1113}$][NTf$_2$] was higher than with other working fluids, on contrary its circulation ratio was the highest among other working fluids.

The higher circulation ratio of ammonia/ionic liquid working fluids also affects the solution mass flowrate per unit of cooling load (R). At same cooling capacity and operation conditions, the R values of the absorption systems working with ammonia/ionic liquid working fluids at same cooling capacity and operation conditions were higher as compared with that of ammonia/LiNO$_3$. The R of the systems working with ammonia/ionic liquid fluid mixtures lies between 8.2 kg/MW·s and 22.8 kg/MW·s whereas the R of the systems working with ammonia/LiNO$_3$ fluid mixtures is as low as 3.275 kg/MW·s. The lowest f among all of studied ammonia/ionic liquid working fluids was shown by ammonia/[EtOHmim][BF$_4$] where as the highest one was shown by ammonia/ [N$_{1113}$][NTf$_2$]. It implies that generally an absorption system working with ammonia/ionic liquids needs more solution to produce cooling than that of ammonia/LiNO$_3$.

In addition, it is also interesting to see from Table 7 that the energy consumption needed to operate the absorption cycle mainly occurs at the generator, and that the mechanical work required for the solution pump is very small in comparison with energy input of the generator (less than 1% in the case of the highest solution pump's work) and thus can be neglected for general calculations or when information on solution density is not available [11].

5.5.2.1. Effect of Generator Temperature

Figure 5.3 shows the effects of generator temperatures on the *COP* of the absorption refrigeration cycles with various working fluids. As illustrated in Figure 4, the *COP* increases when the generator increases and then slightly decreases when the generator temperature is kept increase. For all systems, it also can be observed that there is a low generator temperature limit for each cycle. Each cycle cannot be operated at generator temperatures lower than its limit.

Among all ammonia/ionic liquid mixtures studied working fluid, the highest *COP* was reached by the cycle with ammonia/[N$_{1113}$][NTf$_2$] working fluids. However, this working fluid has the highest generator temperature limit and high *COP* was reached only when it was operated at generator temperature higher than 85ºC. The *COP* of the absorption refrigeration cycle with this working fluid decreases significantly when the generator temperature was operated below 85ºC. On the other hand, other three ionic liquid-based working fluids have similar *COP* behaviour. The *COP* among these three ionic liquid-based working fluid follow an order of [EtOHmim][BF$_4$] > [N$_{111}$(2OH)] [NTf$_2$] > [EtOHmim] [NTf$_2$] for all range of generator temperature. In comparison with ammonia/LiNO3 fluid mixture, the ionic liquid-based working fluids show lower in *COP* except that of ammonia/[N$_{1113}$][NTf$_2$] working fluid at generator temperature higher than 85ºC. The highest *COP* of each cycle working with ammonia/ionic liquid mixtures were lies between 0.55 and 0.64 whereas the maximum *COP* of each cycle working with ammonia/LiNO$_3$ working fluid was 0.63.
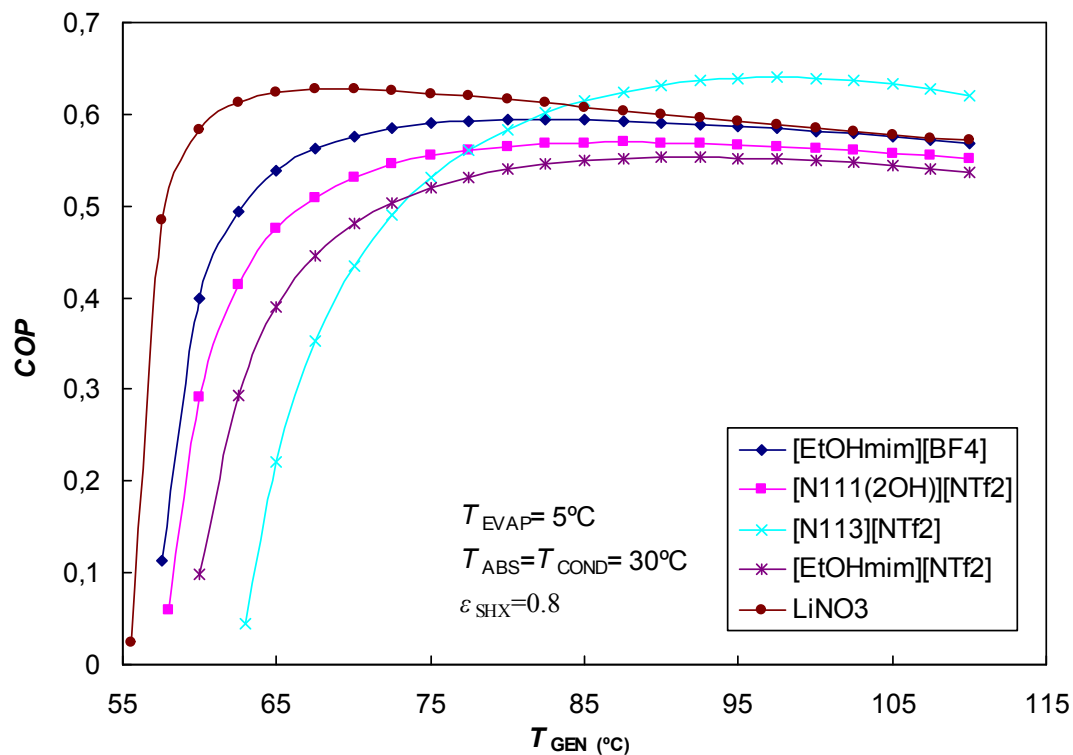
Figure 5.3. Effect of generator temperature on *COP* of the absorption systems

The effects of generator temperature on the solution circulation ratio (*f*) and solution mass flowrate per unit of cooling load (*R*) of the absorption refrigeration cycles with various working fluids are shown in Figure 5.4. As it has been mentioned before, the amount of solution needed to operate the absorption refrigeration cycle at same cooling capacity is different due to their solubility with ammonia. For all studied working fluids, the solution circulation ratio of the absorption cycle decreases when the generator temperature increases as at higher generator temperature the systems are able to produce more refrigerant vapour. The circulation ratio increases significantly when the generator temperature decreases near to its generator temperature limits. The solution circulation ratios of the cycle working with ammonia/ionic liquids are higher than that of ammonia/LiNO$_3$ at all generator temperature range. The *f* values of ammonia/[EtOHmim][BF$_4$] working fluid was the lowest among all three ionic liquids base working fluid, although its values was almost doubled that that of ammonia/LiNO$_3$, followed by the ammonia[N$_{111}$(2OH)][NTf$_2$] and ammonia/[EtOHmim] [NTf$_2$] working fluid, being that of the ammonia/[N$_{1113}$][NTf$_2$] the highest. From Figure 5.4(a), it is also interesting to see

that although the *COP* of the system working with ammonia ammonia/ $[N_{1113}][NTf_2]$ was higher than with other working fluids as discussed above, on contrary its circulation ratio was the highest among other working fluids at all range of generator temperature.

Regarding to the solution mass flowrate per unit of cooling load (*R*), the *R* values of the absorption systems working with ammonia/ionic liquid working fluids at same cooling capacity and operation conditions were higher as compared with that of ammonia/LiNO$_3$. For the systems with ammonia/[EtOHmim][BF$_4$] working fluid, which has the lowest *R* among all three ionic liquids base working fluid, its values was almost doubled that that of ammonia/LiNO$_3$. For the systems with ammonia/[N$_{111}$(2OH)] [NTf$_2$] and ammonia/[EtOHmim] [NTf$_2$], the *R* value was almost three times and four times higher that of ammonia/LiNO$_3$, respectively. The systems with ammonia/ $[N_{1113}][NTf_2]$ shows the highest R with the values more than two times higher than that of ammonia/[EtOHmim][BF$_4$] working fluid. The trends of *R* values are similar to the f values as at the same cooling capacity and operation conditions the circulation ratio was related to the solution mass flowrate per unit of cooling load.
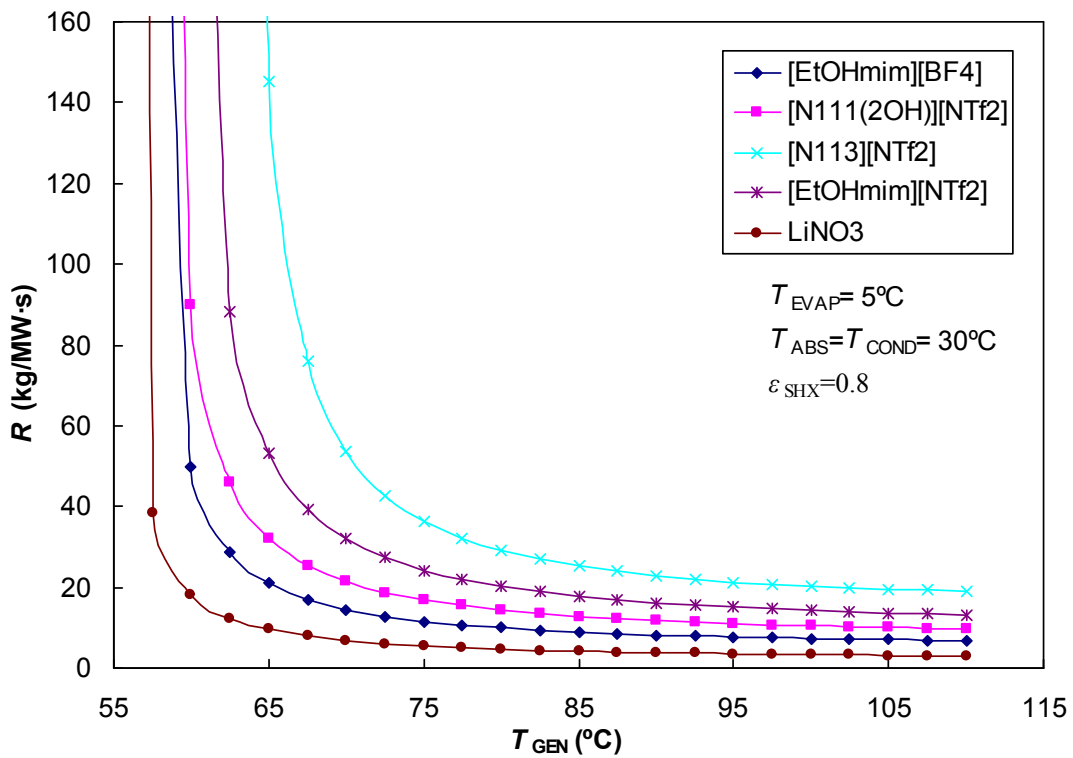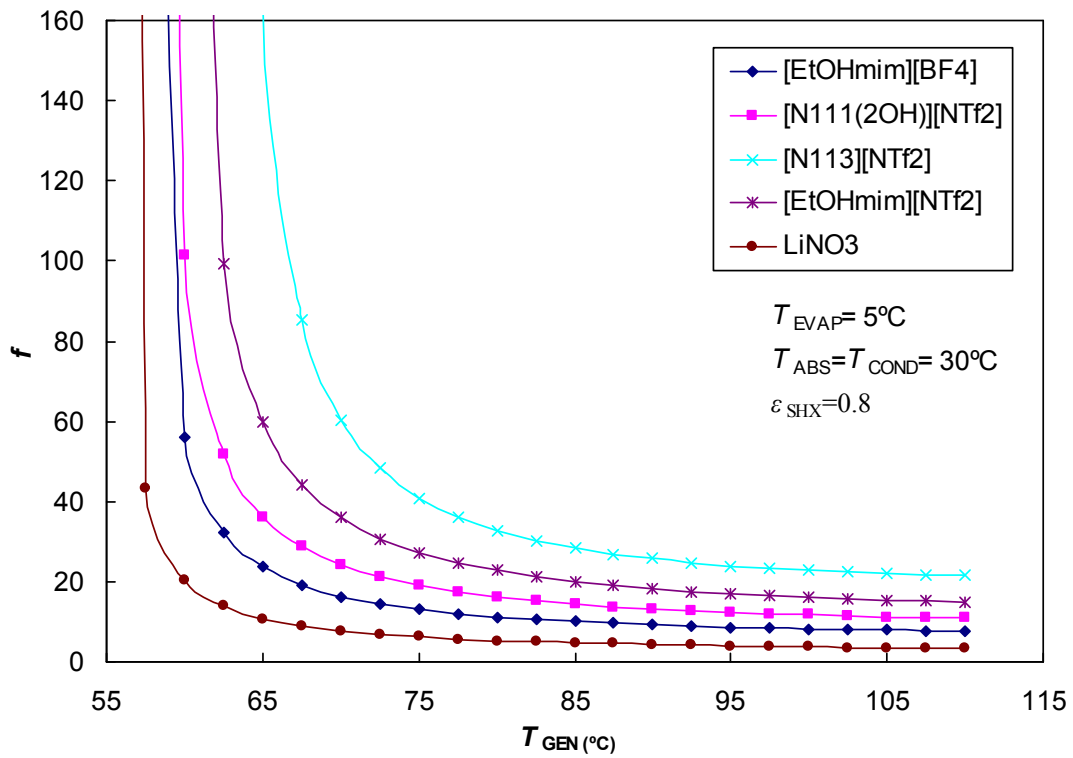
Figure 5.4. Effect of generator temperature on f (a) and R (b) of the absorption systems

5.5.2.2.   *Effect of Cooling Temperature*

The effects of cooling temperature on the performance of the absorption refrigeration systems with different ammonia/ionic liquid working fluids are shown in Figure 5.5. As it can be seen, the *COP* of the systems increases with the increase of the evaporator temperature. It is also interesting to see that the increase of the *COP* of the systems working with ammonia ammonia/$[N_{1113}][NTf_2]$ was more significant than with other working fluids. For other ammonia/ionic liquid working fluids, the *COP* values follow an order of $[EtOHmim][BF_4]$ > $[N_{111}(2OH)]$ $[NTf_2]$ > $[EtOHmim]$ $[NTf_2]$ for a range of cooling temperature from -5ºC to 10ºC. For cooling temperature below 0ºC, which is the refrigeration temperature, the ammonia/$[EtOHmim][BF_4]$ working fluid shows the highest *COP* in comparison with other ionic liquids and on contrary the ammonia/$[N_{1113}][NTf_2]$ working fluid shows the lowest in *COP* than those other working fluids. However, at the evaporator temperature lower than 0ºC the systems with ammonia/$LiNO_3$ working fluid show higher *COP* than the systems with ammonia/ionic liquids studied in this chapter.

Moreover, at cooling temperature higher than 0ºC, particularly at cooling temperature higher than 2ºC, the systems working with ammonia ammonia/$[N_{1113}][NTf_2]$ shows the highest *COP* in comparison with other systems with working fluids even with ammonia/$LiNO_3$ as the *COP* of the systems working with ammonia ammonia/$[N_{1113}][NTf_2]$ was more significant than with other working fluids. Furthermore, at cooling temperature higher than 0ºC the *COP* of other systems working with ammonia/ionic liquid mixtures were lower than the *COP* of the systems with ammonia/LiNO3. At cooling temperature of 10ºC, the *COP* of the systems working with ammonia/LiNO3, ammonia/$[EtOHmim][BF_4]$, ammonia/$[N_{111}(2OH)]$ $[NTf_2]$ and ammonia/$[EtOHmim]$ $[NTf_2]$ were almost similar.
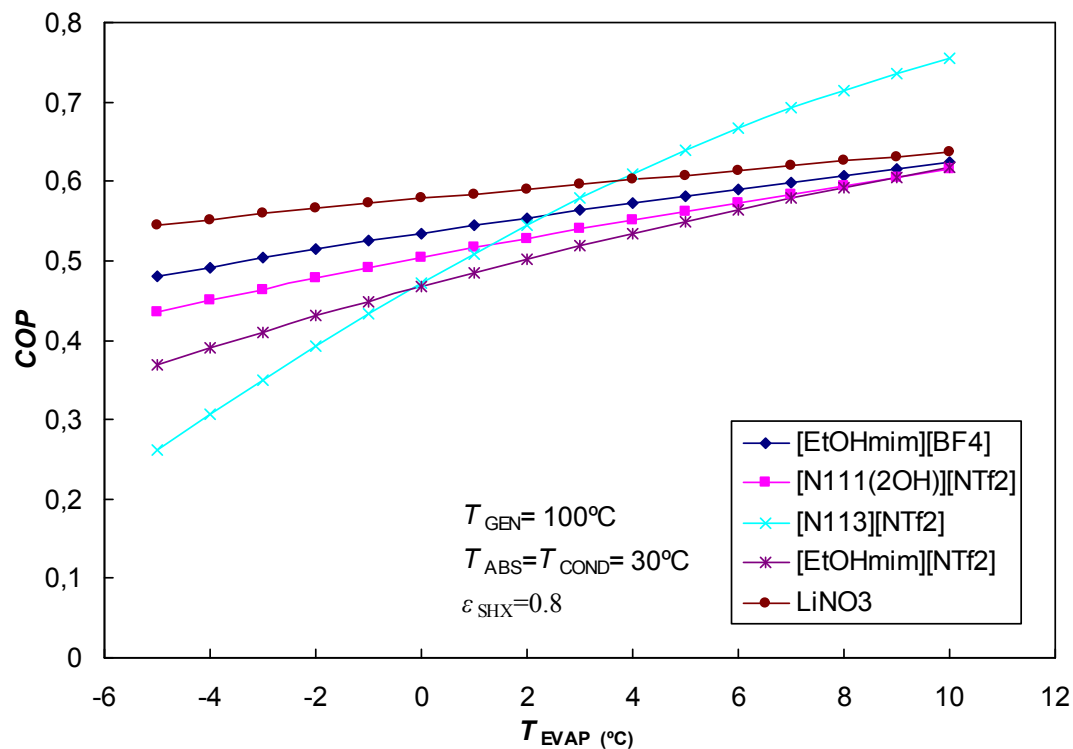
Figure 5.5. Effect of cooling temperature on *COP* of the absorption systems

In terms of solution circulation ratio (*f*) and solution mass flowrate per unit of cooling load (*R*), the increase in cooling temperature will decrease both the circulation ratio (*f*) and solution mass flowrate per unit of cooling load (*R*) as it shown in Figure 5.6. Similarly, the trends of the cooling temperature versus *R* values were identical with those of the *f* values.

Moreover, *R* and *f* values of the cycle working with ammonia/ionic liquids were somehow higher than that of ammonia/LiNO$_3$ at all cooling temperature range. Among all ionic liquids studied here, the *R* and *f* values of ammonia/[EtOHmim][BF$_4$] working fluid is the lowest although its values was almost doubled that that of ammonia/LiNO$_3$, followed by the ammonia[N$_{111}$(2OH)][NTf$_2$] and ammonia/[EtOHmim] [NTf$_2$] working fluid, being that of the ammonia/[N$_{1113}$][NTf$_2$] the highest in *R* and *f*.
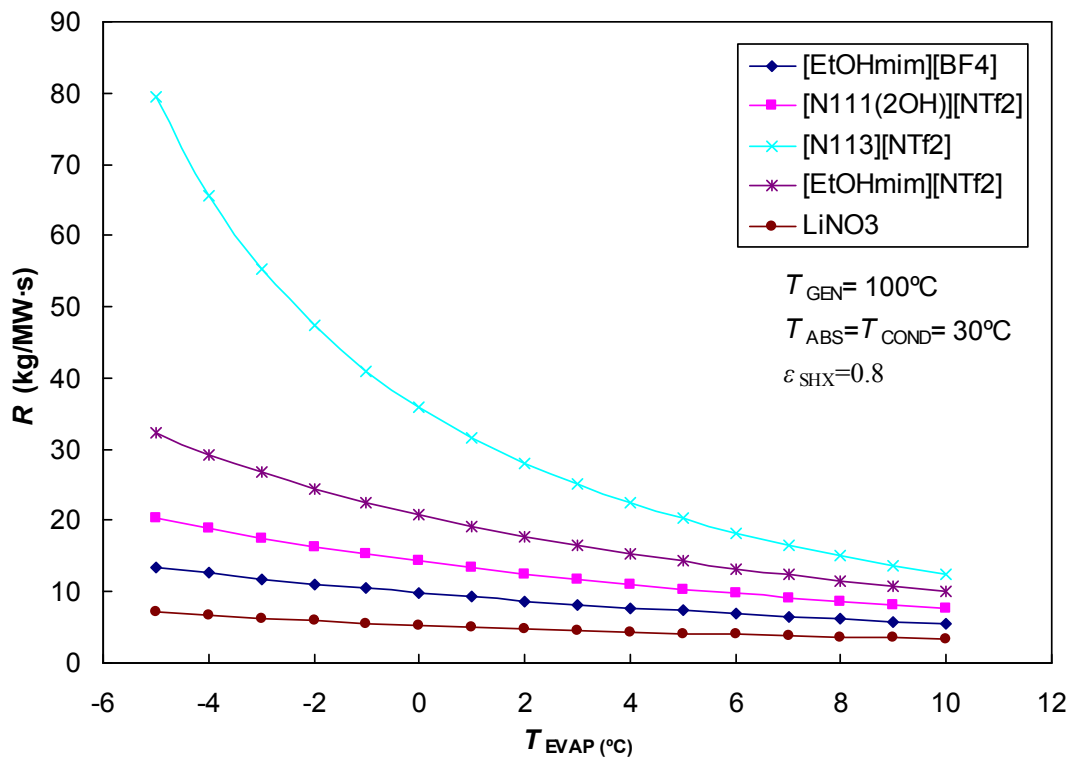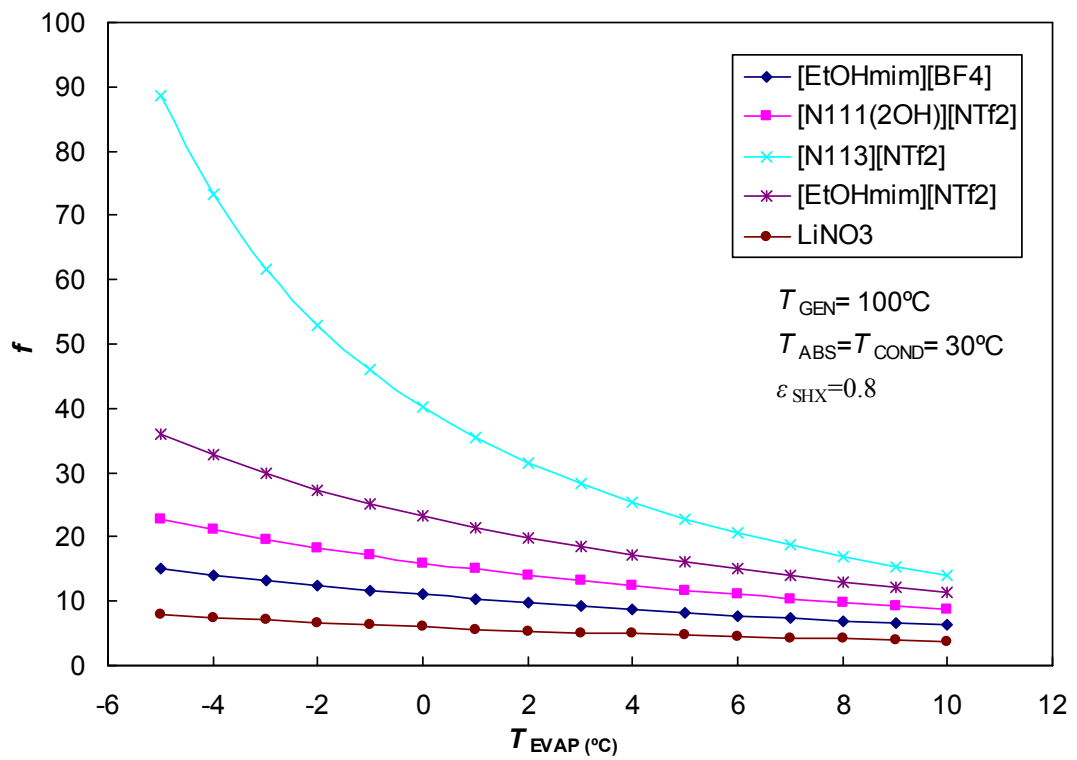
Figure 5.6. Effect of cooling temperature on f (a) and R (b) of the absorption systems

5.5.2.3. *Effect of Absorber and Condenser Temperature*

The effects of absorber and condenser temperature on the performance of the absorption refrigeration systems with different ammonia/ionic liquid working fluids are shown in Figure 5.7. In this case, the absorber and condenser temperature were set at same level, as the condenser and absorber temperatures are usually set at a similar level. From this figure one can observe that the *COP* of the systems decreases with the increase in absorber/condenser temperature. One also can see that the decrease of the *COP* of the systems working with ammonia/$[N_{1113}][NTf_2]$ was more significant than with other working fluids. For absorber/condenser temperature below 31ºC the ammonia/$[N_{1113}][NTf_2]$ working fluid shows the highest *COP* in comparison with other ionic liquids even with ammonia/$LiNO_3$ and on contrary the ammonia/$[EtOHmim][NTf_2]$ working fluid shows the lowest in *COP* than those other working fluids. It implies that absorption systems working with ammonia/$[N_{1113}][NTf_2]$ may be applicable for the systems with water-cooled absorber/condenser. Furthermore, at absorber/condenser temperature lower than 31ºC the *COP* of other systems working with ammonia/ionic liquid mixtures were lower than the *COP* of the systems with ammonia/$LiNO_3$. At absorber/condenser temperature of 25ºC, the *COP* of the systems with ammonia/$LiNO_3$, ammonia/$[EtOHmim][BF_4]$, ammonia/$[N_{111}(2OH)][NTf_2]$ and ammonia/$[EtOHmim][NTf_2]$ were almost similar.

Furthermore, at absorber/condenser temperature higher than 31ºC the systems working with ammonia ammonia/$[N_{1113}][NTf_2]$ shows the lowest *COP* in comparison with other systems with working fluids even with ammonia/$LiNO_3$ as the *COP* of the systems working with ammonia ammonia/$[N_{1113}][NTf_2]$ decreases more significant than with other working fluids. Moreover, at absorber/condenser temperature higher than 31ºC the *COP* of other systems working with ammonia/ionic liquid mixtures were lower than the *COP* of the systems with ammonia/LiNO3. Again, it can be observed that for ammonia/ionic liquid working fluids other than ammonia/$[N_{1113}][NTf_2]$ the *COP* values follow an order of $[EtOHmim][BF_4]$ > $[N_{111}(2OH)][NTf_2]$ > $[EtOHmim][NTf_2]$ for a range of absorber/condenser temperature from 25ºC to 40ºC. At the absorber/condenser temperature lower than

0ºC the systems with ammonia/LiNO$_3$ working fluid show higher *COP* than the systems with ammonia/ionic liquids studied in this chapter.
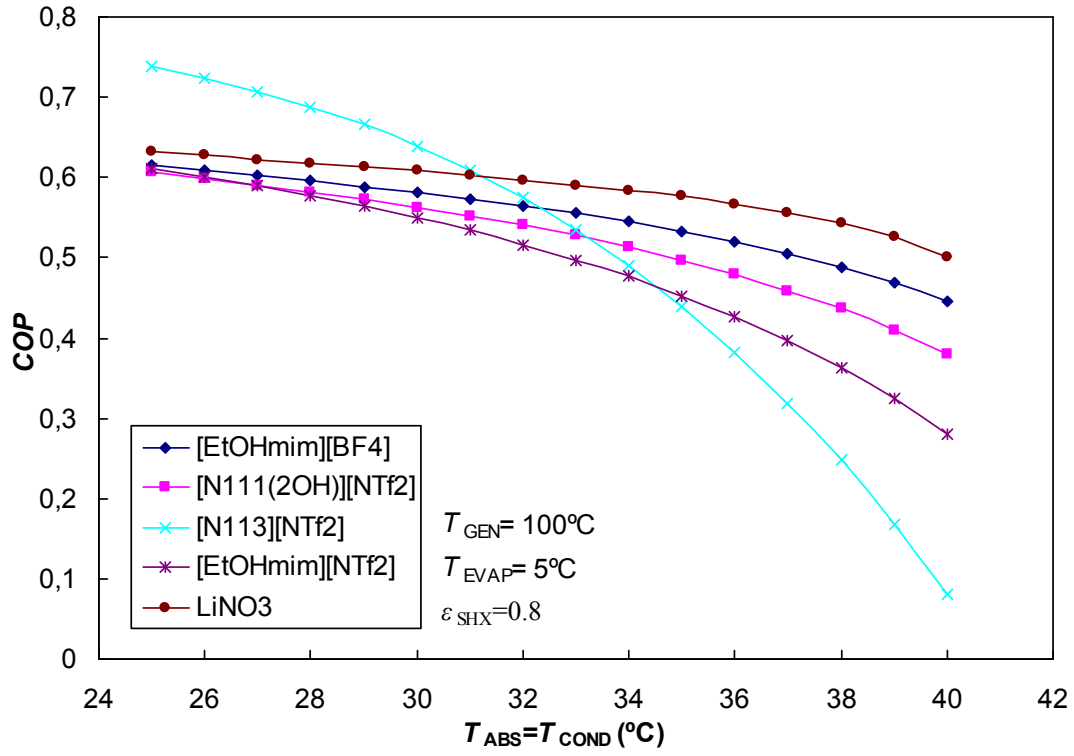
Figure 5.7. Effect of absorber and condenser temperature on *COP* of the absorption systems

The effects of absorber/condenser temperature on the solution circulation ratio (*f*) and solution mass flowrate per unit of cooling load (*R*) are shown in Figure 5.8. The increase in absorber/condenser temperature will increase both the circulation ratio (f) and solution mass flowrate per unit of cooling load (*R*).
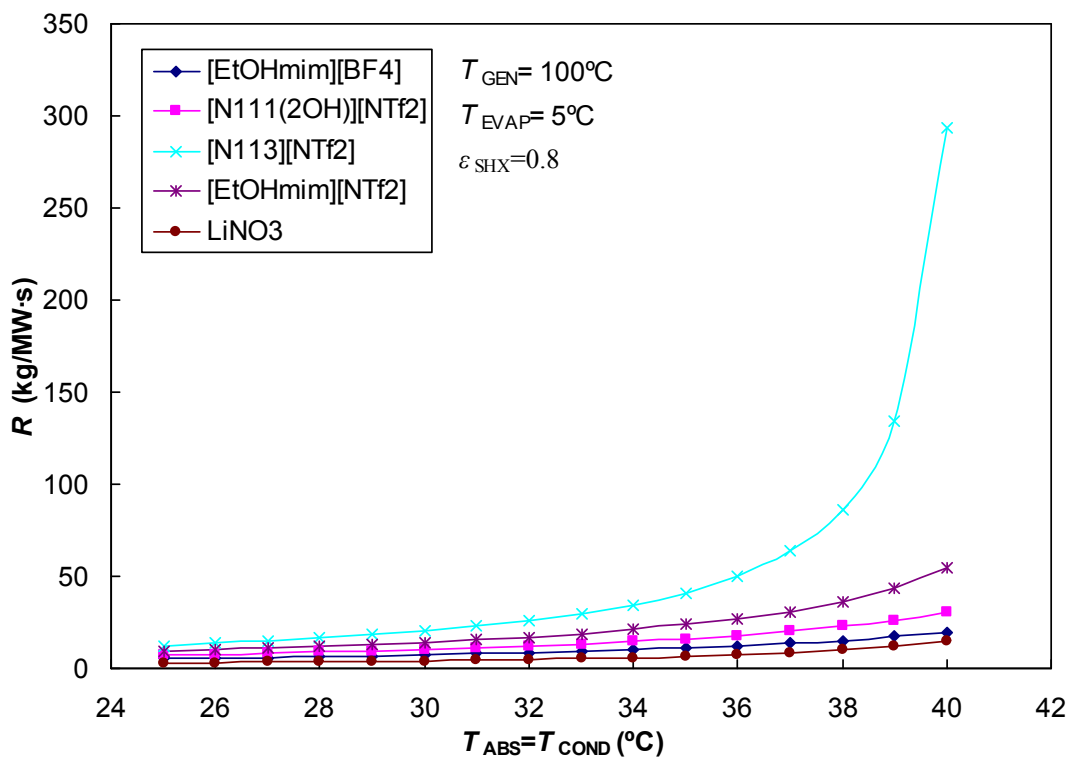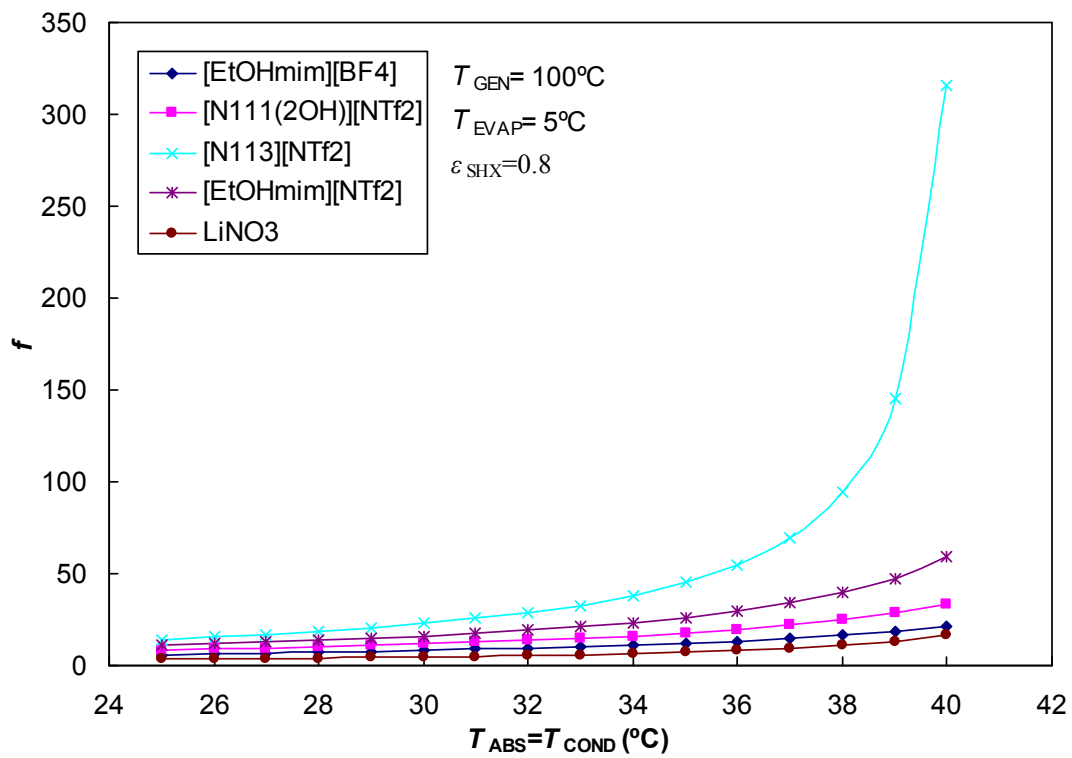
Figure 5.8. Effect of absorber and condenser temperature on f (a) and R (b) of the absorption systems

Similarly, R and f values of the cycle working with ammonia/ionic liquids were somehow higher than that of ammonia/LiNO$_3$ at all absorber/condenser temperature range. Among all ionic liquids studied here, the R and f values of ammonia/[EtOHmim][BF$_4$] working fluid is the lowest although its values was almost doubled that that of ammonia/LiNO$_3$, followed by the ammonia/[N$_{111}$(2OH)][NTf$_2$] and ammonia/[EtOHmim][NTf$_2$] working fluid, being that of the ammonia/[N$_{1113}$][NTf$_2$] the highest in R and f. The R and f values of the systems with ammonia/[N$_{1113}$][NTf$_2$] increases dramatically at the absorber/condenser temperature higher than 35ºC.

5.5.2.4. *Viscosity of ammonia/ionic liquids mixture*

Viscosity plays an important role in the absorption refrigeration systems. Kim et al. [8] reported that higher viscosity of absorbent can cause an increased pressure drop in the compression loop, which would result in larger pumping power or larger pipes and system volume. In addition, according to Römich et al. [9] a high viscosity can influence absorption negatively and increases the pressure drop within the process. Viscosity also plays an important role in the absorption process in the absorber as it influence the overall heat and mass transfer coefficient of the absorber. As compared to conventional absorbent, ionic liquids present relatively higher viscosity. Hence it is important to briefly discuss the viscosity of ammonia/ionic liquid mixtures at inlet and outlet absorber at different operation conditions. The correlation for the viscosity of ammonia/ionic liquid mixtures was taken from Cera-Manjarres [2] whereas the correlation for the viscosity of ammonia/LiNO$_3$ was taken from Libotean et al [10].

Figure 5.9 presents comparison of the viscosities of ammonia/ionic/liquid and ammonia/LiNO$_3$ at inlet absorber at various generator temperatures. As higher generator temperature resulting solution in higher absorbent concentration, thus the viscosity of the solution at inlet absorber increases as the generator temperature increase. Although the viscosity decrease when the temperature decreases, from this figure one can see that the solution concentration gives more effect than solution temperature to the solution viscosity.

The viscosities of ammonia/ionic liquids mixtures are generally higher than that of ammonia/LiNO$_3$ for generator temperature range of 55ºC - 110ºC. However, surprisingly the viscosity of ammonia/[N$_{111}$(2OH)] [NTf$_2$] was lower than that of ammonia/LiNO$_3$ or generator temperature range of 55ºC - 110ºC. The viscosity of ammonia/[N$_{111}$(2OH)] [NTf$_2$] was slightly higher than ammonia/LiNO$_3$ and at generator temperature higher than 100ºC, its viscosity becomes lower than that of ammonia/LiNO$_3$. It is also interesting to see that the viscosities of ammonia/[N$_{1113}$][NTf$_2$] and ammonia/[EtOHmim][BF$_4$] were significantly higher than those other working fluids. In addition, the viscosity of ammonia/[EtOHmim][BF$_4$] increases more dramatically than other working fluids.
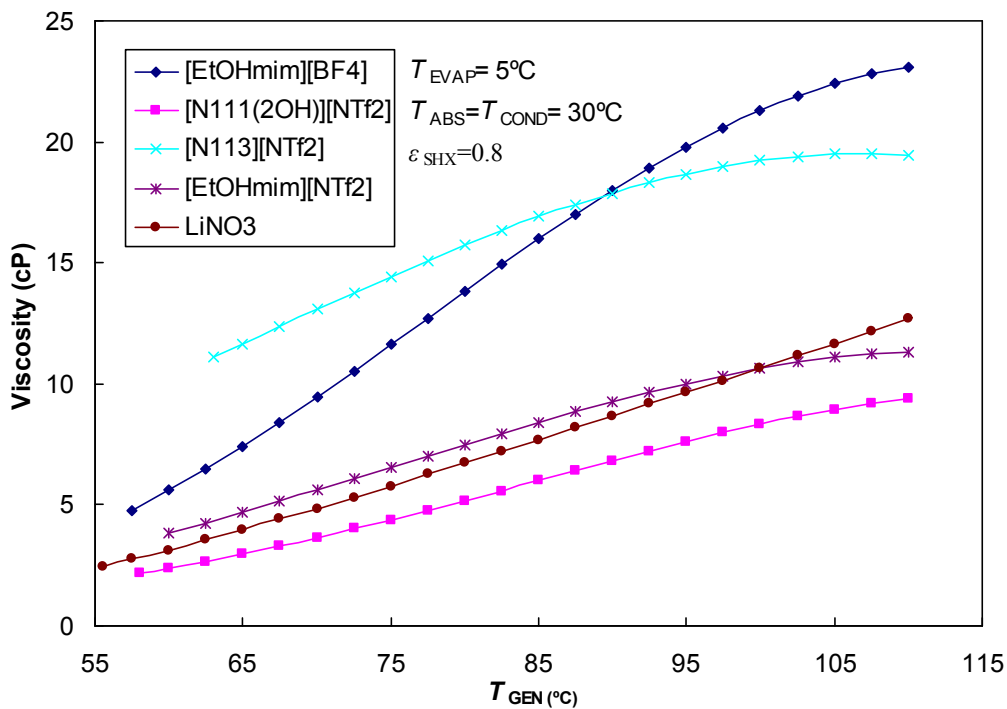
Figure 5.9. Viscosities of ammonia/ionic liquid and ammonia/LiNO$_3$ at inlet absorber at various generator temperatures

Figure 5.10 presents comparison of the viscosities of ammonia/ionic/liquid and ammonia/LiNO$_3$ at outlet absorber at various absorber/condenser temperatures. Similarly, as higher absorber temperature resulting solution in higher absorbent concentration, thus the viscosity of the solution at inlet absorber increases as the

absorber temperature increase and the solution concentration gives more effect than solution temperature to the solution viscosity.

Again, from this figure one can see that the viscosity of ammonia/ionic liquids mixtures were generally higher than that of ammonia/LiNO$_3$ at absorber temperature range of 25ºC - 40ºC. It is also interesting to see that the viscosity of ammonia/[N$_{1113}$][NTf$_2$] was much higher than other working fluids at all absorber temperature range. In addition, although the viscosities of ammonia/[EtOHmim][BF$_4$] and ammonia/[N$_{111}$(2OH)] [NTf$_2$] are much lower than of ammonia/[N$_{1113}$][NTf$_2$], their viscosities were still considerably very high in comparison with ammonia/LiNO$_3$ working fluid. However, the viscosity of ammonia/[N$_{111}$(2OH)] [NTf$_2$] was lower than that of ammonia/LiNO$_3$ at all absorber temperature range.
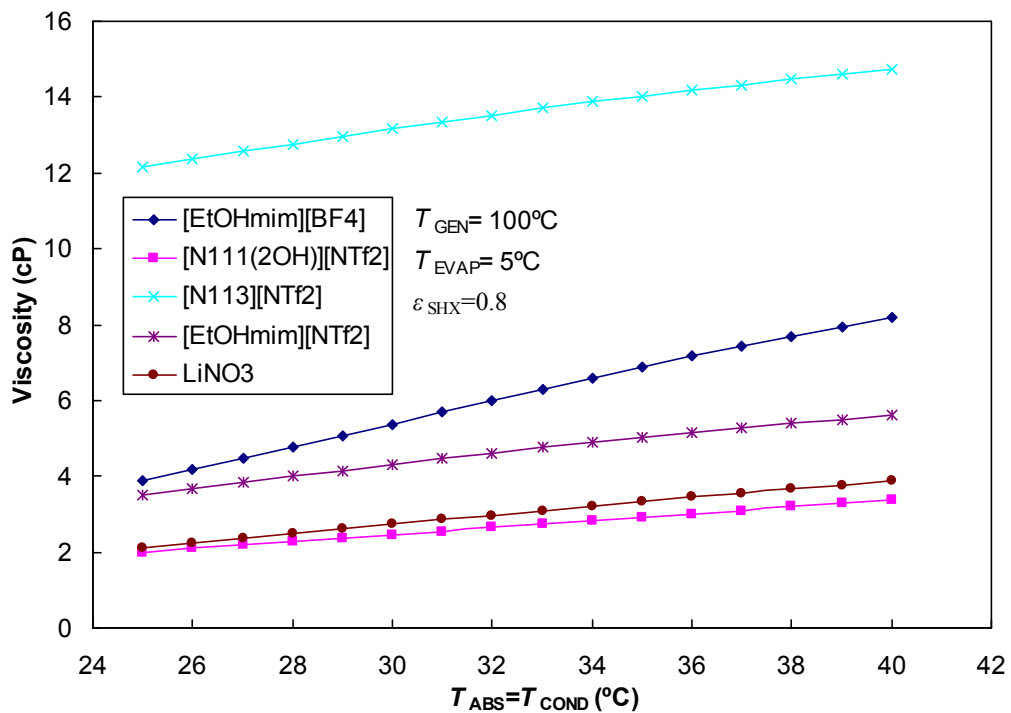

Figure 5.10. Viscosities of ammonia/ionic liquid and ammonia/LiNO$_3$ at outlet absorber at various absorber temperatures

5.6.   Conclusions

In this chapter, the performances of new proposed ammonia/ionic liquid mixtures working pair for absorption refrigeration applications are theoretically

studied and analysed. The 1-(2-Hydroxyethyl)-3-methylimidazolium tetrafluoroborate ([EtOHmim][BF$_4$]), 1-(2-Hydroxyethyl)-3-methylimidazolium bis(trifluoromethyl- sulfonyl)imide ([EtOHmim][NTf$_2$]), (2-hydroxyethyl)-N,N,N-trimethyl bis(trifluoromethyl- sulfonyl)imide ([N$_{111}$(2OH)][NTf$_2$]), and N-Trimethyl-N-propylammonium Bis(trifluoromethane- sulfonyl)imide ([N$_{1113}$][NTf$_2$]) have been selected as new absorbent for ammonia absorption applications. The performance of these ammonia/ionic liquids mixtures is analysed and evaluated. The thermodynamic properties correlation of ammonia/ionic liquid mixture are built using activity coefficient based model non-random two-liquid (NRTL) based on experimental vapor-liquid equilibrium data. Other thermophysical properties necessary for the investigation were correlated from experimental data.

The results show that the NRTL method was able to predict the solubility of ammonia in all ionic liquids studied in this chapter. All solubility predictions were in good agreements in comparison with experimental data. In addition the excess enthalpies for all studied mixture were negative. The coefficient of performance (*COP*) of the absorption systems working with ammonia/ionic liquid working fluids were about similar when compared with ammonia/LiNO$_3$ at same cooling capacity and operation conditions. Among all of ammonia/ionic liquid working fluids studied in this chapter, only [N$_{1113}$][NTf$_2$] presented higher *COP* that that of ammonia/LiNO$_3$ at certain operation conditions. The *COP* of the systems with other ionic liquids as absorbents follows an order of [EtOHmim][BF$_4$] > [N$_{111}$(2OH)][NTf$_2$] > [EtOHmim][NTf$_2$] at all operation conditions. Although the *COP* of the system working with ammonia ammonia/ [N$_{1113}$][NTf$_2$] was higher than with other working fluids at certain operation conditions, on contrary its circulation ratio is the highest among other working fluids. The circulation ratios (*f*) of the absorption systems working with ammonia/ionic liquid working fluids at same operation conditions were somehow higher as compared with that of ammonia/LiNO$_3$. The lowest *f* among all of studied ammonia/ionic liquid working fluids was shown by ammonia/[EtOHmim][BF$_4$] whereas the highest one is shown by ammonia/ [N$_{1113}$][NTf$_2$]. The higher circulation ratio of ammonia/ionic liquid working fluids also affects the solution mass flowrate per unit of cooling load (*R*). At same cooling capacity and operation conditions, the *R* values of the absorption systems working

with ammonia/ionic liquid working fluids at same cooling capacity and operation conditions were higher when compared to that of ammonia/LiNO$_3$. Moreover, energy consumption needed to operate the absorption cycle mainly occurs at the generator, and that the mechanical work required for the solution pump is very small in comparison with energy input of the generator (less than 1% in the case of the highest solution pump's work) and thus can be neglected for general calculations or when information on solution density is not available. Finally the viscosities of ammonia/ionic liquids mixtures were generally higher than that of ammonia/LiNO$_3$ however, surprisingly the viscosity of ammonia/[N$_{111}$(2OH)] [NTf$_2$] was lower than that of ammonia/LiNO$_3$, which may be a competitive absorbent for water absorbent substitution for ammonia-based absorption refrigeration systems in comparison with LiNO$_3$.

5.7. References

[1] Renon, H., Prausnitz, J. M., Local compositions in thermodynamic excess functions for liquid mixtures, *AlChE Journal*, 1968, 14 (1), 135-144

[2] Cerra-Manjarres, A., PhD Thesis, Universitat Rovira i Virgili, Spain, 2015

[3] Tillner-Roth, Harms-Watzenberg, and Baehr, Eine neue Fundamentalgleichung fur Ammoniak, *DKV-Tagungsbericht*, 1993, 20, 167-181,

[4] Yokozeki, A., Shiflett, M.B., Vapor–liquid equilibria of ammonia + ionic liquid mixtures. *Applied Energy*. 2007; 84; 1258-1273

[5] Ruiz, E, Ferro, V.R., de Riva, J., Moreno, D., Palomar, J., Evaluation of ionic liquids as absorbents for ammonia absorption refrigeration cycles using COSMO-based process simulations. *Applied Energy*. 2014; 123; 281–291

[6] Yokozeki, A., Shiflett, M.B., Ammonia solubilities in room-temperature ionic liquids, ammonia solubilities in room-temperature ionic liquids. *Ind. Eng. Chem. Res*. 2007; 46; 1605-1610

[7] Sun, D., Comparison of the performances of NH$_3$-H$_2$O, NH$_3$-LiNO$_3$ and NH$_3$-NaSCN absorption refrigeration systems, *Energy Convers. Mgmt.,* 1998, 39 (5/6), 357-368

[8] Kim, Y. J., Kim, S., Joshi, Y. K., Fedorov, A. G., and Paul, A., Kohl, P. A., Thermodynamic analysis of an absorption refrigeration system with ionic-liquid/refrigerant mixture as a working fluid. *Energy*. 2012; 44; 1005-1016

[9] Roemich C., Schaber K., Berndt J.F., Schubert T.J.S., 2009, Arbeitsstoffgemische mit ionischen Fluessigkeiten fuer Absorptionswaermepumpen und Absorptionskaeltemaschinen, Endreport,

Deutsche Bundesstiftung Umwelt (DBU), Germany, 44

[10] Libotean, S., Martín, A., Salavera, D., Valles, M., Esteve, X., and Coronas, A., Densities, viscosities, and heat capacities of ammonia + lithium nitrate and ammonia + lithium nitrate + water solutions between (293.15 and 353.15) K, *J. Chem. Eng. Data*, 2008, 53, 2383–2388

[11] Sun, D., Comparison of the performances of NH_3-H_2O, NH_3-$LiNO_3$ and NH_3-NaSCN absorption refrigeration systems, *Energy Convers. Mgmt.,* 1998, 39 (5/6), 357-368

Chapter 6

Measurement of Absorption Capacity of Ammonia in Ionic Liquids

6.1. Introduction

Absorption refrigeration system has four main components namely absorber, generator, condenser, and evaporator. Among these, absorber is considered to be the most critical part in the system, both in terms of influence on system performance and cost [1]. Absorption system based on ammonia refrigerant and ionic liquid absorbent is desirable for subzero temperature applications. Thus it is essential to investigate the absorption characteristic of the ammonia vapour into ionic liquid absorbent.

The main objective of this chapter is to undergo comprehensive study on the configurations used in the open literature for both absorber and desorber of the ionic fluids based absorption cooling systems and to develop a measurement setup to study the absorption capacity of the ammonia vapor in ionic liquids in a pool type absorber. This investigation is necessary to find the most suitable ionic liquid as an absorbent for ammonia refrigerant. Furthermore, it is also important to find the most suitable absorber configuration for the proposed ammonia/ionic liquids absorption system.

To achieve the above objectives, a selection on the absorber type suitable for the measurement is carried out based on literature review. Once the absorber type is selected, the measurement setup is then designed and built. The measurement of absorption capacity of ammonia into ionic liquids is performed in several operation conditions. The ionic liquids studied in this work are combinations of two different

cations ([EtOHmim]$^+$ and [emim]$^+$) and three different anions ([BF$_4$]$^-$, [NTf$_2$]$^-$ and [EtSO$_4$]$^-$). The absorption processes are observed within 20 minutes in each experiment at different temperatures and pressures. The detail of the methodology and experimental setup are explained in this chapter and measurement results of absorption capacity of ammonia into ionic liquid are discussed in this chapter..

6.2. Absorption Measurement Setup in the Literature

Absorber is the most critical part in the absorption refrigeration system. Thus as a consequence the selection of absorber type for new working fluid pairs for the initial studies becomes an important step in the starting point before building a complete absorption refrigeration machine.

Generally in all the absorbers the strong solution meets the saturated or superheated vapour coming from the evaporator and absorbs it. During the absorption process the heat is released which is called as heat of absorption and is taken away from the absorber by separate cooling water circuit or blown air in case of air cooled absorbers. To satisfy this condition, it is necessary that the refrigerant concentration of solution and solution temperature returning from generator should be lower and there should be minimal pressure drop across the absorber. At the end, the refrigerant rich weak solution is provided and is pumped to the generator. In exceptional case in spray/adiabatic absorbers the heat of absorption is removed externally due to the difficulties in internal heat removal.

The major characteristic parameters which affects the overall performance of any absorber such as interfacial area, wettability, pressure drop, solution holdup, solution and vapour flow rates, effect of solution inlet temperature and concentration, heat and mass transfer characteristics, effect of cooling water temperature, design difficulty, effectiveness, cost of manufacture and flexibility were compared between all the absorber configurations. With the knowledge gained from the above comparison possible absorber configurations are evaluated for ionic liquid based absorption systems. The critical parameters of ionic liquid based binary solutions are high viscosity, high solution flow rate, high density and the surface tension which are generally negligible at LiBr-water and NH$_3$-water absorption refrigeration systems.

The most common types of absorber for industrial applications are falling film and bubble plate. The former has been recommended to enhance heat and mass transfer during the absorption process. Thin falling film heat transfer mode provides a high heat transfer coefficient and is stable during operation. However, it has a wettability problem that deteriorates the absorption performance.
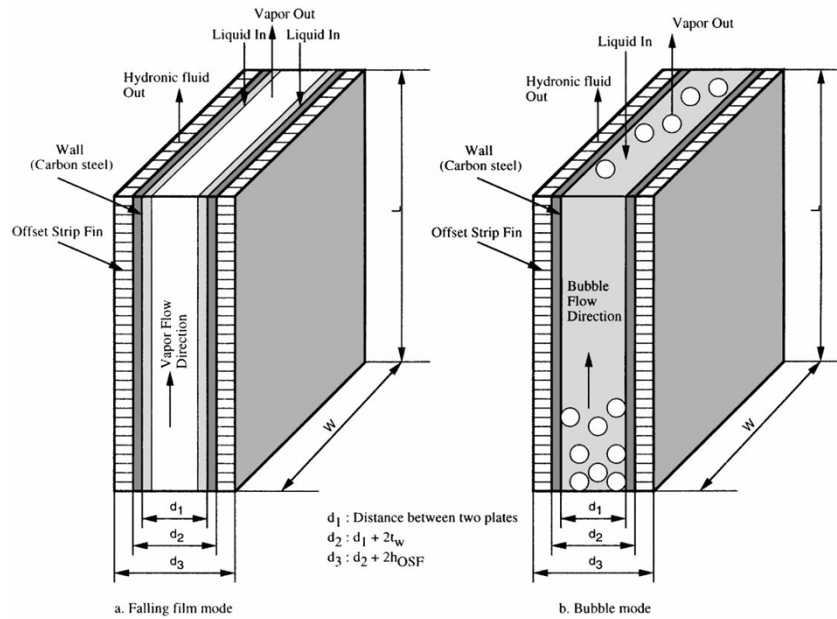
Figure 6.1. Schematic diagram of plate heat exchangers with falling film and bubble absorption modes [2].

Bubble type absorber provides better heat and mass transfer coefficients, and also has good wettability and mixing between the liquid and the vapour [2]. Bubble absorption is in general more efficient than falling-film absorption, especially for low solution flow rates. This fact is explained by the low wetted area in falling film flow under such regimes. These low solution flow rates are more characteristic of low capacity absorber, therefore, the bubble flow is more suitable in such applications [3].

Lee [4] carried out experimental studies on absorption heat and mass transfer performance in ammonia/water adding nanofluids into the system. In their experiment, they measured the effect of nanoparticles on heat and mass transfer aspects of ammonia vapour absorption in ammonia/water solution in a pool type absorber. Their equipment test consists of an absorber test section equipped with vapour distributor, a coolant refrigerator, ammonia cylinder with pressure regulator,

solution outlet line with a balance, and a data acquisition systems. All pipelines as well as the absorber are made of stainless steel to avoid corrosion problems caused by ammonia. The test section unit has dimension of 300 mm width, 300 mm length, and 150 mm height.
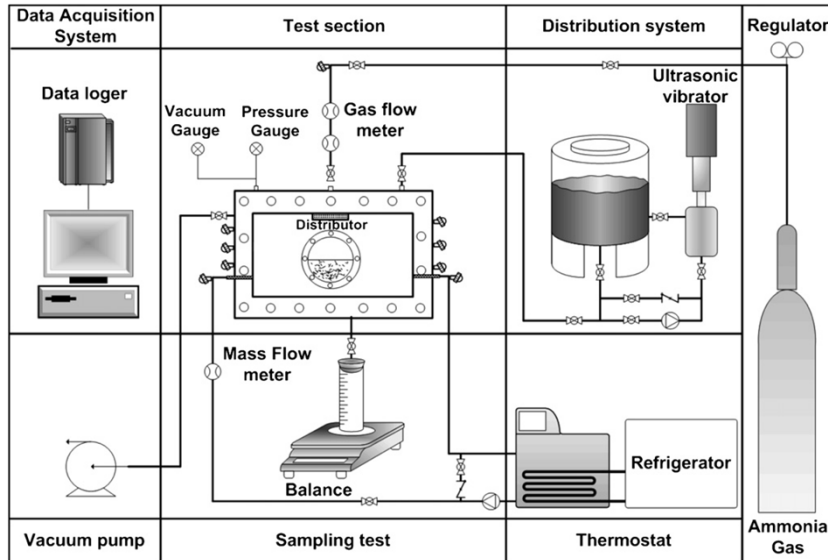
Figure 6.2. Schematic diagram of pool absorber test rig of Lee et al. [4]

To carry out the experiment, the aqueous ammonia of 20% concentration (wt. ammonia) was loaded into the absorber. The ammonia vapour was entered from the gas tank through the pressure gauge at the pressure of 5.0 bar, and was controlled by gas flow meter. The absorption process occurs in the solution surface, hence increasing the solution temperature. To remove the heat, the liquid coolant, which is 30% of ethylene glycol in water entered the absorber at temperature of 15ºC. The inlet temperature of coolant liquid was kept by the refrigerator. Thermocouples were installed in each part of the absorber and coolant line to measure the temperature. In addition, solution and gas flow meter were installed in the coolant line and ammonia gas line, respectively. It is necessary to remove all air within the test section with vacuum pump.
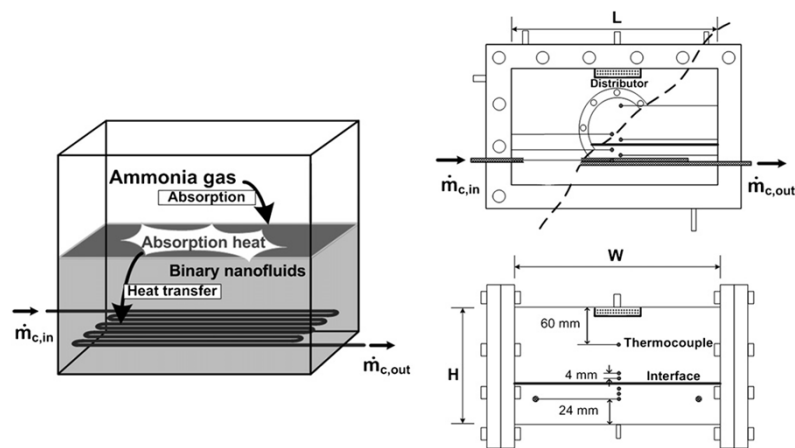
Figure 6.3. Schematic diagram of pool absorber of Li et al [4].

As the ammonia vapour entered the absorber, the absorption process occurs in the solution surface. There is no turbulent motion at the interface such as Marangoni convection during the absorption process because the present experiment is carried out without chemical surfactants. The interface temperature becomes higher as the absorption rate increases. Absorption rate increases rapidly in the incipient stage because the absorption potential (which is the concentration difference between the bulk vapor and the equilibrium vapor at the interface) is the highest in the beginning, and therefore most absorption occurs within about 3 min.

Their results show that the highest solution interface temperature happened within 3 minutes after the absorption processes begin, thus increasing the absorption rate rapidly. The surface temperature increases very quickly just after the absorption starts due to the absorption heat release at the interface between the vapor and the liquid, and starts to decrease gradually after reaching a maximum value for each case. The surface temperature gradually decreases because the absorption potential is the highest in the beginning, and then it decreases as the absorption occurs leading to the increase of the solution concentration.

The absorption processes on a very small bubble type absorber was studied experimentally by Kim et al. [5] in order to find the optimal conditions to design compact absorber for ammonia/water absorption system. In addition, they also tried to find the optimal conditions to design compact absorber for ammonia-water absorption systems. In this study, they considered mechanical treatment and nano technology application to enhance the heat and mass transfer performances. In

mechanical treatment they choose bubble absorption type as the absorption mode and in nano technology application they add the nano particles into the working fluids.

The experimental equipment consists of absorber test unit, a vapour orifice, ammonia gas cylinder and bubble behaviour visualization apparatus. The test section unit has dimension of 20 mm width, 20 mm length, and 200 mm height. The vapour orifice has 2 mm diameter.

The each kind of nano particles with a specific concentration is mixed with the working fluid before the solution is charged into the test section. For the stable distribution of nano particles, the binary nanofluid is stirred by the ultrasonic vibrator for 4 h. The ammonia vapor enters through the orifice with the pressure of 0.16 MPa, which is located at the bottom of the test section. The bubble is generated at the end of the orifice, and the bubble is detached from the orifice after growing, and freely rises in the pool state solution (binary nanofluid). In the present experiment, all of supplied ammonia vapor is absorbed into the binary nanofluid. Under the constant inlet pressure, the vapor flow rate is varied by the absorption performance within the tested solution. That is, since other conditions are exactly same, the absorption rate for the tested solution represents its absorption performance. The solution has concentration between 0.0–18.7% and its temperature is kept constant at 20ºC. The systems is maintained at the pressure of 0.1 MPa.

The results show that the addition of nano particle in the solution can increase the absorption rate of the systems. The addition of nano particles enhances the absorption performance during the bubble absorption process. The maximum effective absorption ratio is 3.21 when Cu nano particles are added 0.10 – 18.7% ammonia solution. Cu is the most effective nano particles among the considered nano particles. The effective absorption ratio increases with increasing the initial ammonia concentration of solution.

The enhancement of heat and mass transfer performance in the ammonia-water bubble absorption process also was investigated by Ma et al [6]. To enhance the heat and mass transfer performance, they used the carbon nanotubes (CNTs)-ammonia binary nanofluid as a working medium.

The experimental tests were conducted in a bubble absorber with 20 mm diameter and 200 mm length. The absorber is connected to the tee valve where the

ammonia vapour was discharged to water tank to adjust its flow rate. After the flowreate is adjusted, the ammonia vapour entered the bottom of the absorber unit through an orifice with 2.7 mm diameter. The absorber temperature was set at 14ºC, but they did not report the absorber pressure as well as cooling procedure for the solution. The ammonia vapour flow rate was measured by gas flowmeter and the total mass of the ammonia solution and absorber was measured using precise electronic balance. The total mass absorbed in the solution could be calculated by measuring the total mass of the solution before and after the experiment.
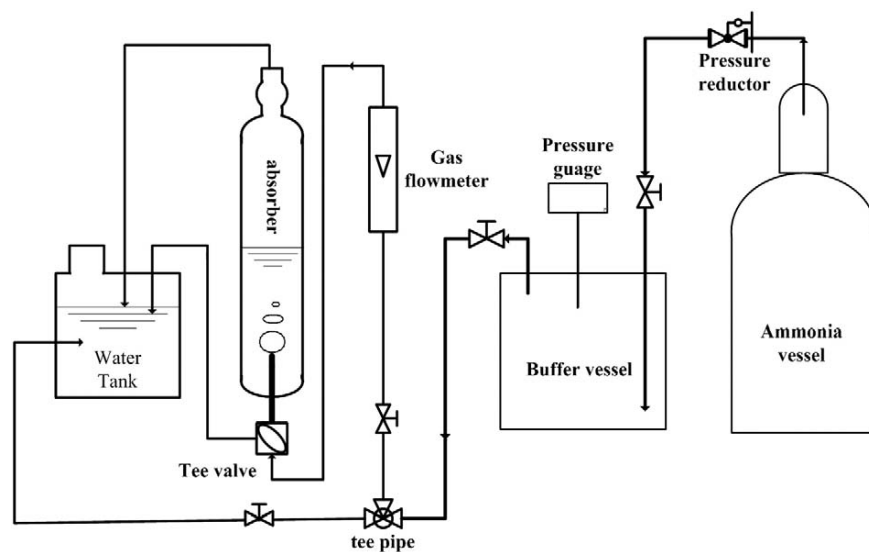
Figure 6.4. Schemactic diagram of bubble absorber test of Ma et al. [6]

Their results show that the absorption ratio increase increases with the mass fraction of CNTs increasing at first, and then decreases. In addition, the effective absorption ratio increases with increasing the initial concentration of ammonia. the effective absorption ratio is vary between 0.25 g/s and 0.05 g/s. In terms of the effect of ammonia vapour flowrate to the effective absorption rate, they conclude that there is no significant different of the effective absorption rate at varied ammonia vapour flowrate.

Pang et al. [7] studied the effect of mono silver (Ag) nanoparticle on mass transfer performance in ammonia-water bubble absorption. Ag nanoparticle has a high thermal conductivity which probably could be a positive contributor to increase

the heat transfer enhancement in nanofluids. In their present work, Ag is chosen to develop binary nanofluids for the absorption application.

The experimental setup consists of the absorber test section, a sampling line with a balance, a refrigerator with thermostats, an ammonia gas cylinder with a regulator, a buffer vessel with pressure gauge, a water tank and a data acquisition system. The absorber test section is carefully insulated to neglect the effect of the heat loss. Prior to the experiments, the air within the test section is completely evacuated by a vacuum pump to remove the effect of non-condensable gases on the absorption performance. Ag solution with a specific concentration is mixed with ammonia aqueous solution before it is charged into the test section. The binary nanofluids prepared with a fixed weight are filled up to the test section and thereafter absorption process begins when ammonia vapor enters the test section.
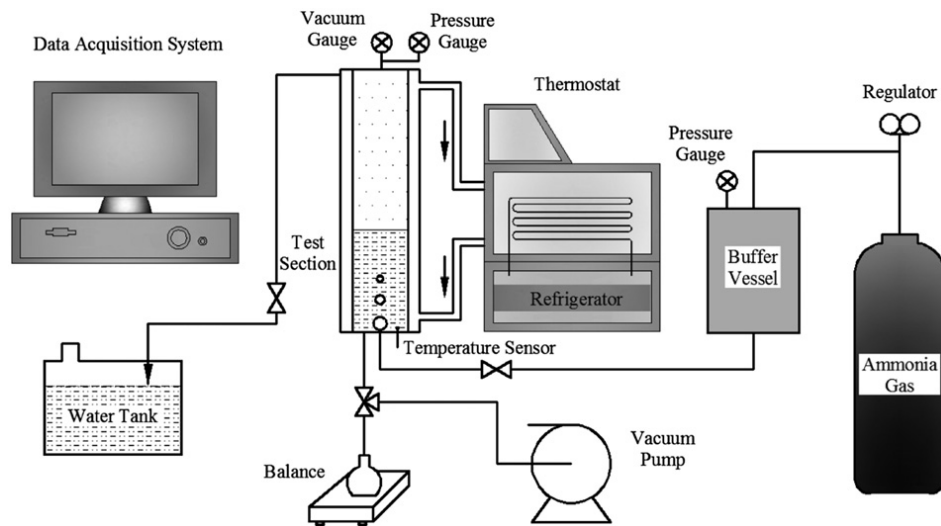
Figure 6.5. Schemactic diagram of bubble absorber test of Pang et al. [7]

The initial pressure of ammonia gas in the buffer vessel is controlled to 200 kPa (absolute pressure) by the regulator. The regulator is shut off during the experiment. Therefore, the initial inlet pressure for the test section is maintained at 200 kPa. The temperature sensor is installed at the bottom of the absorber to measure the temperature of the bulk solution. The inlet coolant temperature is maintained constant at 15ºC and the mass flow rate of cooling water is kept constant at 8 liters per minute and the initial solution temperature is maintained constant at 19.8ºC

The results shows that initially the solution temperature increase when the absorption process started. The solution temperature reached its maximum value within 6-7 minutes after the absorption process started because of a big absorption potential. Both the temperature and temperature gradient decrease gradually as the initial concentration of ammonia increases. The effective mass absorption rate lay between 0.16 and 0.35 g/min.

Kim et al [8] investigated the effect of nano particles on the absorption rate and heat transfer on water-LiBr falling film absorber. In their investigation, they used falling film type absorber which consists of the absorber test section, a chiller and a reservoir tank with an auxiliary solution tank. The absorber test section has eight copper tubes with diameter of 15 mm and the length of 500 mm. The test section chamber is a rectangular channel with a gap distance of 500 mm and made of stainless steel with 10 mm thickness. The system pressure is kept at 0.01 bar. The coolant from the refrigerator flows inside the copper tube from the bottom to the top while the solution from the solution pump is distributed by the solution distributor on the top of the test section, and flows down on the horizontal tube rows. Therefore, there is a counter-cross falling film flow between the solution and the coolant flows. A sight glass is installed in the front side of the absorber test section to visualize the falling film flow of the solution. The test section except the sight glass is completely insulated by the insulating materials.
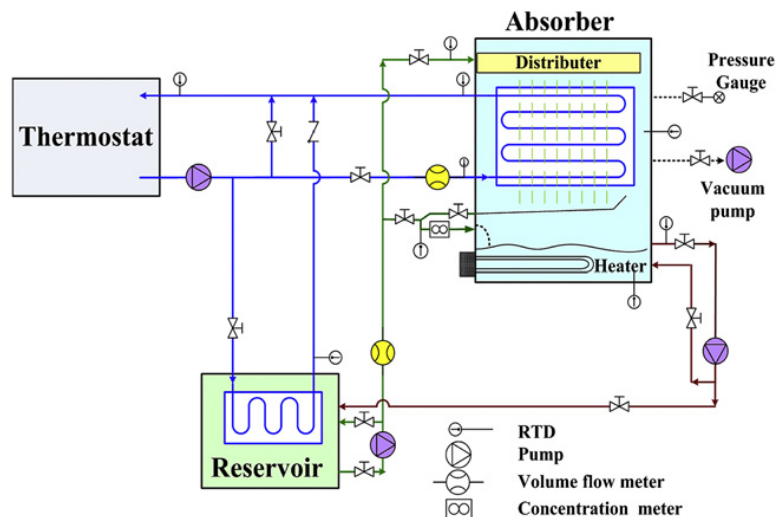

Figure 6.6. Schemactic diagram of bubble absorber test of Kim et al. [8]

Water vapor is generated by two electric heaters (4 kW each) which are installed at the bottom of the test section. The water vapor flows up and is absorbed into the solution liquid on the tube wall. The solution inside the test section is then pumped into the reservoir tank where the solution temperature is cooled down to the absorber inlet temperature by the coolant from the refrigerator. The solution inside the reservoir tank is pumped to the solution distributor by a magnetic solution pump and then flows down on the horizontal tube bank. The solution mass flow rate is measured by a precise electronic volume flow meter just before the solution distributor. The solution is collected at the bottom of the tube bank by a solution collector where the solution outlet temperature is measured. The solution collected at the bottom of the test section is heated by the electric heaters to generate the water vapor and the solution is pumped to the reservoir tank. The coolant from the refrigerator is splitted into the absorber test section and the solution reservoir tank. The coolant is the cooling water with 30% of ethylene glycol (EG).

Their results show that when the surfactants are not added, the heat transfer performance is enhanced by adding nano-particles. The maximum improvements of heat transfer and mass transfer rates reach 46.8% and 18%, respectively, when the concentration of SiO2 nano-particle is 0.005 vol%. The nano-particles improve the heat and mass transfer performance by their convective characteristic such as Brownian motion. But by adding them too much, it is postulated that nano-particles formed in the process hinder mutual movement or motion, reducing the heat and mass transfer performances. In addition, the enhancement ratios increase when the nano-particles and the surfactant are added. But it is found that the synergetic enhancement does occur by the nano-particles and the surfactant which induces the Marangoni convection by reducing the surface tension of solution. The performance enhancement with only the nanoparticles becomes higher than that with both the nanoparticles and the surfactant. This is because the convective motion of nano-particles such as Brownian movement gives a big impact on the absorption performance in SiO2 binary nanofluids and then the surfactant makes the convective motion of nano-particles weak.

Wu et al. [9] investigated the a new method for enhancing absorption in an ammonia/water bubble-type absorber by adding Fe3O4 nanoferrofluid in

combination with the application of an external magnetic field and its effects on bubble absorption.

The experimental test consist of a bubble absorber with electric magnetic field and magnetic field generator, ammonia gas cylinder with pressure gauge and gas flowmeter, and water cooling system.
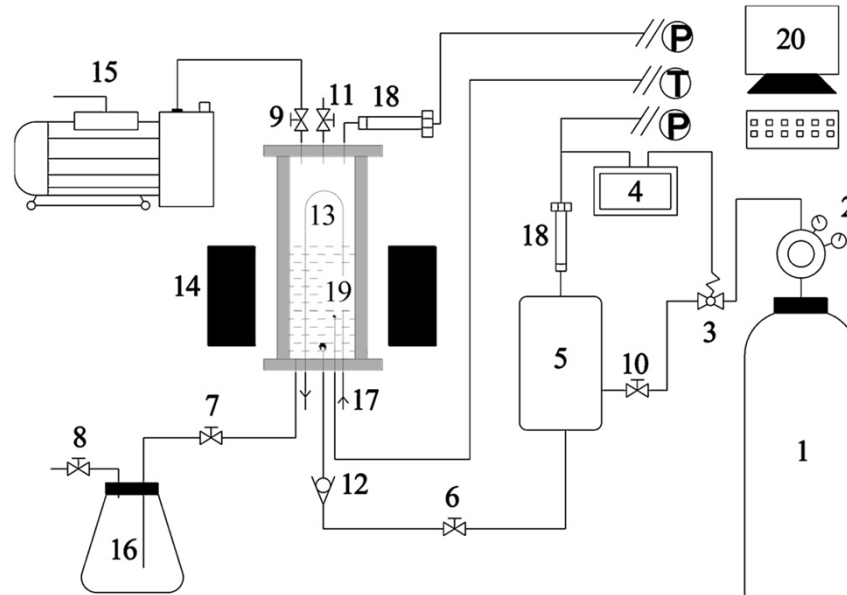
Figure 6.7. Schemactic diagram of bubble absorber test of Wu et al. [9]

The ammonia gas entered to the absorber via gas reservoir, and its pressure is controlled by pressure reducing valbe and pressure control. When bubble absorption experiments are performed, the pressure control devices are shut down and needle valve (in direction to the absorber) is completely open, and the ammonia gas flows from the ammonia gas reservoir through the check valve and is continuously bubbled into the absorber, which is filled with a predetermined quantity of absorption solution (40 g in each experiment). Before being filled with absorption solution, the absorber is completely evacuated to eliminate the influence of non-condensable gases on absorption performance. The external magnetic field intensity, which is measured with a digital TESLA meter (accuracy: 2.0%), is adjusted by changing the distance between the two permanent magnets. The absorption heat generated in the process is removed by circulating cooling water in the cooling loop as required. The relevant temperature and pressure parameters were measured using a platinum resistance sensor and a pressure sensor, respectively, and the real-time temperature and pressure

signals were acquired and recorded by a data acquisition system. The amount of ammonia absorbed into the solution during the process was determined by measuring pre- and post-absorption solution mass with a high-precision electronic balance. The time it takes for each test was constant (i.e. 5 min or 300 s), which was strictly reckoned and controlled by a stopwatch.

Their results show that as the absorption process begin, the solution temperature increase and reached its maximum value after about 100 s. After reached its maximum value, the temperature decrease gradually until the absorption process is stopped. The results also show that increasing magnetic field intensity can increasethe absorption rate. The absorption rate lays between 0.71 g/min and 0.73 g/min without magnetic field and the absorption rate increase up to between 0.72 g/min and 0.75 g/min.
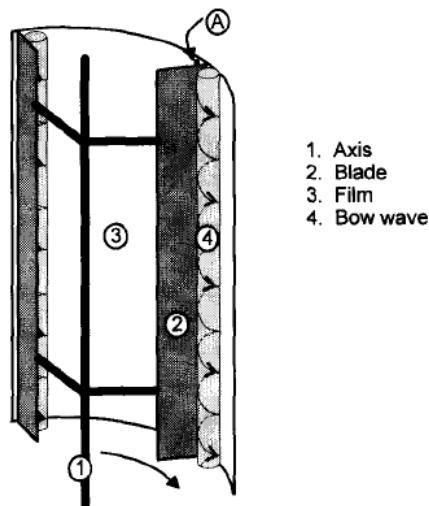
Figure 6.8. Schematic diagram of wipred-film evaporator [10].

In addition to the types of absorber configuration mentioned above, there are some other configurations which are investigated for the absorption characteristic of a refrigerant into an absorbent at relatively small flow rates. A novel design and configuration of wiped-film evaporator has been proposed for high viscosity working fluids [10-11]. Since the basic principle of evaporation process is a reverse process of absorption, this configuration may be applied and be adjusted for the application of absorption process. For instance, Mc Kenna [10] proposed a design model of a wiped-film evaporator for the devolatilisation of polymer solutions. He reported that

wiped film evaporators (WFE) can be used in chemical process operations where heat and/or mass transfer steps are rate limited since they can be adapted to treat liquids with a wide range of viscosities while maintaining short residence times. Both Heimgartner [12] and Biesenberger [13] indicated in their reviews on the applications of such devices that they can operate at liquid viscosities ranging from 1 poise up to 105 poise.

In this study, the pool type absorber configuration is selected to examine the absorption rate of ammonia refrigerant into ionic liquid absorbent as this configuration is suitable for the measurement of absorption capacity in liquid static conditions. In addition, this configuration is suitable to handle high viscosity fluid like ionic liquids.

6.3. Materials and Experimental Setup

6.3.1. Materials

The anhydrous ammonia (purity 99.98% by mass, CAS no. 7664-41-7) is obtained from Carburos Métalicos and is used directly without any further purification. Commercial ionic liquids, 1-ethyl-3-methylimidazolium ethyl sulfate ([emim][EtSO$_4$], assay ≥95%, MW=236.29, CAS no. 342573-75-5) is obtained from Aldrich Chemistry, whereas 1-ethyl-3-methylimidazolium tetrafluoroborate ([emim][BF$_4$], assay >98%, MW=197.97, CAS no. 143314-16-3), 1-ethyl-3-methylimidazolium bis[(trifluoromethyl)sulfonyl]imide ([emim][NTf$_2$], assay 99%, MW=391.31, CAS no. 174899-82-2), 1-(2-hydroxyethyl)-3-methylimidazolium tetrafluoroborate ([EtOHmim][BF$_4$], assay >98%, MW=213.97, CAS no. 374564-83-7) and 1-(2-hydroxyethyl)-3-methylimidazolium bis(trifluoro-methylsulfonyl)imide ([EtOHmim][NTf$_2$], assay 99%, MW=2407.31, CAS no. 374564-83-7) are obtained from Iolitec. Chemical structure of cations and anions of ionic liquids used in this study are shown in figure 6.9. Ionic liquids are dried in a vessel under vacuum and simultaneously stirred and heated for at least 48 hours to reduce their water contents before used. The water content of ionic liquids after drying process is determined using Karl Fisher coulometer (Mettler Toledo model C20). The results show that the water content for all ionic liquids is below 200 ppm (by mass).
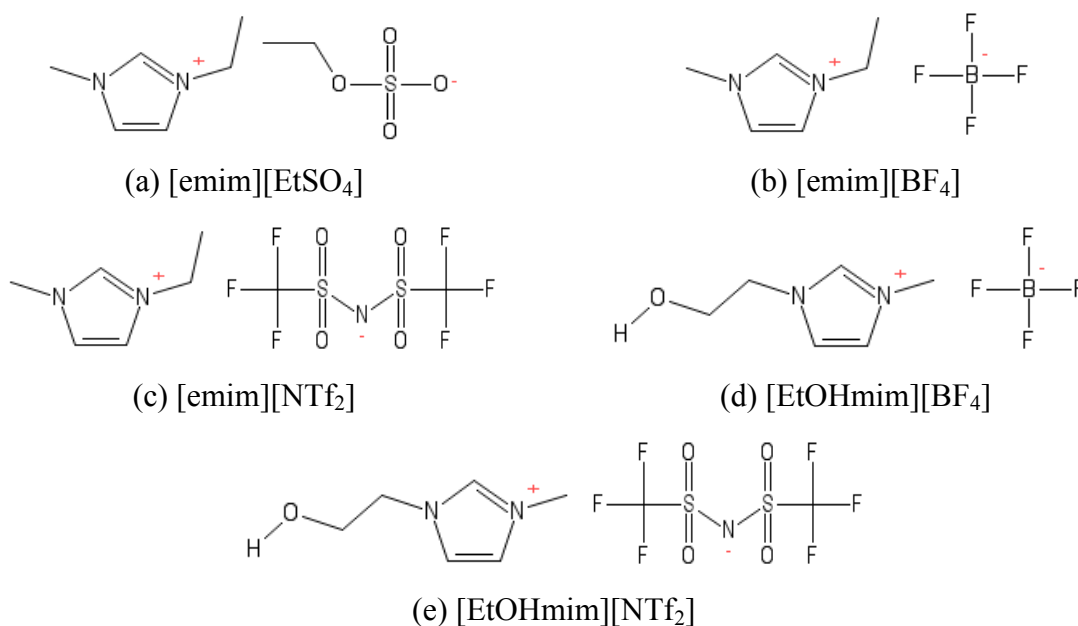

(a) [emim][EtSO$_4$]

(b) [emim][BF$_4$]

(c) [emim][NTf$_2$]

(d) [EtOHmim][BF$_4$]

(e) [EtOHmim][NTf$_2$]

Figure 6.9. Chemical structures of studied ionic liquids

6.3.2. Experimental Setup and Procedures

In this study, static pool type absorber is selected to examine the absorption rate of ammonia refrigerant into ionic liquid absorbent as this configuration is suitable for the measurement of absorption capacity in liquid static conditions [10]. In addition, this configuration is suitable to handle high viscosity fluids such as ionic liquids.

The main components of the experimental set-up for absorption measurement are liquid cell, mass flow controller, temperature and pressure sensor, data logger, thermal bath, magnetic stirrer, ammonia tank and vacuum pump.

The liquid cell is a cylinder and is made up of stainless steel to avoid corrosion problems due to ammonia contact. It has inner volume of 14 ml, outside diameter of 30 mm and wall thickness of 2 mm. The liquid cell has a temperature sensor (PT-100) and pressure sensor (Wika S-20 pressure transducer). The temperature and the pressure sensors are connected to the data logger (DataTaker DT80) to record the temperature and pressure in a certain interval of time. The cell is immersed in a thermal bath to maintain the temperature, and is placed over a magnetic stirrer to agitate the liquid absorbent inside the cell in order to ensure that

the ionic liquid/ammonia solution is in homogenous condition and the liquid surface is less than equilibrium condition so that the absorption process can occur until the solution reaches the equilibrium condition with the refrigerant vapor. The detailed schematic diagram of the measurement setup is shown in figure 6.10 and the detailed drawing of measurement cell is shown in figure 6.11.
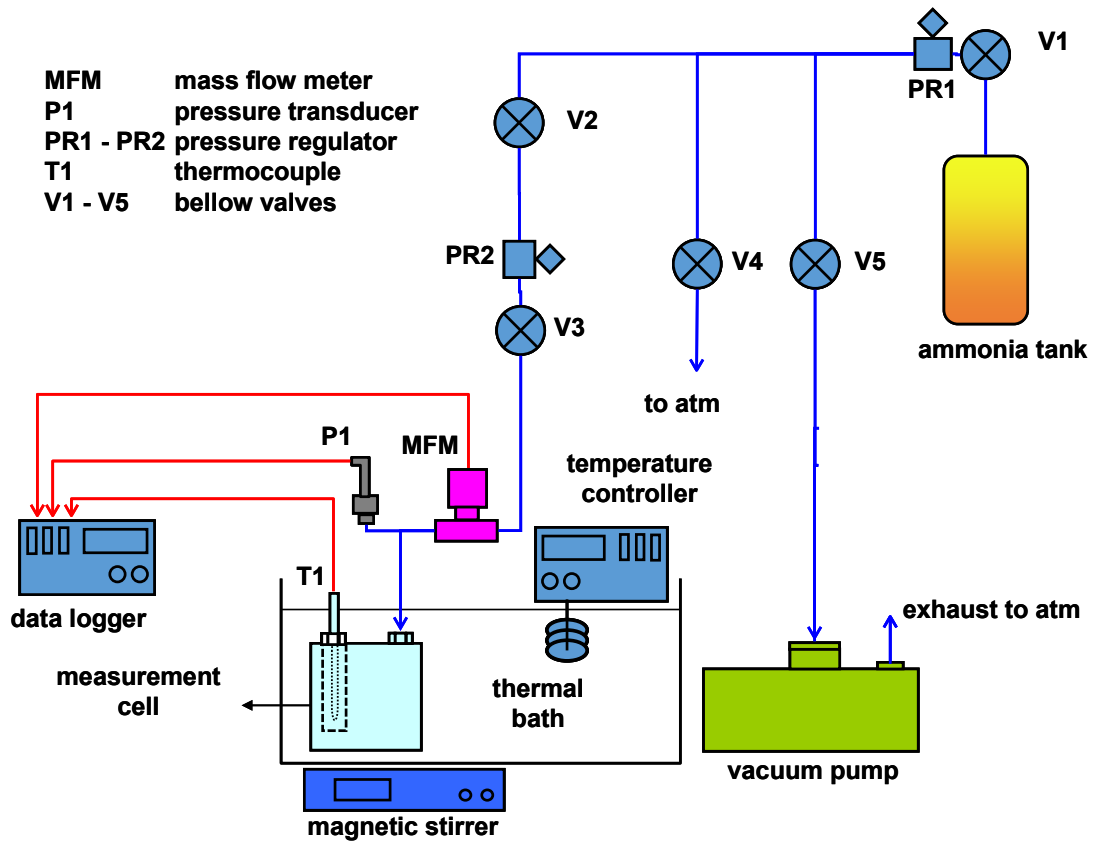
Figure 6.10. Schematic diagram of the experimental measurement setup

The main ammonia line is connected to the ammonia tank which has a valve and a pressure regulator. A mass flow controller (Alicat gas flow controller, model MCS-500SCCM-D) is installed in the ammonia line close to the cell to record ammonia mass flow. Another valve and a pressure regulator are installed in the setup to control the pressure and to start and terminate the measurement. In addition, the ammonia line has a connection to the vacuum pump to remove non-absorbable gas inside the system.

TOP VIEW FRONT HALF - SECTIONAL VIEW

BOTTOM VIEW

ALL DIMENSIONS ARE IN MM
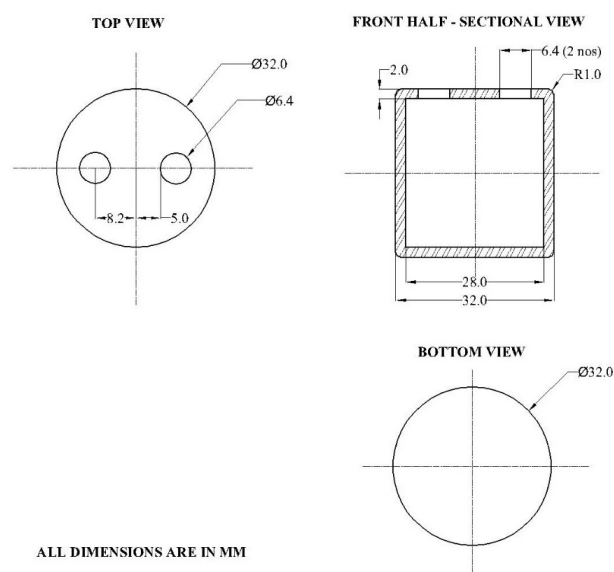
Figure 6.11. Design of ionic liquid measurement cell

Experimental Procedure

In this section, the procedure for the measurements is described. It is divided into three main stages: leakage test (which is carried out under vacuum conditions as well as pressure conditions); measurement; and cleaning of the equipment.

1. Leakage test under vacuum conditions

    With the argon cylinder connected to the setup gas line, the line-to-vacuum valve is opened and the vacuum pump is activated to decrease the system's pressure until a minimum possible value of approximately 0.01 mbar. Once the target pressure is reached, the line-to-vacuum valve is closed and, with the gas line being isolated from the outside by the closed valves, the pressure transducers' readings are monitored; if pressure in the line increases, it means there is leakage at some point in the circuit. After finishing the leakage test, the line-to-atmosphere valve is opened to finish the vacuum conditions.

2. Leakage test under pressure conditions

    Argon gas is used to carry out the leakage test under pressure. With the argon cylinder connected to the setup gas line, the main valve and the line-reactor valve are

both opened to increase the system's pressure until 5 bar. Once the target pressure is reached, the cylinder-to-circuit valve is closed and the pressure transducers' readings are monitored; if pressure in the line decreases, it means there is leakage at some point in the circuit. After finishing the leakage test, the line-to-atmosphere valve is opened to release the contained argon.

3.   Absorption of refrigerant into absorbent

An amount of about 5 ml of ionic liquid is taken using a syringe and weighted on a digital mass balance Mettler AE 260 DeltaRange (±0.1 mg) , and then is injected carefully into the cell via injection line.

After the liquid is inserted into the cell, all the lines are connected properly. Before starting the measurement, it is important to remove the non-absorbable gas trapped both in the line and the cell. To remove the non-absorbable gas, vacuum is applied to the whole gas pipeline and the cell, in order to remove the air inside them. The vacuum pressure is monitored with the digital Pirani gauge meter, until that segment reaches vacuum (c.a. 0.01 bar). After removing the non-absorbable all valves are closed. The temperature and pressure sensors are connected to the data logger. The cell is then immersed into the thermal bath placed over the magnetic stirrer.

The final step before starting the measurement is to set the ammonia pressure regulator to the desired pressure. The first step to set the ammonia pressure is to ensure that the ammonia tank valve and the pressure regulator are closed, and then to reduce the pressure by opening the release valve. The second step is to open the ammonia tank valve and then carefully open the pressure regulator until reach the desired pressure.

To start the measurement, the valve (V3) is opened. The pressure and the temperature are recorded every two seconds until these parameters become invariant and then the measurements and experiment are stopped.

After finishing the last desorption stage, all valves areclosed and line-to-atmosphere valve (valve V4) is opened slowly to bring the system back to atmospheric pressure. Then, valve V4 is closed, the cell is detached from the gas pipeline and the thermocouple is removed from inside the cell. The cell is then

emptied by just turning it upside down and put the ionic liquid and ammonia solution into a labelled bottle. Due to the IL's high viscosity, the emptying can take some time, even with the cell being at high temperature.

4. Cleaning the Equipments

Once the measurement is completed, the ammonia tank valve is then closed, and the ammonia pressure is released by opening the release valve. The cell is then uninstalled from all connection as well as from the temperature and pressure sensor. To clean up, the cell is cleaned with acetone for several times and then is connected to the water line and the water flows slowly into the cell for about 15 minutes. Afterwards, the water pH exit from the cell is checked using pH indicator paper. If the water exiting from the cell still has high pH (indicated by blue-purple colour) then the water is kept flowed for another 15 minutes until the water exit from the cell has neutral pH (indicated by yellow colour). After the cell is clean, then the next step is to dry the cell by keeping the cell inside the dehumidifying chamber at temperature of about 80ºC for 30 minutes – one hour.

6.3.3. Data Reduction

Three parameters, mass absorption, mass absorption flux, and absorber thermal load are used to analyse the absorption capacity of ammonia into ionic liquids. The following equations are used for processing and analysing the data obtained from the measurements.

1. Mass Absorption Capacity

Mass absorption rate can be defined as the total mass of refrigerant absorbed into the absorbent in a unit of time. This mass absorption rate can be used to determine the total mass absorbed into ionic liquids and ammonia mass concentration in the solution. In a formula, it can be calculated as

$$m_{NH_3} = \int \dot{m}_{NH_3} \, dt \qquad (6.1)$$

where $\dot{m}_{NH_3}$ represents the ammonia mass flow rate (g/s), $\dot{m}_{NH_3}$ is the total mass of the solution (g), and t is the time (s).

In addition, ammonia mass concentration in the solution can be expressed as

$$X_{NH_3}(\%) = \frac{m_{NH_3}}{m_{NH_3} + m_{IL}} \cdot 100 \qquad (6.2)$$

where X_{NH_3} is the ammonia mass concentration in the solution (%) and m_{IL} is the mass of ionic liquid in the solution.

2. Mass Flux

Mass flux which is defined as the mass absorption rate per unit area can be calculated using

$$m_f = \frac{\dot{m}_{NH_3}}{A} \qquad (6.3)$$

where m_f is mass flux (g/s cm^2) and A is interface area (cm^2).

3. Absorber thermal load

Absorber thermal load is defined as total heat released from the absorber to the ambient due to absorption process. This parameter can be calculated from mass and energy balance using

$$Q = m_{NH_3}h_{NH_3} + m_{IL}h_{IL} - m_s h_s \qquad (6.4)$$

where Q is absorber thermal load and h_{NH_3}, h_{IL}, and h_{sol} are enthalpy of ammonia, pure ionic liquids and ammonia-ionic liquid solution, respectively. The enthalpies of ammonia, ionic liquids, and ammonia-ionic liquid solutions can be calculated using equations described in previous chapter.

Mass balance during the absorption process can be expressed as

$$m_{sol} = m_{NH_3} + m_{IL} \qquad (6.5)$$

6.4. Results and Discussion

The absorption capacity of ammonia into five ionic liquids in a static pool type absorbent is studied in this work. Pool type absorber is chosen due to its ability

to measure the absorption capacity of absorbent having low solubility with the refrigerant by small quantity of absorbent [14].

The ionic liquids studied in this work are combinations of two different cations ([EtOHmim]$^+$ and [emim]$^+$) and three different anions ([BF$_4$]$^-$, [NTf$_2$]$^-$ and [EtSO$_4$]$^-$). The absorption processes are observed within 20 minutes in each experiment at different temperatures and pressures.
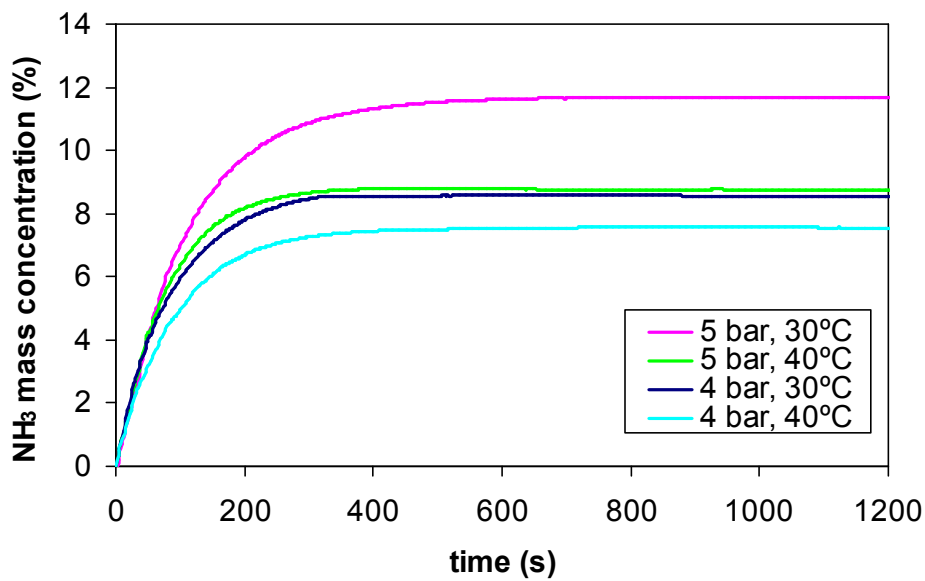
6.4.1. *Effect of temperature and pressure*

It is known that the ammonia solubility in ionic liquids decreases when the temperature is increased and the ammonia solubility in ionic liquid increases when the system pressure is increased [11-13]. However, it is interesting to understand the behaviour of ammonia absorption into ionic liquids at different temperatures and pressures.

The effect of initial temperature on the absorption process of ammonia into [emim][BF$_4$] is shown in figure 6.12. When the initial temperature is increased, the absorption rate decreases and thus decreasing the heat releases to the ambient, resulting the decrease of temperature different (ΔT) (see figure 6.12 (a)). From figure 6.12 (b) it can be confirmed that the ammonia absorption capacity in ionic liquid decreases when the initial temperature is increased. For instance, the ammonia concentration at pressure of 5 bar decrease from 11.67% at initial temperature of 30ºC to 8.75% at initial temperature of 40ºC. Similarly, at pressure of 4 bar the ammonia concentration slightly decreases from 8.56% at initial temperature of 30ºC to 7.54% at initial temperature of 40ºC.
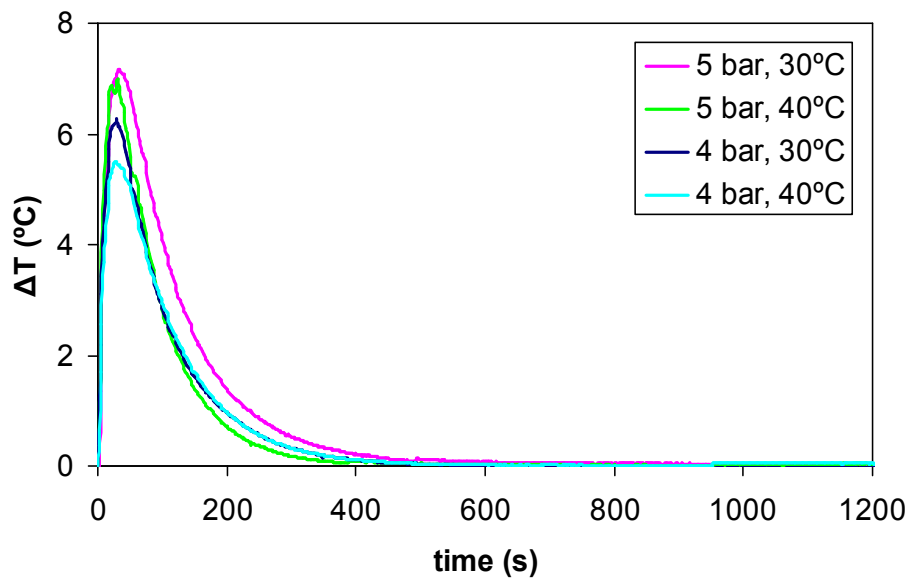
(a)

(b)

Figure 6.12. Temperature difference profile (a) and NH_3 mass concentration profile (b) of [emim][BF_4] at different temperatures and pressures

Figure 6.13 shows the effect of pressure to the absorption process of ammonia into [EtOHmim][NTf2]. This figure confirms that the ammonia absorption capacity in ionic liquid increases when the system pressure is increased. As shown in figure 6.13 (a), the ammonia mass flow rate increases when the system pressure is

increased. The ammonia concentration at pressure of 5 bar decreases from 11.19% to 9.72% at pressure of 40ºC and decreases to 7.58% at pressure of 3 bar (see figure 6.13 (b)).
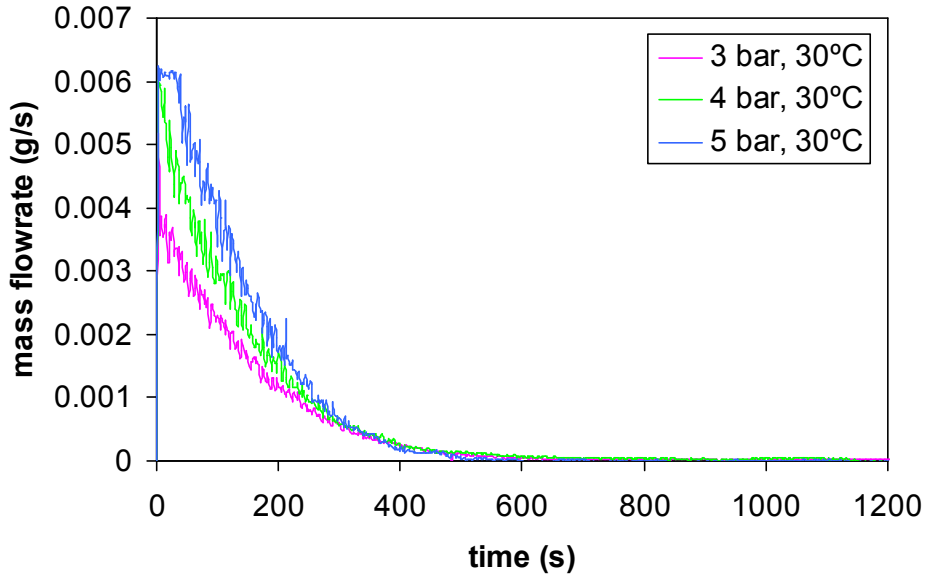
(a)
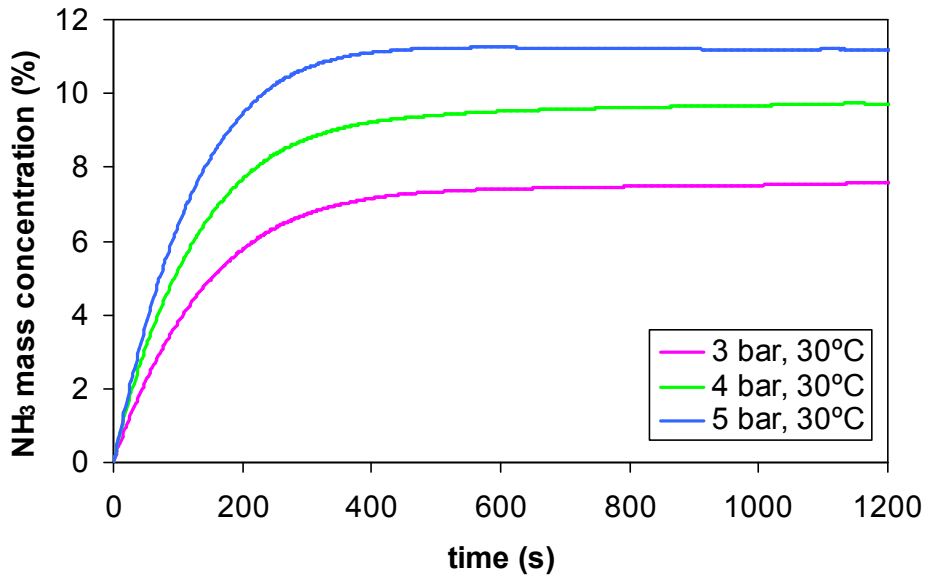
(b)

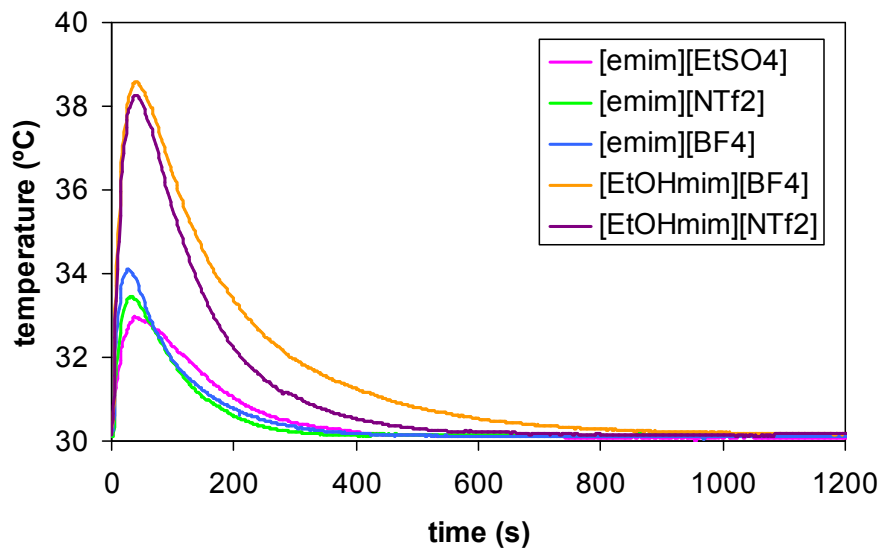**Figure 6.13.** Mass absorption flux profile (a) and ammonia mass concentration profile (b) of [EtOHmim][NTf$_2$] at temperature of 30ºC and different pressures

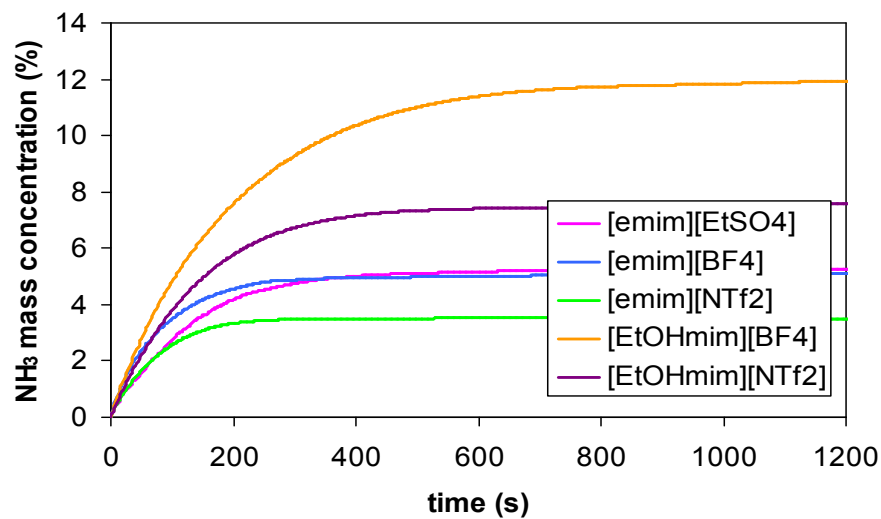### 6.4.2. Temperature and mass concentration profile

Figure 6.14 (a) shows the temperature profile during absorption process at initial temperature of 30ºC and pressure of 3 bar. It can be seen that the pool type absorber with small volume can give relatively significant in temperature change considering that ionic liquid has relatively low solubility in ammonia. It also can be seen that the temperature increase significantly in the beginning of the measurement as in this time the absorption capacity is in its highest rate, and the heat is released to the system. The temperature then decreases as the absorption rate decrease until the solution reach equilibrium. For all ionic liquid studied, the temperature increases in the beginning of absorption process which indicates that the absorption processes for all studied ionic liquids are exothermic process.

The temperature increase of ionic liquids with $[EtOHmim]^+$ cation is higher as compared to those ionic liquids with $[emim]^+$ cation which means that ionic liquids with $[EtOHmim]^+$ cation release more heat as compared to other ionic liquids. The temperature difference between peak temperature and initial temperature (ΔT) of $[EtOHmim][BF_4]$ and $[EtOHmim][NTf_2]$ at initial temperature of 30ºC and pressure of 3 bar lays about 8.6ºC and 8.2ºC, respectively whereas temperature differences of $[emim]^+$ based ionic liquids just lay around 3–4ºC which are less than half of the temperature difference of $[EtOHmim]^+$ based ionic liquids.

In terms of same cation, it can be clearly seen from figure 3 that ionic liquids having $[BF_4]^-$ anion give higher temperature difference as compared to other anion. For instance, $[EtOHmim][BF_4]$ shows higher temperature difference than $[EtOHmim][NTf_2]$ and $[emim][BF_4]$ has higher temperature difference than $[emim][NTf_2]$ and $[emim][EtSO_4]$. In addition, for same cation ionic liquid with $[NTf_2]$ anion has higher temperature difference than that of $[EtSO_4]^-$ anion. However, although for same cation $[BF_4]^-$ has higher temperature difference than other anions, these differences are much lower as compared to those given by different cations. In a simple way, it can be said that different cations can give more influence in temperature differences as compared to different anions.

(a)

(b)

Figure 6.14. Temperature profile (a) and ammonia mass concentration profile (b) at temperature of 30ºC and pressure of 3 bar

Figure 6.14 (b) shows the ammonia mass concentration profile during the absorption process. This figure shows that similarly with the trends of temperature differences, at the end of each measurement for operation condition at temperature of 30ºC and pressure of 3 bar the [EtOHmim]⁻ based ionic liquids can absorb more ammonia as compared to [emim]⁺ based ionic liquids. In addition, [EtOHmim][BF$_4$] has the highest ammonia concentration and [emim][NTf$_2$] has the lowest ammonia

concentration as compared to the other ionic liquids. At the end of measurement, the ammonia mass concentration in [EtOHmim][BF$_4$] and [EtOHmim] [NTf$_2$] is 11.94% and 7.58%, respectively. For [emim] based ionic liquids, the ammonia mass concentration at the end of measurements follows the trend [BF$_4$]$^-$>[EtSO$_4$]$^-$>[NTf$_2$]$^-$. The ammonia mass concentrations for these three ionic liquids are 5.23%, 5.11%, and 3.50%, respectively.

Although [EtOHmim]$^+$ based ionic liquids absorbs more ammonia, it is interesting to see that in the beginning of the process [emim][BF$_4$] absorbs slightly faster than [EtOHmim][NTf$_2$]. This trend occurs until the process takes place for around 70 s. After 70 s, the ammonia concentration of [emim][BF$_4$] remains lower than [EtOHmim] [NTf$_2$] as [emim][BF4] absorbs less ammonia. On the other hand, faster absorption of ammonia in the beginning of the process is shown by [emim][BF$_4$] in comparison with [emim][EtSO$_4$] and [emim] [NTf$_2$] in comparison with [emim][EtSO$_4$].

6.4.3. *Mass Absorption Flux*

Mass absorption flux is calculated using eq. (2) and mass absorption rate is recorded directly from gas mass flow controller using data logger. When the absorption process is started, the ionic liquid is in its highest purity and thus absorbs ammonia quickly. As the absorption process continues, the absorption rate decreases until the solution reaches equilibrium condition. This process can be confirmed in figure 6.15 (a) which shows mass absorption flux of ammonia into ionic liquids at operation condition of 30ºC and 3 bar, was very high in the beginning of the process as the absorption and then decreases until the solution reach equilibrium. The initial mass flux for all ionic liquids in this operation condition lays between 4×10^{-4} g/cm^2 s and 14×10^{-4} g/cm^2 s.

Mass absorption flux at temperature of 30ºC and pressure of 5 bar is shown in figure 6.15 (b). From this figure it can be seen that the mass absorption flux was much higher in the beginning of the process as compared with those at pressure of 3 bar.
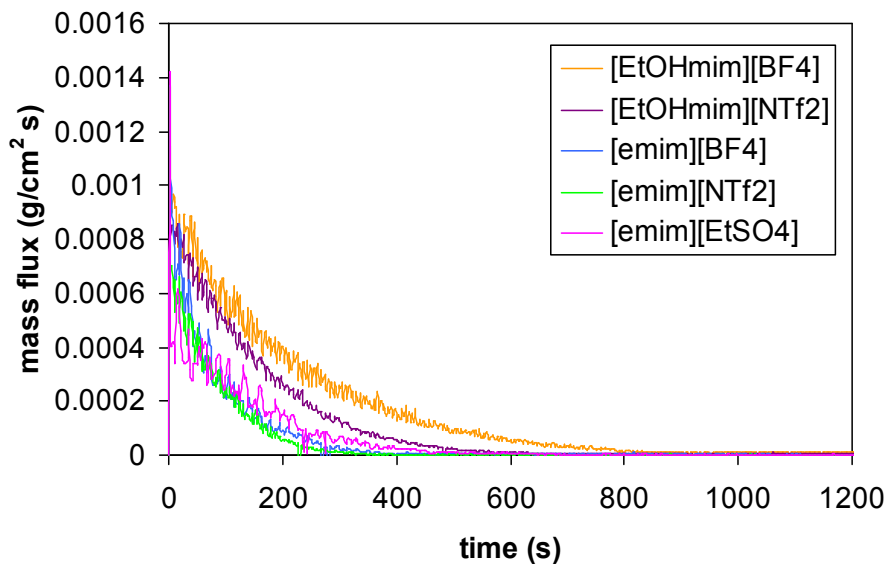
(a)
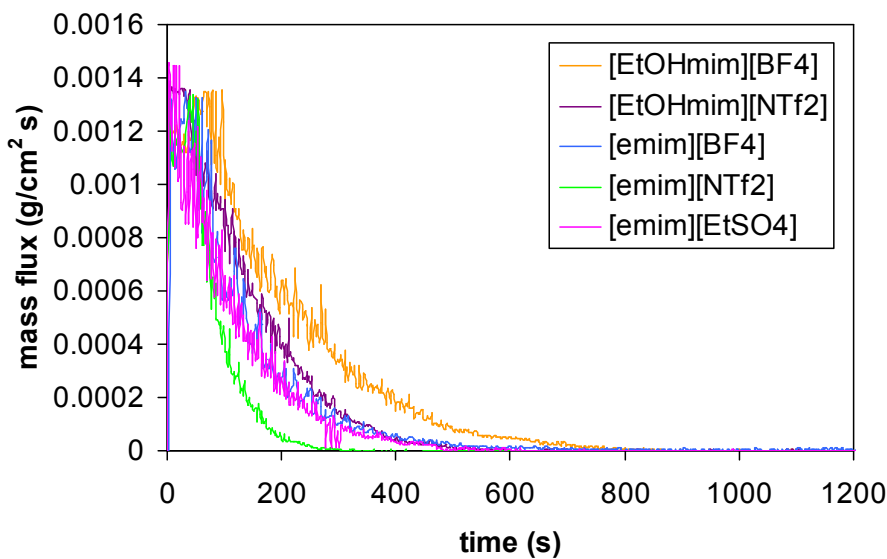
(b)

Figure 6.15. Ammonia mass flux at temperature of 30ºC and at pressure of (a) 3 bar and (b) 5 bar

The initial mass absorption flux for all ionic liquids in this operation condition lays between 11×10^{-4} g/cm^2 s and 15×10^{-4} g/cm^2 s. However, different with those at pressure condition of 3 bar, the mass absorption flux at pressure condition of 5 bar remains high until the absorption process takes place for around 2 minutes and after the mass absorption flux decreases sharply. From figure 6 it is also interesting

to note that although the absorption process may take place for more than an hour [12] the mass absorption flux of both 3 bar and 5 bar pressure conditions remains similar after 5 minutes.

6.4.4. Absorber thermal load

Apart of temperature, pressure, and mass absorption profile, it is also interesting to analyse the absorber thermal load to get information about the absorber thermal load for different working fluids at similar absorber configuration. The heat flow, total heat, and total heat released per unit refrigerant mass absorbed at several operation conditions were analysed.

Figure 6.16 (a) shows the heat flow of different working fluids at temperature of 30ºC and at pressure of 3 bar. It can be seen that the heat flow from the cell to the ambient increase significantly in the beginning of the measurement as in this time the absorption capacity is in its highest rate, and the heat is released from the system. The heat flow then decreases as the absorption rate decrease until the solution reach equilibrium and the heat flow reach zero. For all ionic liquid studied, the heat flow increases in the beginning of absorption process which confirms that the absorption processes for all studied ionic liquids are exothermic process.

In addition, it is also interesting to see that in the terms of same cation the heat flow increase of ionic liquids with $[NTf_2]^-$ anion is higher as compared to those ionic liquids with other anion which means that ionic liquids with $[NTf_2]^-$ anion release more heat as compared to other ionic liquids. Both $[EtOHmim][NTf_2]$ and $[emim][NTf_2]$ show highest peak in heat flow than other ionic liquids. As a results, the ionic liquids having $[NTf_2]^-$ anion shows higher total thermal load than ionic liquids with same cation and different anion, as it is shown in figure 6.16 (b). The total heat released by $[EtOHmim][NTf_2]$ is about 1.35 kJ and the total heat released by $[EtOHmim][BF_4]$ is only 1.28 kJ.
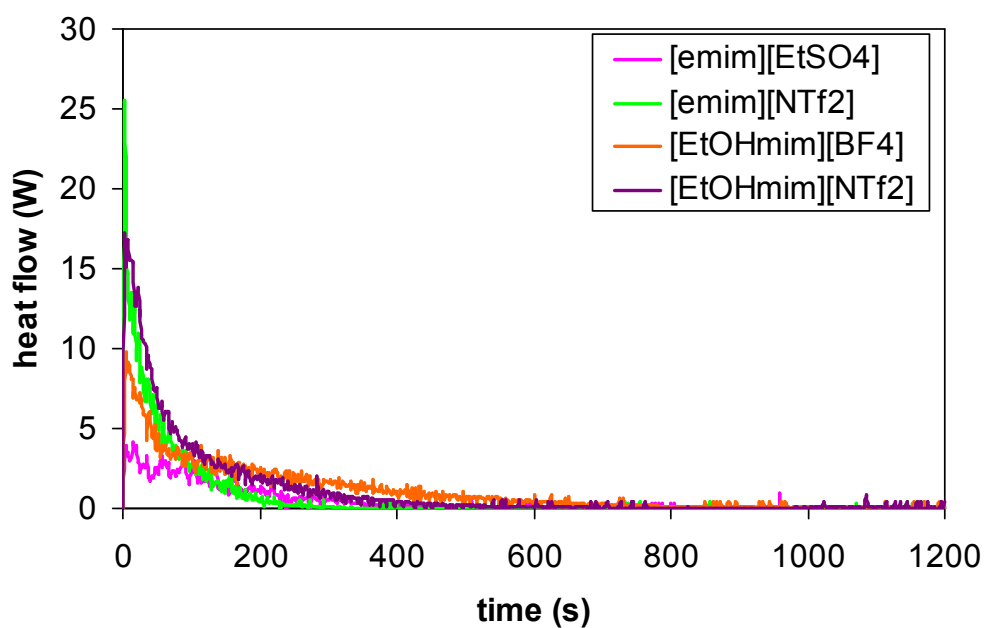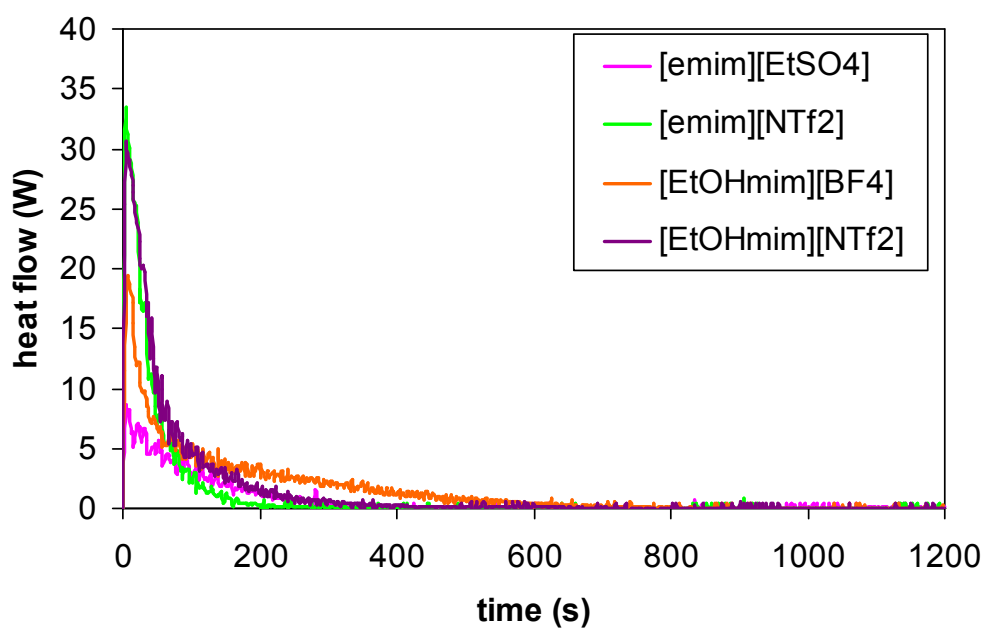
(a)
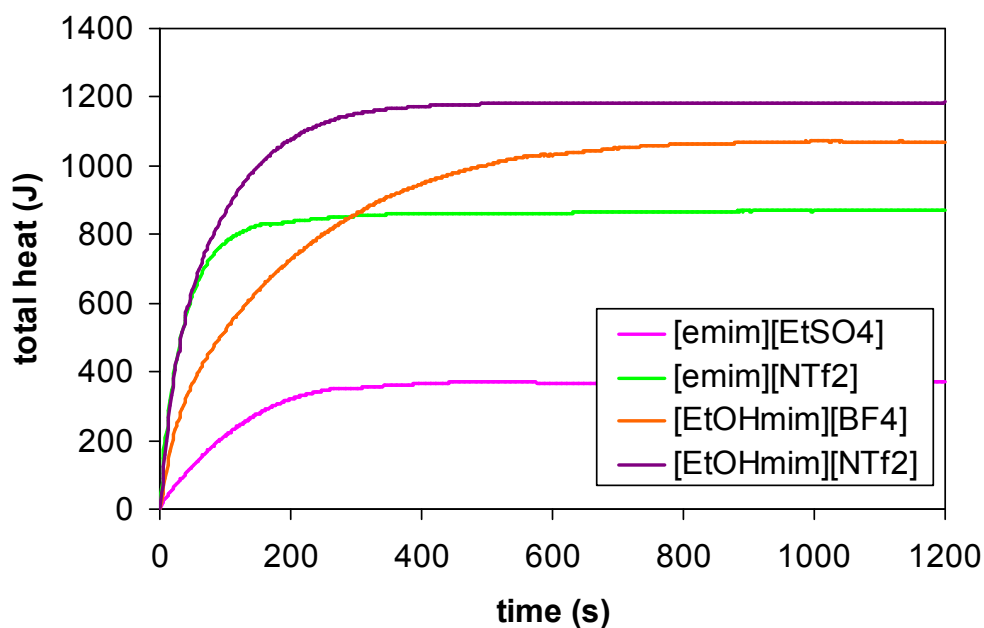
(b)

Figure 6.16. Heat flow (a) and total heat (b) released at temperature of 30ºC and at pressure of 3 bar

In the terms of same anion, it can be clearly seen from figure 6.16 (a) that ionic liquids having [EtOHmim]$^+$ cation give higher heat flow peak when compared to other cation although this difference does not give significant effect to the heat

flow when compared with that of difference of anion. For instance, [EtOHmim][NTf$_2$] shows higher heat flow peak than [emim][NTf$_2$] and [emim][BF$_4$] Howeever, although this difference does not give significant effect to the heat flow, the ionic liquids having [[EtOHmim]$^-$ cation shows higher total thermal load than ionic liquids with same anion and different cation as it can be seen in figure 6.16 (b). For instance, the total heat released by [EtOHmim][NTf$_2$] is about 1.35 kJ and the total heat released by [emim][NTf$_2$] is only 0.87 kJ.

Figure 6.17 (a) shows the heat flow of different working fluids at temperature of 40ºC and at pressure of 5 bar. Again, the heat flow from the cell to the ambient increase significantly in the beginning of the measurement as in this time the absorption capacity is in its highest rate, and the heat is released from the system. The heat flow then decreases as the absorption rate decrease until the solution reach equilibrium and the heat flow reach zero. For all ionic liquid studied, the heat flow increases in the beginning of absorption process which confirms that the absorption processes for all studied ionic liquids are exothermic process.

Moreover, it is also interesting to see that in the terms of same cation the heat flow increase of ionic liquids with [NTf$_2$]$^-$ anion is higher as compared to those ionic liquids with other anion which means that ionic liquids with [NTf$_2$]$^-$ anion release more heat as compared to other ionic liquids. Both [EtOHmim][NTf$_2$] and [emim][NTf$_2$] show highest peak in heat flow than other ionic liquids, even in this case their highest peak were almost at same value. As a results, the ionic liquids having [NTf$_2$]$^-$ anion shows higher total thermal load than ionic liquids with same cation and different anion, as it is shown in figure 6.17 (b). The total heat released by [EtOHmim][NTf$_2$] is about 1.81 kJ and the total heat released by [EtOHmim][BF$_4$] is slightly higher 1.83 kJ.

(a)

(b)

Figure 6.17. Heat flow (a) and total heat (b) released at temperature of 40ºC and at pressure of 5 bar

In the terms of same anion, again, it can be seen from figure 6.17 (a) that ionic liquids having [EtOHmim]$^+$ cation give higher heat flow peak when compared to other cation although this difference does not give significant effect to the heat flow
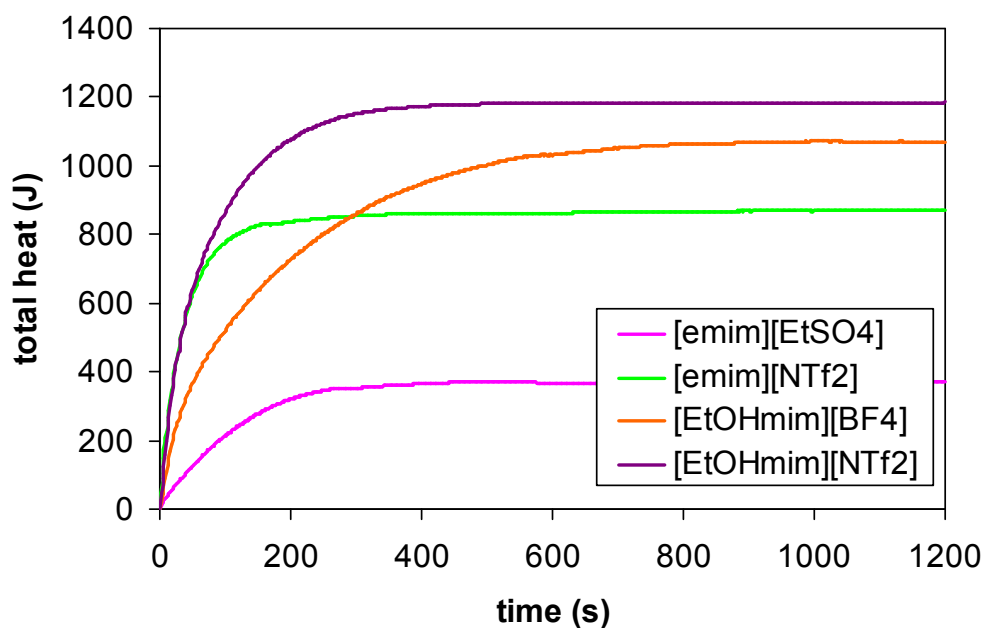
when compared with that of difference of anion. For instance, [EtOHmim][NTf$_2$] shows higher heat flow peak than [emim][NTf$_2$] and [emim][BF$_4$] However, although this difference does not give significant effect to the heat flow, the ionic liquids having [EtOHmim]$^-$ cation shows higher total thermal load than ionic liquids with same anion and different cation as it can be seen in figure 6.16 (b). For instance, the total heat released by [EtOHmim][NTf$_2$] is about 1.81 kJ and the total heat released by [emim][NTf$_2$] is only 1.36 kJ.

Figure 6.18 shows the total heat released per unit refrigerant mass absorbed at (a) temperature of 40ºC and at pressure of 5 bar temperature of 40ºC and (b) at pressure of 5 bar. From these figures, it can be seen that the total heat released per unit refrigerant mass of ionic liquids with [Ntf$_2$]$^-$ anion is higher as compared to those ionic liquids with other anion and same cation. In terms of same anion, it can be clearly seen from figure 6.18 that ionic liquids having [emim]$^+$ cation give higher total heat released per unit refrigerant mass as compared to other cation with the same anion as ionic liquids with [emim]$^+$ cation absorbed less refrigerant than other ionic liquids with different cation.

At operation condition of 30ºC and 3 bar, at the end of the absorption process, the total heat released per unit refrigerant mass of [emim][NTf$_2$] and [EtOHmim][NTf$_2$] are 3.18 kJ/g and 2.18 kJ/g, respectively, which are much higher than other ionic liquids with different anion, [emim][EtSO$_4$] and [EtOHmim][BF$_4$], which have total heat released per unit refrigerant mass of 1.62 kJ/g and 1.42 kJ/g, respectively. The trends are similar for operation condition of 40ºC and 5 bar. At this operation condition, at the end of the absorption process, the total heat released per unit refrigerant mass of [emim][NTf$_2$] and [EtOHmim][NTf$_2$] are 3.29 kJ/g and 2.43 kJ/g, respectively, which are much higher than other ionic liquids with different anion, [emim][EtSO$_4$] and [EtOHmim][BF$_4$], which have total heat released per unit refrigerant mass of 1.90 kJ/g and 1.65 kJ/g, respectively.
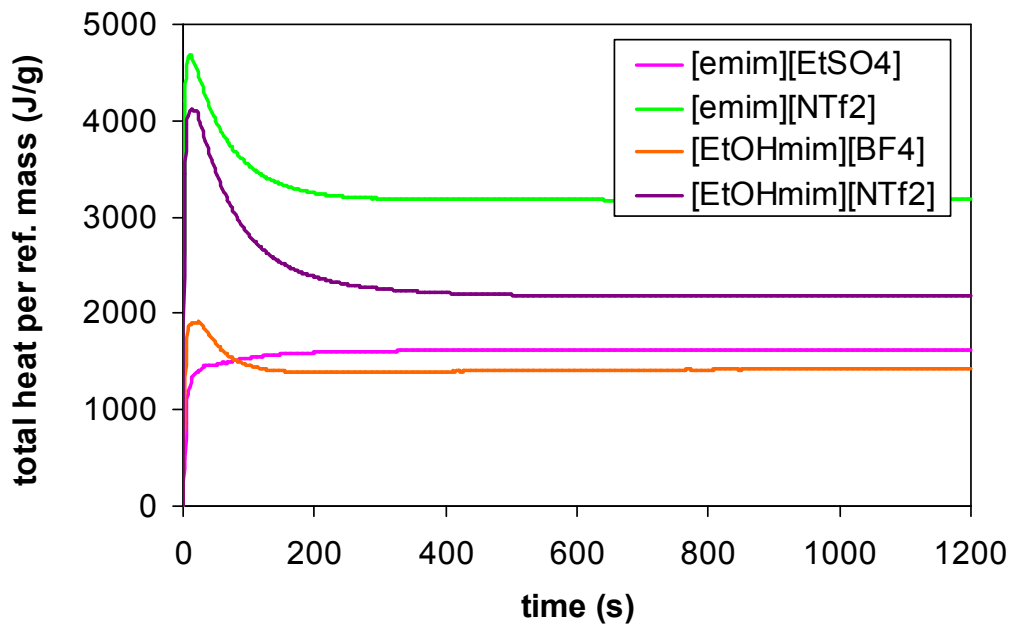
(a)
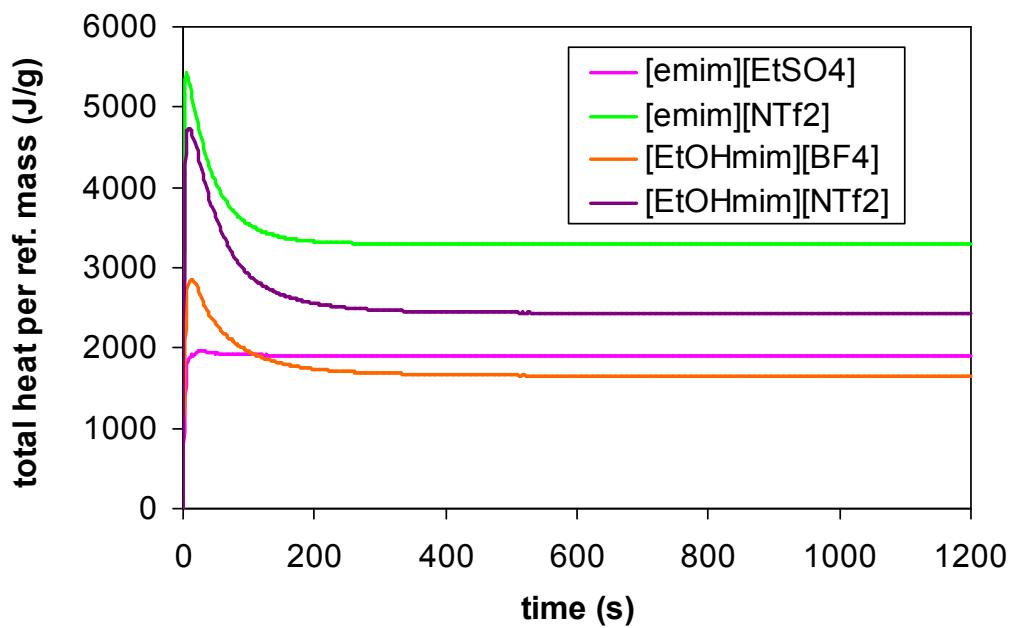
(b)

Figure 6.18. Total heat released per unit refrigerant mass absorbed at (a) temperature of 40ºC and at pressure of 5 bar temperature of 40ºC and (b) at pressure of 5 bar

6.5. Conclusions

In this work, a measurement setup to study the absorption capacity of the ammonia vapor in ionic liquids in a pool type absorber is developed and studied. This investigation is necessary to find the most suitable ionic liquid as an absorbent for ammonia refrigerant. Furthermore, it is also important to find the most suitable absorber configuration for the proposed ammonia/ionic liquids absorption systems.

Considering the literature review about the most suitable for the absorber and desorber of absorption refrigeration cycle with the working fluid mixtures under study, flooded/pool type column having inner volume of 14 ml is constructed to study the absorption capacity of the ammonia vapor in ionic liquids.

The absorption capacity of ammonia into five ionic liquids is measured using static pool type absorber at different temperatures and pressures. The measurement confirms that pool type absorber is able to measure the absorption capacity of absorbent having low solubility with the refrigerant by relatively small quantity of absorbent. It is also confirmed that the ammonia solubility in ionic liquids decrease when the temperature is increased and the ammonia solubility in ionic liquid increases when the system pressure is increased.

Among all ionic liquids presented in this chapter, [EtOHmim]$^+$ based ionic liquids shows higher absorption capacity than [emim]$^+$ based ionic liquids, which means that the OH structure in the cation may improve the absorption capacity of ammonia. In addition [BF$_4$]$^-$ anion shows slightly higher absorption capacity than other anions with same cation. However, in the beginning of the process [emim]$^+$ based ionic liquids show higher absorption capacity than [EtOHmim]$^+$ based ionic liquids.

In the terms of absorption thermal load, heat flow peak of ionic liquids with [NTf$_2$]$^-$ anion is higher as compared to those ionic liquids with other anion which means that ionic liquids with [NTf$_2$]$^-$ anion release more heat as compared to other ionic liquids. As a results, the ionic liquids having [NTf$_2$]$^-$ anion shows higher total thermal load than ionic liquids. Similarly, the total heat released per unit refrigerant mass of ionic liquids with [Ntf$_2$]$^-$ anion is higher as compared to those ionic liquids with other anion and same cation. However, in the terms of same anion, ionic liquids

having [emim]$^+$ cation give higher total heat released per unit refrigerant mass as compared to other cation with the same anion as as ionic liquids with [emim]$^+$ cation absorbed less refrigerant than other ionic liquids with [EtOHmim]$^+$ cation.

Moreover, although [EtOHmim][BF$_4$] shows high absorption capacity, it is necessary to study its other properties (e.g. viscosity) to have deeper understanding about its feasibility to be a suitable absorbent for ammonia refrigerant.

6.6. References

[1] Killion, J. D., and Garimella, S., A critical review of models of coupled heat and mass transfer in falling-film absorption, International Journal of Refrigeration, (2001), 24, 755-797

[2] Tae Kang Y., Akisawa A., Kashiwagi T., Analytical investigation of two different absorptionmodes: falling film and bubble types. Int. J. Refrig. 2000;23;430-443

[3] Castro J., Oliet C., Rodríguez I., Oliva A., Comparison of the performance of falling film andbubble absorbers for air-cooled absorption system. Int. J. Therm. Sci. 2009;48;1355-1366.

[4] Lee J.K, Koo J., Hong H., Kang Y.T., The effects of nanoparticles on absorption heat and mass transfer performance in nh3/h2o binary nanofluids. Int. J. Refrig. 2010;33;269–275

[5] Kim J.K., Jung J.Y., Kang Y.T., The effect of nano-particles on the bubble absorption performance in a binary nanofluid, Int. J. Refrig. 2006;29;22–29

[6] X. Ma, F. Su, J. Chen, T. Bai, Z. Han, International Communications in Heat and Mass Transfer, 36 (2009) 657–660

[7] C. Pang, W.Wub, W. Sheng, H.Zhang, Y. T. Kang, International Journal of Refrigeration, 35 (2012) 2240–2247

[8] H. Kim, J. Jeong, Y.T. Kang, International Journal of Refrigeration, 35 (2012) 645–651

[9] W.D. Wu, G. Liu, S.X. Chen, H. Zhang, Energy and Buildings 57 (2013) 268–277

[10] McKenna T.F., Design model of a wiped film evaporator applications to the devolatilisation of polymer melts, Chemical Engineering Science 1995;50(3);453-467

[11] Cvengros J., Lutisan J., Evaporator with wiped film as the reboiler of the vacuum rectifying column, Separation and Purification Technology 1999;15;95-100

[12] Heimgartner, E., 1980, Devolatilisation in the thin-film vaporiser, in

Devolatilisation of Plastics, pp. 69-97. VDIVerlag Gmbh, Dusseldorf.

[13] Biesenberger, J. A., 1983, Thin film evaporators, in Devolatilization of Polymers (Edited by J. A. Biesenberger), pp. 51-63. Macmillan, New York.

[14] Ariyadi, H. M., Maiya, P. M., Valles, M., Salavera, D., and Coronas, A., Measurement of Ammonia Absorption in New Absorbent - Preliminary Results, *Proc. 28th Int. Conf. on Efficiency, Cost, Optimization, Simulation and Environmental Impact of Energy Systems*, Pau, France 2015

[15] Yokozeki, A., Shiflett, M.B., Vapor–liquid equilibria of ammonia + ionic liquid mixtures. *Applied Energy*. 2007; 84; 1258-1273

[16] Yokozeki, A., Shiflett, M.B., Ammonia solubilities in room-temperature ionic liquids, ammonia solubilities in room-temperature ionic liquids. *Ind. Eng. Chem. Res*. 2007; 46; 1605-1610

[17] Li, G., Zhou, Q., Zhang, X., Wang, L., Zhang, S., Lia, J., Solubilities of ammonia in basic imidazolium ionic liquids. *Fluid Phase Equilibria*. 2010 ;297(1); 34–39

Chapter 7

Conclusions and Recommendations

7.1. Conclusions

The research for this thesis was aimed to analyse the feasibility and the performance of ionic liquids as an absorbent for ammonia refrigerant in absorption refrigeration systems. Ionic liquids, novel and tailor-made absorbents, can be used with ammonia as working pairs for absorption refrigeration cycles and give some advantages such as elimination of the rectification process in ammonia/water systems. In the beginnig of this research, an overview of absorption technologies and working fluids has been discussed with an emphasized to ionic liquid as alternative absorbent for ammonia refrigerant. The properties of ammonia/ionic liquid working pairs have been gradually examined in recent years. However, the information related to the thermophysical properties of the mixtures of ammonia/ionic liquid systems are still remains scarce. The information related with thermophysical properties of ammonia/ionic liquid working fluids is limited to the solubility of ammonia in few ionic liquids mostly in imidazolium based ionic liquids. Other information, such as excess enthalpy of ammonia/ionic liquid mixture which is important property for absorption simulation, so far is not available in the literature. Furthermore, experimental studies on the absorption refrigeration systems working with ammonia/ionic liquid fluids are so far not reported in the literature. Investigations related to the application of ammonia/ionic liquid working fluids in absorption refrigeration systems are so far limited to the theoretical studies and computational simulation. In addition, the simulation results were undoubtedly dependent to the thermodynamic model and the availability of thermophysical

property data. Therefore it is necessary to select an appropriate model (from equation of state (EOS) or activity coefficient-based methods) to describe the vapour-liquid equilibrium properties of the binary systems of ammonia/ionic liquid mixtures.

The ability of four different models to calculate the phase equilibrium prediction of ammonia/ionic liquid mixtures, namely Non-Random Two Liquid (NRTL) model, Reidlich-Kwong-Soave Equation of State (RK-Soave EOS), are studied and analyzed in the next step of this research. Both NRTL and RK-Soave model show their ability to calculate the vapor-liquid equilibrium of ammonia/ionic liquid mixtures with high accuracy. Although the calculation results using NRTL model were slightly less accurate than those of RK-Soave model, NRTL model is considered as the simplest model in comparison with other thermodynamic models studied in this chapter. Due to its simplicity, this model has been used to correlate the vapor-liquid equilibrium and to predict the excess properties of ammonia/ionic liquid mixture [4, 26-27]. If the critical properties of ionic liquids are available or can be predicted, the cubic EOS also can be used, such as have been done by some authors [6-7]. PC-SAFT model, although it is not as simple as NRTL model and RK-Soave model, this model is able to predict whether two pure compounds are soluble or not. Furthermore, PC-SAFT model are rarely used to calculate the solubility of absorption refrigeration working fluids especially for thermodynamic performance analysis purpose. Finally, UNIFAC model is so far not recommended to be used to predict the phase-equilibrium of ammonia/ionic liquids mixture due to its limitation in group parameters available in the database.

The performances of several ammonia/ionic liquid mixtures working pair available in the literature were then theoretically studied and analysed for absorption refrigeration applications using selected NRTL model. The ammonia/ionic liquid working fluids selection was mainly based on the availability of their thermodynamic property data in the literature. All the calculation and simulation works were carried out using commercial software ASPEN Plus.

Among five ammonia/ionic liquid working fluids studied, at certain operation conditions, the ammonia/[emim][NTf$_2$] working fluid presented the highest *COP* than that of other ammonia/ionic liquid mixtures. The *COP* of the systems with ionic liquids as absorbents follows an order of [emim][NTf$_2$] > [emim][SCN] >

[bmim][PF$_6$] > [bmim][BF$_4$] > [emim][EtSO$_4$]. However, although the *COP* of the system working with ammonia ammonia/[emim][NTf$_2$] was higher than the systems with other working fluids, it is also interesting to see that its circulation ratio was the highest among other working fluids. On contrary, although the *COP* of the system working with ammonia ammonia/[bmim][BF$_4$] was lower than the systems with other working fluids, its circulation ratio was the lowest among other working fluids. Similarly, although the *COP* of the system working with ammonia/[emim][NTf$_2$] mixture was higher than the systems with other working fluids, its *R* was the lowest among other working fluids. It means that at the same ionic liquid mass flow rate and at the same operation conditions, the systems working with ammonia/[emim][NTf$_2$] mixture produces lower cooling capacity. In contrary, although the *COP* of the system working with ammonia ammonia/[bmim][BF$_4$] mixture was lower than the systems with other working fluids, on contrary its *R* value was the highest among other working fluids, which means that at the same ionic liquid mass flow rate and at the same operation conditions, the systems working with ammonia/[bmim][BF$_4$] mixture can produce higher cooling capacity.

Apart of ammonia/ionic liquid mixture available in the literature, new selected ammonia/ionic liquid mixtures working pair for absorption refrigeration applications are theoretically studied and analysed. The 1-(2-Hydroxyethyl)-3-methylimidazolium tetrafluoroborate ([EtOHmim][BF$_4$]), 1-(2-Hydroxyethyl)-3-methylimidazolium bis(trifluoromethyl- sulfonyl)imide ([EtOHmim][NTf$_2$]), (2-hydroxyethyl)-N,N,N-trimethyl bis(trifluoromethyl- sulfonyl)imide ([N$_{111}$(2OH)][NTf$_2$]), and N-Trimethyl-N-propylammonium Bis(trifluoromethane-sulfonyl)imide ([N$_{1113}$][NTf$_2$]) have been selected as new absorbent for ammonia absorption applications. The results show that all solubility predictions were in good agreements in comparison with experimental data. In addition the excess enthalpies for all studied mixture were negative. The coefficient of performance (*COP*) of the absorption systems working with ammonia/ionic liquid working fluids were about similar when compared with ammonia/LiNO$_3$ at same cooling capacity and operation conditions. Among all of ammonia/ionic liquid working fluids studied in this chapter, only [N$_{1113}$][NTf$_2$] presented higher *COP* that that of ammonia/LiNO$_3$ at certain operation conditions. The *COP* of the systems with other ionic liquids as absorbents

follows an order of [EtOHmim][BF$_4$] > [N$_{111}$(2OH)][NTf$_2$] > [EtOHmim][NTf$_2$] at all operation conditions. Although the *COP* of the system working with ammonia ammonia/ [N$_{1113}$][NTf$_2$] was higher than with other working fluids at certain operation conditions, on contrary its circulation ratio is the highest among other working fluids. The circulation ratios (*f*) of the absorption systems working with ammonia/ionic liquid working fluids at same operation conditions were somehow higher as compared with that of ammonia/LiNO$_3$. The lowest *f* among all of studied ammonia/ionic liquid working fluids was shown by ammonia/[EtOHmim][BF$_4$] whereas the highest one is shown by ammonia/ [N$_{1113}$][NTf$_2$]. The higher circulation ratio of ammonia/ionic liquid working fluids also affects the solution mass flowrate per unit of cooling load (*R*). At same cooling capacity and operation conditions, the *R* values of the absorption systems working with ammonia/ionic liquid working fluids at same cooling capacity and operation conditions were higher when compared to that of ammonia/LiNO$_3$. Moreover, energy consumption needed to operate the absorption cycle mainly occurs at the generator, and that the mechanical work required for the solution pump is very small in comparison with energy input of the generator (less than 1% in the case of the highest solution pump's work) and thus can be neglected for general calculations or when information on solution density is not available. Finally the viscosities of ammonia/ionic liquids mixtures were generally higher than that of ammonia/LiNO$_3$ however, surprisingly the viscosity of ammonia/[N$_{111}$(2OH)] [NTf$_2$] was lower than that of ammonia/LiNO$_3$, which may be a competitive absorbent for water absorbent substitution for ammonia-based absorption refrigeration systems in comparison with LiNO$_3$.

In addition to the simulation and theoretical investigation, a measurement setup to study the absorption capacity of the ammonia vapor in ionic liquids in a pool type absorber was also developed and studied. This investigation is necessary to find the most suitable ionic liquid as an absorbent for ammonia refrigerant. Furthermore, it is also important to find the most suitable absorber configuration for the proposed ammonia/ionic liquids absorption systems. Among all measured ionic liquids, [EtOHmim]$^+$ based ionic liquids shows higher absorption capacity than [emim]$^+$ based ionic liquids, which means that the OH structure in the cation may improve the absorption capacity of ammonia. In addition [BF$_4$]$^-$ anion shows slightly higher

absorption capacity than other anions with same cation. However, in the beginning of the process [emim]$^+$ based ionic liquids show higher absorption capacity than [EtOHmim]$^+$ based ionic liquids.

In the terms of absorption thermal load, heat flow peak of ionic liquids with [NTf$_2$]$^-$ anion is higher as compared to those ionic liquids with other anion which means that ionic liquids with [NTf$_2$]$^-$ anion release more heat as compared to other ionic liquids. As a results, the ionic liquids having [NTf$_2$]$^-$ anion shows higher total thermal load than ionic liquids. Similarly, the total heat released per unit refrigerant mass of ionic liquids with [Ntf$_2$]$^-$ anion is higher as compared to those ionic liquids with other anion and same cation. However, in the terms of same anion, ionic liquids having [emim]$^+$ cation give higher total heat released per unit refrigerant mass as compared to other cation with the same anion as as ionic liquids with [emim]$^+$ cation absorbed less refrigerant than other ionic liquids with [EtOHmim]$^+$ cation.

Finally, from this research it can be said that the ionic liquid has a great potential to be an alternative absorbent for ammonia refrigerant. The ammonia/ionic liquid working fluid can provide competitive performance in comparison with conventional absorbent for ammonia refrigerant. However, some drawbacks are still remains to be solved such as relatively low solubility of ammonia into ionic liquids which affects to the solution circulation mass flow ratio and relatively high viscosity of ionic liquid in comparison with other conventional absorbent which may affects to the performance of absorber and solution pump. In addition, to date the availability of the thermophysical properties of ammonia/ionic liquids mixtures are very few and limited. Therefore, it is recommended to deeply explore other ionic liquids that may be a better candidate as an absorbent for ammonia refrigerant and has thermophysical properties suitable for absorption refrigeration applications. Moreover the measurement of the thermophysical properties of ionic liquids and their mixtures with ammonia is urgently needed to provide adequate thermophysical data to further investigate the characteristic and performance of ionic liquid as an alternative absorbent for ammonia refrigerant.

7.2. Recommendations and Future Works

As it has been mentioned in porevious section, deep exploration and investigation on other ionic liquids that may be a better candidate as an absorbent for ammonia refrigerant and has thermophysical properties suitable for absorption refrigeration applications is indeed necessary. Moreover the measurement of the thermophysical properties of ionic liquids and their mixtures with ammonia is urgently needed to provide adequate thermophysical data to further investigate the characteristic and performance of ionic liquid as an alternative absorbent for ammonia refrigerant. The investigation on ionic liquids for absorbent should be extended to not only imidazolium-based ionic liquids. As it has been concluded, the non-imidazolium- based ionic liquid may give a better potential as an absorbent for ammonia refrigerant as it has relatively high solubility in comparison with other ionic liquids and it has lower viscosity even when compared with ammonia/LiNO$_3$ solution.

In addition to above recommendations, as future works it will be interesting to study not only the feasibility of ionic liquids as absorbent for ammonia but a slo their feasibility as absorbent for other natural refrigerant such as water and alcohol-based refrigerant like 2,2,2-trifluoroethanol (TFE). Moreover, depending to the characteristic of the natural refrigerant/ionic liquid working fluids, it is also great opportunity to investigate the use of natural refrigerant/ionic liquid mixtures as working fluids for other absorption applications such as heat transformer and heat pumps or even for combine cooling/heating and power applications.

Finally, the experimental investigations on the performance of ammonia/ionic liquid working fluids for absorption refrigeration applications are still remain open and thus need to be developed and studied. The interest on experimental research is not only limited on the performance of ammonia/ionic liquid working fluids for absorption refrigeration but also can be extended to the performance and characteristic of absorption processes in some typical absorbers as well as the vapour generation processes in the generator.